STRUCTURAL SEQUENCE AND PETROGENESIS OF THE POLYPHASE DEFORMED PRECAMBRIAN TERRANE OF THE VILA NOVA REGION, STATE OF RIO GRANDE DO SUL, SOUTHERN BRAZIL

BRENO CORREA DA SILVA FILHO

Thesis presented for the degree of
DOCTOR OF PHILOSOPHY
Department of Geology, University of Glasgow
February, 1984

OTHON HENRY LEONARDOS JR. with his interest when I applied for a grant, allowed me to start this work; PROF. BERNARD E. LEAKE, DR. P.W.G. TANNER with their support and my WIFE with her inestimable help and encouragement allowed to accomplish it. This Thesis is dedicated to THEM.

Page

Page

Page

Page

LIST OF TABLES

LIST OF FIGURES

ABSTRACT

Evidence is presented concerning the nature and development of the structural pattern existing in the region of Vila Nova, State of Rio Grande do Sul, Southern Brazil.

A supracrustal rock assemblage made up predominantly of quartzofeldspathic gneisses ranging in composition from dioritic to granodioritic; migmatites, and associated layers and lenses of amphibolite, have undergone an extensive polyphase deformational and metamorphic history, within which multiple igneous injections played a prominent role. This mixed rock assemblage which is here designated "Vila Nova Complex" forms part of the Precambrian rocks of the Sulriograndence Shield.

Despite the high degree of structural complexity it has been possible to establish a deformational sequence mainly on the basis of refolding and cross-cutting relationships seen in the field. Correlation between different areas of outcrop has been carried out on the basis of eleven phases of deformation that have been recognized, and their relationships with various intrusive masses. A gneissose foliation, formed during the first deformational phase (D_1), and folds of varying style and size and related igneous intrusions, developed during the third deformational phase (D_3), are key elements in the elucidation of the geological development of the rock complex.

The dominant foliation (S_1) which generally parallels the original layering (S_o) is commonly associated with and axial-planar to isoclinal, intrafolial, rootless folds (F_1).

The main phases of igneous activity took place during both late D_2 and D_3 with the emplacement of structurally-controlled tonalitic to trondhjemitic and granodioritic masses, respectively. The complex fold patterns displayed by various neosomes are the result of polyphase deformation rather than ptygmatic activity.

On the basis of different structural features representing a long-lasting progressive deformation three markedly distinct general compressive stress-systems have been distinguished in the course of the orogeny which caused the formation of the Vila Nova Complex. This orogeny appears to have occurred along convergent plate boundaries involving a continent-continent collision model.

I. INTRODUCTION

The Sulriograndense Shield, in Southern Brazil, as many other shield areas in the world is made up of an entangled association of a variety of structurally complex rock types in which quartzofeldspathic gneisses, migmatites, amphibolites and minor intrusions play an outstanding role. A small part of this shield in the region of the village of Vila Nova (Fig. 1) has been the subject of the present work and new information is given, on the basis of structural analysis and geochemical investigation, permitting a time sequence of events to be established, to relate structural events to metamorphic activity and leading to the setting up of an overall geological evolution. This approach follows most used in tightly deformed terranes, for example, in the Precambrian Lewisian Complex of Northwestern Scotland (Dash, 1969; Bowes & Hopgood, 1969; Findlay, 1970; Hopgood 1971; Hopgood & Bowes, 1972); in migmatites, gneisses and schists of the Baltic Shield in Finland (Hopgood, Bowes & Addison, 1976; Koistinen, 1981; Halden, 1982); in the schists of the Caledonides of Scotland (Bowes & Wright, 1973; Bowes, 1979) and elsewhere in the world (Skinner, Bowes & Khoury, 1969; Joubert, 1971; Naha & Halyburton, 1977; Marjoribanks *et al.*, 1980).

The rocks dealt with are polyphase deformed gneisses of different compositions and igneous masses that can be put in an overall structural sequence and in an overall structural, metampophic and igneous pattern rather than vaguely referred to as "Formation" or "Group", as if the studied area were simply made up of a metamorphosed sedimentary pile. This means that this work not only deals with gneisses, amphibolites and migmatites in a small area but that the concepts emerging from this study lead to the conclusion that previous ideas of processes of development in the Precambrian of Southern Brazil need to be re-evaluated.

No attempt is made here to make an extensive review of the many papers relating to the geological characteristics of the

Sulriograndense Shield. Rather, a general description of the principal works relating the rock assemblage dealt with is presented.

Carvalho (1932) described some of these rocks in different areas and on the basis of metamorphic grade divided them into two different units as follows: (1) a unit formed by rocks of high metamorphic grade, assumed to represent the Archean, and (2) a unit of low metamorphic grade rocks, considered as representing the Algonchean, and assembled under the designation of Porongos Group.

Goni (1962) dealing specifically with the geology of the Vila Nova region considered the high grade metamorphic rocks cropping out along Cambai river as making up the type section of his Cambai Formation. Similarly to Carvalho (1932), Goni (1962) on the basis of metamorphic grade ascribed to this "Formation" an Early Precambrian age and considered it as forming the basal unit of the Sulriograndense Shield. According to Goni et al. (1962) the Cambai Formation is underlying unconformably rocks of low metamorphic grade (Carvalho's (1932) Porongos Group).

Ribeiro et al. (1966) described a variety of gneisses, migmatites, amphibolites and marbles, crosscut by a number of pegmatites and displaying ptygmatic folds, as representing the Cambai Formation in the Caçapava region (Figure 1). These workers pointed out however that the unconformity reported by Goni et al. (1962) as existing between the Cambai Formation and Porongos Group was not found. On account of this they included Goni's (1962) Cambai Formation in Carvalho's (1932) Porongos Group.

Jost & Villwock (1966) dealing with a rock assemblage in the São Gabriel region (Fig. I) similar to that described by Goni (1962) claimed to have found out an angular unconformity between the rocks of high metamorphic grade and those less metamorphosed. In addition, these workers assumed the high grade metamorphic rocks as related to the oldest orogeny that took place in the Sulriograndense Shield and based on their lithological and metamorphic complexity suggested they should constitute a Group rather than a Formation. On structural grounds they referred to their "Group" as forming a regional holomorphic pattern of alternating anticlines and synclines.

The present study has shown, however, that the mixed rock assemblage dealt with (which includes Goni's (1962) type section) apart from being structurally extremely complex cannot be treated as a "normal stratified sedimentary sequence". Therefore, the previous designations either Cambai Formation or Cambai Group are absolutely inadequate and must be abandoned. Hence, the most appropriate designation "Vila Nova Complex" is here suggested.

II. GEOGRAPHICAL SETTING

The studied area is located in the Vila Nova region (Fig. I) and access to it is fairly good, since it is crossed in a direction E-W by the paved road (BR-290) which links Porto Alegre, the capital of the State of Rio Grande do Sul, with Uruguaiana in the border with Argentina. Such a road cuts across the village of Vila Nova. In addition, connecting a number of farms with Vila Nova there are a great deal of small unpaved roads which allow to go by car till very close to the principal outcrops of the region.

Outcrops are limited along the whole region surrounding Vila Nova. On account of this fact the studied area as a whole was divided into four subareas, which were designated by the Roman numerals I to IV (Fig.I). For the sake of clarity it must be stressed that such a division of the area into subareas was dictated by the availability of exposures rather than by structural characteristics, so that the term "domain" (Turner & Weiss, 1963) was not used in this case.

The best exposures are seen along the Cambai river (Fig.I, subarea I).

Other places with fairly good exposures are the Roma creek (Fig.I, subarea II) and the Tessari creek (Fig.I, subarea IIIa and IIIb). A road-cutting in the south side of the BR-290, 6 km to the west of Vila Nova, provides about 100 m of excellent exposures (subarea IV).

The localization of points of reference for each subarea is shown in figure I, in terms of plane co-ordinates.

III. TERMINOLOGY

Certain terms used in geological literature are given different meanings by different authors. Thus for the sake of clarity some of the definitions used in this thesis are set out here to avoid confusion.

Banded - A descriptive, non-genetic term for layers of alternating composition in metamorphic rocks (cf. Mason, 1978).

Gneissose banding or gneissosity - Metamorphic banding with an alternation of bands rich in quartz and feldspar with bands rich in ferromagnesian minerals (cf. Mason, 1978).

Composite layering - Applied to the case in which part of the gneissose banding is tectonic in origin.

Gneiss - A metamorphic rock containing medium to coarse bands of differing texture and mineralogy. The bands consist of layers relatively rich in quartz and feldspar, alternating with those containing ferromagnesian minerals (cf. Ehlers & Blatt, 1980).

Granitic gneiss - Gneiss which in outcrop has the appearance of a foliated granite (sensu latu).

Injection gneiss - A gneiss which has been formed by the injection of granite (sensu latu) magma along schistosity planes (cf. Mason, 1978).

Tonalitic gneiss - A gneiss with the composition comparable to that of tonalites.

Dioritic Gneiss - A gneiss which has the composition comparable to that of diorites.

Amphibolite - A medium to coarse-grained rock consisting predominantly of an amphibole (usually hornblende) and plagioclase (Ehlers & Blatt, 1980).

Quartzite - A granoblastic metamorphic rock consisting mainly of quartz, formed by recrystallization of sandstone or chert (Ehlers & Blatt, 1980).

Adamellite - A granitic rock in which plagioclase accompanies an alkali feldspar in approximately equal amounts (Hatch, Wells & Wells, 1972).

Granodiorite - A granitic, quartz-rich rock in which plagioclase is the dominant feldspar (Hatch, Wells & Wells, 1972).

Trondhjemite - A grandioritic rock in which alkali-feldspar is completely (or almost completely) suppressed and consist of plagioclase of the appropriate range of composition for granodioritic rocks (oligoclase-andesine) together with quartz and small quantities of biotite, sometimes proxied by hornblende (Hatch, Wells & Wells, 1972).

Granitic - A term applied to all holocrystalline igneous rocks of medium to coarse grain that are composed essentially of quartz and one or more feldspar, usually with some ferromagnesian mineral in addition (cf. Nockolds et al., 1978).

Granitoid - Applied with the same meaning as granitic.

Migmatite - Megascopically composite rock consisting of two or more petrographically different parts, one is the country rock in a more or less metamorphic stage, whereas the other one is of pegmatitic, aplitic or granitic, generally plutonic, appearance (Dietrich & Mehnert, 1960; Mehnert, 1968).

Paleosome - Parent rock of a migmatite (Mehnert, 1968).

Neosome - Newly formed part of a migmatite (Mehnert, 1968).

Cataclasis - Brittle deformation leading to breaking, crushing and pulverising of the grains of a rock (Best, 1982).

Cataclastic - Applied to a rock texture formed by granulation without loss of cohesion, accompanied, in many cases, by partial recrystallization (Park, 1983).

Mylonite - A fine-grained crush rock formed under ductile conditions by continuous recrystallization or flow (Park, 1983).

Cataclastic flow - Brittle deformation of a rock on a granular scale involving frictional sliding of broken fragments past one another (Best, 1982).

Foliation - A general term covering any planar surface produced in a rock as a result of deformation (Park, 1983).

Schistosity - A foliation marked by the parallel orientation of tabular minerals in a metamorphic rock with a sufficiently coarse-grain size (Park, 1983).

Fracture cleavage - A foliation marked by a set of closely-spaced fractures (Park, 1983).

Shear cleavage - A type of fracture cleavage in which there is differential movement (slip) along the fracture planes (Billings, 1942).

Lineation - Parallel arrangement of linear structures penetrative in handspecimen or in small exposures (Turner & Weiss, (1963).

Plunge - The angle a lineation makes with the strike line of a vertical plane which is parallel to it.

Rake - The angle a lineation makes with the strike line of an inclined plane which is parallel to it.

IV. ROCK UNITS

IV.1 GENERAL CHARACTER

The rocks of the area consist mainly of well-foliated quartzofeldspathic gneiss with bands or lenses of amphibolite. Associated with the gneisses there is a magmatic intrusive suite which varies in composition from gabbro, through diorite, tonalite and trondhjemite suite to a granitoid suite. The latter includes granodiorite, adamellite, rhyolite and pegmatites. Rare thin layers of quartzite occur in granitic gneiss. The whole rock sequence constitutes a banded assemblage which was involved in polyphase deformation and metamorphism.

Quartzofeldspathic gneiss is the dominant rock-type in the area. It is regularly banded, medium to coarse grained in texture, and varies in colour from light to dark grey. This colour variation is a reflection of the relative proportion of the major mineral constituents, which are quartz, feldspars, biotite and hornblende. In general the dimensional orientation of the mineral grains parallel to the gneissose banding is well developed, except where there is a local preponderance of granoblastic minerals (Fig.IV a, b).

On the basis of the relative proportion of those major constituents, the gneisses are referred to as biotite-gneiss, biotite-hornblende-gneiss and hornblende-biotite-gneiss. These different varieties of gneiss are inter-related and sometimes it appears that some types grade into one another with no apparent definite pattern of distribution in the field. This makes mapping of individual types an impossible task.

Medium grey biotite-gneiss, in a few places displaying small crystals of pink garnet, is the most common rock in the area. In places there is a strong reduction of the proportion of the leucocratic material accompanied by a relative increase in the content of biotite. This results in the formation of highly melanocratic bands, which look like bands of biotite schist. These micaceous bands are sometimes related to shear zones or zones of high strain. By contrast, there are wider leucocratic bands which have an igneous aspect and resemble injection gneisses.

On the basis of variation in the proportion of the major mineral constituents, mainly the variation in quartz content, for practical purposes, two main groups of gneisses can be recognized in the field, namely (1) dioritic gneisses, and (2) granitic gneisses.

The intrusion of the granitic rocks as concordant sheets or discordant veins and pegmatites, in relation to the dominant gneissose banding, gave rise to the formation, in places, of migmatites. Although the intrusion of these neosomes took place early in terms of the overall deformational pattern of the area and they have been deformed, they still preserve a clear igneous character. They are here described as tonalites, granodiorites, etc. The modal composition of the different rocks are given in Table I.

IV.2. PETROGRAPHY

IV.2.1 Quartzofeldspathic gneisses

IV.2.1.1. Dioritic gneisses

IV.2.1.1.1. Biotite-gneiss

a) General characteristics

A well foliated, dark grey, medium-grained rock, with irregularly spaced thin leucocratic bands of quartzofeldspathic material. Very small crystals of pyrite are found either dispersed throughout the groundmass, or aligned parallel to the foliation planes. On account of the character of the banding, in which the mafic bands are much thicker than the felsic ones, this rock-type in outcrops looks much more like a schist rather than a gneiss.

Under the microscope it can be seen that the mafic bands are composed dominantly of biotite (Fig.IV 2.a), with rare hornblende crystals, whilst the felsic material is quartz and plagioclase. Apart from forming the dominant foliation, biotite can also be seen making different foliations cross-cutting the former at different angles. As a rule the biotites making up the dominant foliation are larger than those aligned along the other ones.

Fractures, filled with carbonate, albite and pyrite, are seen cross-cutting the rock either parallel to the dominant foliation or at a high angle to it.

b) Mineralogy

Biotite - This mineral varies in size depending on whether it is making the dominant foliation (up to 1 mm in length) or at different angles to the latter (0.2 to 0.5 mm in length). The pleochroism is pale yellow to reddish brown. In some places, mainly close to fractures, it is altered to chlorite. In some thin sections it was seen also associated with a few crystals of amphibole. It has apatite, sphene, pyrite and epidote as inclusions and, commonly, exhibits lenses of albite or carbonate along the cleavage planes. Inclusions of zircon give rise to pleochroic haloes. Sometimes, it is seen enclosed by quartz or plagioclase.

Amphibole - This mineral is very rare in these rocks and only in some places it occurs as small prismatic, pale green crystals partly altered to biotite. Its characteristics suggest the presence of actinolitic amphibole.

Plagioclase - There are two plagioclase compositions in this rock: andesine (An_{32-41}) and albite.

Andesine - The crystals are hipidioblastic and vary in size from 0.30 up to 0.65 mm. Some of them exhibit a very prominent undulose extinction. They vary also from very saussuritized to practically fresh crystals. The alteration develops irregularly along twin planes, i.e., along some planes there is alteration while along others there is not. Some crystals are, in addition, zoned. Lobate contact with biotite or other plagioclase crystals is common. Apatite, opaques and carbonate occur as inclusions. In some instances biotite is seen recrystallizing along fracture planes cutting-across some plagioclase crystals.

Albite - This plagioclase occurs in two different ways, namely, (1) as hipidioblastic crystals with grey birefringence colour, and (2) as xenoblastic grains showing a yellow birrefringence colour. The hipidiomorphic crystals may exhibit alteration while the xenoblastic grains are always fresh-looking. In addition, the latter exhibit granulation and undulose extinction and commonly occur as elongate crystals in the quartzofeldspathic bands, with lobate contacts very accentuated with other mineral grains.

Quartz - This mineral varies in both shape and size. In shear zones it exhibits a ribbon-like shape up to 1.2 mm in length but normally displays a xenoblastic shape, with lobate contact with other mineral grains. Commonly what seems to be a single crystal under plane-polarized light, appears as an aggregate of smaller grains, when the nicols are crossed. Fracturing is very common, as well as, undulose extinction.

Accessories - The most common accessory minerals are apatite, sphene and zircon. Sericite is common as an alteration product together with carbonate. As opaque mineral, pyrite is the most important. Garnet is sometimes found as an accessory mineral (Fig. IV.2.b and IV.3.a).

IV.2.1.1.2. Hornblende-biotite gneiss

a) General characteristics

This type of gneiss is generally dark coloured, on account of the dominance of the mafic bands over the felsic ones. These are seen in places as a very thin veining varying in thickness from 1 mm to 2 mm. The felsic thin veining is continuous contrasting with another type of quartzofeldspathic bands which apart from being thicker are discontinuous. The mesoscopic appearance of this rock is that of a well foliated mafic rock.

Under the microscope, the leucocratic bands are seen to be composed mainly of plagioclase, with subordinate quartz, and exhibit a granoblastic texture (Fig.IV.3.b). Sometimes in these granoblastic bands the plagioclase crystals form a polygonal pattern. The mafic layers are formed by dimensionally oriented biotite and hornblende. The preferential orientation of hornblende prisms, in some places, give rise to a nematoblastic texture. The dominant foliation, parallel to the gneissose banding, is defined by both biotite and hornblende crystals but other foliations at different angles are only marked by small biotite flakes (mean size = 0.2 mm).

Fractures parallel to the dominant foliation are seen filled with albite and carbonate. The width of these fractures is variable from 0.1 mm up to 0.9 mm. The granulation and undulose extinction displayed by albite, indicates that movement took place along such fractures after the crystallization of this plagioclase. Another set of very irregular fractures are also seen in thin-section to cross-cut the dominant foliation at a high angle. These fractures are very thin (about 0.08 mm wide) and are filled with albite. Associated with the fractures parallel to the dominant foliation there are crystals of pyrite. In addition, the crystals of plagioclase along these zones of fractures, display very thin cracks filled with albite, and disposed obliquely in relation to the orientation of the former. In some places the "parallel" fractures are filled, in addition, with an isotropic or cryptocrystalline brownish material which could be devitrified pseudo-tachylite.

b) Mineralogy

Hornblende - The crystal size varies from 0.2 to 0.6 mm. The pleochroism in basal section is light yellow or yellowish green to brownish green, while in prismatic sections varies from light or yellowish green to green. The prismatic section tends to show a high length/width ratio. The angle $C \wedge Z$ varies from 10^{o} to 26^{o}. On the basis of such characteristics it appears that besides hornblende there is some actinolite in this rock. Some hornblende have a corona which exhibits pleochroism in bluish-green while the core displays pleochroism in yellow to green. Locally the amphibole crystals are seen altered to biotite, epidote and sphene.

Apatite, zircon and opaques are seen as common inclusions in this mineral.

Biotite - The biotite flakes vary in length from 0.18 up to 1.2 mm. Pleochroism is light yellow to reddish brown or brown. Close to fractures the biotite is altered to chlorite and associated with sphene and epidote. Sometimes it can be seen to have resulted from alteratinn of hornblende. It can be also seen as inclusion in plagioclase or crystallized along fractures which cut this mineral. Lobate contact with plagioclase is very common. As inclusions it presents apatite, zircon, which originates pleochroic haloes, sphene and some opaques.

Plagioclase - Compositions in the ranges An_{15-27} and An_{31-43} were recognized on the basis of the angle of extinction of the polysynthetic twinning, apart from another type without twinning which was considered as representing albite. The oligoclase and andesine are generally moderately altered to sericite but such alteration becomes very strong along fracture zones. The width of the twinning lamellae change from one type to another, probably reflecting the anorthite content. Some crystals exhibit an incipient zoning. Offset of twin lamellae due to fracturing is common. Apatite, zircon, biotite and hornblende are found as inclusions.

Albite is seen into two different types as far as birefringence colour and shape are concerned. One type is represented by hipidioblastic grey crystals, under crossed nicols, which exhibit some alteration. This type has zircon, sphene and biotite as inclusions. The other type is represented by xenoblastic, yellow crystals, under crossed nicols, which can reach 2.1 mm in length. They are seen generally along fractures and do not show evidence of alteration, on contrary, they are very fresh-looking crystals. A distinctive characteristic of this type of albite is that what seems to be a large crystal in plane-polarized light appears as an aggregate of smaller grains with undulose extinction, when the nicols are crossed. In some places it appears that albite has been formed along biotite cleavage planes, pulling them apart and taking up a lens-shaped form.

Quartz - Its abundance in these rocks is very low. It varies in size from 0.2 mm to 0.9 mm. It is always xenoblastic displaying lobate contact with other minerals, mainly plagioclase. Normally is very granulated and the larger crystals are formed by an aggregate of smaller grains that display undulose extinction. Some crystals show a small angle 2V. Quartz is seen predominantly in the quartzo-feldspathic layers, but sometimes is making up monomineralic veins, parallel to the dominant foliation, up to 1.2 mm wide. In the more cataclastic zones quartz is seen together with albite but displaying sharp contacts. It encloses normally apatite needles, but very small, aligned bubbles are extremely common.

Accessories - Apatite, zircon, sphene, chlorite, carbonate, epidote and opaques. Sphene varies from rare up to about 1% of the mineral composition and is an important accessory mineral. It is normally associated with the mafic minerals. Chlorite is found as an alteration product of biotite. Carbonate is seen associated with altered plagioclase or in fractures together with albite. Epidote is characteristically a product of alteration associated with biotite, hornblende and plagioclase. The most common opague mineral is pyrite which occurs as hipidiomorphic to idiomorphic crystals.

It is very difficult to establish a representative modal composition for these gneisses, on account of the great variation presented by the mafic minerals, not only from band to band but also along the band themselves. The greatest variation is, however, in a direction perpendicular to the dominant foliation what suggests the existence of transitional types. Depending on the part of the thin section studied the result may be a biotite-rich band, a band with approximately equal amounts of biotite and hornblende and, still, a band in which hornblende is the only mafic mineral present.

Thus, in general terms, the three principal constituents of these gneisses show the following variation: biotite - 7 to 20% hornblende - 3 to 40% and plagioclase - 30 to 40%. An estimate average modal composition is shown in Table I.

IV.2.1.2. Granitic gneisses

a) General characteristics

These rocks are medium-grained, grey tonalitic to granodioritic (Fig. IV.1.a,b) gneisses composed of plagioclase, quartz, K-feldspar and biotite. The colour of these rocks is variable depending upon the amount of biotite, since in a general sense they can be termed biotite-gneisses.

Foliation is normally distinct, resulting from the dimensional orientation of the biotite flakes. A banding of variable width from milimeters up to a few centimeters and made up by quartzo-feldspathic material is a common characteristic of these rocks.

Compositionally there is a great similarity between some of these gneisses poorer in quartz and K-feldspar, and those belonging to the dioritic sequence. They differ, however, in textural characteristics because the tonalitic gneisses vary from approximately equigranular to heteroblastic, depending on their position in relation to movement zones. The heteroblastic texture arises as a result of (1) development of porphyroblasts of feldspar in a former grained groundmass, (2) mortaring and (3) myrmekitization.

b) Mineralogy

Quartz - Occurs as xenoblastic grains showing undulose extinction, and very sutured margins. Small rounded grains are seen within crystals of plagioclase.

Plagioclase - Varies in composition from An_{25} to An_{30} and occurs either as equigranular grains or as larger hipidiomorphic crystals, commonly with lobate contacts.

Microcline - Is irregularly distributed in variable amounts, but always subordinate in relation to plagioclase. As microcline becomes more common it normally forms embayed contacts with plagioclase and in suchcases the formation of myrmekites is very frequent. In places, the amount of microcline increases as to give to the rock a grano-dioritic composition.

Biotite - Biotite flakes are aligned parallel to distinct orientations. The most prominent and abundant crystals are seen parallel to the dominant foliation. Its pleochroism is in light yellow or yellowish brown to brick red or dark brown. The types with pleochroism in light yellow to brick red are smaller, fresher and mark foliations that cross-cut the dominant one. Biotites altered to chlorite show pale green to brownish pleochroism.

Accessories - Sphene, associated with biotite, zircon, which sometimes generates pleochroic haloes within biotite flakes, epidote and carbonate.

IV.2.2 Amphibolites

These rocks occur as bands or lenses, are very common in the area, and are concordant with the dominant foliation of the host gneisses. Discordant amphibolites originated from younger minor igneous intrusions are of very limited occurrence. The concordant amphibolites may, in turn, be divided into two types, namely (1) fine-grained well foliated amphibolite and (2) very coarse-grained amphibolite displaying no foliation. The former type varies in size from a few centimeters to more than 1 meter, whereas the coarser grained type which shows hornblende crystals up to 3 cm long, is more than 5 meters wide.

IV.2.2.1 Fine-grained concordant amphibolites

a) General characteristics

Are melanocratic rocks with a well developed foliation marked by the dimensional orientation of the mafic constituents. In places they are banded, consisting of alternating feldspar and hornblende-rich bands. The individual bands may be so thin as 1 mm. Their major mineral constituents are green hornblende, biotite and plagioclase.

b) Mineralogy

Hornblende - It occurs as prismatic or basal section aligned parallel to the dominant foliation of the rock. Pleochroism is in brownish yellow or greenish yellow to deep green. Simple contact twins are seen occasionally. Inclusions of opaques and euhedral crystals of plagioclase are common.

Plagioclase - This mineral normally occurs with very irregular shapes, displaying pronounced lobate-type contact with other plagioclase crystals or with hornblende. The most common shape is elongate, xenoblastic, parallel to the dominant foliation. It appears that there are different types of plagioclase in terms of An contents, on the basis of the variation in width displayed by the twinning bands. However, the crystal sections available in general were not suitable for use of the Michel Levy method to determine An content. Nevertheless, a few determinations were possible and show that some plagioclases fall in the compositional range An_{33-40}. Some fresher-looking and untwinned crystals appear to represent albite. Some crystals are altered to sericite but in places they are limpid and form aggregates of small grains displaying a polygonal texture.

Biotite - There is clear evidence of several generations of this

mineral as indicated by distinct orientations.
Parallel to these different foliations biotide is seen as elongate flakes with a high length/width ratio. It is pleochroic in light or brownish yellow to dark brown. A few crystals, however, are seen unrelated to any foliation in the rock. They occur as large almost equidimensional flakes (basal section) brown or deep green in colour. The dominant foliation is seen to bow around such large crystals which enclose smaller crystals or hornblende, plagioclase and sphene.

Accessories - Sphene is the most important accessory mineral, occurring in relatively high proportion associated with the mafic constituents of the rock, together with opaques, in some places. Some crystals are idioblastic, but the most common type of occurrence is as granular aggregates. Apatite occurs as inclusions normally in plagioclase; zircon generating pleochroic haloes in some biotites and opaques, sometimes dispersed poikiloblastically within hornblende, sometimes forming oriented trains of rounded grains in the same mineral.

IV.2.2.2. Coarse-grained concordant amphibolites

a) General characteristics

These are melanocratic, dark green rocks in outcrop or handspecimen, which are outstanding on account of the size of the hornblende crystals. The lack of a defined foliation in mesoscopic scale is confirmed under the microscope. The general texture of this rock is decussate with the large hornblende crystals randomly oriented. Commonly, the large hornblende crystals are surrounded by aggregates of small grains of hornblende and biotite.

b) Mineralogy

Hornblende - Occurs as large hipidiomorphic crystals with pleochroism in yellow to green in the prismatic sections. It displays twinning and in some crystals the twinning planes are offset by shear fractures along which biotite crystallized (Fig. IV.4.a). The large crystals enclose smaller ones, biotite and plagioclase.

Biotite - Occurs normally as inclusion in the large crystals of hornblende as thin and long crystals, or less commonly as short (Fig.IV.4.a) wide flakes. When it is not an inclusion it is seen in the corona of granulated crystals around the large crystals of amphibole. Within the hornblende it can be seen in several directions, but it appears that there is a direction related to a fracture set which is represented in different hornblende crystals. Its pleochroism is in light yellow to light brown or brown. It is altered to chlorite, mainly in the zones of granulation. A few crystals exhibit kink bands.

Plagioclase - Forms aggregates of grains of irregular shape and very much altered to sericite. Lobate contacts with hornblende are common. Small, less altered crystals, are seen around larger crystals, displaying a polygonal texture as evidenced by triple junctions (Fig. IV.4.b). The plagioclase aggregates are separated from one another by the hornblende crystals, so that no bands are formed. Actually, these aggregates could be described as "islands" in a sea of hornblende. No suitable crystal for determining the An content was found.

Accessories - The most significant accessory minerals are sphene and opaques which are seen associated to the mafic minerals, mainly to the amphiboles. In places, sphene is seen surrounding grains of opaques, what lead to think that the opaques are represented by ilmenite (Fig. IV.5.a). The colour of sphene is reddish brown. Chlorite is seen as alteration of biotite and very rare epidote was found along a fracture zone.

IV. 2.2.3 Discordant amphibolites

a) General characteristics

These rocks are dark coloured (dark green) fine-grained and do not present a conspicuous foliation. Foliations are barely seen only after careful examination of the rock surface, as marked by the alignment of very small biotite flakes, or some crystals of amphibole. Pyrite is seen either disseminated in the groundmass or concentrated in quartz veins which cut the rock.

Under the microscope the texture is dominantly granoblastic as controlled by the size and amount of plagioclase crystals. Reflecting the character seen in handspecimens, foliations are incipiently marked by the dimensional orientation of biotite and hornblende. Some of the foliations are marked only by small biotite flakes. Poikiloblastic textures are displayed by crystals of hornblende which enclose biotite, sphene, apatite and zircon. Inclusions of apatite and zircon in the biotites are common. Thin cross-cutting veins filled with chlorite, muscovite and carbonate are seen.

In some thin sections remnants of an original igneous texture are still preserved so that these rocks may represent the metamorphosed equivalents of dioritic intrusions (meladiorites?). On account of that in following sections these discordant amphibolites are referred to as diorites, for short.

b) Mineralogy

Hornblende - Normally occurs as prismatic crystals varying in size from 0.2 to 0.3 mm. In some places it is very altered into biotite, sphene and opaques. Twins are common. The colour in plane polarized light is green, with pleochroism in light yellow (X), olive green (Y) to dark green (Z). The extinctions angle varies from 10^{o} to 30^{o} with the great majority in the range 10^{o} - 20^{o}. This fact together with the fibrous aspect that some crystals display indicates that some hornblende has altered to actinolitic hornblende.

Biotite - The size of the flakes varies from 0.2 to 1.5 mm, but normally they are less than 1.0 mm, in length. The pleochroism is in light yellow to reddish brown. The contact with amphibole crystals can be sharp or transitional. Sometimes hornblende can still be recognized within some biotite flakes. It alters to chlorite mainly in zones close to fractures. In such situations it is also seen associated with sphene. Some flakes exhibit kink bands.

Plagioclase - This mineral normally forms the groundmass of the rock together with hornblende, with a mean size about 0.25 mm. Sometimes, however, it can be found as phenocrysts 3 mm in length. In the places where these phenocrysts are seen the texture of the rock close resembles that of an andesite. There are two distinct types of plagioclase. The first type is represented by hypidioblastic crystals, some of them zoned, and is normally very saussuritized. This type of plagioclase has the composition An_{15-31}. The second type is characterized by xenomorphic grains, normally untwinned but when displaying twins the lamellae are wider than in the former type. The undulose extinction of these lamellae has, however, prevented the determination of the An content. The boundaries of the plagioclases are commonly extremely lobate, what appears to be the result of partial replacement of the plagioclase by the surrounding crystals of plagioclase or mafic minerals. Where there are biotite flakes or amphibole prisms at the boundary it has been fixed and between the crystals involved the lobes in the boundary bulge into the plagioclase. As inclusions, in the plagioclase crystals, there are epidote, apatite, biotite and zircon. Some crystals are cut by fractures in which recrystallization of red biotite took place.
Albite has also been found as xenoblastic untwinned crystals

enclosing biotite and epidote.

Accessories - The most important accessory mineral is sphene which is found in relatively high proportions. It occurs as idiomorphic or xenomorphic crystals, varying in size from very small grains up to 0.5 mm. The colour varies from dark brown to almost colourless. Some of these crystals appear to show no relation with alteration of the mafic constituents of the rock.

Epidote is rare, and can be seen associated with hornblende and plagioclase.

Apatite occurs as prismatic crystals as inclusions in hornblende, biotite and, mainly, in plagioclase.

Zircon is also seen as a minor accessory mineral within some biotites or plagioclases.

Quartz is extremely rare and when present is of small size (about 0.2 mm) and shows undulose extinction.

Chlorite occurs as alteration of biotite.

Carbonate is normally filling fractures which cross-cut the rock, and rarely within plagioclase.

IV.2.3 Quartzites

a) General characteristics

Concordant, thin bands of quartzitic composition are found restrictly (subarea II, middle part), within very weathered granitic gneiss. On account of the contrasting behaviour in relation to weathering the quartzitic layers are readily recognized. In surface they vary in colour in shades of orange and reddish on account of dissemination of iron oxide, but in fresh cuts they are white with some pink zones due to the presence of potassium feldspar. In handspecimens they exhibit a very pronounced mylonitic banding, in which lensoid quartz and K-feldspar can be seen dimensionally oriented. Very thin layers of biotite, with some muscovite occurs widely apart, parallel to the dominant foliation which, in turn, parallels the mylonitic handing (Fig. IV.5.b).

b) Mineralogy

This rock is composed essentially of quartz, together with feldspar and very small proportions of biotite.

Quartz - It is the dominant constituent of the rock and varies in both grain size and shape. Some grains form ribbons parallel to the mylonitic banding (Fig. IV.5.b) while others display a mosaic and sutured fabric. Smaller grains are generally rounded and commonly are enclosed by the bigger ones, or by microcline. Undulose extinction is a very common characteristic.

Plagioclase - It is normally untwinned and lens-shaped dimensionally oriented. Some large grains show a more rounded outline, with sutured margins. The existence of smaller grains associated with these large porphyroclasts suggests that granulation of the latter took place during deformation generating a mortar texture. The optical characteristics of some of the plagioclase suggests the presence of albite, together with oligoclase.

Microcline - As the quartz grains, microcline is extremely variable in both grain size and shape. Some grains are very elongate parallel to the mylonitic banding while others are xenoblastic, displaying very irregular contacts with both quartz and plagioclase. In places it is seen clearly replacing plagioclase whose polysynthetic twinning can still be seen with continuity in its both sides. It is common the formation of myrmekites in the contacts (normally lobates) with plagioclase. Apart from being found in the granulated matrix of the rock, microcline is also seen along fractures which cut the dominant foliation at a high angle.

Biotite - Is a minor constituent of the rock, occurring as very small flakes oriented parallel to the mylonitic handing

(Fig.IV.5.b). It is pleochroic in light brown to dark brown, in the case of the fresher-looking crystals, or in brownish yellow to dark green, when altered. The alteration is commonly to chlorite, but some flakes are seen altered to muscovite, as well.

Accessories - Apart from the presence of chlorite and muscovite as alteration products of biotite, there are some rare occurrences of epidote, forming fine granular aggregates, mainly close to transversal fractures.

IV.2.4. Gabbro-tonalite-trondhjemite suite

IV.2.4.1. Gabbro

a) General characteristics

This rock-type has been found as isolated boulders which represent bands parallel to the dominant foliation of the gneisses in subarea III. The contacts are covered with soil and the exposures are about 1.5 m wide. This figure is, therefore, the minimum width of this igneous mass. It is a prophyritic, dark coloured rock, in which laths of plagioclase up to 4 mm long are seen in a medium-grained groundmess.

Under the microscope it has an ophitic texture, still well preserved, and represented by disoriented euhedral laths of plagioclase within plates of a mixture of amphibole with chlorite (Fig.IV.6.a). All traces of the original pyroxene have been destroyed by alteration. Neither olivine nor its alteration products has been found.

b) Mineralogy

Amphibole - The amphibole is the result of pseudomorphosis after pyroxene due to uralitization process. It is represented by fibrous-looking pale-green to bluish-green crystals, probably of actinolitic amphibole. The interlacing with chlorite is pronounced so as to prevent determinations of pleochroism scheme.

Plagioclase - Normally very altered, mainly to sericite. Less commonly carbonate and epidote are seen as alteration products. Plagioclase shows combined Carlsbad-albite twinning with some of the individuals making up the twinned crystals being less altered than the others. Some altered crystals are brownish, probably due to a general dissemination of iron oxides. Their composition has been determined as sodic labradorite (An_{52}). This sodic character of labradorite may be related to the extensive alteration of the rock, or, alternatively, to the absence of olivine in the original magma (cf. Nockolds et al, 1978). The plagioclase commonly exhibit very irregular outlines with the amphiboles which are seen replacing the former. In some cases around the plagioclase laths there are coronas of pale-green amphibole.

Accessories - It has already been mentioned the intimate association of the amphibole with chlorite which shows pleochroism in colorless to light green. Apart from this mineral and the presence of sericite in the plagioclases, the presence of very rare epidote and carbonate, and opaques associated with the amphiboles can be observed.

IV.2.4.2. Tonalite

a) General characteristics

It is a grey, medium to coarse-grained rock. In hand specimens the major mineral constituents, plagioclase, quartz and biotite, are readily recognized. The quartz grains have a characteristic blue hue. The biotite flakes define several different oriented foliations.

Under the microscope the dominant texture is granoblastic on account of the much larger size of the plagioclase and quartz crystals as compared to the biotite flakes. Some plagioclase and quartz crystals have undergone granulation, giving rise to a mortar texture, along zones of shear movement.

b) Mineralogy

Plagioclase - Is the major mineral constituent of this rock and is, (1) andesine (An_{32}) and (2) albite.
The andesine crystals range in size from 1.2 to 9.0 mm. Zoned crystals are common, exhibiting an altered core. In general, however, alteration is not pronounced in this type of plagioclase except for the places in which the rock was influenced by shearing.
Sometimes they have lobate boundaries displaying irregular contacts with other crystals, with the development of epidote and carbonate in the contact zone.
The crystals are commonly fractured and show undulose extinction. Some kinked lamellae have also been found. Zircon, carbonate, epidote and biotite are seen as inclusions, and sometimes oriented along the cleavage planes of the crystals. Albite ranges in size from 0.8 to 3.6 mm. It occurs characteristically with birefringence in the range of first order yellow. The crystals are xenoblastic, and may contain andesine and biotite as inclusions. In places they form elongate granular aggregates.

Quartz - Normally occurs in crystals larger than 5 mm and together with plagioclase is responsible for the granoblastic texture of the rock. Under the microscope the grains are xenoblastic and show undulose extinction (Fig.IV.6.b).
In zones affected by shear is lensoid or ribbon-like and very granulated. In places, between two large crystals of plagioclase, quartz occurs as small grains displaying triple junctions.

Biotite - Its size is variable and its distribution in the rock clearly reflects distinct phases of generation. It is pleochroic in light brown to reddish brown. Flakes enclosed in plagioclase show pleochroism in light brown to deep red. In sheared zones biotite is completely altered to chlorite. Sphene and epidote are also seen as its alteration products.

Accessories - Hornblende: it is very rare in these rocks. It is pleochroic in greenish yellow to dark green in the fresher crystals. However, is normally altered to a pale green fibrous variety (actinolite), to biotite, epidote and sphene.

Sphene: it is very common, sometimes makes about 1% of the rock constituents. It varies in size from 0.05 to 0.15 mm, generally exhibiting the euhedral rhombic section, but grain aggregates, sometimes elongate parallel to shear planes, are also common. Normally associated with biotite, mainly close to shear zones (Fig.IV.7a)

Epidote: characteristically as a product of alteration of other minerals. Commonly associated with biotites and saussuritized plagioclases. Sometimes it forms coronas in plagioclase crystals. It is also seen in fractures which cross-cut the rock. It varies in size from 0.27 to 0.75 mm (Fig.IV.7.b)

Chlorite: very common as a product of alteration of biotite in shear zones (Fig.IV.6.b)

Muscovite: extremely rare. It occurs as very small flakes (0.07 mm) within plagioclase crystals or in contact with biotite.

Carbonate: it can be found between plagioclase crystals in zones in which granulation took place or within some more altered plagioclases.

Opaques: they occur as very small grains (about 0.08mm) mainly associated with biotite. Sometimes enclosed in plagioclases in zones in which the latter have been remobilized by strain. Very common as elongate crystals parallel to shear planes.

Apatite: it occurs as rare, very small prismatic crystals sometimes showing a perfect hexagon-shaped basal section. Normally enclosed in plagioclase, but also in biotite or chlorite.

Zircon: it is found as inclusions in biotite or plagioclase. The crystals are, generally, very small but may reach 0.36 mm in length. When occurring as inclusions in biotite, normally, they give rise to the formation of pleochroic haloes.

IV.2.4.3 Trondhjemite

a) General characteristics

These rocks occur as sheets concordant with the dominant foliation and display pinch-and-swell features. They are banded rocks, composed of biotite-rich layers a few centimeters thick alternating with quartzofeldspathic bands several centimeters thick. The banding is irregular both in thickness and in the form of the bands along the sheets. The texture varies from fine to medium-grained in the mafic bands to very coarse in the leucocratic ones. As a rule, quartz is always seen in the neck zones of the pinch-and-swell structures (Fig.VII.43b). The presence of secondary foliations cross-cutting the dominant one is quite obvious as marked by dimensionally oriented biotite flakes. Carbonate is seen filling thin fractures and disseminated in the groundmass, as well (Fig.VII.46b)

Under the microscope the general texture is granoblastic but its heterogeneity indicates that the rock has undergone strong dynamic metamorphism. In many places small new crystals of quartz are developed both between quartz and quartz and between quartz and plagioclase. Strips of granular quartz can be seen between plagioclases or between granoblastic aggregate of quartz and plagioclase. As a rule quartz crystals display undulose optical extinction and is quite common what seems to be a single ribbon-like crystal, under plane-polarized light, appears as an aggregate of small crystals when nicols are crossed. In the contact with these rock-sheets the host gneiss concentrating higher strains was intensively mylonitized (Fig.IV.8.a)

b) Mineralogy

Plagioclase - Oligoclase (An_{26-30}) represents an early type of plagioclase in these rocks. The size varies from 0.54 up to 5.6 mm. The crystals normally exhibit irregular forms on account of the lobate-type of contact with other crystals, mainly with quartz. Some crystals are completely saussuritized, while other displaying some zoning are altered to sericite only in the core. Some exhibit twin planes disturbed by deformation. Carbonate, biotite, muscovite, quartz, apatite, zircon and some epidote are seen as inclusions. In places some crystals are cut by fractures filled with quartz, epidote and an untwinned feldspar which may be potash-feldspar.

Albite occurs in xenoblastic crystals ranging in size from 0.45 to 2.5 mm. The biggest (ribbon) crystals are seen in cataclastic bands together with quartz. Under crossed nicols it shows yellow colour of birefringence. The crystals are very limpid with irregular contacts with the other minerals. Its inclusions are represented by apatite (about 0.03 mm), altered plagioclases and biotite altered to chlorite.

Quartz - Varies in size from 0.54 up to 2.6 mm. Granulated, exhibiting undulose optical extinction and, sometimes, small 2V. Always xenoblastic, with lobate-type contact with other minerals, mainly albite and oligoclase. Under crossed nicols shows a birefringence colour in the range of grey to dark grey, what allow it to be discriminate in relation to untwinned limpid albite crystals. The presence of fractures is common. Apatite, very small bubbles and biotite are present as inclusions. Biotite is more common in zones affected by cataclasis.

Accessories - Chlorite, muscovite, epidote, carbonate, apatite, zircon and rare pyrite.

IV.2.5 Granitoid suite

IV.2.5.1 Granodiorite

a) General characteristics

On a fresh surface these rocks are light grey in colour and are fine to medium-grained. In places they show either a prominent foliation or a strong fracturing relating several directions of shear planes. In handspecimens the major constituents, quartz, feldspar and biotite, can be distinguished. The dissemination of pyrite in the groundmass is very conspicuous, as well.

Under the microscope, depending on the provenance of the samples, the textures can be granoblastic or cataclastic. Nevertheless, even the most granoblastic specimens show mortar texture between large crystals of plagioclase. The cataclastic textures, however, are by far the most common. In those places in which dynamic metamorphism acted more strongly there is a change from slightly foliated granodiorite to a well foliated granitic gneiss. The dominant mylonitic banding can be seen crenulated by younger shear planes.

b) Mineralogy

Quartz - It is extremely variable in shape and its grain size varies from 0.8 up to 2.5 mm. Invariably it shows undulose extinction,and sutured boundaries are very common. Between crystals of quartz or plagioclase, quartz can be be seen forming a mortar texture. Strips of granular or ribbon-shaped crystals can be seen between granoblastic aggregate of quartz and feldspars. In these bands of crystal aggregates quartz is most commonly seen as lensoid grains. Some crystals show a small angle 2V. Aligned, small bubbles can be seen within some quartz grains.

Plagioclase - The plagioclase is either oligoclase (An_{24-29}) or albite. Oligoclase is normally zoned displaying a more altered core in relation to the outer zones. This alteration, which decreases towards the crystal margins, is represented by saussuritization. It commonly forms porphyroclasts which contrast with the surrounding granoblastic aggregates of quartz and plagioclase making up the bands generated by granulation of the older rock texture (Fig. IV.8.b). In places, a foliation marked by biotite is seen wrapped around these porphyroclasts which sometimes exhibit a rounded shape, on account of the granulation of the corners of the original hypidimorphic crystals during rotation. Sometimes, oligoclase crystals show undulose extinction and evidence of lattice dislocations. (Fig.IV.9.a). In the less cataclastic rocks plagioclase commonly displays lobate boundaries which appear to have developed by this partial replacement by the surrounding crystals of quartz and microcline. The presence of myrmekites in the zones of contact between plagioclase and microcline is not uncommon.

Albite occurs as xenoblastic crystals sometimes forming ribbons parallel to the shear planes. In places it can be seen filling fractures cutting-across different minerals in the groundmass.

K-Feldspar - The dominant potash-feldspar is microcline. It varies in size from 0.4 to 1.9 mm. The largest crystals are elongate parallel to the shear planes. Usually it occurs as marginal or intergranular patches, displaying lobate boundaries. Its most characteristic feature, however, is to occur replacing plagioclase, which sometimes can be seen as inclusions in its interior. Some crystals appear to be, in turn, the result of replacement after orthoclase and show perthites.

Biotite - Occurs normally represented by small flakes, varying in size from 0.2 to 0.55 mm. Its pleochroism depends upon the degree of alteration to chlorite, but the fresh-looking crystals are brownish yellow to dark brown. The alteration to chlorite is very common even in the rocks showing the least effects of deformation by shear. When altered to chlorite the pleochroism is pale green to brown. Biotite is seen forming a foliation which parallels the most prominent mylonitic banding and is also dimensionally oriented parallel to shear cleavages that cross-cut and deform the former. It also alters to muscovite and sphene in some places. Some crystals show pleochroic haloes due to the inclusion of zircon.

Accessories - Muscovite is seen varying in size from 0.20 to 0.75 mm. It appears to have been formed as a primary constituent of the original igneous rock, apart from the typically secondary origin as an alteration product of biotite. It can be seen in equilibrium with the surrounding minerals or displaying lobate boundaries when in contact with plagioclase. Its presence within crystals of oligoclase is more pronounced when the plagioclase is more altered.

Epidote occurs associated with biotite or within crystals of plagioclase, mainly in zones more affected by shearing.

Carbonate occurs either as a product of alteration within plagioclase or forming veins parallel to shear planes.

Apatite is a common accessory mineral, occurring as very small (0.02 to 0.04 mm) prisms within plagioclase, potash feldspar, quartz or albite.

Zircon is not very common, being restricted to small inclusions in some biotites.

Garnet is very rare and locally developed as idioblastic

pink crystals (Fig.IV.9.b)
Opaques are of restricted occurrence and represented by small crystals of pyrite disseminated in the groundmass.

IV.2.5.2 Adamellite

a) General characteristics

These are light grey, fine to medium-grained rocks. In places rare phenocrysts of plagioclase, up to 1 cm long, can be seen. In handspecimens, quartz, plagioclase, biotite, muscovite, pyrite and carbonate can be identified. Carbonate occurs either disseminated in the groundmass or filling very fine fractures. The biotite flakes, which are very small and make up a low percentage in the mineral composition, show ill-defined different preferential orientation.

Under the microscope the general aspect of the texture is granuloblastic but the most striking feature is the pronounced effect of dynamic metamorphism (Fig.IV.10.a). This effect is represented by an intense granulation with development of mortar textures. In the whole there is a textural heterogeneity due to the presence of a variety of grain sizes, grain boundary types and grain shapes.

b) Mineralogy

Quartz - The crystals range in size from 0.55 to 2.4 mm and show marked undulose extinction. The boundaries between quartz crystals have a distinct sutured form. In many places, new crystals are developed both between quartz and quartz and between quartz and feldspar. The small grains are not set strained as the large ones, and often make up a mosaic texture. In places, quartz forms a band of granulated crystals between plagioclase porphyroclasts and a granoblastic aggregate of quartz and potash feldspar. The presence in different samples of quartz aggregates displaying undulose extinction, with no clear separation between the different individuals and quartz forming a mosaic texture with distinct separate grains, indicates that apart from granulation, annealing took place as deformation proceeded.

K-Feldspar - The potash feldspar is represented by orthoclase perthite and microcline. The microcline exhibits low triclinicity and is clearly recrystallized after orthoclase. It is very common the presence of orthoclase perthite partially replaced by microcline (Fig.IV.10.b)

Plagioclase - There are two types of plagioclase, namely (1) highly saussuritized twinned crystals of andesine (An_{34}) and, (2) fresh xenomorphic grains of untwinned albite. Andesine commonly displays deformed or spindle-like twinning lamellae. In places, there are porphyroclasts of andesine displaying very irregular outlines (lobate boundaries) due to partial replacement by albite, quartz or microcline. When microcline is involved in this phenomenon of partial replacement, the generation of myrmekites is very common. Another common feature associated with andesine is its alteration to epidote minerals.

Biotite - The biotite flakes are in general very small, with an average size about 0.27 mm. Fresh crystals are rare, and show pleochroism in brownish red to red. Normally it is altered to chlorite.

Accessories - Muscovite is normally seen in all the studied samples, but always in very small amounts. The size of the crystals ranges from 0.10 to 0.63 mm. It occurs within plagioclase or along small fractures. In places it results from alteration of biotite.
Chlorite is a very common alteration product of biotite and sometimes show a greenish pleochroism.

Epidote constitutes a prominent product of alteration of plagioclase together with sericite and is also associated with biotite.

Apatite occurs as very small prismatic crystals (average size is about 0.07 mm) normally within plagioclase or quartz, and less commonly in K-feldspar.

Carbonate is also an alteration product seen in plagioclase crystals, but sometimes is found filling very thin fractures.

IV.2.5.3 Rhyolite

This rock forms a dyke which cuts across the dominant foliation of the host rock at high angle. It is reddish in colour and displays a prominent banding, marked by alternating thin bands varying in both colour intensity and texture. The general texture is porphyritic with quartz phenocrysts dispersed in an aphanitic matrix.

Under the microscope it can be seen that apart from the most easily discernible quartz phenocrysts, in handspecimens, there are phenocrysts of very altered plagioclase, K-feldspar and some rare biotite flakes. The matrix is formed by a devitrified cryptocrystalline brownish material. Dispersed in the matrix there are some vesicles filled either with intergrowths of quartz and K-feldspar or with quartz (Fig.IV.11.a)

The quartz phenocrysts are, normally, very embayed, but still present the bipyramidal habit characteristic of the original high-temperature form (Fig.IV.11.b)

The plagioclase and K-feldspar occur as euhedral laths dimensionally oriented parallel to the banding of the rock (Fig.IV.12.a) whereas the best developed biotite flakes are positioned at an angle with regard to that orientation. The smaller and most altered (to muscovite) biotite flakes are, however, oriented parallel to the banding, as well.

Both K-feldspar and plagioclases are very altered, but some crystals still display a noticeable Carlsbad-twinning which allow to consider them as being represented by sanidine. In places carbonate is seen dispersed in the matrix.

The banding can be interpreted as due to differential flow during the emplacement of the magma, and is marked by alternating bands of different grain size making up the matrix together with,the referred to above,differences in colour shades.

IV.2.5.4.Pegmatites

Occur as veins of variable thickness from a few centimeters to about 1 meter. Their texture is also variable from homogeneous very coarse-grained to typically porphyritic. The general composition is granitic with quartz, feldspar and biotite readily recognisable.

Under the microscope two different types of pegmatites are identified: one type is characterized by the presence of orthoclase perthite, while the other shows limpid crystals of microline. It appears, therefore, that orthoclase was replaced by microcline.

K-feldspar is the porphyritic constituent of the rock. Quartz, plagioclase and biotite are found as smaller crystals then the K-feldspars, making up aggregates in the interstices of the phenocrysts. These are commonly fractured and mortar texture is a very frequent feature along the contacts between two crystals. In these granulated zones the granoblastic material is formed by aggregates of small, strained quartz crystals and altered plagioclase.

Orthoclase is often seen replacing plagioclase which in places appears as isolated grains displaying optical continuity, within the former (Fig.IV.12.b). Along the boundaries between K-feldspar and plagioclase development of myrmekites is a very common feature (Fig.IV.13.1)

Plagioclase is normally altered to sericite and, occasionally to epidote. This is a great difference with regard the K-feldspars which are, in general fresh-looking. Some crystals less altered and with twin-lamellae not distorted were determined as oligoclase (An_{10-16}).

Quartz is represented either by xenomorphic grains exhibiting undulose extinction or by aggregates of small strained crystals. The large xenomorphic grains are often seen replacing both potash feldspars and plagioclase (Fig.13.b).

Biotite is seen as short and wide flakes with pleochroism in brownish yellow to dark brown. Sometimes is altered to chlorite and in such cases shows pleochroism in brownish yellow to green. Some crystals show several inclusions of apatite.

Hornblende is found occasionally as remnants of altered green crystals displaying lobate boundaries with plagioclase.

Opaques are very rare and found as small inclusions in plagioclase and biotite.

It is difficult to define a representative modal composition for the pegmatites, in general, on account of the textural variations referred to above. A modal composition which can be considered as a representative average of their granitic character is shown in Table I.

TABLE I. MODAL COMPOSITION (%) OF THE DIFFERENT ROCK UNITS MAKING UP THE VILA NOVA COMPLEX

	I		II		III			IV	V			VI		VII
	Ia	Ib	IIa	IIb	IIIa	IIIb	IIIc		Va	Vb	Vc	VIa	VIb	
Quartz	15	5	15	25	Tr			75		15	30	20	25	15
Plagioclase	45	40	60	50	30	10	40	15	48	73	65	35	35	10
K-Feldspar				10				9			3	15	34	60
Biotite	35	15	20	10	25	9	15	1		10		5	3	15
Hornblende		35			40	80	35		50					
Epidote					5	1	5	Tr	Tr				1	
Sphene								Tr						
Opaques								2						
Carbonate														
Accessories	5	5	5	5			5			2	2	5	2	

I -Dioritic gneisses
Ia -Biotite gneiss
Ib -Hornblende-biotite-gneiss
II -Granitic gneisses
IIa-Tonalitic gneiss
IIb-Granodioritic gneiss
III-Amphibolite
IIIa-Fine-grained concordant amphibolite
IIIb-Coarse-grained concordant amphibolite
IIIc-Discordant amphibolite
IV -Quartzites
V -Gabbro-tonalite-trondhjemite suite
Va -Gabbro
Vb -Tonalite
Vc -Trondhjemite
VI -Granitoid suite
VIa -Granodiorite
VIb -Adamellite
VII -Pegmatites
Tr -Traces

FIGURES IV.1 TO IV.13

Figure IV. 1.a. Handspecimen of quartzofeldspathic dioritic gneiss showing the dominant foliation parallel to a prominent banding.

Figure IV.1.b Handspecimen of quartzofeldspathic dioritic gneiss showing the dominant foliation and the contact between a medium-grained band with predominance of quartz and plagioclase and a fine-grained hornblende-rich band.

a

b

Figure IV.2.a Photomicrograph of quartzofeldspathic dioritic gneiss (biotite-gneiss) showing the dominant foliation (S_1) marked by the orientation of biotite flakes and aggregates of quartz and feldspar; subarea IV (XN, X 10).

Figure IV.2.b Photomicrograph of quartzofeldspathic dioritic gneiss (biotite-gneiss) showing an idioblastic crystal of garnet with quartz inclusions; subarea I, northern part (OL, X 10).

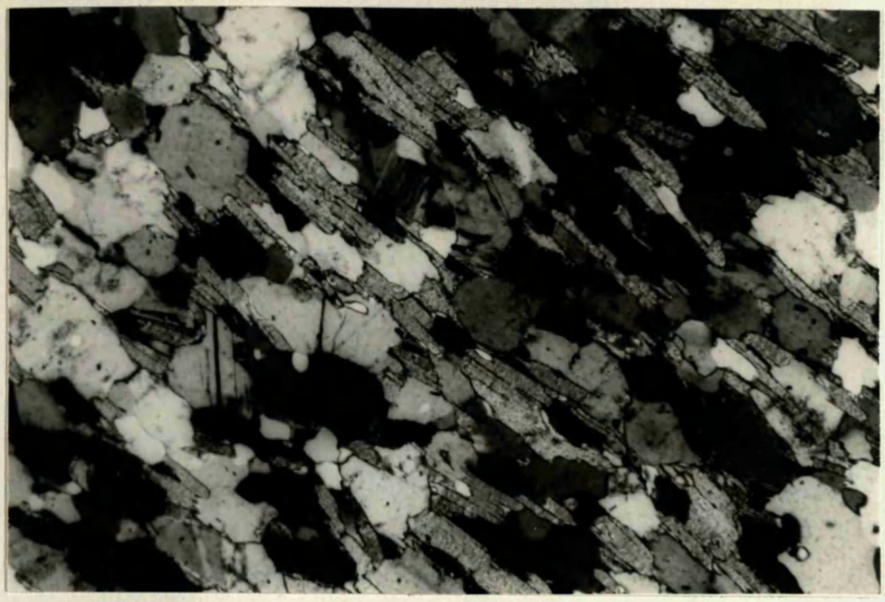

a

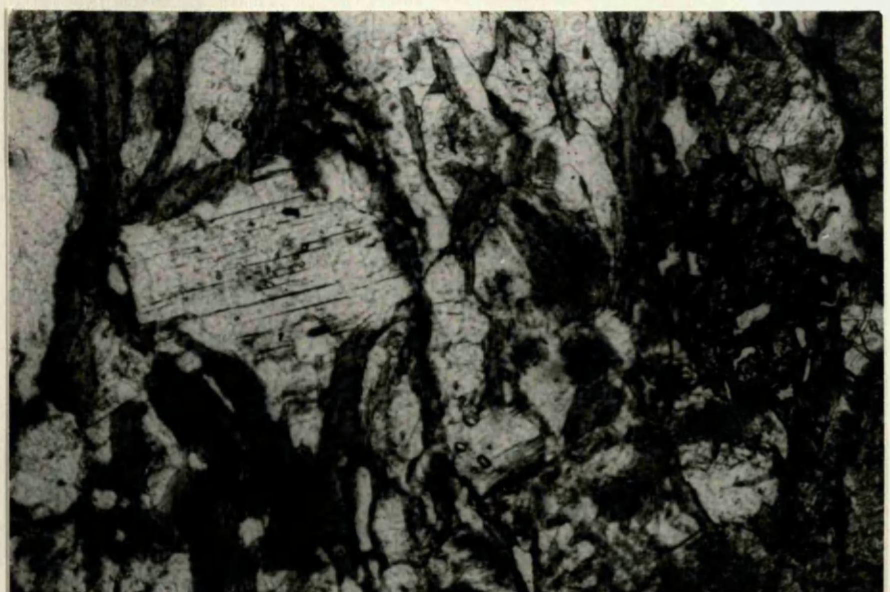

b

Figure IV.3.a. Photomicrograph of quartzofeldspathic dioritic gneiss (biotite-gneiss) showing recrystallization of quartz in zones of pressure shadows associated with a crystal of garnet; subarea I, northern part (XN, X 40).

Figure IV.3.b Photomicrograph of quartzofeldspathic dioritic gneiss (hornblende-biotite-gneiss) showing the dominent foliation (S_1) marked by the alingnment of mafic minerals together with hipidioblastic to xenoblastic plagioclase grains; subarea IV (XN, X 25).

a

b

Figure IV.4.a. Photomicrograph of a coarse-grained concordant amphibolite showing twin lamellae in a hornblende crystal off-set by shear planes; biotite growth took place; subarea I, southern end (XN,X 10).

Figure IV.4.b. Photomicrograph of a coarse-grained, concordant amphibolite, showing mosaic texture developed in an aggregate of plagioclase grains; subarea I, southern end (XN, X 10).

a

b

Figure IV.5.a Photomicrograph of a coarse-grained concordant amphibolite, showing an opaque crystal (ilmenite?) surrounded by grains of sphene; subarea I, southern end (XN, X 25).

Figure IV.5.b Photomicrograph of a quartzite showing mylonitic banding. Note between ribbon-like grains of quartz, aggregates of small grains with irregular boundaries parallel to the dominant fabric of the rock (S_1). Some rare oriented biotite flakes are also seen; subarea II, middle part (XN, X 10).

a

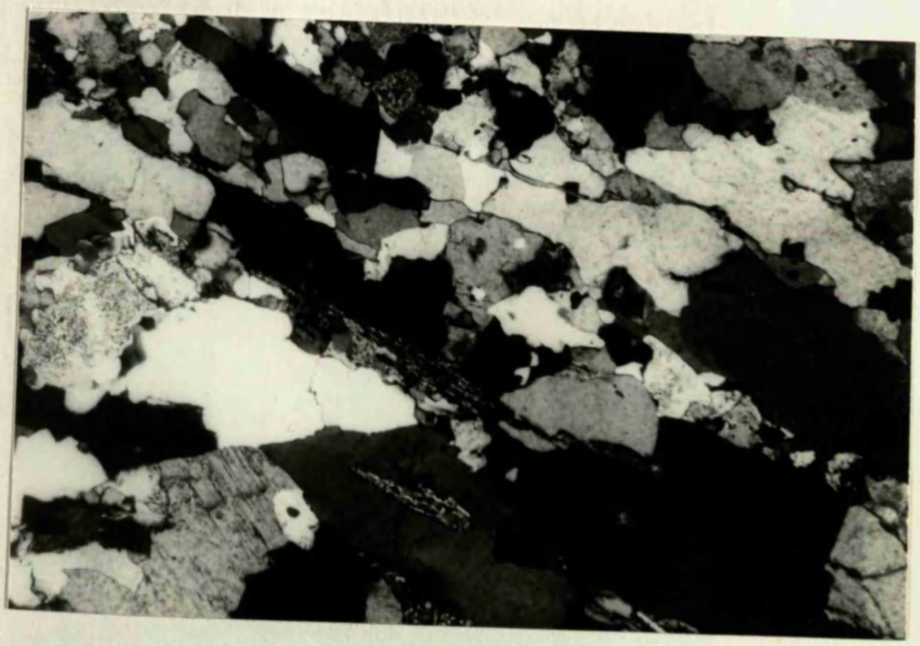

b

Figure IV.6.a. Photomicrograph of a gabbro showing laths of plagioclase enclosed in a matrix of hornblende altered to a mixture of fibrous amphibole (actinolite) and chlorite; subarea IIIb (XN, X 10).

Figure IV.6.b Photomicrograph of a sheared tonalite showing shadowed quartz aggregates and deformed chlorite (after biotite); subarea IV (XN, X 10).

a

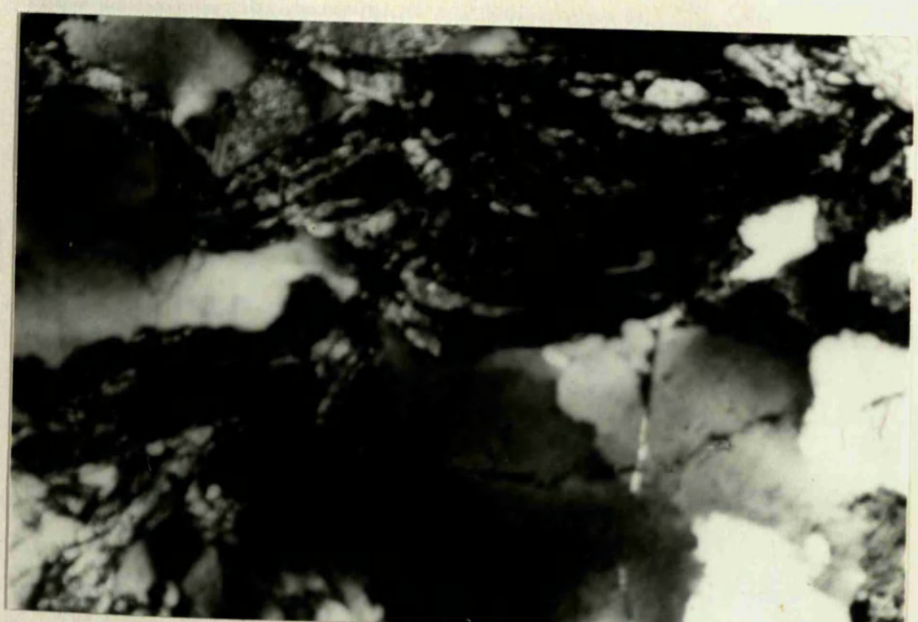

b

Figure IV.7.a Photomicrograph of a tonalite showing plagioclase replacing biotite and displaying inclusions of oriented grains of sphene which resulted from alteration of the biotite; subarea IV. (OL, X 10).

Figure IV. 7.b Photomicrograph of a tonalite showing a crystal of plagioclase (in extinction) surrounded by a corona of epidote; subarea IV (XN, X 25).

a

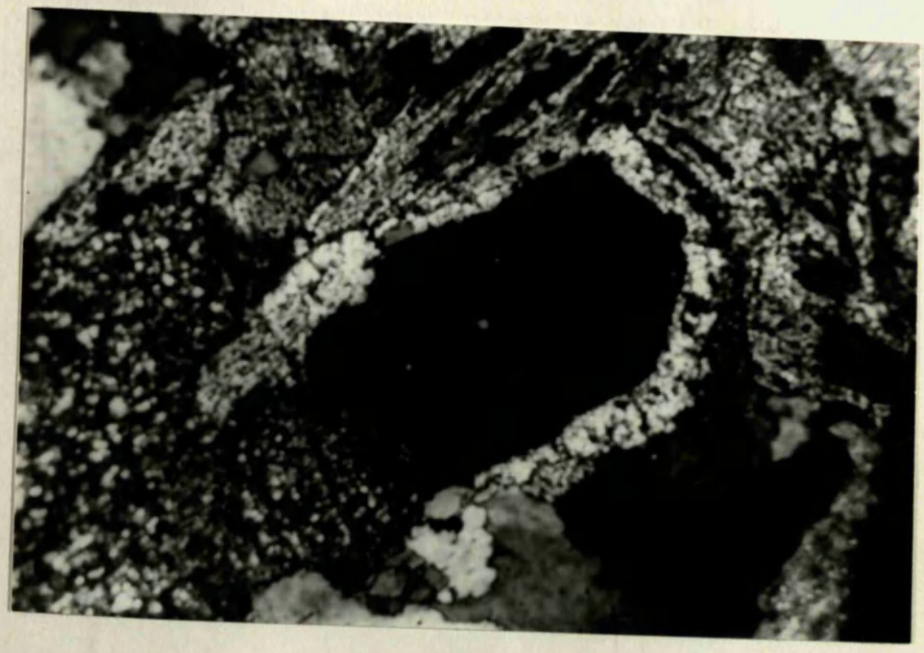

b

Figure IV.8.a Photomicrograph showing the contact zone of a trondhjemite sheet (granuloblastic texture) with the host quartzofeldspathic gneiss which displays an oriented fabric parallel to the contact zone; subarea IV (XN, X 10).

Figure IV.8.b Photomicrograph of a cataclastic granodiorite showing a zoned plagioclase porphyroclast displaying evidence of having undergone rotation under the influence of a sinistral shear displacement; subarea I, middle part (XN, X 10).

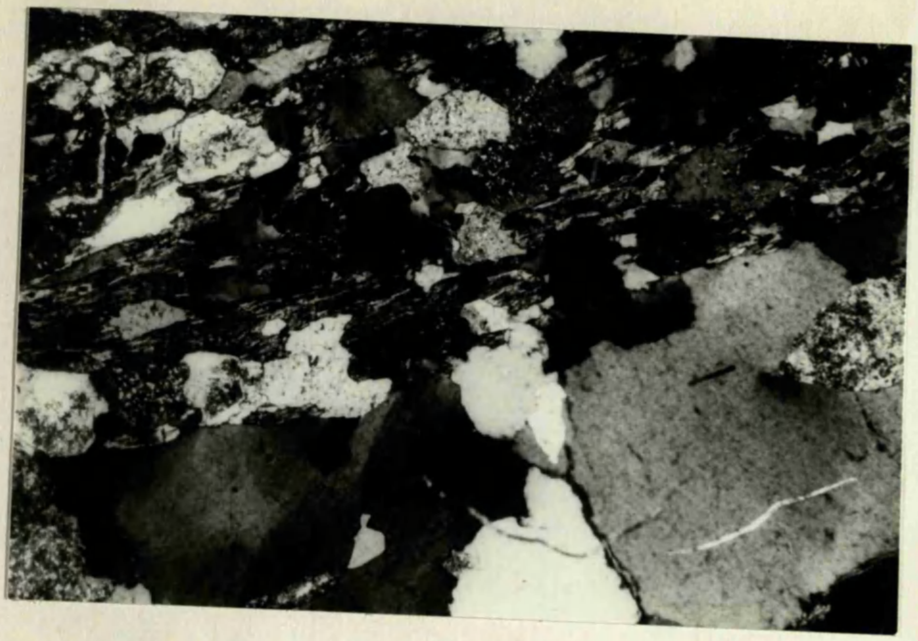

a

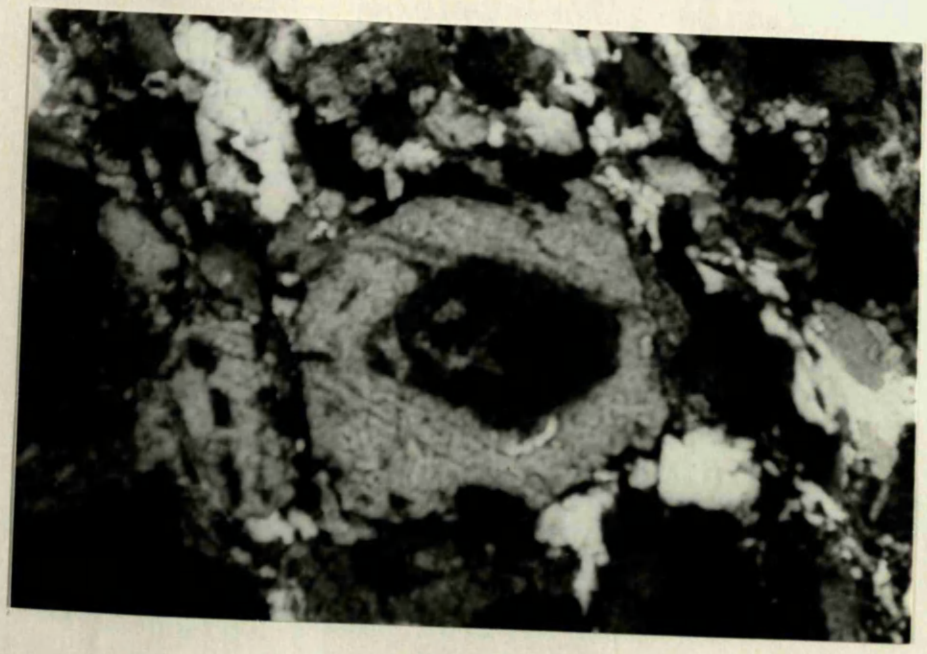

b

Figure IV.9.a. Photomicrograph of a granodiorite showing dislocations features in a strained plagioclase crystal; subarea IV (XN, X 10).

Figure IV.9.b Photomicrograph showing the presence of an idioblastic crystal of garnet in grandiorite; subarea I, middle part (OL, X 10).

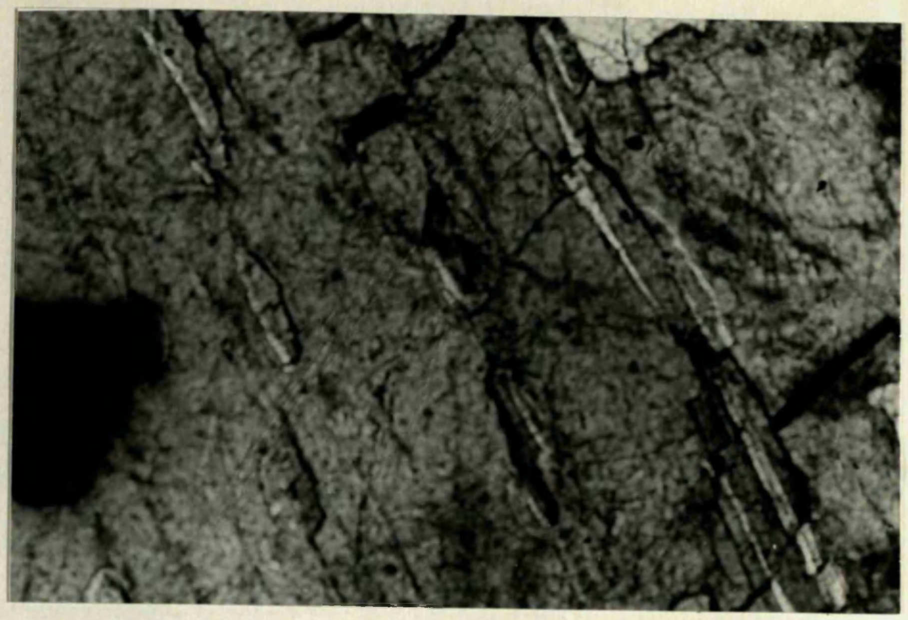

(a)

(b)

Figure IV.10.a Photomicrograph showing microline porphyroclast with sutured boundaries in mylonitic banding in an occurrence of adamellites; subarea IIIc (XN, X 10).

Figure IV.10.b Photomicrograph showing microcline replacing orthoclase perthite in adamellite; subarea IIIb (XN, X 10).

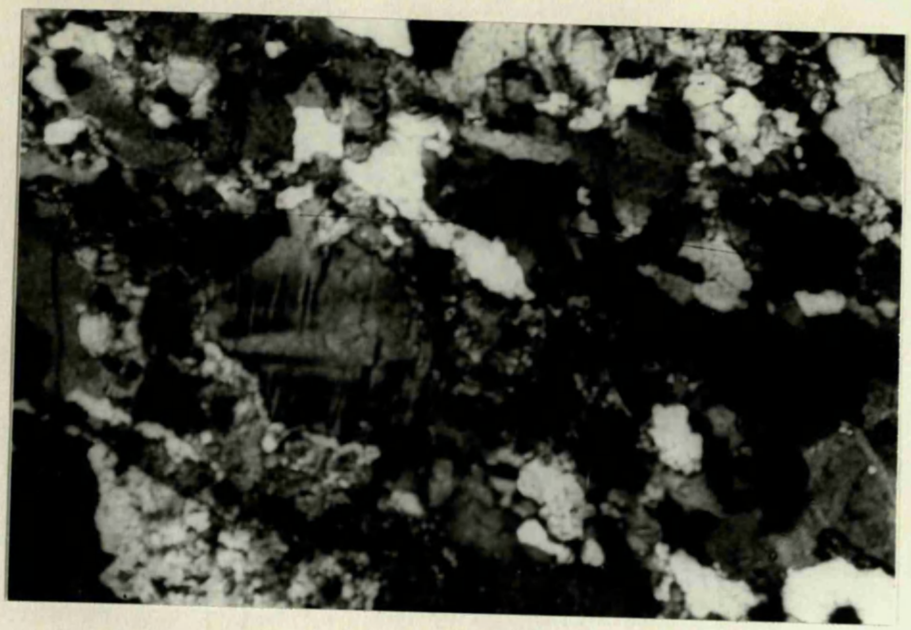

a

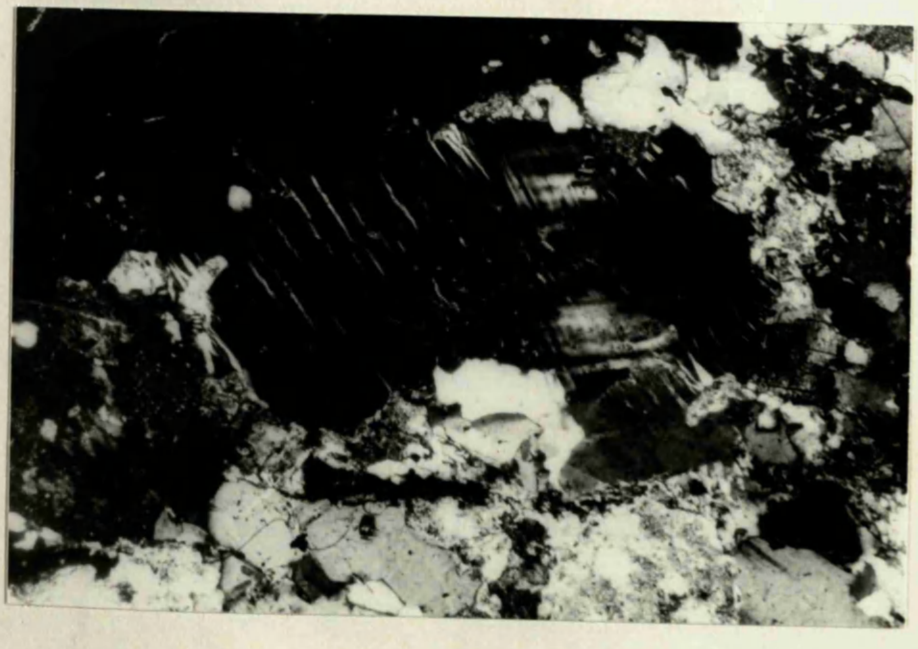

b

Figure IV.11.a	Photomicrograph showing intergrowth of quartz and K-feldspar in a vesicle in rhyolite; subarea IIIb (XN, X 31).
Figure IV.11.b	Photomicrograph showing bipyramidal embayed quartz in rhyolite; subarea IIIb (XN, X 40).

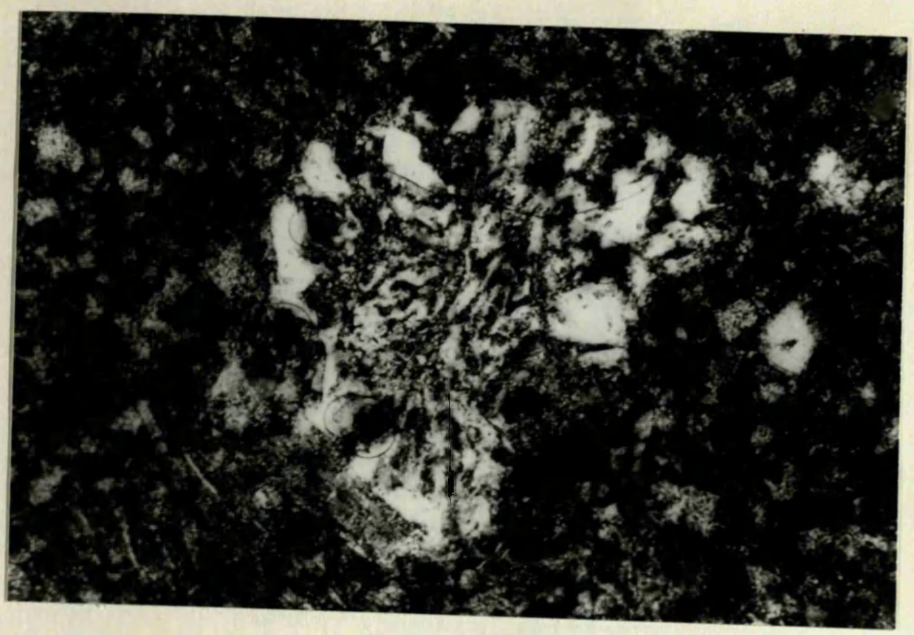

a

b

Figure IV.12.a Photomicrograph showing K-feldspar laths oriented parallel to the flow banding in rhyolite; subarea IIIb (XN, X 31).

Figure IV.12.b Photomicrograph showing corrosion of plagioclase by orthoclase in granitic pegmatite. The isolated fragment of plagioclase within the orthoclase has maintained its optical continuity in relation to the rest of the crystal; subarea II, southern end (XN, X 40).

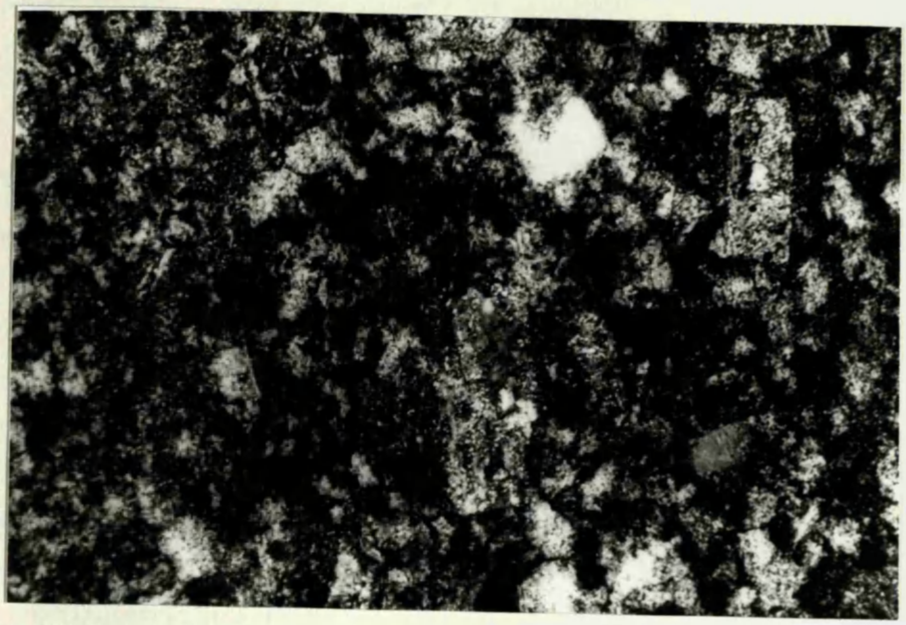

(a)

(b)

Figure IV.13.a Photomicrograph showing myrekite development in the contact between orthoclase perthite and plagioclase in granitic pegmatite; subarea II, southern part (XN, X 25).

Figure IV.13.b Photomicrograph showing xenoblastic quartz displaying irregular contact with plagioclase in granitic pegmatite; subarea II, southern end (XN, X 10).

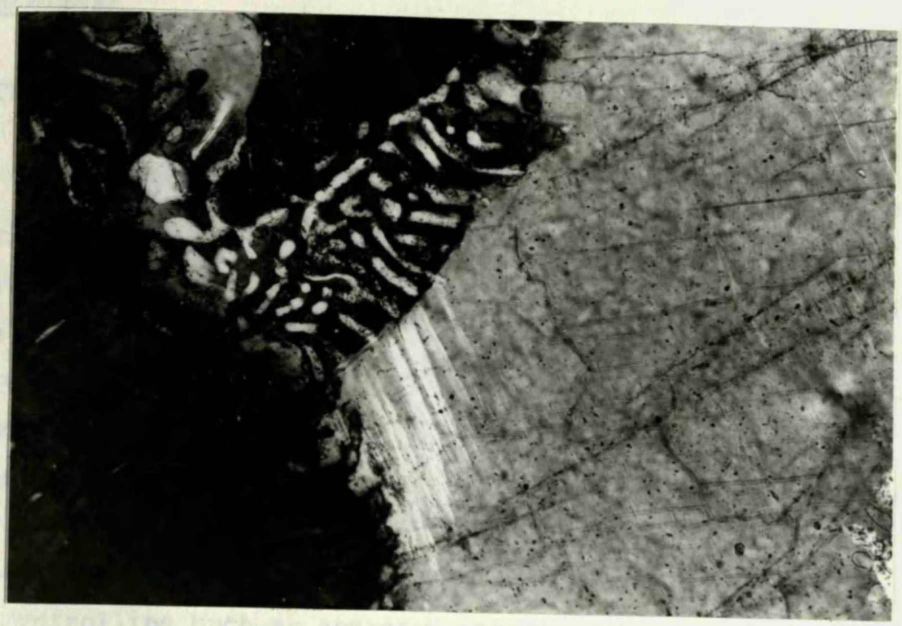

a

b

V. GEOCHEMISTRY

V.1. INTRODUCTION

The chemistry of the rocks of the Vila Nova Complex was investigated in order to throw light on their origin. Interpretation is, however, problematical because of the relatively small size of the area investigated, the limited availability of outcrops, which are mostly small occurrences along the Cambai River valley, and the general absence of exposed spatial relationships between the different rock-types. Hence, the criterion upon which this study was based consisted in the selection of the rock-units whose field relationships are the most unambiguous. A very strong factor in controlling such an approach was the relationships of rock units with well understood structural features. On these grounds, subarea IV which can be considered as having provided the basis for the setting out of the structural sequence, on account of well exposed deformational features which can be timed due to different phases of igneous intrusions, was selected as being the most favourable for petrogenetic interpretations. In this subarea there is a sequence of amphibolitic rocks which grades to leucocratic, banded quartzofeldspathic gneisses, through transitional members represented by hornblende-biotite and biotite-gneisses. This rock-sequence (named broadly as dioritic gneisses) was intruded by concordant to subconcordant (in relation to the dominant foliation) tonalitic-trondhjemitic sheets, a minor dioritic body and either concordant or discordant granodiorite veins. The discordant granodiorite veins, which are pegmatitic in some places, are readily seen as the youngest intrusive materials in this subarea.

The gneissic sequence which constitutes the host rocks for the intrusive masses display evidence relating the first deformational phase and the geochemical study which follows is mainly concerned with it and the associated igneous intrusions.

V.2 ANALYTICAL METHODS

The determination of Al_2O_3, Fe_2O_3, K_2O, Na_2O and MgO was carried out by atomic absorption spectrometry; FeO was determined by the method of titration with potassium-dichromate; SiO_2, P_2O_5 and TiO_2 were determined by using the conventional method of colorimetry. Volatile contents were determined by measuring loss on ignition. This work was carried out at the Department of Geology of the Federal University of the State of Rio Grande do Sul, Brazil.

Trace element analysis were carried out at the Department of Geology of the University of Glasgow, by running pelletized rock powders in a Philips fully automatic XRF spectrometer.

V.3. CHEMICAL DATA

Tables II to VII show the chemical analyses in terms of major and trace elements, as well as the corresponding normative compositions and Niggli numbers for the rock-sequence of subarea IV, apart from one amphibolite (RPH-57)from subarea II (southern end) and two granitic gneisses, AL-7 and C-1, from subareas IIIc and I (middle part), respectively.

In general the major elements give a continuous trend from the most basic to the most acidic types, whether using SiO_2 (Fig. V.1) or Kuno's solidification index (S.I; Fig.V.2) as fractionation indexes.

The analyses span a considerable range of composition with SiO_2 ranging from 49 to 76%. There is a fairly continuous range of dioritic gneisses with SiO_2between 52 and 62% and a very continuous range of intrusive rocks with SiO_2 between 63 and 74%. The most basic rock-types are represented by amphibolites.

Fe,Mg, Ca and Ti show a consistent negative correlation with both SI and SiO_2, for every different rock unit. K_2O shows a very interesting behaviour; for SiO_2 contents above 70% two trends occur: one with decreasing K_2O is given by the trondhjemites, while the other, with increasing K_2O, is given by the granitoids.

The S.I plot shows two features, (1) there is a constant "step" in the trend lines of the different oxides plotted, at S.I = 10, and (2) the points representing the diorites plot above the general trend line.

The trondhjemites have less than 15% Al_2O_3 and therefore can be classified as low Al_2O_3-type, according to Barker et al. (1976). Their CaO contents are high, ranging from 3.10 to 3.92%, while the average K_2O content (1.33%) is consistent with the composition of primary trondhjemites (Barker & Millard, 1979). Most of the trondhjemites, and many of the associated tonalites, are corundum normative, irrespective if they are of low or high Al_2O_3 type.

On the basis of major-element contents it can be concluded that the trondhjemites differ markedly from the tonalites in having higher Si and lower Mg and Ca. Some tonalites exhibit trondhjemitic affinities as shown in figure V.6.

With respect to trace-element analyses, when plots are carried out using SiO_2 as a differentiation index, it is apparent that Co, Pb, Zn and, to a less extent, Ga present a good correlation with that oxide (Fig. V.3). Other elements such as Zr, Cr, Ni, Th, U, Ce and Nb vary both within and between compositional groups, with no clear correlations.

The trondhjemites have relatively low Ba and high Sr, in contrast to the granitoids which have high Ba and low Sr abundances. The Sr abundances of the dioritic gneisses, tonalites and trondhjemites is approximately the same (about 500 ppm). Like Ba, Rb is low in the trondhjemites, moderate in the tonalites and high in the granitoids. Generally, tonalites and trondhjemites have similar K/Rb ratios (300-400) while the granitoids show a large variation from about 350 to more than 700 (Fig. V.4). The tonalites, however, differ from the trondhjemites in having, in general, higher Rb/Sr, Ba/Rb and Ba/Sr ratios. The low Rb/Sr ratios of some tonalites are, however, typical of trondhjemitic rocks (Barker et al., 1979: Peterman, 1979 in Arth & Millard, 1979).

The tonalites are slightly enriched in both, light and heavy rare earth elements (LREE and HREE, respectively) relatively to the trondhjemites. In general terms, the whole tonalite-trondhjemite suite shows highly fractionated petterns with La varying from 110 to 130 times chondrites and Y considered as representing the behaviour of HREE, since it behaves geochemically very much like Yb (cf. Cox et al., 1979) less than 6 times chondrites (Fig. V.14).

V.4 PETROGENESIS

V.4.1 Overall relationships

A classification of the igneous intrusive rocks based on the alkalis contents is given in figure V.5. In this figure the rocks plot along a linear trend from tonalites-trondhjemites to rhyolites and pegmatites evidencing a well marked negative correlation between Na and K. On the basis of mutual relationships seen in the field between differnt intrusive masses it is suggested that this negative correlation between Na and K is time related. A normative plot of Ab-An-Or (Fig. V.6)shows that the intrusive rocks are, basically represented by a tonalite-trondhjemite suite and granites.

On a AFM diagram the intrusive rock-sequence lies along a typical calc-alkaline trend and the tonalitic-trondhjemitic rocks closely fit the gabbro-trondhjemite trend line established by Barker & Arth (1976) for the trondhjemitic suite of SW Findland (Fig. V.7).

A K-Na-Ca diagram (Fig. V.8) shows that the whole intrusive sequence differs from the "normal" calc-alkaline trend (cf. Nockolds & Allan, 1953) but has a close resemblance with the gabbro-trondhjemite trend of the suite of SW Finland (Barker & Arth, 1976). However, the rocks of the Vila Nova region differ from the Finnish suite in having Lower K levels.

This tendency to follow a gabbro-trondhjemite trend is also shown on a normative Q-Ab-Or diagram (Fig.V.9).

It is apparent fromfigures V.8 and V.9 that the dioritic trondhjemitic rocks of the Vila Nova region follow a trondhjemitic calc-clkaline trend. In fact, it is brought out clearly by figure V.8 that such rocks follow a K-rich calc-alkaline trend.

V.4.2. Quartzofeldspathic gneisses

V.4.2.1 Dioritic gneisses

The origin of the dioritic gneisses is considered first since these rocks display the earliest-recognized folds (F_1).

As evidenced in figure V.1. these gneisses make up a continuous range of gneisses from very basic types (amphibolitic) to rocks about 63% SiO_2. Figure V.10 shows that these rocks plot within, or very close, to the andesite field of Church (1975). However, plots of Niggli (al-alk) against c (Fig. V.11) and c against mg (Fig.V.12) show clearly that these rocks, despite having compositions which chemically resemble intermediate igneous rocks, are actually metamorphosed pelite-dolomite mixtures.

The distribution of points in figure V.12 is consistent with the transition seen in the field, in subarea IV, from amphibolites to biotite-garnet-gneisses. The occurrence of marble layers to the north of subarea IV (Picada & Lowarsky, 1962) is also consistent with the original sedimentary sequence here established.

V.4.2.2. Granitic gneisses

These rocks constitute restricted occurrences as compared to the widespread occurrence of the sioritic gneisses. They are of two different types: one is stripped, very rich in thin quartzofeldspathic bands of neosome and the other is most homogeneous, with the appearance of a foliated granite. This latter type was found always very weathered so that samples were not collected for chemical analysis. However, its association with quartzitic layers with which they are interlayered displaying in places gradational features (subarea II, middle part) suggests they have a sedimentary origin.

The striped type varies in composition from tonalite to granodiorite (Fig. V.5) and in the Harker's variation diagram (Fig. V.1) they are seen associated with the dioritic gneisses normally in the transition zone with the area in which the tonalites plot.

This association with the dioritic gneisses is also seen in plots of Niggli (al-alk) against c and c against mg (Fig. V.11 and V.12). In figure V.11 these gneisses plot away from the trend line corresponding to granitic rocks and tend to the field of semi-pelites (cf. Evans & Leake, 1960). In figure V.12, sample C-1 plots very close to the field of pelitic materials while sample A /-7 plots similarly to the dioritic gneisses, along the trend-line corresponding to pelite-dolomite mixtures. Therefore, on the basis of these evidence, it is considered that these gneisses originated from sedimentary materials in which semi-pelite represented an important constituent.

V.4.3. Amphibolites

The amphibolites have been divided into (1) concordants and (2) discordants, in relation to the dominant gneissose banding. The condordant types can be further divided into two types, viz. (1) amphibolite layers associated with the dioritic gneisses and (2) amphibolite layers associated with granitic gneisses. The discordant amphibolites are represented by bodies cross-cutting the gneissose banding and have a composition which corresponds to andesites (Fig.V.10). These rocks are, therefore, interpreted as resulting from the metamorphism of dioritic minor intrusions.

The fine-grained concordant amphibolite, associated with quartzfeldspathic granite gneisses in subarea II (southern end) has a composition corresponding to basalt (Fig.V.10). However, on a Niggli c against mg diagram it plots away from the Karroo dolerites trend line (Evans & Leake, 1960) and is also considered as likely metamorphosed pelite-dolomite mixtures (Fig. V.12).

The coarse-grained concordant amphibolites, which in places are actually hornblendites, have not been chemically analysed due to the impossibility of collecting fresh samples, but their petrography suggests an igneous origin. They have characteristics of cumulate rocks associated with basic intrusions.

V.4.4. Gabbro-tonalite-trondhjemite suite

V.4.4.1 General

The elucidation of the origin of the gabbro-tonalite-trondhjemite suite appears to be of great significance for understanding the overall igneous activity of the area.

The most generally accepted ideas concerning the genesis of tonalitic-trondhjemitic suites are those related to a basaltic source (Arth, 1979). The opinions, however, diverge with respect to the mechanism leading to the final formation of such rocks, as they have been considered as originating by either partial melting or fractional crystallization (Barker et al, 1976; Barker & Arth, 1976; Barker, 1979; Arth, 1979).

Barker et al (1976) have suggested that low-Al_2O_3 trondhjemitic-tonalitic rocks are related to a process which left plagioclase as a residual phase in either partial melting or a fractional crystallization model. Low Sr with negative Eu anomalies are chemical features of some of these rocks that are consistent with plagioclase being a residual or fractionated phase in either process. The presence of plagioclase in the residue restricts the depth of magma generation to less than 60 km (Arth, 1979).

The high-Al_2O_3-type of tonalitic-trondhjemitic liquids form either by fractionation of wet basalt or by partial melting of a basaltic parent in a process in which little or no plagioclase remains in the residue.

Some workers (Hanson & Goldish, 1972; Arth & Hanson, 1975; Arth & Barker, 1976: Arth, 1979) have claimed that partial melting of amphibolites at less than 60km satisfactorily explains the genesis of some high-Al_2O_3 trondhjemitic rocks. The HREE depletion of such rocks was originally ascribed to the presence of garnet as a residual phase in the eclogitic residue resulting from melting at mantle depths. This opinion, however, evolved on the basis of studies of the partitioning of rare earths and Arth & Barker (1976) suggested that melting of amphibolite at less than 60 km depth could equally produce liquids depleted in HREE leaving hornblende as a residue, in much the same way as the model involving eclogite as a residual product at high-pressure conditions.

As referred to by Arth (1976) models relating to fractional crystallization for explaining the formation of high-Al_2O_3 trondhjemites have appeared long ago. In fact, Goldschmidt (1922) used such a model for explaining the origin of the suite of the Trondheim area, Norway, while Hietanen (1943) has tried the same approach in relation to the trondhjemitic rocks of S.W Finland.

The opinion of Goldschmidt (1922) and Hietanen (1943) that trondhjemitic-tonalitic magmas could be generated by differentiation of the wet basaltic liquid has been supported by isotopic and chemical studies of the rocks of the Uusikaupunki-Kalanti area, in Southern Finland, carried out by Barker & Arth (1976).

A characteristic feature of the suites from Norway and Finland is the association of rocks ranging from gabbro, through diorite, tonalite to trondhjemite.

Other hypothesis concerning the origin of soda-rich and trondhjemitic rocks include the metasomatic introduction of Na in older rocks, normally under the influence of water (Battey, 1956) and anatexis of graywackes during metamorphosis (Winkler, 1967; Cheney & Stewart, 1975).

Winkler (1967) concluded that tonalitic-trondhjemitic liquids may be derived by partial melting of K-poor graywacke at crustal levels. Lambert & Willie (1970), however, argued that to generate a melt of tonalitic composition at crustal levels is necessary a temperature very high (about $1000^{o}C$ for $P_{H2O} = P_{Total}$).

On the basis of what has been presented concerning the origin of trondhjemitic rocks some attemps can be made to try to fit the Vila Nova rocks into some general model.

V.4.4.2 Origin

The relatively low large ions lithophile (LIL) trace elements concentrations of the trondhjemites under investigation, apart from the typical intrusive characteristics they exhibit, rules out the possibility that these rocks have resulted from either metasomatic or anatectic processes.

A possibility relating the trondhjemitic sheets to vapour phase transport is again ruled out, for these rocks, as illustrated in figure V.13, closely related to the igneous trend shown by Holloway (1971) who has experimentally determined composition of silicate liquids and vapours in the basalt-H_2O-CO_2 system, as referred to by Payne & Strong (1979). Therefore, the most likely source for such rocks is a parent material of basaltic composition.

This conclusion is consistent with the accordance of the suite of dioritic rock-tonalites-trondhjemites with the trend of the gabbro-trandhjemite suite from Finland (Barker & Arth, 1976) Fig. V.9). However, such an accordance implies only a crystal-liquid equilibrium which can be due to either crystal fractionation or partial melting.

The relatively high K_2O content of the dioritic gneisses suggests that any tonalitic melt would be generated by partial melting of these rocks only if an early more potassic (adamellite) melt were first removed (Hanson & Goldish, 1972). Field evidence, however, clearly demonstrates that more potassic rocks are younger than the tonalitic suite, so that the possibility of the latter to represent melts of the dioritic gneisses cannot be accepted.

On the variation diagrams represented in figure V.3 and V.4 this suite shows a reasonable coherence, likely illustrating the course of chemical evolution of liquids, as manifested by clear liquid line-of-descent. However, as pointed out by Cox et al., (1979) a regular pattern of data points in a variation diagram does not prove the corresponding rocks are genetically related, despite the fact that a coherent trend may be compatible with such a relationship. Therefore, some additional information is needed in order to allow a more precise evaluation of the degree of relationship that exists between the different studied rocks. In addition, supporting what has been said above, concerning the origin of magmatic material it should be stressed that rock suites showing reasonable coherence simply illustrate the course of the chemical evolution of liquids which may have been formed by fractional crystallization or progressive partial melting.

As the liquid line-of-descent represents the chemical evolution of liquids it follows that it represents a relatively continuous trend of compositions. Sometimes, however, this is not so, since symbols on diagrams may be referring to various rocks groups distinguished on the basis of age or structural relationships. In such cases, as pointed out by Cox et al. (1979) the idea of a parental magma fractionating progressively to give rise to the members of a rock series may be replaced by the idea of a fractionation process which is reproducible at different times. The presence of the dioritic rocks in figure V.4 which, on the basis of field evidence are younger than the tonalites and older than the trondhjemites, strongly supports this idea as applied to the Vila Nova rock sequence.

Figure V.4 shows that the diorites follow a trend parallel to that determined by the majority of the rocks. Therefore, it appears that the different rocks are consanguineous on the basis they are all products of a basaltic parental material but generated in different episodes of magma formation involving, in turn, distinct degrees of differentiation or partial melting. The existence of relatively massive bodies of very coarse-grained amphibolites (practically hornblendites, in places) resembling cumulate rocks, strongly supports an origin by fractional crystallization of a wet parental basaltic magma.

According to Verhoogen et al., (1970) if fractional crystallization operates, the successive liquids formed from basaltic magmas will be progressively enriched in (Na+K)/Ca, Fe^{2}/Mg and (Na+K)/Fe^{2}. Data in Table VIII supports the hypothesis of fractional crystallization. The decrease of Al_2O_3, CaO, FeO and MgO with increasing SiO_2, apart from the abundance of hornblende in the more basic rocks, suggest that differentiation was probably controlled by hornblende and plagioclase fractionation.

The association of the tonalitic-trondhjemitic suite with gabbro and dioritic rocks, suggests the existence of a rock sequence similar to that of the Uusikaupunki-Kalanti area, in Finland (Hietanen, 1943; Arth et al., 1974; Barker & Arth, 1976). This opinion is supported by the gabbro-trondhjemite trend exhibited by the Vila Nova rocks when plotted on the K-Na-Ca and the normative Q-Ab-Or diagrams (Fig. V.8 and V.9, respectively). The compositional variation from gabbro to tonalite involves fractionation of high percentages of hornblende, as well as, an enrichment in quartz and plagioclase of magmas of intermediate composition to account for the more siliceous members of the rock sequence.

In the fractionation process, there is an increase in K_2O and REE until the content of SiO_2 in the liquid is about 60%. Beyond this point, as SiO_2 increases the contents of both K_2O and REE decreases as a result of the dilution effect of accumulated quartz and plagioclase (in the cases of K_2O and REE) and the fractionation of hornblende(in the case of REE), according to Barker & Arth (1976) and Arth (1979). In terms of the Vila Nova rocks the variation in K_2O as a function of the variation of the SiO_2 content in the liquid is clearly seen in figure V.1. The REE behaviour is shown in figure V.14 in comparison with the Finnish suite (Arth et al., 1978). As can be seen in figure V.14 the variation in REE sympathetically with SiO_2 is clear as demonstrated by the average values determined for the diorites, tonalites and trondhjemites. It is worth noting that even the buffering of the REE contents of the Finnish rocks with less than 60% SiO_2, pointed out by Arth (1979), is accompanied by the Vila Nova dioritic rocks. The only discrepancy in relation to the Finnish rocks is represented by the less HREE depleted character of the trandhjemites from Vila Nova, even at high SiO_2 contents. The decrease in the overall REE abundances of the Vila Nova trondhjemites when compared with the tonalites of the same suite is similar to the behaviour of the rocks making up the Finnish suite. This sort of behaviour is, according to Barker & Arth (1976) likely the result of fractional crystallization of hornblende and plagioclase. This opinion, therefore, supports what has been suggested above in relation to the nature of the processes which have controlled the chemical characteristics of the tonalitic-trondhjemitic suite from Vila Nova.

A further evidence of plagioclase and hornblende crystallization during a late stage of fractionation leading to the generation of the trondhjemitic liquids is provided by figure V.15.A. In this figure it is clearly shown that tonalites and trondhjemites exhibit very distinct trends, and assuming Y as representing the behaviour of HREE and remembering that field evidence show the trondhjemites are younger than the tonalites, the following conclusions can be drawn:

1) The tonalitic trend ends exactly in the intersection with the trend of the trondhjemites;
2) There is a decrease in HREE, accompanied by very small, or no increase at all of LREE in the tonalites when they tend toward the trend line of the trondhjemites:
3) The trondhjemites trend line is parallel to the Ce/Y axis, implying in a constant HREE content and variable LREE abundances;
4) The HREE abundance of the trondhjemites is equivalent to the final value reached by the tonalites, assuming an evolutive Process within the suite.

The interpretation of the evidence provided by figure V.15A lead to the conclusion that some hornblende was fractionated during the evolution of the tonalitic liquids, leaving the depleted HREE abundance which is displayed by the trondhjemites. These, on the other hand, were slightly enriched in LREE, what is in accordance with the behaviour of such elements in low-Al_2O_3-type trondhjemite (Barker & Arth, 1976). In addition, the distribution of points on a CaO versus Y diagram (Fig. V.15.B) show a general trend which relates positively CaO to Y. Such a behaviour is in accordance with the J-type trend of Lambert & Holland (1974) which can be most easily explained by hornblende fractionation.

The negative correlation between Y and SiO_2(Fig. V.15.C) can be explained on the basis of the suggestion of Arth et al.,(1978, in Tarney et al., 1979) that hornblende liquid partition coefficients for REE(especially HREE) increases with the increasing SiO_2 content of the magma. Much in the same way, the negative correlation between TiO_2 and SiO_2 (Fig. V.1) may be ascribed to removal of Ti by hornblende during magmatic differentiation, despite the fact that biotite and ilmenite might also account for some Ti depletion in the liquids. The positive correlation between Y and TiO_2 (Fig. V.15.D) displaying a trend which does not pass through the origin of the graph but intercepts the Y axis is, in fact, suggestive of biotite fractionation, which removed Ti but not Y (cf. Tarney et al, 1979). This fact is consistent with the high proportions of biotite in the tonalites as compared to the trandhjemites.

The interception of the Y axis by the general trend line in the graph TiO_2-Y, may be assumed as an evidence supporting the conclusion that garnet was not involved in the fractionation process which led to the formation of the tonalitic-trandhjemitic liquids (cf. Tarney et al., 1979).

On the basis that hornblende was a major controlling mineral phase in the fractional crystallization process leading to the formation of the tonalitic liquids, it may be concluded that this phase of magma generation took place at high P_{H_2O} conditions, deep in the crust.

If the fractionation of the basaltic parental magma started under conditions of high water pressure, plagioclase fractionation would be suppressed (Yoder & Tilley, 1962) relative to that of hornblende, resulting then liquids rich in CaO and Al_2O_3. This would ensure that the first materials to crystallize from these liquids would have plagioclase more calcic than the late formed ones. As calcic plagioclase has lower partition coefficients for Sr than intermediate plagioclase (Philpoths, 1970) this would give rise to liquids enriched in Sr (cf. Tarney et al., 1979). This suggests that the high levels of Sr in the trondhjemites may be explained assuming that these rocks were generated at shallower depths than the tonalites. Thus the uprising tonalitic magma undergoing fractionation would originate the more siliceous trondhjemitic liquids. The decrease in the Al_2O_3 content of the trondhjemites in relation to the tonalites may be accounted for plagioclase fractionation in the course of the continued fractionation.

In summary, on the basis of both, the chemical evidence which has been discussed and the field relationships, it is concluded that the most likely origin for the gabbro-diorite-tonalite-trondhjemite suite and related hornblende-rich cummulate rocks is that based on the fractional crystallization model of basic magmas. It is worth noting the fact that the existence of hornblende-cummulate rocks associated with the suite of Southern Finland led Arth et al., (1978, in Tarney et al., 1979) to retain a similar model for explaining the origin of those rocks.

V.4.5 Granitoid suite

V.4.5.1 General

As summarized by Hughes (1982) there are four different ways in which granitic rocks may originate as follows:

1) Advanced fractionation of basaltic magmas;
2) Anatexis of salic crustal material under the influence of very high thermal gradients originated, for instance, by the intrusion of large volume of mafic magmas;
3) Effects of different processes leading to granitization in areas of generation of migmatitic complexes;
4) Assimilation of crustal material by basic magmas generated at mantle depths.

On the basis of the present state of knowledge of the studied area, and according to what has been discussed in the foregoing headings, the hypothesis (1) and (2) seems to be the most likely for explaining the origin of the granitoid suite.

A remarkable characteristic of these rocks is the shape of the intrusive bodies. The grantoids do not make up discordant features similar to stocks. They are represented by sheet-like masses of variable thickness, from a few centimeters up to more than five meters, deformed by folds. These igneous masses are concordant with the dominant foliation, except for fold hinge zones. Such characteristics are strong evidence of syntectonic intrusion of magmas which should have a rather low viscosity.

The normative Q-Ab-Or proportion of these granitoids (Fig.V.16) show they fall within the 53% contour in the frequency distribution for 1,190 granitic rocks as determined by Winkler & von Platen (1961). These rocks tend to cluster around the minimum melting point composition for the system Q-Ab-Or-H_2O, at P_{H_2O} = 2Kbar (Fig. V.16). In addition, on a Ab-An-Or diagram the adamellites plot within the low-temperature granite trough (cf.Kleeman, 1965) (Fig.V.6).

This demonstrates that crystal-liquid equilibria have controlled their compositions (cf. Tuttle & Bowen, 1958). Thus, on the basis of the clustering of points around the minimum melting point composition, within the low-temperature "basin" on the quartz-feldspar boundary, it can be concluded that the granitoids represent an ideal granite composition (Hughes, 1982).

According to James & Hamilton (1969) the only compositions to have last liquids of minimum composition during equilibrium crystallization at low water pressure, lie on a tie line from the Q apex to the point Ab/Or = 1 on the Ab-Or side of the Q-Ab-Or diagram. As can be seen in figure V.16 there are no rocks plotting along the tie line referred to above. This fact leads to the conclusion that the granitoids are not related to a process of equilibrium crystallization, and an origin relating crystal fractionation or partial melting is, actually, favoured.

As referred to by Hughes (1982) grantic rocks include compositions that can be regarded as residual liquids capable of being produced by fractional crystallization processes, and thus complementary to basic rocks. This is consistent with the fractional crystallization processes which have been considered as related to the generation of the tonalitic-trondhjemitic liquids.

However, the Vila Nova trondhjemites,as referred to above, have chemical characteristics of primary trondhjemites (Barker & Millard, 1979). This means that the K_2O content of these rocks is typical of trondhjemites which have not differentiated further to grandodioritic of quartz-monzonitic rocks by the setling of plagioclase at relatively shallow crustal levels. Therefore, if an origin from differentation of basaltic material is to be invoked for the granitoids, they could not be regarded as the more evolved representatives of the trondhjemitic liquids. Hence, this high K_2O suite, which is the most differentiated of any of the major intrusive rock-types in the Vila Nova Complex, cannot be considered as originated from the residual liquids remaining after crystallization of the tonalites and trondhjemites.

On the other hand, there exists some evidence suggesting an origin by partial melting of crustal material. Hence, as shown in Table VI,all granitoids are corundum normative and have a Al(Na+K+Ca/2) ratio greater than 1.10, being, therefore, peraluminous. This fact together with the presence of relict fragments of biotite gneiss within granodiorite, in some places, may suggest that these rocks can be classified as S-type granitoids, according to White & Chappell (1977).

The low Sr and Y contents these rocks present suggest that whatever the way in which they originate i.e. either by partial melting or fractional crystallization during the differentiation of a basaltic magma, the process must have involved phases such plagioclase and amphibole. The fractionation of plagioclase or, alternatively, its presence in a residual sub-solidus mineral assemblage, indicates that the generation of the acidic magmas did not take place under high pressure conditions. Therefore, an origin based upon the hypotheses of Green & Ringwood (1966) of generation of acidic magmas from wet basaltic parents at depths of 100-150 Km is rules out.

Verhoogen *et al* (1970) have claimed that the most likely origin of granodioritic magmas is that related to partial melting of crustal rocks deep in the crust. The association graywacke-shale-andesite is, according to them, the most suitable rock assemblage for producing such magma type. These rocks under crustal conditions corresponding to P_{H_2O}= 2 Kbar and T=700-770^oC may yield large liquid fractions in the compositional range granodiorite-granite. A granodoritic magma generated under such conditions could move upward in the crust while fractionating towards truly granitic liquids, whose compositions are found to be always in the field of minimum liquids temperature in the system Q-Ab-Or.

The presence of perthites in the granitoids indicates crystallization at low water pressure, or a rapid cooling (Tuttle & Bowen, 1958). The low water pressure hypothesis is consistent with the minimum melting point composition at P_{H_2O}= 2 Kbar (Fig.v.16), but the influence of a rapid cooling cannot be disregarded, for instance, for the area where the presence of an intrusive breccia is suggestive of a fast upward movement of the magma. Such a breccia, on the other hand, represents some escape of gases from the rising magma, which must have reached crustal levels corresponding to low total pressure, shallower than the critical vesiculation depth (Hughes, 1982). This breccia is itself intruded by granitoid material that ascended after pressure was released. The dominantly protoclastic character of this breccia which distinguishes it from a typically explosive one, suggests that the explosive activity took place at a late stage in the consolidation of the granitoids. The presence of gas in these magmas is consistent with the low viscosity which has been considered as an important factor controlling the way by which the emplacement of the granitoids took place.

On the basis of the foregoing, in terms of rock genesis it can be concluded that the grantoids probably resulted from partial melting of the dioritic gneisses under P-T conditions compatible with those existing in the amphibolite facies metamorphic environment.

V.4.5.2. Rhyolite

The origin of the magma which formed the rhyolite which occurs as a small dyke in subarea IIIb appears to have been more complex than that of the other granitoids. Thus, if no Rb was introduced into this rock after its formation, on the basis of figure VIII.1, it can be concluded that the generation of the rhyolitic magma took place deep in the crust. The very low Sr content and the relatively high abundances of Rb, Th and U as compared to the other granitoids, apart from the K_2/Na_2O ratio far in excess of unity (cf. Green & Ringwood, 1968), support this opinion. However, the small size of the occurrence which is the only one found in the surveyed area, makes any further discussion on genetic grounds pointless.

The rhyolite, as seen in subarea IIIb is flow banded and exhibits some rare drusy cavities, and at the contact with the host gneiss formed localized incipient brecciation. The rarity of drusy cavities can be explained by a lowered water content due to the early escape of water vapour from the magma, so that the concentration necessary to the formation of a separate water phase, was never reached. Such features are in accord with the epizonal emplacement of a degassed viscous magma (cf. Hughes, 1982), along a fracture which enhanced the escape of volatiles. The high viscosity of this magma was responsible for the banded character and fine texture of this rock (Hughes, 1982) and it may also account for the fact that the rhyolite did not reach a minimum melting composition, as shown in figure V.16. Such characteristics are contrasting with those of the other granitoids in which an increasing percentage of water lowered the melting point and decreased the viscosity, resulting in protracted crystallization and coarser textures (cf. Hughes, 1982).

V.4.5.3. Pegmatites

Associated with the granitoids there is a number of pegmatites. Such an association suggests the pegmatites were derived from magmas with relatively high water content (Luth et al., 1964). The pronounced alteration of the phenocrysts of the granitoids is ascribed to increased late-stage deuteric activity.

The association of granitoids with pegmatites is characteristic of subsolvus granites (Tuttle & Bowen, 1958). This is consistent with the fact that the granitoids are of two-feldspar-type and corundum normative, as shown in Table VI (cf. Luth et al., 1964).

The normative Ab-An-Or proportions of some pegmatites indicate compositions corresponding to those in the low temperature trough in the Ab-An-Or-SiO_2 system (Fig. V.6) according to Kleeman (1965). Due to the extremely high content of K_2O and low Na_2O, the pegmatites do not show similarity with the granitic rocks. Their normative Q-Ab-Or proportion (Fig. V.16) differ markedly from those of the granitoids.

TABLES II. TO VII.

MAJOR ELEMENTS IN %
TRACE ELEMENTS IN PPM

TABLE II. CHEMICAL COMPOSITION (MAJOR AND TRACE ELEMENTS), CIPW NORMS AND NIGGLI NUMBERS OF THE QUARTZOFELDSPATHIC GNEISSES OF THE VILA NOVA COMPLEX

D I O R I T I C G N E I S S E S

Field n°	GR-2	GR-3	GR-10	GR-8	GR-5	GR-7	GR-4	GR-9
SiO_2	58.66	58.64	58.15	52.00	57.57	59.18	57.83	57.33
TiO_2	1.10	0.80	0.81	1.19	0.89	0.80	0.86	0.87
Al_2O_3	17.45	16.65	17.04	18.23	17.68	17.60	18.05	16.09
Fe_2O_3	0.67	0.55	0.74	0.42	0.32	0.28	0.38	2.03
FeO	5.80	6.06	5.69	7.43	6.66	5.47	6.17	6.03
MnO	0.15	0.14	0.26	0.30	0.31	0.12	0.13	0.14
MgO	3.05	3.12	3.41	5.23	3.67	2.81	3.14	3.80
CaO	4.23	5.11	4.53	6.57	5.15	3.87	4.12	4.67
Na_2O	3.44	3.71	4.10	4.25	3.52	4.23	3.90	3.82
K_2O	2.46	2.08	1.48	1.21	1.68	1.94	2.27	3.17
P_2O_5	0.25	0.26	0.28	0.22	0.29	0.03	0.30	0.26
H_2O	0.44	0.29	0.30	0.48	0.36	0.67	0.45	0.33
LOI	1.73	2.12	2.66	1.85	1.38	2.68	2.74	1.88
Total	99.43	99.53	99.45	99.38	99.48	99.63	100.34	100.42
S	663	736	688	698	344	1285	1201	491
Nb	6	8	6	6	7	8	7	9
Zr	128	143	131	149	125	145	140	126
Y	26	20	23	24	18	22	20	18
Co	19	14	21	41	24	17	21	24
Sr	521	580	519	505	506	610	580	370
Cr	108	116	118	137	160	108	100	119
U	3	2	1	4	3	3	3	3
Ce	45	42	40	28	42	48	45	43
Rb	64	53	42	34	41	51	62	76
Ba	659	632	457	349	552	518	576	643
Th	7	6	4	5	3	5	3	3
La	14	20	17	14	30	18	20	13
Pb	13	10	10	10	9	10	11	7
Ga	20	19	18	17	18	21	20	20
Zn	77	72	79	66	78	79	76	75
Cu	60	60	70	66	34	108	98	52
Ni	27	34	39	94	36	32	34	41

TABLE II. CONTINUED

DIORITIC GNEISSES

Field n°	GR-6	GR-1	A38-1	A38-2	A38-3	A-1	A-2
SiO_2	58.97	59.25	58.44	56.55	59.83	62.00	59.18
TiO_2	0.88	0.73	0.74	0.76	0.81	0.88	0.88
Al_2O_3	16.04	16.87	17.73	18.20	16.36	15.87	16.67
Fe_2O_3	0.10	0.41	0.34	0.59	0.13	0.03	0.03
FeO	6.21	5.59	6.02	5.85	5.73	6.50	6.60
MnO	0.13	0.13	0.24	0.11	0.15	0.13	0.11
MgO	3.15	3.14	2.89	3.04	2.82	3.14	4.13
CaO	4.19	6.39	3.59	3.86	3.71	4.05	5.47
Na_2O	3.77	3.50	4.23	4.54	4.25	3.30	3.76
K_2O	2.70	2.06	1.97	2.06	2.02	2.53	1.99
P_2O_5	0.29	0.21	0.29	0.28	0.29	0.24	0.29
H_2O	0.19	0.21	0.46	0.57	0.56	0.42	0.29
LOI	2.77	1.75	2.66	3.04	3.08	1.27	0.86
Total	99.35	100.24	99.60	99 58	99.70	100.38	100.28
S	1198	663				735	
Nb	9	5				7	
Zr	146	139				143	
Y	27	20				22	
Co	24	23				24	
Sr	491	506				521	
Cr	126	126				97	
U	2	2				3	
Ce	64	39				40	
Rb	68	50				61	
Ba	738	431				480	
Th	7	6				4	
La	23	20				18	
Pb	11	13				10	
Ga	20	19				14	
Zn	72	74				74	
Cu	115	46				43	
Ni	54	48				37	

TABLE II. CONTINUED

	DICRITIC GNEISSES					GRANITIC GNEISSES	
Field n°	A-3	A-4	A-5	B-7	AR-1	C-1	Al-7
SiO_2	60.35	61.48	55.10	59.56	57.67	61.42	64.18
TiO_2	0.73	0.81	1.05	0.81	0.81	0.66	0.77
Al_2O_3	17.42	16.34	16.28	16.58	17.13	17.08	15.84
Fe_2O_3	0.08	0.53	0.04	0.15	1.60	0.44	0.11
FeO	5.65	6.03	7.49	6.24	5.39	4.73	5.53
MnO	0.11	0.14	0.14	0.17	0.13	0.24	0.10
MgO	2.48	3.14	5.54	3.48	3.95	2.64	1.98
CaO	3.73	4.11	6.80	5.27	7.27	2.83	2.13
Na_2O	3.76	3.22	3.86	3.50	3.44	4.67	3.89
K_2O	2.78	2.47	1.85	1.66	1.57	1.96	3.00
P_2O_5	0.24	0.23	0.27	0.25	0.19	0.22	0.22
H_2O	0.13	0.14	0.37	0.08	0.12	0.37	0.32
LOI	1.92	1.63	1.34	1.93	1.22	2.86	1.95
Total	99.38	100.27	100.13	99.68	100.49	100.12	100.02
S		596			119		769
Nb		3			6		9
Zr		149			105		241
Y		21			23		21
Co		23			27		12
Sr		538			375		311
Cr		114			145		29
U		2			1		0
Ce		38			21		56
Rb		63			44		92
Ba		463			456		665
Th		7			4		5
La		22			12		30
Pb		13			6		10
Ga		16			18		16
Zn		80			65		62
Cu		36			17		25
Ni		36			46		9

TABLE II. CONTINUED

D I O R I T I C   G N E I S S E S

	GR-2	GR-3	GR-10	GR-8	GR-5	GR-7	GR-4	GR-9
q	17.35	15.83	18.09	1.35	13.99	18.19	17.02	9.59
or	14.54	12.29	8.75	7.15	9.93	11.46	13.41	18.73
ab	29.10	31.38	34.68	35.95	29.78	35.78	32.99	32.31
an	8.42	10.25	3.83	19.46	14.93	2.38	1.16	9.58
hy	15.73	16.98	16.85	24.21	19.57	15.22	17.17	17.32
mt	0.97	0.80	1.07	0.61	0.46	0.41	0.55	2.94
il	2.09	1.52	1.54	2.26	1.69	1.52	1.63	1.65
ap	0.58	0.60	0.65	0.51	0.67	0.07	0.70	0.60
cc	3.93	4.82	6.05	4.21	3.14	5.98	6.23	4.28
c	6.04	4.54	7.29	2.80	4.60	7.67	8.75	2.86
py	0.13	0.13	0.13	0.13	0.06	0.24	0.22	0.09
si	198.03	193.25	192.47	140.54	181.59	205.27	190.19	176.69
al	34.72	32.34	33.24	29.04	32.87	35.98	34.98	29.23
fm	33.42	33.39	34.41	38.71	35.58	31.12	33.30	37.71
c	15.30	18.04	16.07	19.03	17.41	14.38	14.52	15.42
alk	16.56	16.23	16.28	13.22	14.15	18.52	17.20	17.65
ti	2.79	1.98	2.02	2.42	2.11	2.09	2.13	2.02
k	0.32	0.27	0.19	0.16	0.24	0.23	0.28	0.35
mg	0.46	0.46	0.49	0.54	0.48	0.47	0.46	0.46

TABLE II. CONTINUED

DIORITIC GNEISSES

	GR-6	GR-1	A38-1	A38-2	A38-3	A-1	A-2
q	17.03	14.10	18.03	14.42	19.86	19.21	10.13
or	15.96	12.17	11.64	12.17	11.94	14.95	11.76
ab	31.89	29.61	35.78	38.41	35.95	27.92	31.81
an	1.38	19.27	0.90	1.83	1.89	10.50	19.81
hy	17.47	16.40	16.75	16.57	16.10	18.13	20.93
mt	0.14	0.59	0.49	0.85	0.19	0.04	0.04
il	1.67	1.39	1.40	1.44	1.54	1.67	1.67
ap	0.67	0.49	0.67	0.65	0.67	0.56	0.67
cc	6.30	3.98	6.05	6.89	6.62	2.89	1.96
c	6.41	1.82	8.97	9.17n	7.88	3.86	1.07
py	0.22	0.13	0.00	0.00	0.00	0.13	0.00
si	201.38	190.15	199.79	185.75	212.78	216.45	183.23
al	32.28	31.91	35.72	35.23	34.29	32.65	30.42
fm	34.02	31.01	32.81	32.41	32.34	35.39	36.22
c	15.33	21.97	13.15	13.59	14.14	15.15	18.15
alk	18.36	15.11	18.32	18.77	19.24	16.80	15.22
ti	2.26	1.76	1.90	1.88	2.17	2.31	2.05
k	0.32	0.28	0.23	0.23	0.24	0.34	0.26
mg	0.47	0.48	0.45	0.46	0.46	0.46	0.53

TABLE II. CONTINUED

	DIORITIC GNEISSES					GRANITIC GNEISSES	
	A-3	A-4	A-5	B-7	AR-1	C-1	AL-7
q	17.92	20,73	2.10	17.79	10.76	20.14	23.81
or	16.43	14,60	10.93	9.81	9.28	11.58	17.73
ab	31.81	27.24	32.65	29.61	29.10	39.51	32,91
an	4.80	8.58	21.63	21.31	27.11	1,44	1.44
hy	15.28	16.99	25.03	18.66	17.05	13.81	13.56
mt	0.12	0.77	0.06	0.22	2.32	0.64	0.16
il	1,39	1.54	1.99	1.54	1.54	1.25	1.46
ap	0,56	0.53	0,63	0.58	0.44	0.51	0.51
cc	4.37	3.71	3.05	4.39	2.77	5.05	3.80
c	6.47	5.22	0.00	4.51	0.01	7.80	6.72
py	0.00	0.11	0.00	0.00	0.02	0,00	0.15
si	214.29	213,08	151.57	196.00	169.98	226.66	257.12
al	36.45	33.38	26.39	32.16	30.07	37.15	37.40
fm	30.12	35.08	40.02	34.61	34.19	30.34	30.68
c	14.19	15.26	20.04	18.58	22.96	11.19	9.14
alk	19.24	16.28	13.54	14.65	12,78	21.32	22.78
ti	1.95	2.11	2.17	2.00	1.86	1.83	2.32
k	0.33	0.34	0.24	0.24	0.23	0.22	0.34
mg	0.44	0.46	0.57	0.49	0.51	0.48	0.39

TABLE III. CHEMICAL COMPOSITION (MAJOR AND TRACE ELEMENTS), CIPW NORMS AND NIGLI NUMBERS OF AMPHIBOLITES OF THE VILA NOVA COMPLEX.

Field n°	EB-1	EB-2	EB-3	EB-4	RPM-57
SiO_2	51.92	52.44	50.57	53.40	49.75
TiO_2	1.52	1.56	1.50	1.31	1.66
Al_2O_3	17.45	18.77	17.86	17.15	16.12
Fe_2O_3	0.77	0.28	0.23	0.22	2.08
FeO	7.32	7.91	7.44	6.83	9.21
MnO	0.14	0.28	0.29	0.13	0.13
MgO	4.31	4.31	3.94	4.29	6.19
CaO	7.84	7.45	7.82	6.86	7.11
Na_2O	4.38	3.54	4.90	4.23	3.63
K_2O	1.98	2.04	2.16	2.54	2.52
P_2O_5	0.46	--	0.40	0.45	0.46
H_2O	--	0.17	0.39	0.44	0.45
LOI	1.95	1.74	1.80	1.77	1.15
Total	100.04	99.49	99.30	99.62	100.46
S	1398	867	1247	742	1398
Nb	15	10	9	9	15
Zr	226	223	221	217	211
Y	26	25	28	23	19
Co	29	35	33	40	43
Sr	714	691	656	653	778
Cr	76	83	63	99	153
U	1	0	4	3	3
Cr	55	51	48	42	52
Rb	43	45	48	56	53
Ba	669	656	761	859	602
Th	2	1	6	3	4
La	27	25	21	24	28
Pb	6	8	10	6	6
Ga	24	22	21	22	21
Zn	89	91	92	89	88
Cu	61	63	75	62	179
Ni	46	39	34	45	138

EB-1 to EB-4 : Discordant amphibolites

RPM-57 : Fine-grained concordant amphibolite

TABLE III.(Continued)

Field nº	EB-1	EB-2	EB-3	EB-4	RPM-57
q	0.00	1.15	0.00	0.00	0.00
or	11.70	12.06	12.76	15.01	14.89
ab	37.05	29.95	37.48	35.78	30.71
an	22.11	25.96	20.36	19.90	20.25
di	1.20	0.00	3.67	0.00	3.90
hy	12.66	22.26	0.00	18.86	4.93
mt	1.12	0.41	0.33	0.32	3.02
il	2.89	2.96	2.85	2.49	3.15
ap	1.07	0.00	0.93	1.05	1.07
cc	4.43	3.96	4.09	4.02	2.61
c	0.00	1.22	0.00	0.15	0.00
py	0.26	0.17	0.22	0.13	0.26
ol	5.50	0.00	13.82	1.38	15.18
ne	0.00	0.00	2.15	0.00	0.00
si	139.13	141.62	135.57	150.63	122.12
al	27.56	29.88	28.22	28.51	23.32
fm	35.17	35.78	32.89	34.62	45.39
c	22.51	21.56	22.46	20.73	18.70
alk	14.76	12.78	16.43	16.14	12.58
ti	3.06	3.17	3.02	2.78	3.06
k	0.23	0.27	0.22	0.28	0.31
mg	0.49	0.48	0.48	0.52	0.50

TABLE IV. CHEMICAL COMPOSITION (MAJOR AND TRACE ELEMENTS) AND CIPW NORMS OF TONALITES OF THE VILA NOVA COMPLEX

Field n°	B3-B	B-11	T-1	T-2	T-3	T-4	T-4A	T-4B
SiO_2	63.92	66.78	66.27	67.70	60.74	64.10	66.10	65.49
TiO_2	0.70	0.80	0.61	0.34	0.86	0.51	0.47	0.48
Al_2O_3	17.08	14.28	16.69	15.94	17.42	17.70	16.49	16.52
Fe_2O_3	0.56	0.49	0.32	0.25	1.07	0.64	0.77	1.00
FeO	4.73	5.11	3.64	3.07	5.23	2.76	3.50	3.34
MnO	0.09	0.16	0.14	0.06	0.12	0.07	0.08	0.09
MgO	1.44	2.22	1.17	1.15	1.68	1.86	1.30	1.22
CaO	4.31	3.63	3.79	3.78	5.71	4.16	4.69	4.86
Na_2O	3.95	2.82	4.00	3.71	3.76	4.92	3.88	4.13
K_2O	2.03	2.34	1.70	1.87	1.92	1.93	1.85	2.04
P_2O_5	0.28	0.22	0.22	0.10	0.29	0.19	0.17	0.17
H_2O	0.12	0.11	0.15	0.15	0.15	0.18	0.10	0.10
LOI	1.08	1.44	0.70	1.40	1.29	0.55	0.58	0.57
Total	100.29	100.40	99.40	99.52	100.24	99.57	99.98	100.01
S	1181		651	180	378	112	114	
Nb	11		13	8	4	11	11	
Zr	351		278	327	318	212	198	
Y	20		16	13	36	14	11	
Co	10		7	7	16	10	11	
Sr	519		504	463	464	441	452	
Cr	44		20	27	27	37	26	
U	2		3	2	2	1	2	
Ce	94		84	49	78	61	68	
Rb	54		48	44	47	47	48	
Ba	831		718	617	720	537	572	
Th	11		9	6	7	11	10	
La	54		58	23	42	40	30	
Pb	13		11	11	10	9	10	
Ga	18		17	16	20	19	18	
Zn	63		55	50	70	50	48	
Cu	74		40	16	27	10	13	
Ni	10		5	6	6	0	1	
q		31.40	26.76	31.05	17.83	24.25	16.77	21.40
or		13.83	10.05	11.05	11.35	10.93	11.41	12.06
ab		23.86	33.84	31.38	31.81	32.82	41.62	34.94
an		7.47	12.94	9.25	18.28	18.49	15.92	19.40
di		0.00	0.00	0.00	0.00	0.00	0.00	0.00
hy		13.19	8.18	7.69	11.40	7.23	7.31	7.55
mt		0.71	0.46	0.36	1.55	1.12	0.93	1.45
il		1.52	1.16	0.65	1.63	0.89	0.97	0.91
ap		0.51	0.51	0.23	0.67	0.39	0.44	0.39
cc		3.27	1.59	3.18	2.93	1.32	1.25	1.30
c		4.37	3.53	4.42	2.46	1.33	1.68	0.41
py		0.00	0.13	0.04	0.07	0.02	0.02	0.00

TABLE IV. CONTINUED

Field n°	T-5	B3-A	B3-B	B3-D	B3-E	RPJ-3	ARD-1	ARD-2
SiO_2	62.48	68.80	63.92	68.50	62.08	62.53	67.58	65.79
TiO_2	0.71	0.24	0.70	0.25	0.73	0.67	0.52	0.53
Al_2O_3	17.68	15.82	17.08	16.00	16.63	18.28	15.78	17.04
Fe_2O_3	0.02	0.14	0.56	0.61	0.42	0.56	0.73	0.61
FeO	5.16	2.84	4.73	2.11	5.03	2.90	3.07	3.26
MnO	0.10	0.05	0.09	0.06	0.10	0.17	0.07	0.07
MgO	1.51	1.01	1.44	1.15	1.44	1.50	1.37	1.36
CaO	4.72	4.65	4.31	3.02	5.06	4.40	3.48	3.63
Na_2O	4.04	3.98	3.95	4.41	3.77	5.60	3.91	3.84
K_2O	1.81	1.63	2.03	2.13	1.92	1.79	2.05	2.22
P_2O_5	0.27	0.12	0.28	0.14	0.26	0.28	0.20	0.23
H_2O	0.00	0.95	0.12	0.19	0.09	0.28	0.27	0.25
LOI	1.58	0.16	1.08	1.40	2.19	0.58	0.65	0.60
Total	100.08	100.39	100.29	99.97	99.72	99.45	99.68	99.43
S	316	172	1181	423	409	86	108	113
Nb	12	12	11	6	13	13	6	6
Zr	321	246	351	124	309	222	275	276
Y	25	12	20	14	35	13	14	16
Co	15	2	10	8	20	8	11	10
Sr	506	490	519	575	491	571	444	467
Cr	20	30	44	44	20	39	32	29
U	2	2	2	3	2	1	2	3
Ce	90	43	94	95	91	55	97	102
Rb	47	39	54	52	61	60	48	47
Ba	599	459	831	538	781	283	992	956
Th	10	5	11	18	9	8	11	12
La	43	26	54	48	46	37	54	49
Pb	10	13	13	13	10	15	8	7
Ga	21	16	18	19	21	25	16	16
Zn	67	45	63	33	68	81	63	63
Cu	15	16	74	27	25	10	19	18
Ni	4	5	10	5	2	11	5	5
q	21.02	26.76	22.42	29.42	23.06	12.01	27.94	25.35
or	10.70	9.63	12.00	12.59	11.35	10.58	12.11	13.12
ab	34.18	33.67	33.41	37.31	31.89	47.37	33.08	32.48
an	11.66	20.49	12.73	5.22	9.56	16.33	11.85	12.71
di	0.00	0.66	0.00	0.00	0.00	0.00	0.00	0.00
hy	11.95	6.84	10.40	5.74	11.19	7.47	7.57	7.87
mt	0.03	0.20	0.81	0.88	0.61	0.81	1.06	0.88
il	1.35	0.46	1.33	0.47	1.39	1.27	0.99	1.01
ap	0.63	0.28	0.65	0.32	0.60	0.65	0.46	0.53
cc	3.59	0.36	2.46	3.18	4.98	1.32	1.48	1.36
c	4.80	0.00	3.72	4.53	4.85	1.14	2.79	3.66
py	0.06	0.04	0.22	0.07	0:07	0.02	0.02	0.02

TABLE V. CHEMICAL COMPOSITION (MAJOR AND TRACE ELEMENTS) AND CIPW NORMS OF TRONDHJEMITES OF THE VILA NOVA COMPLEX

Field n^{o}	M-1	M-2	B3-C	M-28-3	M-28-4	M-28-5	M-28-6	M-28-7	M-28-8
SiO_2	72.85	73.47	71.62	72.04	71.39	71.02	72.71	72.54	72.78
TiO_2	0.16	0.18	0.31	0.27	0.22	0.30	0.14	0.23	0.15
Al_2O_3	14.32	13.81	12.66	13.14	14.51	15.10	14.18	13.55	14.14
Fe_2O_3	0.13	0.00	0.61	0.22	0.18	0.24	0.30	0.13	0.19
FeO	1.71	1.54	1.97	2.28	1.82	1.05	1.66	1.80	1.81
MnO	0.04	0.03	0.05	0.05	0.05	0.04	0.04	0.04	0.04
MgO	0.58	0.48	0.83	0.91	0.57	0.38	0.50	0.61	0.64
CaO	3.79	3.46	3.92	3.31	3.67	3.10	3.85	3.50	3.18
Na_2O	4.22	3.97	3.77	4.35	4.58	4.79	3.98	4.28	4.30
K_2O	1.81	1.02	1.69	1.27	1.26	1.28	1.33	1.17	1.12
P_2O_5	0.08	0.05	0.13	0.12	0.10	0.08	0.07	0.09	0.10
H_2O	0.00	0.04	0.09	0.09	0.13	0.12	0.00	0.09	0.17
LOI	0.69	1.24	2.00	1.50	1.17	1.28	1.08	1.41	0.80
Total	100.13	99.29	99.65	99.55	99.65	99.38	99.84	99.44	99.42
S	120	113	174	627	118	85	107	239	425
Nb	3	4	6	2	3	7	7	6	6
Zr	157	119	251	183	101	78	88	172	149
Y	9	7	12	11	6	5	5	8	9
Co	1	1	6	5	5	0	2	4	4
Sr	498	495	517	475	527	532	476	500	482
Cr	29	18	34	44	32	24	27	41	19
U	2	3	2	1	0	2	1	1	1
Ce	102	53	67	107	47	16	16	83	120
Rb	24	27	39	28	31	26	30	29	24
Ba	416	319	460	267	402	441	325	305	344
Th	18	9	9	16	4	5	3	14	19
La	53	21	38	57	21	10	13	43	61
Pb	11	12	13	10	13	13	13	13	11
Ga	16	13	17	14	15	15	14	13	15
Zn	25	21	35	29	22	21	18	25	25
Cu	11	11	9	44	6	10	5	8	15
Ni	0	0	3	3	3	0	1	1	0
q	33.25	40.73	40.57	35.71	33.41	34.22	37.46	37.59	36.89
or	10.70	6.03	9.99	7.50	7.45	7.56	7.86	6.91	6.62
ab	35.70	33.58	28.51	37.64	38.74	40.52	33.67	36.21	36.38
an	13.92	9.00	5.95	6.15	10.16	6.76	11.82	7.86	10.07
hy	4.19	3.70	4.63	5.70	4.23	2.16	3.79	4.30	4.43
mt	0.19	0.00	0.88	0.32	0.26	0.35	0.43	0.19	0.27
il	0.30	0.34	0.59	0.51	0.42	0.57	0.27	0.44	0.28
ap	0.19	0.12	0.30	0.28	0.23	0.19	0.16	0.21	0.23
cc	1.57	2.82	4.55	3.41	2.66	2.91	2.46	3.21	1.82
c	0.32	2.89	3.10	2.19	1.89	3.36	1.86	2.36	2.16
py	0.02	0.02	0.04	0.11	0.02	0.02	0.02	0.04	0.07

TABLE VI. CHEMICAL COMPOSITION (MAJOR AND TRACE ELEMENTS) AND CIPW NORMS
OF ADAMELLITES, GRANODIORITES AND A RHYOLITE OF THE VILA NOVA COMPEX

	A D A M E L L I T E S							
Field n°	C-13	AT-6	AT-4	AL-1	AL-2	RPM-54	RPM-55	RPJ-4
SiO_2	72.44	72.73	73.19	73.12	74.95	72.86	74.48	73.89
TiO_2	0.23	0.06	0.12	0.14	0.11	0.13	0.18	0.22
Al_2O_3	14.86	14.12	13.50	14.02	13.84	14.98	14.08	13.31
Fe_2O_3	0 26	0.38	0.84	0.41	0.00	0.18	0.23	0.35
FeO	0.42	1.44	1.51	0.98	1.10	0.58	1.03	0.94
MnO	0 02	0.05	0.05	0.04	0.03	0.02	0.03	0.03
MgO	0.10	0.29	0.32	0.28	0.29	0.16	0.29	0.35
CaO	1.48	1.69	1.84	1.50	1.70	1.67	1.76	2.49
Na_2O	3.81	3.62	3.52	3.47	3.22	3.46	3.50	3.57
K_2O	4.97	4.46	3.80	4.56	4.19	5.08	3.91	3.85
P_2O_5	0.02	0.04	0.05	0.05	0.02	0.00	0.01	0.05
H_2O	0.09	0.21	0.15	0.03	0.23	0.08	0.23	0.03
LOI	0.68	0.54	0.68	0.83	0.51	0.36	0.40	0.49
Total	99.78	99.63	99.57	99.43	100.19	99.56	100.13	99.57
S	80	94	60	53	45	64	161	38
Nb	2	10	13	5	4	1	8	7
Zr	58	140	141	124	99	40	114	84
Y	14	14	12	8	6	8	19	5
Co	0	0	1	1	2	2	1	5
Sr	316	223	228	235	291	315	343	411
Cr	14	20	20	32	39	1	9	19
U	3	3	3	4	3	3	2	2
Ce	23	50	53	43	21	105	21	31
Rb	63	66	67	63	51	58	49	60
Ba	1660	919	968	1066	1082	408	1163	1170
Th	5	7	6	7	2	4	5	2
La	8	16	27	19	5	51	27	13
Pb	34	17	16	18	18	29	18	17
Ga	13	17	15	13	15	13	15	14
Zn	3	36	36	19	12	7	14	20
Cu	14	3	10	10	8	14	25	10
Ni	0	1	1	3	0	1	1	0
q	29.78	31.13	34.90	33.71	36.72	30.14	35.45	33.52
or	29.37	26.36	22.46	26.95	24.76	30.02	23.11	22.75
ab	32.23	30.62	29.78	29.35	27.24	29.27	29.61	30.20
an	2.91	4.71	4.50	1.87	5.08	6.01	6.14	8.92
hy	0.40	2.93	2.67	1.91	2.56	1.08	2.08	1.94
mt	0.38	0.55	1.22	0.59	0.00	0.26	0.33	0.51
il	0.44	0.11	0.23	0.27	0.21	0.25	0.34	0.42
ap	0.05	0.09	0.12	0.12	0.05	0.00	0.02	0.12
cc	1.55	1.23	1.55	1.89	1.16	0.82	0.91	1.11
c	2.14	1.61	1.95	2.69	2.15	1.59	1.84	0.00
py	0.02	0.02	0.02	0.02	0.00	0.02	0.04	0.00

TABLE VI. CONTINUED

Field n°	ADAMELLITES AT-5	ADAMELLITES AL-3	GRANODIORITES C-6-B	GRANODIORITES RB-3	GRANODIORITES C-8	GRANODIORITES G-1	GRANODIORITES C-6-A	RHYOLITE RT-R
SiO_2	72.62	72.90	71.99	70.77	71.70	72.58	71.59	74.45
TiO_2	0.15	0.17	0.30	0.30	0.23	0.15	0.24	0.00
Al_2O_3	14.12	14.53	15.05	15.88	14.53	14.11	15.17	12.22
Fe_2O_3	0.24	0.00	0.29	0.26	0.14	0.05	0.26	0.55
FeO	1.41	1.29	1.79	1.66	1.56	1.34	1.89	0.95
MnO	0.04	0.03	0.12	0.05	0.05	0.03	0.06	0.03
MgO	0.32	0.25	0.45	0.78	0.25	0.41	0.50	0.17
CaO	2.17	1.39	1.68	2.57	2.16	2.65	2.59	1.29
Na_2O	3.37	3.16	3.90	3.55	3.63	4.10	3.91	1.82
K_2O	4.58	4.62	3.34	3.65	3.48	2.64	3.19	6.74
P_2O_5	0.07	0.02	0.08	0.10	0.04	0.03	0.09	0.02
H_2O	0.04	0.23	0.08	0.16	0.59	0.06	0.06	0.49
LOI	0.71	0.72	0.62	0.38	0.97	1.11	0.88	1.35
Total	99.84	99.31	99.69	100.11	99.33	99.26	100.43	100.08
S	46	32	33	61	40	307	42	59
Nb	6	4	9	8	5	6	7	27
Zr	134	116	177	182	109	63	178	94
Y	11	8	12	15	16	6	12	59
Co	0	0	0	2	0	2	3	4
Sr	239	282	271	350	229	434	274	48
Cr	9	16	46	49	23	36	34	31
U	2	4	3	2	3	3	3	6
Ce	48	39	53	56	39	19	64	25
Rb	66	60	78	55	73	51	77	277
Ba	1020	1284	766	1084	925	599	746	560
Th	8	6	9	8	7	2	7	25
La	25	19	30	32	24	12	36	10
Pb	19	20	17	14	19	17	17	40
Ga	17	13	17	16	16	15	16	21
Zn	29	14	38	32	31	16	36	22
Cu	9	11	5	8	5	42	7	6
Ni	0	0	0	6	0	4	0	6
q	31.52	34.56	33.01	29.74	33.95	34.49	31.69	37,29
or	27.07	27.30	19.74	21.57	20.57	15.60	18.85	39.83
ab	28.51	26.73	33.00	30.03	30.71	34.68	33.08	15.40
an	5.82	2.21	3.89	9.69	4.32	5.93	6.70	0.13
hy	2.94	2.71	3.67	4.26	2.99	3.13	4.10	1.69
mt	0.35	0.00	0.42	0.38	0.20	0.07	0.38	0.80
il	0.28	0.32	0.57	0.57	0.44	0.28	0.46	0.00
ap	0,16	0.05	0.19	0.23	0.09	0.07	0.21	0.05
cc	1,61	1.64	1.41	0.86	2.21	2.52	2.00	2.30
c	1.49	3.52	3.59	2.54	3.21	2.33	2.83	1.98
py	0.00	0.00	0.00	0.02	0.00	0.06	0.00	0.02

TABLE VII. CHEMICAL COMPOSITION (MAJOR AND TRACE ELEMENTS) AND CIPW NORMS OF PEGMATITES OF THE VILA NOVA COMPLEX

Field n°	RPM-50	RPM-51	RPM-52	RPM-53	RPM-56	RPM-58
SiO_2	69.62	70.32	73.10	71.57	70.41	70.07
TiO_2	0.12	0.07	0.07	0.07	0.17	0.05
Al_2O_3	16.65	17.31	15.74	16.12	16.68	16.91
Fe_2O_3	0.12	0.00	0.03	0.00	0.00	0.00
FeO	0.78	0.39	0.24	0.39	0.49	0.33
MnO	0.02	0.01	0.01	0.01	0.01	0.01
MgO	0.29	0.08	0.08	0.04	0.12	0.04
CaO	0.91	1.36	0.94	0.59	0.56	0.24
Na_2O	2.22	3.02	2.55	2.22	2.01	2.35
K_2O	8.35	6.60	6.79	8.41	8.94	8.74
P_2O_5	0.04	0.02	0.02	0.00	0.00	0.00
H_2O	0.07	0.12	0.16	0.12	0.25	0.17
LOI	0.29	0.36	0.31	0.30	0.31	0.30
Total	99.48	99.66	100.04	99.84	99.95	99.21
S	161	48	40	49	41	40
Nb	2	2	1	3	3	0
Zr	12	20	21	9	17	10
Y	2	2	2	2	3	2
Co	0	0	0	0	0	0
Sr	857	784	650	783	745	761
Cr	24	12	12	12	10	12
U	1	1	1	0	1	2
Ce	17	10	6	8	8	5
Rb	93	70	73	86	102	107
Ba	9021	5141	3347	7738	6545	9512
Th	0	1	1	0	1	0
La	4	8	10	0	2	6
Pb	29	27	25	29	36	33
Ga	10	13	11	10	10	8
Zn	8	2	0	1	3	0
Cu	19	15	12	14	13	14
Ni	4	0	0	1	0	0
q	22.77	25.22	30.91	25.69	23.69	22.65
or	49.35	39.00	40.13	49.70	52.83	51.65
ab	18.78	25.55	21.57	18.78	15.00	19.88
an	2.42	4.34	2.57	1.03	0.82	0.00
hy	1.81	0.80	0.50	0.70	0.92	0.62
mt	0.17	0.00	0.04	0.00	0.00	0.00
il	0.23	0.13	0.13	0.13	0.32	0.09
ap	0.09	0.05	0.05	0.00	0.00	0.00
cc	0.66	0.82	0.70	0.68	0.70	0.43
c	3.07	3.61	3.25	2.99	3.40	3.58
py	0.04	0.00	0.00	0.00	0.00	0.00

TABLE VIII. AVERAGE (Na+K)/Ca, Fe^{+2}/Mg AND $(Na+K)/Fe^{+2}$ RATIOS FOR THE DIFFERENT IGNEOUS ROCKS OF THE VILA NOVA COMPLEX

	(Na+K)/Ca	Fe^{+2}/Mg	$(Na+K)/Fe^{+2}$
DIORITES	1.38	0.98	1.80
TONALITES	2.35	1.48	3.23
TRONDHJEMITES	2.63	1.63	7.10
GRANODIORITES	4.78	2.18	8.50
ADAMELLITES	6.72	2.28	16.38
RHYOLITE	8.76	3.18	15.25
PEGMATITES	24.70	2.95	45.39

TABLE IX. AVERAGE COMPOSITION OF THE TRONDHJEMITIC ROCKS OF THE VILA NOVA COMPLEX COMPARED TO TRONDHJEMITIC ROCKS OF OTHER PARTS OF THE WORLD

	A	B	C	D	E	F	G	H
SiO_2	72.27	65.25	61.42	64.18	75.40	73.20	70.40	71.72
TiO_2	0.22	0.56	0.66	0.77	0.15	0.18	0.29	0.22
Al_2O_3	13.93	16.71	17.08	15.84	13.70	13.50	16.10	15.98
Fe_2O_3	0.22	0.55	0.44	0.11	0.85	0.73	0.79	0.49
FeO	1.74	3.72	4.73	5.53	1.20	2.50	1.42	0.88
MnO	0.04	0.09	0.24	0.10	0.04	0.10	0.07	0.03
MgO	0.61	1.42	2.64	1.98	0.33	0.70	0.66	0.53
CaO	3.53	4.26	2.83	2.13	1.50	1.90	2.27	2.83
Na_2O	4.25	4.05	4.67	3.89	4.30	4.00	4.84	5.56
K_2O	1.33	1.95	1.96	3.00	1.50	2.00	2.59	1.21
P_2O_5	0.09	0.21	0.22	0.22	0.04	0.06	0.09	0.06
H_2O	0.08	0.21	0.37	0.32				
LOI	1.40	0.98	2.86	1.95				
Zr	144	239		241				
Sr	500	455		311	101	217	547	634
Rb	29	49		92	28	45	76	23
Zn	25	57		62				
Cu	13	23		25				
Ba	364	659		665	617	180	855	329
Ce	68	76		56				
La	35	42		30				
Nb	5	9		9				
Ga	15	18		16				
Pb	12	11		10				
Co	3	10		12				
Ni	1.2	5		9				
Cr	30	28		29				
Y	8	17		21				
Th	11	10		5				
U	1.4	2.1		0				
K/Rb	381	330		271	445	387	299	437
Rb/Sr	0.058	0.108		0.296	0.394	0.368	0.148	0.036
Ba/Rb	12.55	13.45		7.23	22.03	4.00	11.25	14.30
Ba/Sr	0.728	1.448		2.138	6.109	0.829	1.234	0.519
K/Ba	30	25		37	20.19	96.75	26.58	30
Ce/Y	8.5	4.5		2.7				
Y/Nb	1.6	1.9		2.3				

VILA NOVA COMPLEX

A - Average composition of 9 trondhjemites
B - Average composition of 16 tonalites
C - Quartzofeldspathic gneiss (subarea I)
D - Quartzofeldspathic gneiss (subarea II)

OTHER ROCKS

E - Average composition of the Rio Brazos trondhjemite, New Mexico, USA (Barker <u>et al</u>, 1976)
F - Average composition of the Twilight gneiss, Colorado, USA (Barker <u>et al</u>, 1976)
G - Average composition of the Kroenke granodi rite, Colorado, USA (Barker <u>et al</u>, 1976)
H - Trondhjemite from the Trondheim region, Norway (Barker & Millard Jr , 1979)

FIGURES V.1 TO V.16

Figure V.1 Harker's variation diagram for all analysed rocks of the Vila Nova Complex.

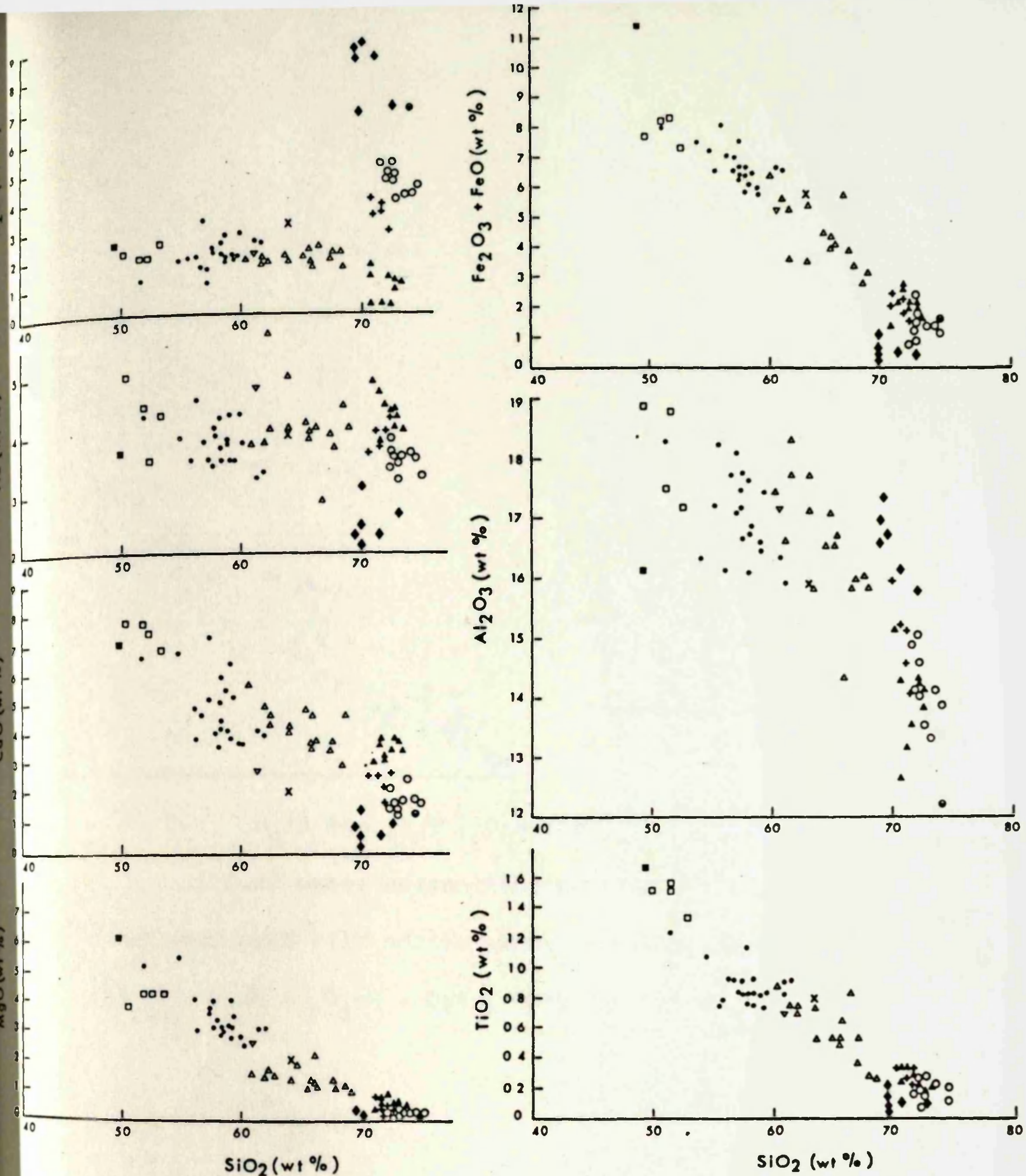

- ◆ GRANITIC PEGMATITE
- ⊖ RHYOLITE
- ◎ ADAMELLITE
- \+ GRANODIORITE
- ▲ TRONDHJEMITE
- △ TONALITE
- ● DIORITIC GNEISS
- □ DISCORDANT AMPHIBOLITE
- ■ FINE-GRAINED CONCORDANT AMPHIBOLITE

Figure V.2 Plots of MgO, $FeO+Fe_2O_3$, TiO_2 and Al_2O_3 against Kuno's solidification index (S.I) for all analysed rocks of the Vila Nova Complex. (S.I = 100 MgO/(MgO + FeO + Fe_2O_3 + Na_2O + K_2O)).

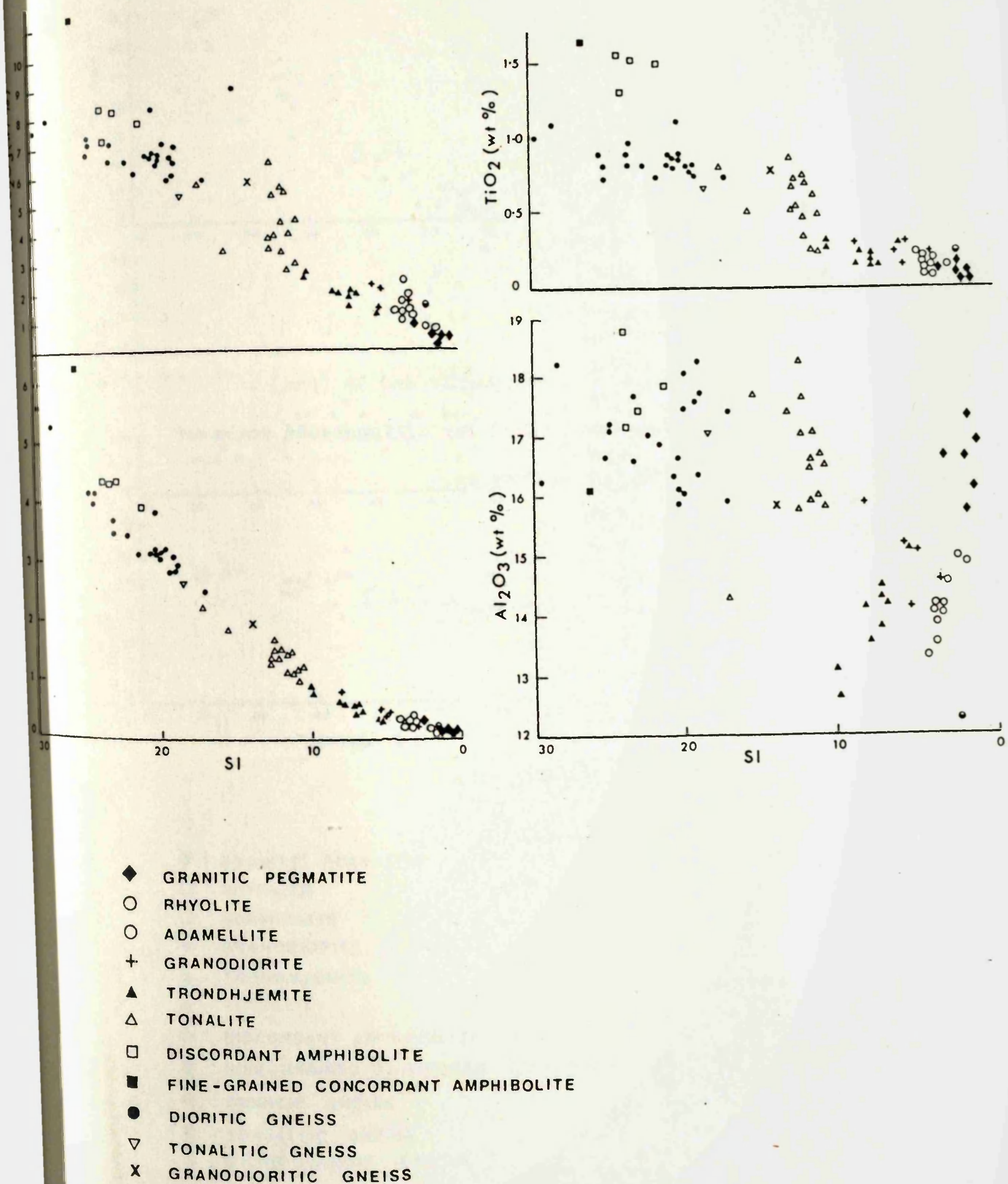

TiO2 (wt %)
Al2O3 (wt %)
SI
SI
GRANITIC PEGMATITE
RHYOLITE
ADAMELLITE
GRANODIORITE
TRONDHJEMITE
TONALITE
DISCORDANT AMPHIBOLITE
FINE-GRAINED CONCORDANT AMPHIBOLITE
DIORITIC GNEISS
TONALITIC GNEISS
GRANODIORITIC GNEISS

Figure V.3 Plots of Co, Pb, Ga, Zr and Sr (ppm) against SiO_2 (wt%) for all analysed rocks of the Vila Nova Complex.

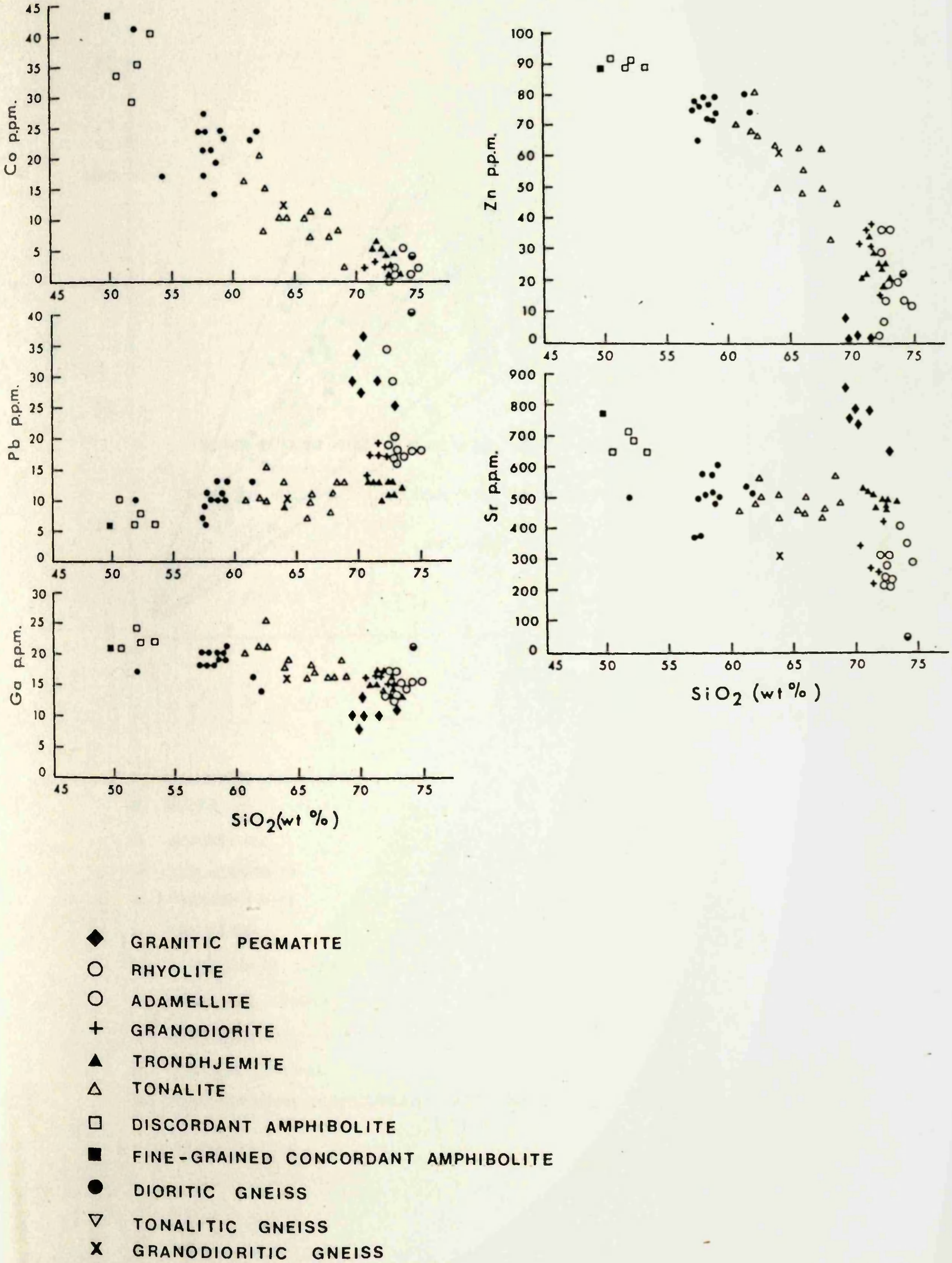

Co p.p.m.
Pb p.p.m.
Ga p.p.m.
SiO_2(wt %)
Zn p.p.m.
Sr p.p.m.
SiO_2 (wt %)
GRANITIC PEGMATITE
RHYOLITE
ADAMELLITE
GRANODIORITE
TRONDHJEMITE
TONALITE
DISCORDANT AMPHIBOLITE
FINE-GRAINED CONCORDANT AMPHIBOLITE
DIORITIC GNEISS
TONALITIC GNEISS
GRANODIORITIC GNEISS

Figure V.4 Plot of Rb against K for whole-rock samples of the analysed rocks of the Vila Nova Complex.

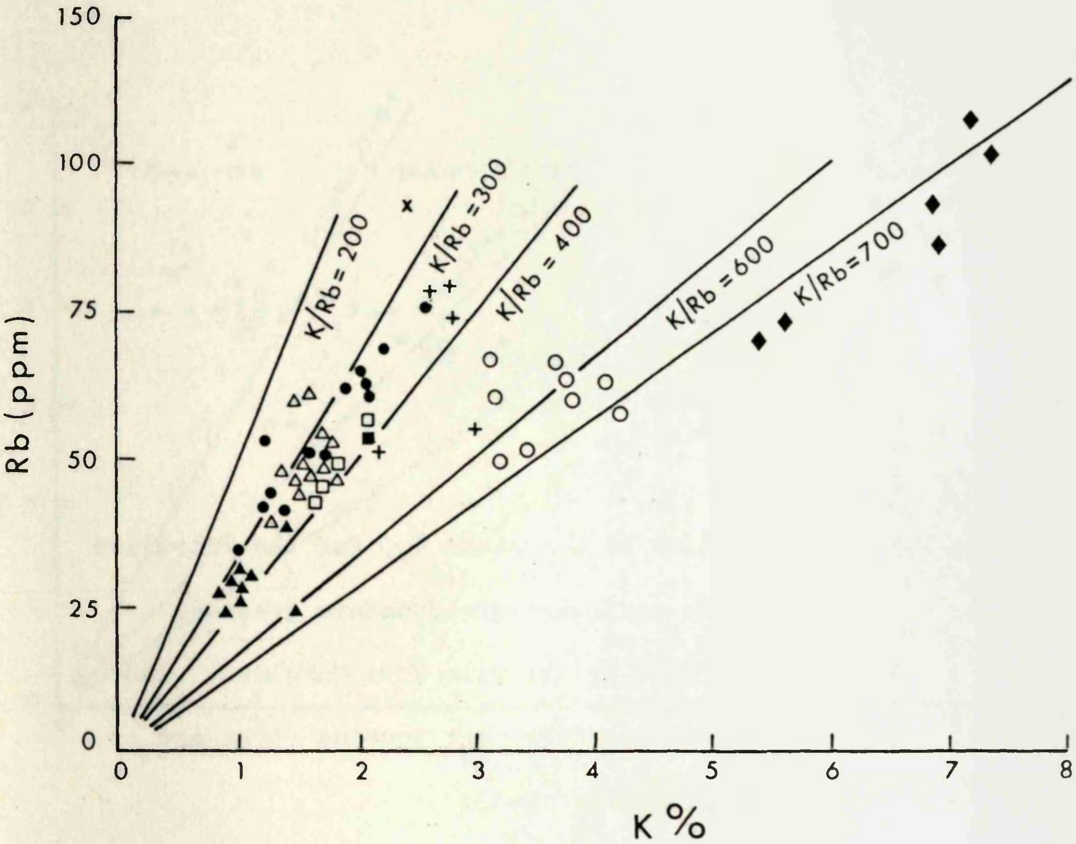

◆ GRANITIC PEGMATITE
⊖ RHYOLITE
○ ADAMELLITE
+ GRANODIORITE
▲ TRONDHJEMITE
△ TONALITE
□ DISCORDANT AMPHIBOLITE
▽ TONALITIC GNEISS
x GRANODIORITIC GNEISS
● DIORITIC GNEISS
■ FINE-GRAINED CONCORDANT AMPHIBOLITE

Figure V.5 Plot of Na_2O against K_2O for the intrusive rocks and quartzofeldspathic granitic gneisses of the Vila Nova Complex. The fields for different igneous rocks are from Harpum (1963).

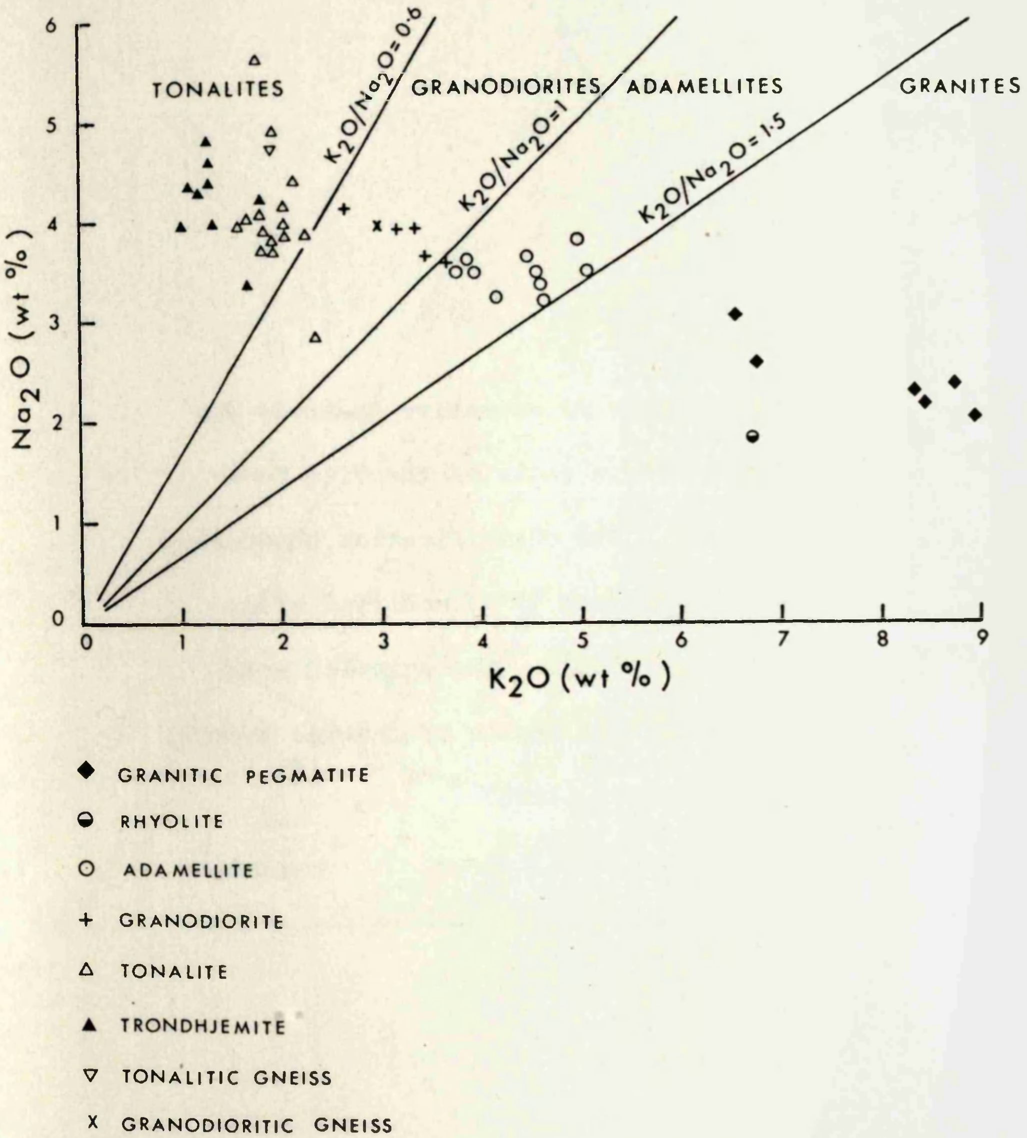
TONALITES
GRANODIORITES
ADAMELLITES
GRANITES
$K_2O/Na_2O=0{\cdot}6$
$K_2O/Na_2O=1$
$K_2O/Na_2O=1{\cdot}5$
Na_2O (wt %)
K_2O (wt %)
0
1
2
3
4
5
6
7
8
9
GRANITIC PEGMATITE
RHYOLITE
ADAMELLITE
GRANODIORITE
TONALITE
TRONDHJEMITE
TONALITIC GNEISS
GRANODIORITIC GNEISS

Figure V.6 Ternary plot of normative Ab-An-Or for the intrusive rocks of the Vila Nova Complex. The classification boundaries are from Barker (1979) modified after O'Connor (1965). The stippled area represents the region of thermal trough, after Kleeman (1965)

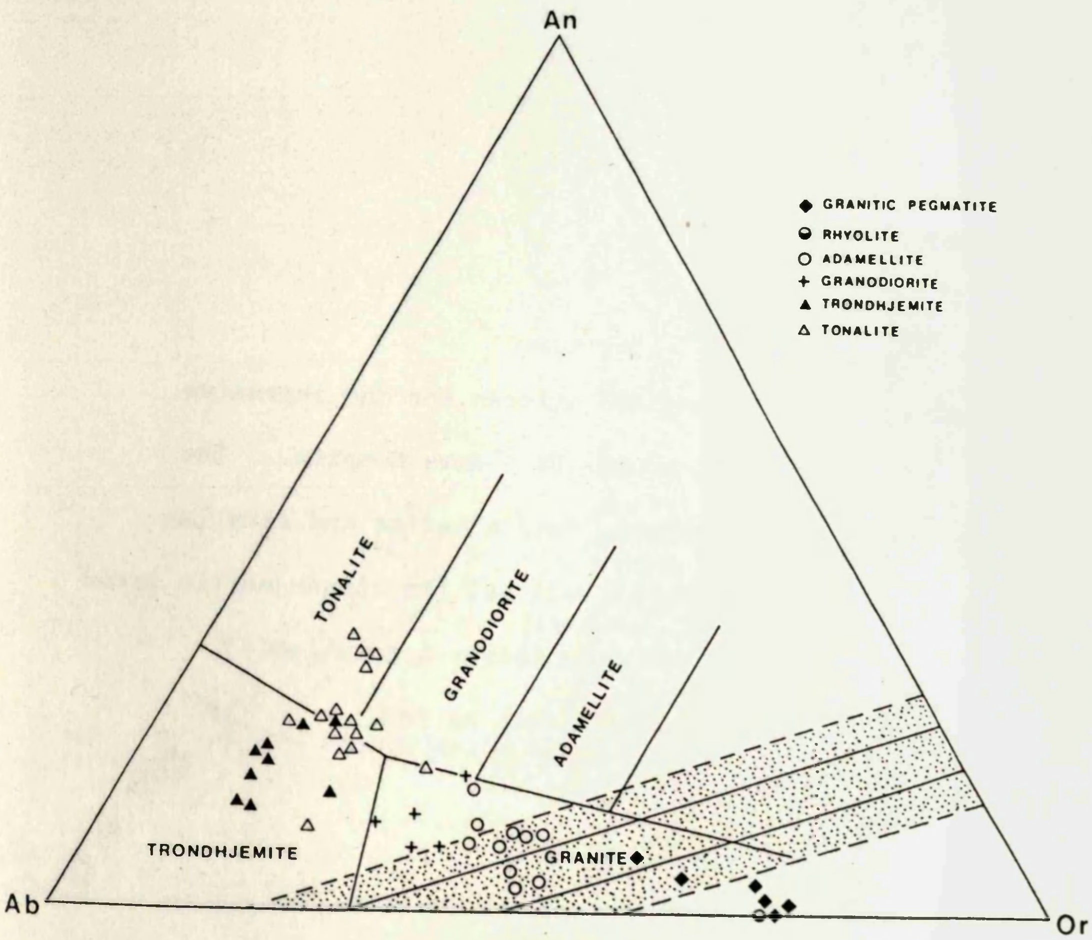
An
Ab
Or
TONALITE
GRANODIORITE
ADAMELLITE
TRONDHJEMITE
GRANITE
GRANITIC PEGMATITE
RHYOLITE
ADAMELLITE
GRANODIORITE
TRONDHJEMITE
TONALITE

Figure V.7 Ternary AFM diagram for the intrusive rocks of the Vila Nova Complex. The tholeiitic, calc-alkaline and alkaline fields, as well as, the trondhjemitic trend line are from Barker & Arth (1976). FeO^* = total iron as FeO.

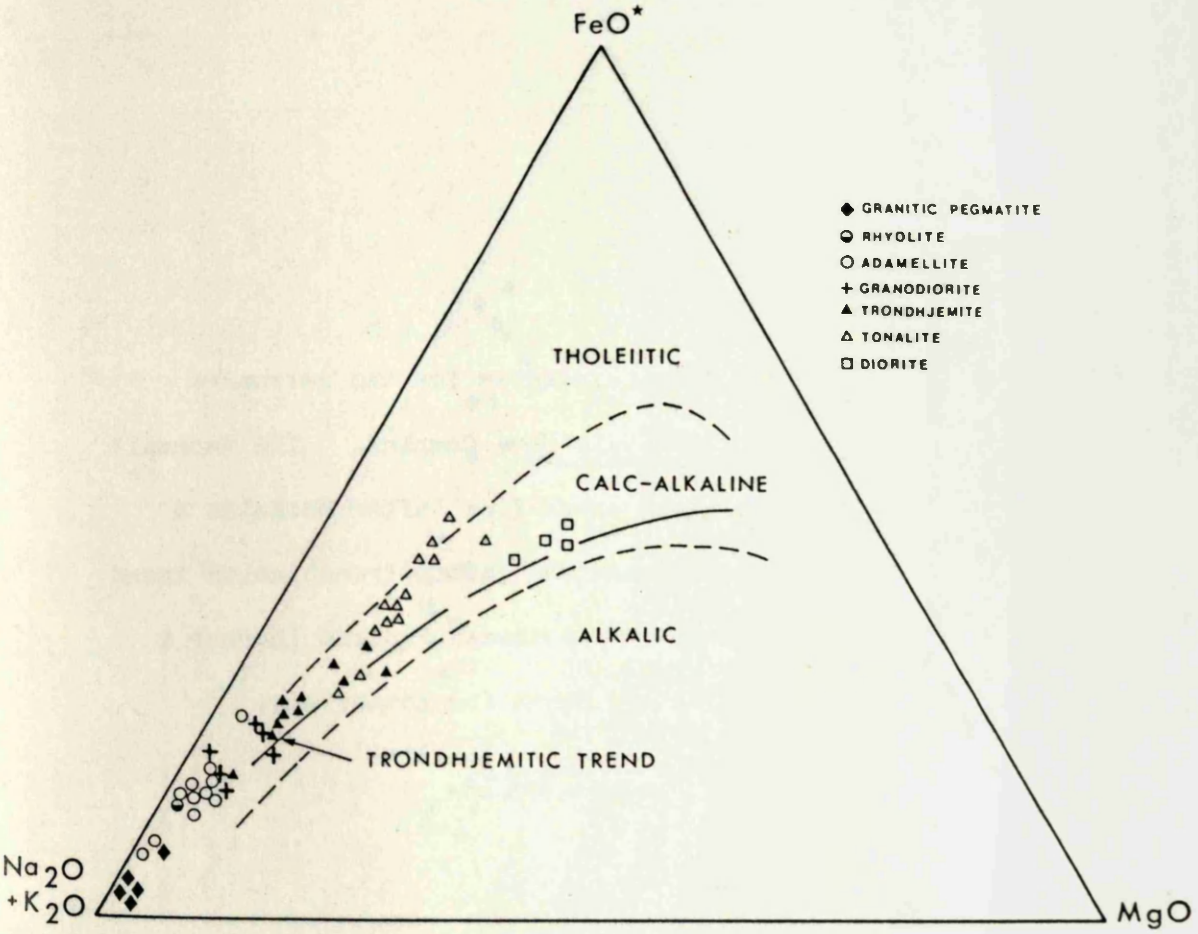
FeO*
GRANITIC PEGMATITE
RHYOLITE
ADAMELLITE
GRANODIORITE
TRONDHJEMITE
TONALITE
DIORITE
THOLEIITIC
CALC-ALKALINE
ALKALIC
TRONDHJEMITIC TREND
Na_2O $+K_2O$
MgO

Figure V.8 Ternary K-Na-Ca diagram for the intrusive rocks of the Vila Nova Complex. The "normal" calc-alkaline trend line (after Nockolds & Allen, 1953) and the gabbro-trondhjemite trend of the suite of southwest Finland (Barker & Arth, 1976) are given for comparison.

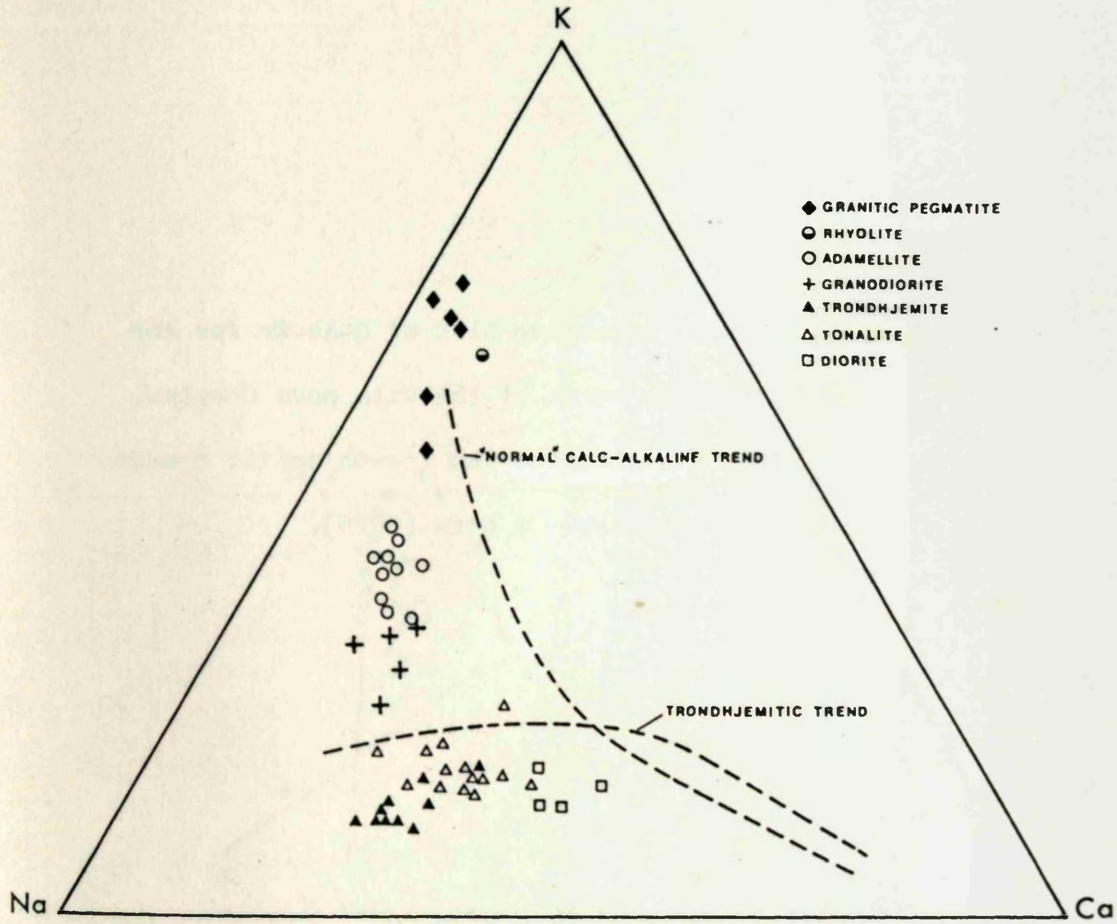

K
Na
Ca
GRANITIC PEGMATITE
RHYOLITE
ADAMELLITE
GRANODIORITE
TRONDHJEMITE
TONALITE
DIORITE
"NORMAL" CALC-ALKALINE TREND
TRONDHJEMITIC TREND

Figure V.9 Ternary normative plot of Q-Ab-Or for the intrusive rocks of the Vila Nova Complex. The calc-alkaline and trondhjemitic trends are from Barker & Arth (1976).

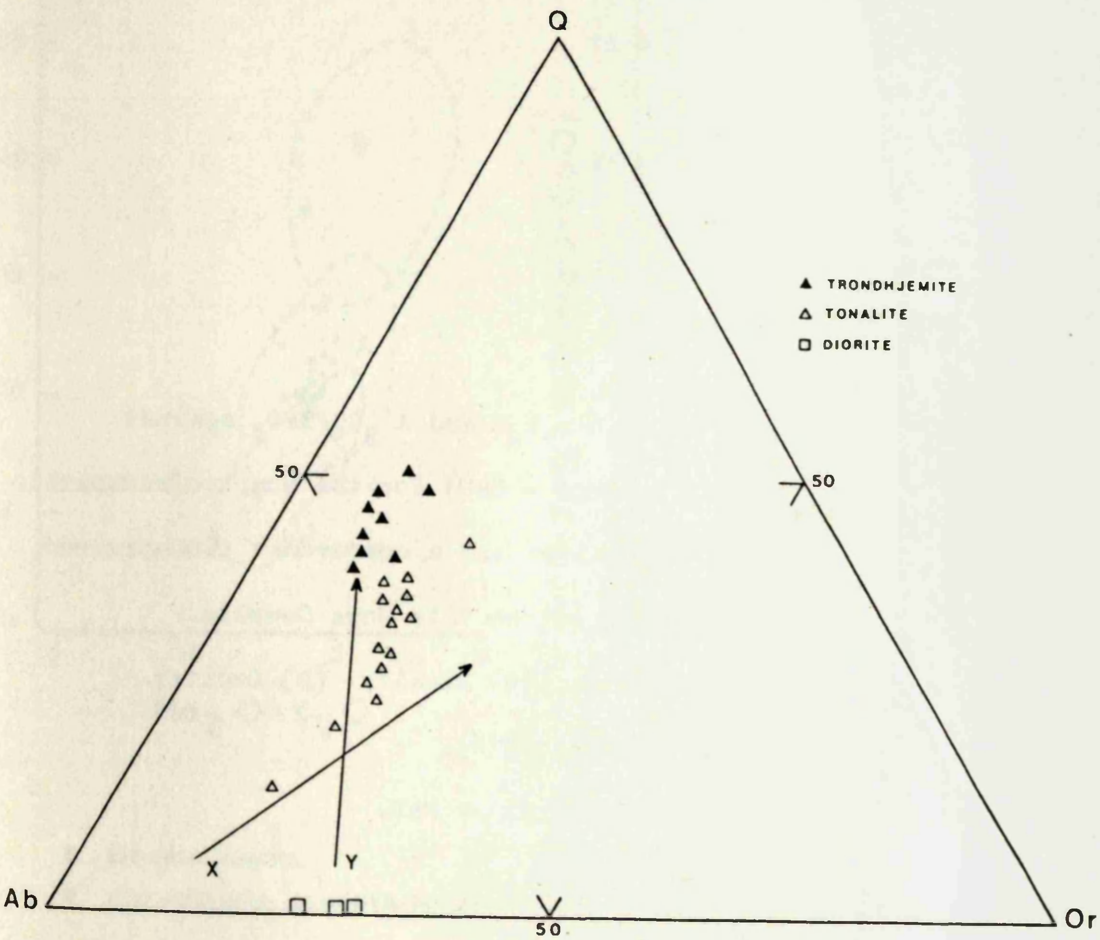
Q
Ab
Or
50
50
50
X
Y
TRONDHJEMITE
TONALITE
DIORITE

Figure V.10 Plot of $Na_2O + K_2O$ and Al_2O_3/SiO_2 against $FeO^* + 1/2(MgO - CaO)$ for the quartzofeldspathic diorite gneisses and a concordant fine-grained amphibolite of the Vila Nova Complex.

(A) Andesite; (B) Basalt; (D) Dacite;

(after Church, 1975).

FeO^* = total iron as FeO.

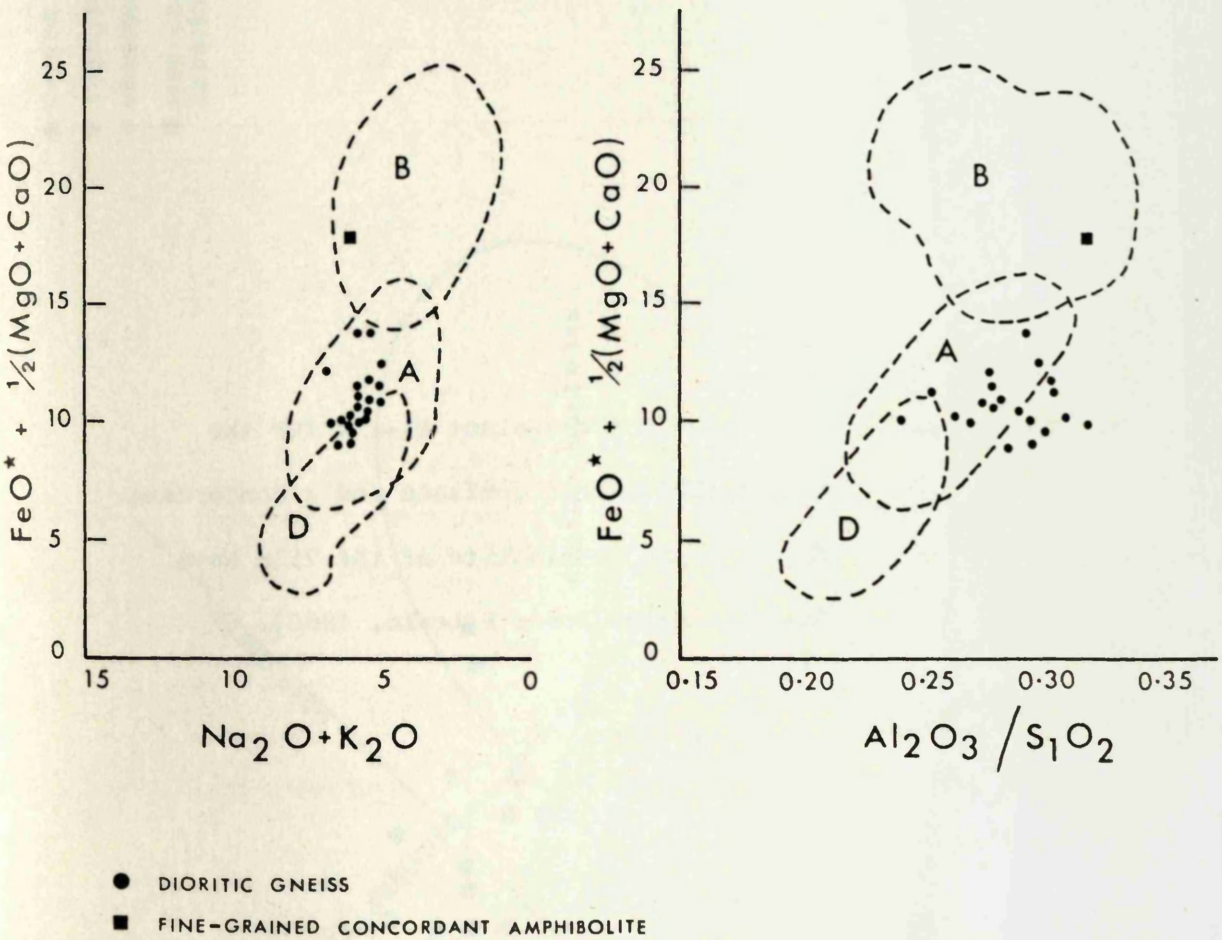

25
20
15
10
5
0
15
10
5
0
FeO* + ½(MgO+CaO)
Na_2O+K_2O
B
A
D
0·15
0·20
0·25
0·30
0·35
Al_2O_3/SiO_2
DIORITIC GNEISS
FINE-GRAINED CONCORDANT AMPHIBOLITE

Figure V.11. Plot of Niggli c against al-alk for the quartzofeldspathic gneisses and a concordant fine-grained amphibolite of the Vila Nova Complex (after Evans & Leake, 1960).

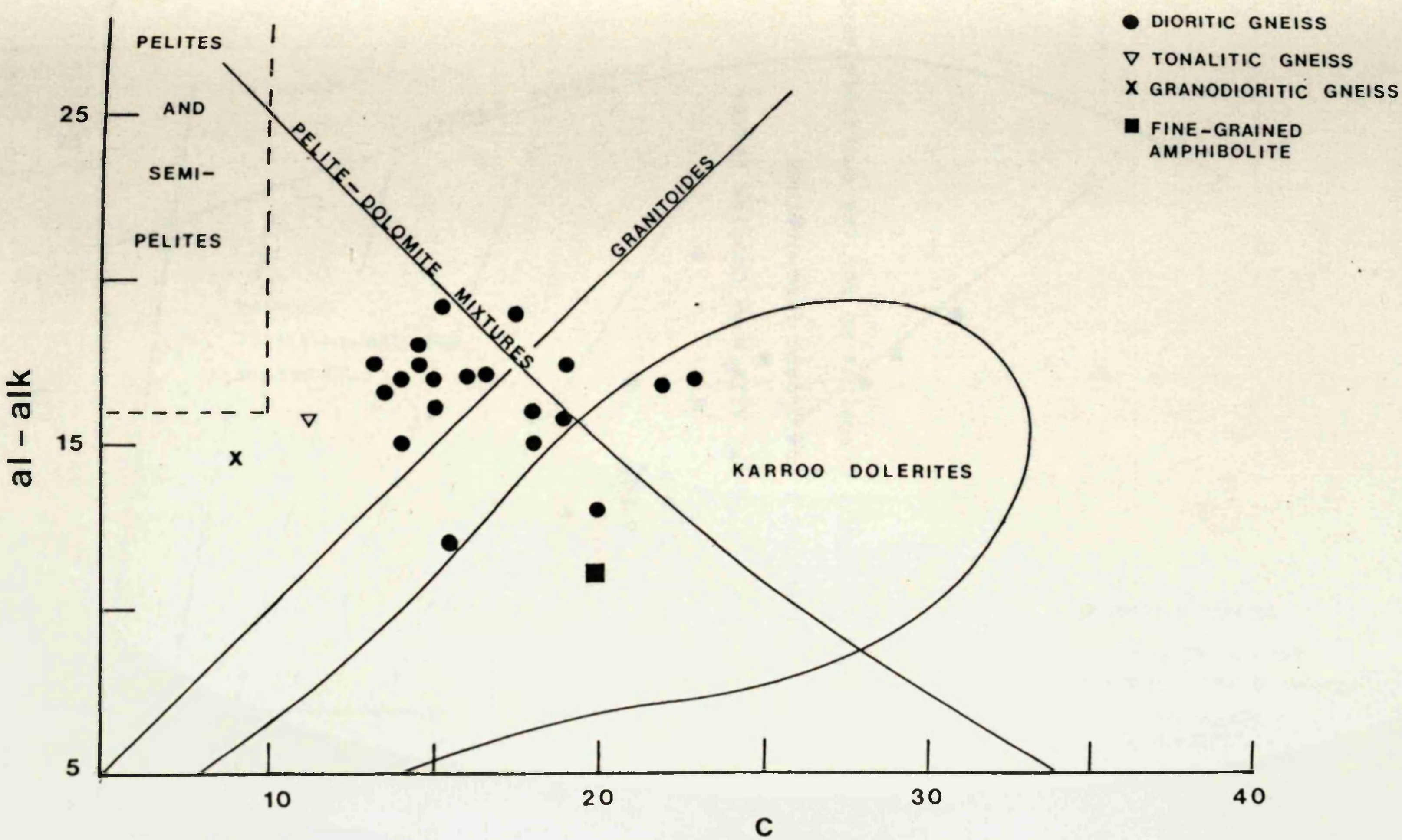
DIORITIC GNEISS
TONALITIC GNEISS
GRANODIORITIC GNEISS
FINE-GRAINED AMPHIBOLITE
PELITES AND SEMI-PELITES
PELITE-DOLOMITE MIXTURES
GRANITOIDES
KARROO DOLERITES
al - alk
C
5
15
25
10
20
30
40

Figure V.12 Plot of Niggli c against mg for the quartzofeldspathic gneisses and a concordant fine-grained amphibolite of the Vila Nova Complex (after Leake, 1964).

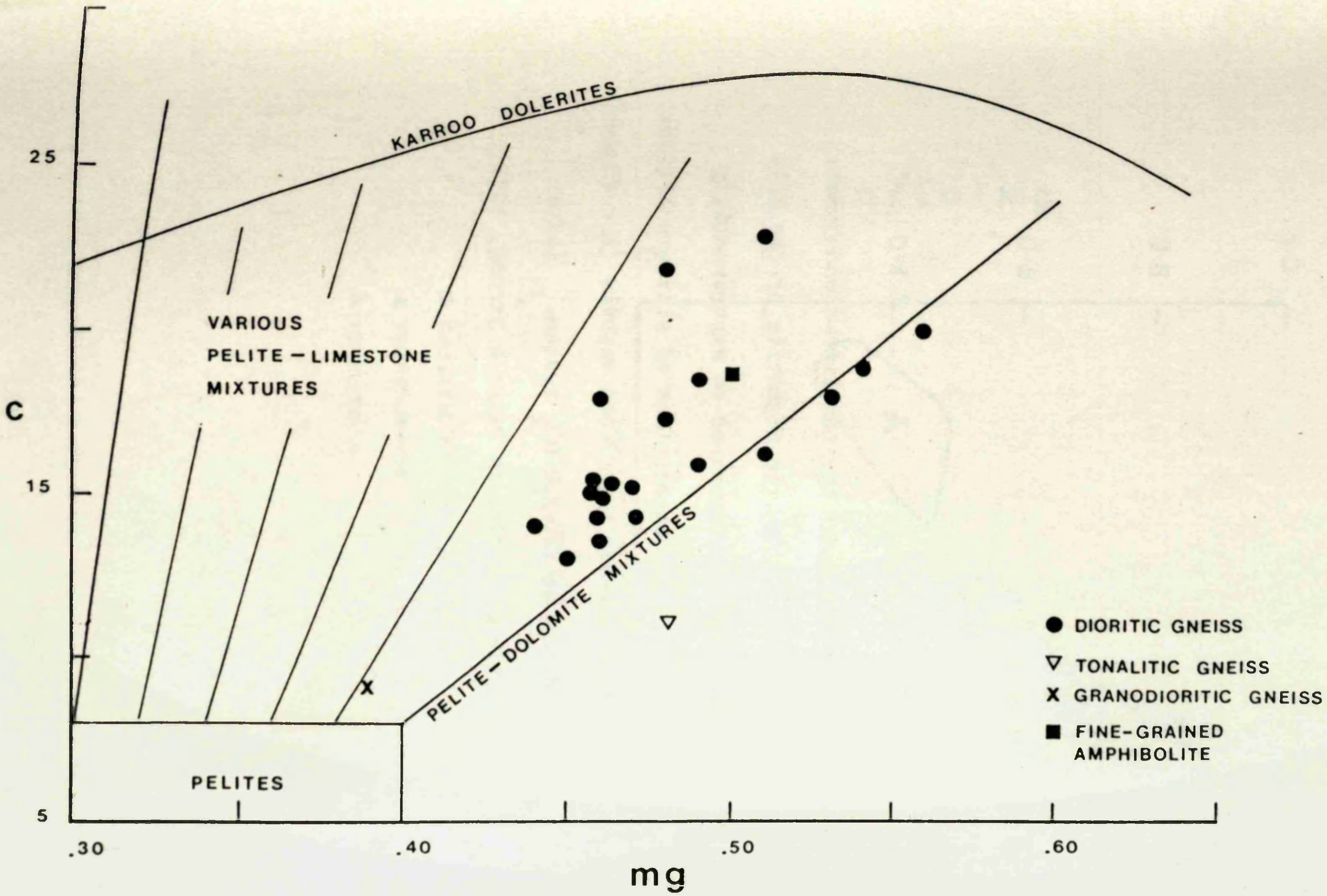
KARROO DOLERITES
VARIOUS
PELITE – LIMESTONE
MIXTURES
PELITE – DOLOMITE MIXTURES
PELITES
C
25
15
5
.30
.40
.50
.60
mg
DIORITIC GNEISS
TONALITIC GNEISS
X GRANODIORITIC GNEISS
FINE-GRAINED AMPHIBOLITE

Figure V.13 Composition of the tonalite-trondhjemite suite and granitic pegmatite of the Vila Nova Complex compared to experimentally determined compositions of silicate liquids (B = igneous trend) and vapours (A = fluids) in the basalt-H_2O-CO_2 system. (After Holloway, 1971, in Payne & Strong, 1979)

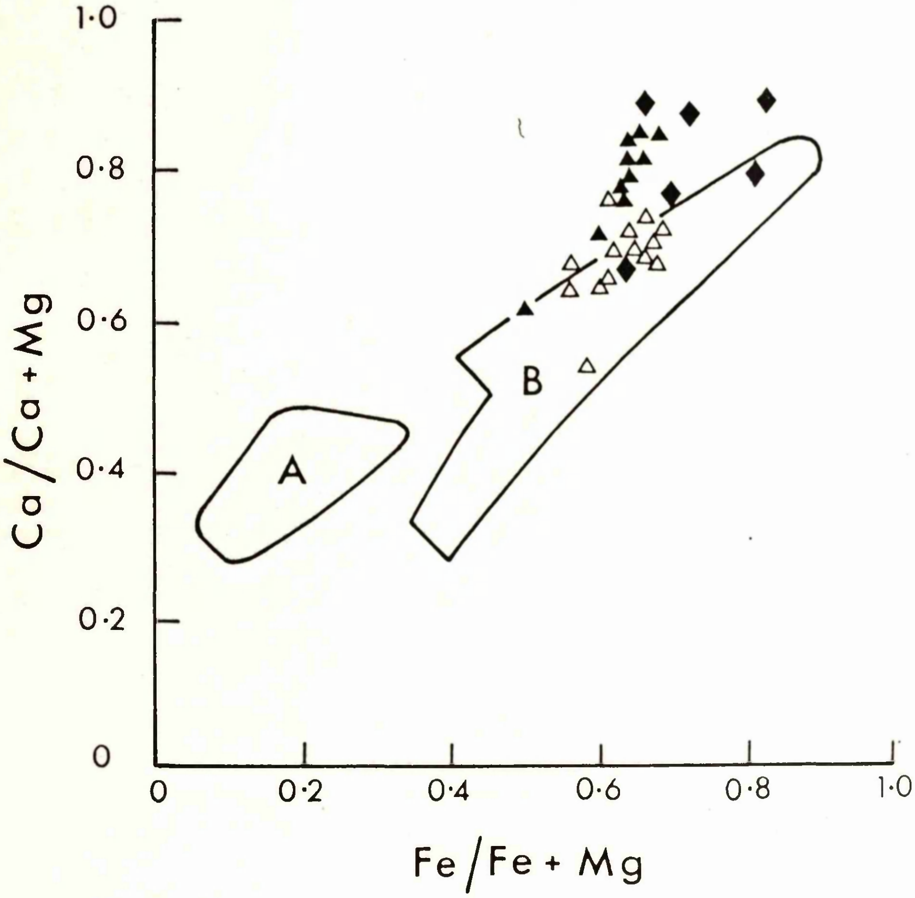

◆ GRANITIC PEGMATITE

▲ TRONDHJEMITE

△ TONALITE

Figure V.14 Chondrite-normalized La, Ce and Y for the tonalites, trondhjemites and diorites of the Vila Nova Complex, compared to the chondrite-normalized REE patterns of the gabbro-diorite-tonalite-trondhjemite suite from southwest Finland (cf. Arth *et al.*, 1978 in Arth, 1979).

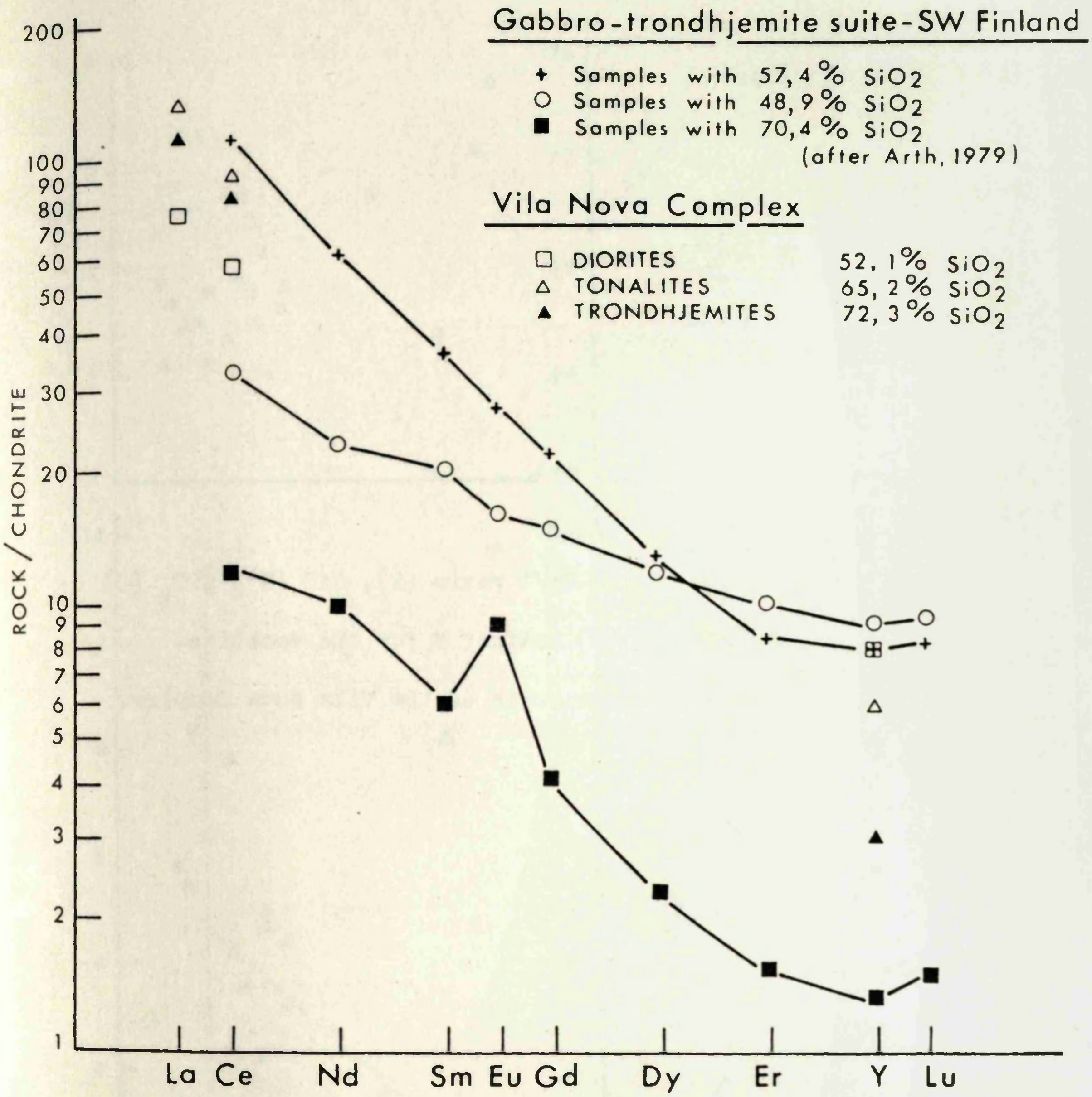
Gabbro-trondhjemite suite-SW Finland
+ Samples with 57,4 % SiO2
○ Samples with 48,9 % SiO2
■ Samples with 70,4 % SiO2
(after Arth, 1979)
Vila Nova Complex
□ DIORITES 52,1% SiO2
△ TONALITES 65,2% SiO2
▲ TRONDHJEMITES 72,3% SiO2
ROCK / CHONDRITE
200
100
90
80
70
60
50
40
30
20
10
9
8
7
6
5
4
3
2
1
La Ce Nd Sm Eu Gd Dy Er Y Lu

Figure V.15 Plot of the Ce/Y ratio (A), CaO (B), SiO_2 (C) and TiO_2 (D) against Y for the tonalite-trondhjemite suite of the Vila Nova Complex.

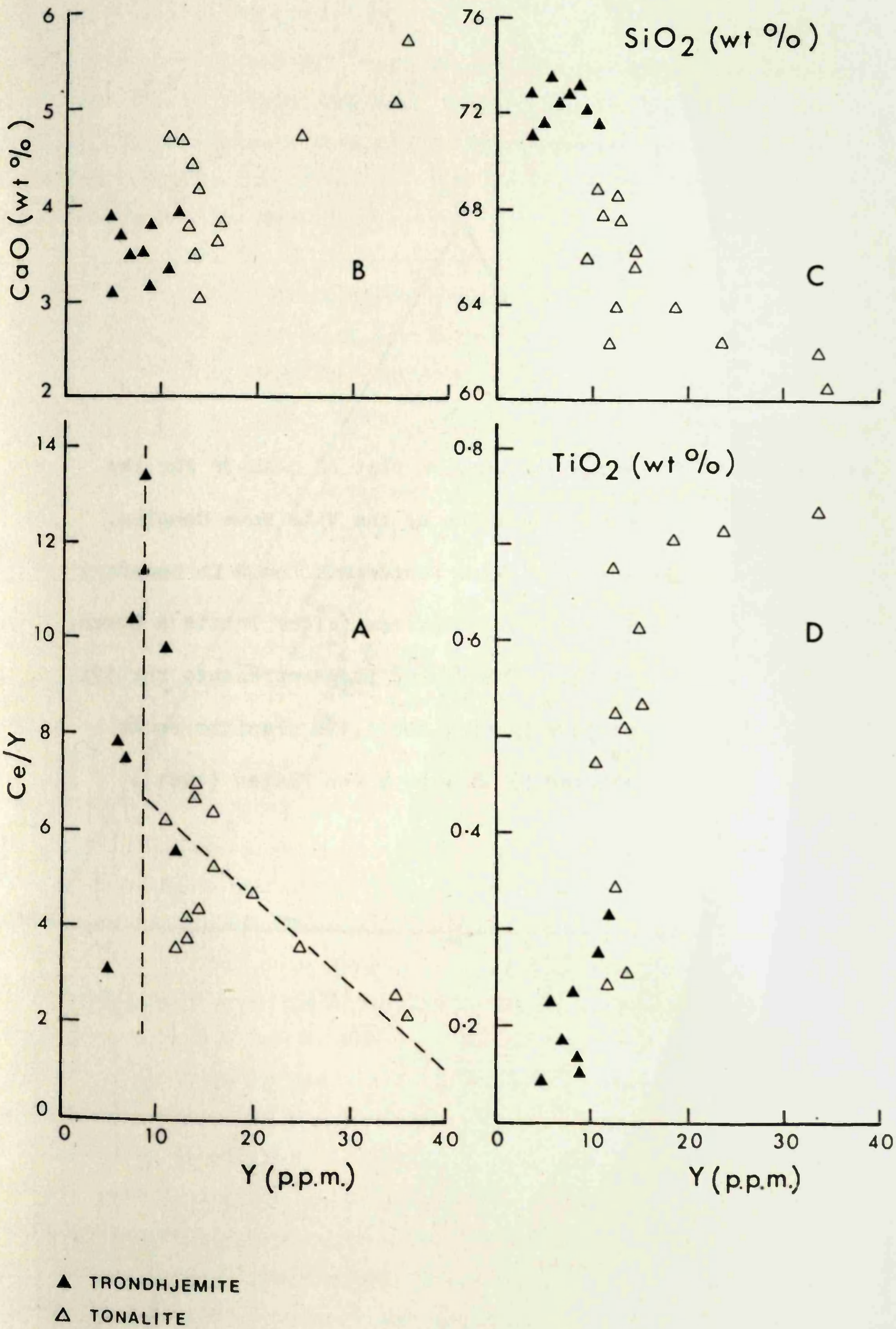

CaO (wt %)
SiO2 (wt %)
TiO2 (wt %)
Ce/Y
Y (p.p.m.)
A
B
C
D
TRONDHJEMITE
TONALITE

Figure V.16 Ternary normative plot of Q-Ab-Or for the intrusive rocks of the Vila Nova Complex. The solid line represents the 2 Kb boundary in the granite system (after Tuttle & Bowen, 1958). The dashed line represents the 53% contour line of the 1,190 granitic rocks studied by Winkler & von Platen (1961).

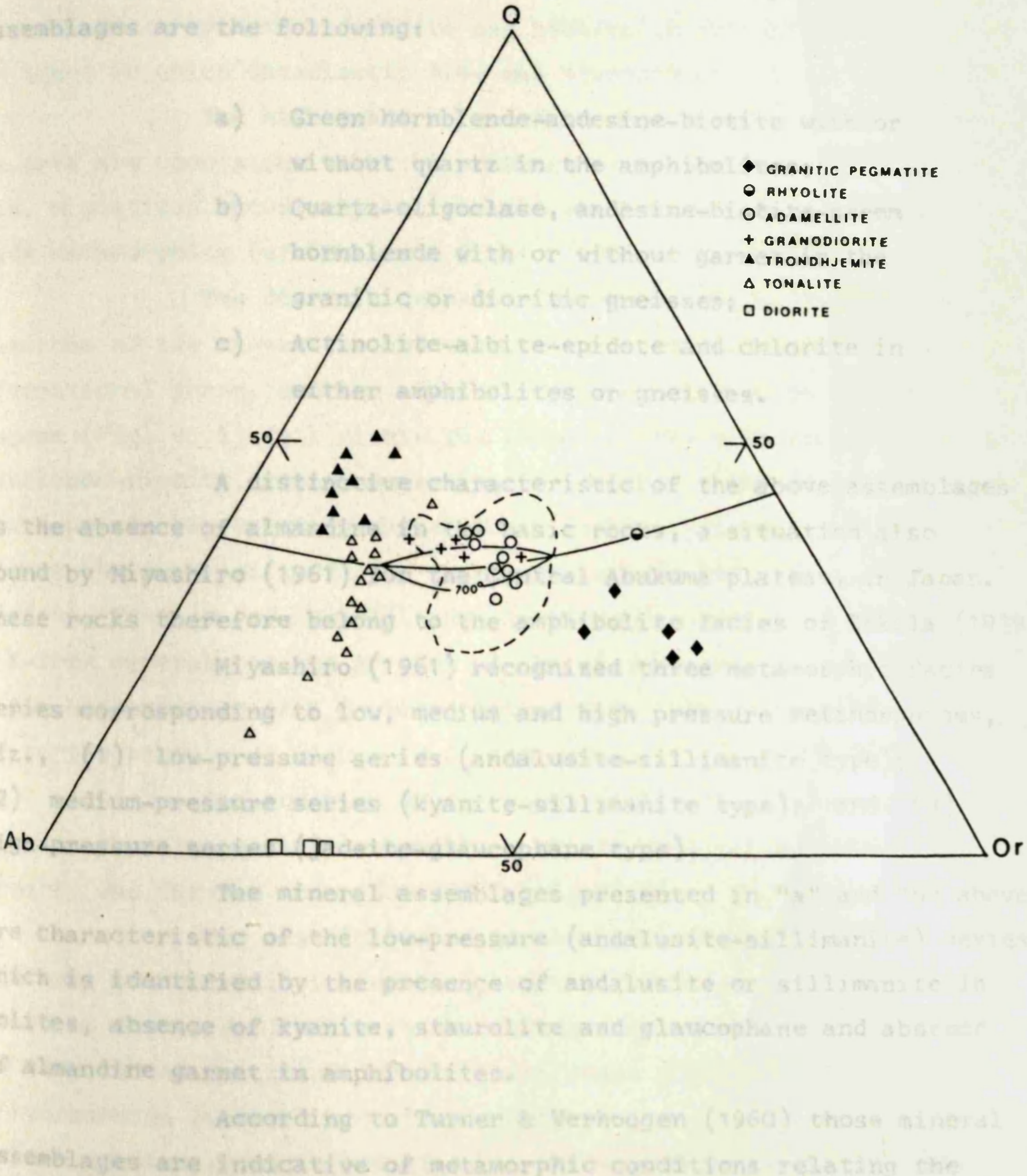
Q
◆ GRANITIC PEGMATITE
⊖ RHYOLITE
○ ADAMELLITE
+ GRANODIORITE
▲ TRONDHJEMITE
△ TONALITE
□ DIORITE
50
50
700°
Ab
Or
50

VI. METAMORPHISM

On the basis of the petrographic characteristics of the different rock-types existing in the area it can be concluded that the mineral assemblages and textures observed have resulted from a polymetamorphic process. The general metamorphic assemblages are the following:

a) Green hornblende-andesine-biotite with or without quartz in the amphibolites;

b) Quartz-oligoclase, andesine-biotite-green hornblende with or without garnet in the granitic or dioritic gneisses;

c) Actinolite-albite-epidote and chlorite in either amphibolites or gneisses.

A distinctive characteristic of the above assemblages is the absence of almandine in the basic rocks, a situation also found by Miyashiro (1961) for the Central Abukuma plateau, in Japan. These rocks therefore belong to the amphibolite facies of Eskola (1939).

Miyashiro (1961) recognized three metamorphic facies series corresponding to low, medium and high pressure metamorphisms, viz., (1) low-pressure series (andalusite-sillimanite type); (2) medium-pressure series (kyanite-sillimanite type); and (3) high-pressure series (jadeite-glaucophane type).

The mineral assemblages presented in "a" and "b" above are characteristic of the low-pressure (andalusite-sillimanite) series which is identified by the presence of andalusite or sillimanite in pelites, absence of kyanite, staurolite and glaucophane and absence of almandine garnet in amphibolites.

According to Turner & Verhoogen (1960) those mineral assemblages are indicative of metamorphic conditions relating the sillimanite-almandine-muscovite sub-facies of the almandine-amphibolite facies. Therefore, a low-pressure high-temperature amphibolite facies represents the maximum level of metamorphism in the area.

The mineral assemblage represented by actinolite-albite-epidote and chlorite is indicative of a retrograde metamorphic process which placed the rocks in the greenschist facies.

Dynamic metamorphism was a major element in this retrogressive process, as clearly evidenced by the break down of plagioclase in epidote and albite and biotite in chlorite, along the zones in which cataclastic flow was strongly operative.

The high-grade metamorphic conditions determined for the area are consistent with the presence of migmatites since, as a rule, migmatites occur only in terranes which have undergone high-grade metamorphism (cf. Ehlers & Blatt, 1980).

The dioritic gneisses, which in subarea IV are the paleosome of the migmatites and show features related to the first deformational phase, and the amphibolites when plotted on an ACF diagram (Fig. VI.1) fall within the compatibility triangle plagioclase-hornblende-biotite, relating amphibolite facies. The distribution of the points representing these rocks, is, in addition, similar to that of the amphibolite facies rocks with excess SiO_2 and K_2O of Orijärvi, Finland (cf. Eskola, 1915 in Miyashiro, 1973). The absence of K-free minerals on the AF side of the diagram can be accounted for by the high content of K_2O which reacted with them to form biotite, and to the paucity of Al_2O_3, Fe_2O_3 and MgO.

The position of the rocks within the amphibolite facies suggests that the maximum temperature of the regional metamorphism probably was between about 600-700^oC (Fig.VI.2).

The restriction of garnet in biotite-gneisses to areas adjoining grandioritic intrusions, together with the usual euhedral nature of the garnet indicates that the garnet growth is related to the very end of the third deformational phase (chapter VII), when nonhydrostatic stresses had stopped deforming the rocks but a high thermal gradient, due to granitic intrusions, was still in existence. The clouded plagioclases could be related to the effect of this thermal event, as well (cf.Poldervaart & Gilkey, 1954).

Considering the development of migmatites related to metamorphic conditions in which $P_{H_2O} = P_{total}$ (cf. Ehlers & Blatt, 1980) and on the basis of figure V.16 which shows that the granitic suite cluster around the eutectic composition for the system Ab-Q-Or-H_2O at 2Kb water pressure and temperature about 700°C, it can be concluded that by the end of the third deformational phase the rocks were subjected locally to thermal gradient about 100°C/km . This conclusion supports the inference regarding the formation of post-tectonic garnets in some rocks of the studied sequence.

FIGURES VI.1 - VI.2

Figure VI.1 Quartzofeldspathic dioritic gneisses; discordant amphibolites and a fine-grained concordant amphibolite of the Vila Nova Complex plotted on a ACF diagram for rocks with excess SiO_2 and K_2O in the low-pressure amphibolite facies (after Orville, 1969)

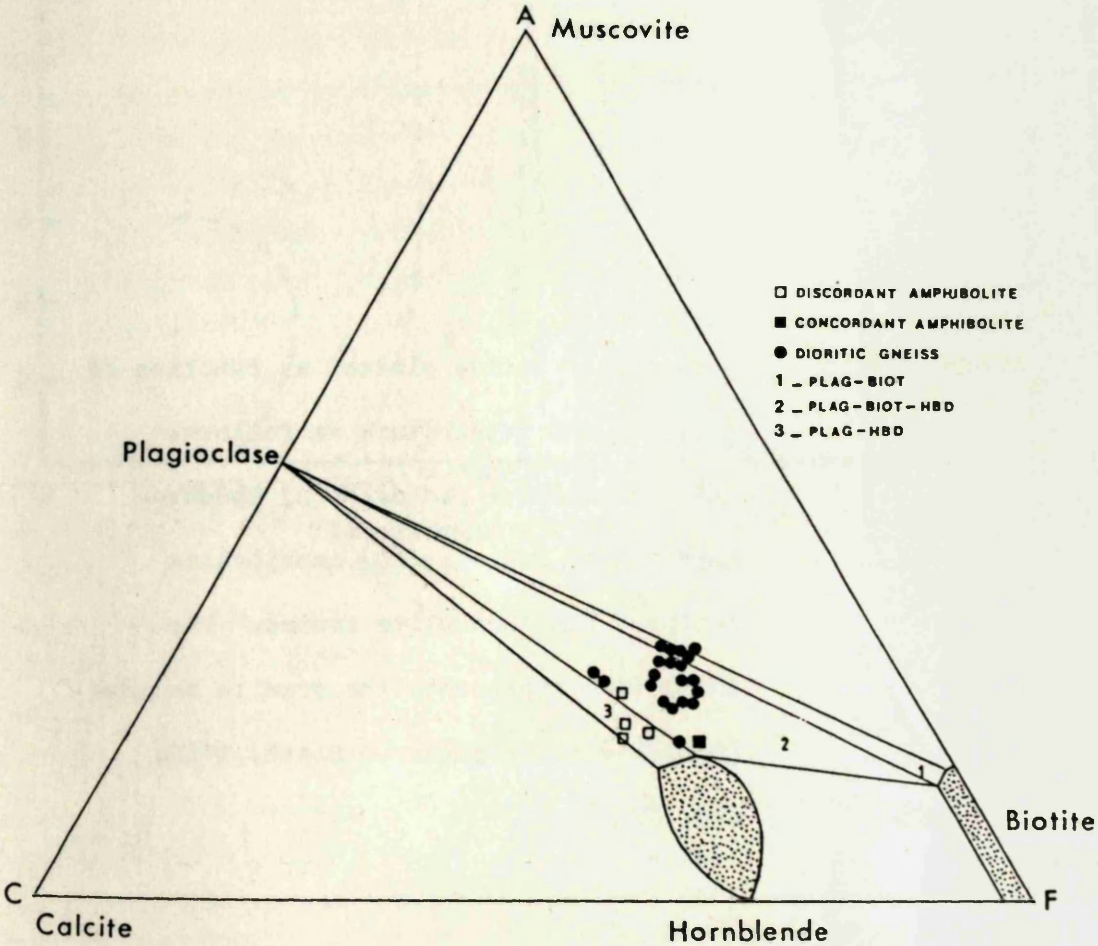

A
Muscovite
DISCORDANT AMPHIBOLITE
CONCORDANT AMPHIBOLITE
DIORITIC GNEISS
1 _ PLAG-BIOT
2 _ PLAG-BIOT-HBD
3 _ PLAG-HBD
Plagioclase
3
2
1
Biotite
C
Calcite
Hornblende
F

Figure VI.2 Metamorphic facies plotted as function of pressure and temperature as follows: (A) Greenschist facies; (B) Epidote-Amphibolite facies; (C) Amphibolite facies; (D) Granulite facies. The solid line represents the granite solidus (modified after Ehlers & Blatt, 1980, fig. 20.1)

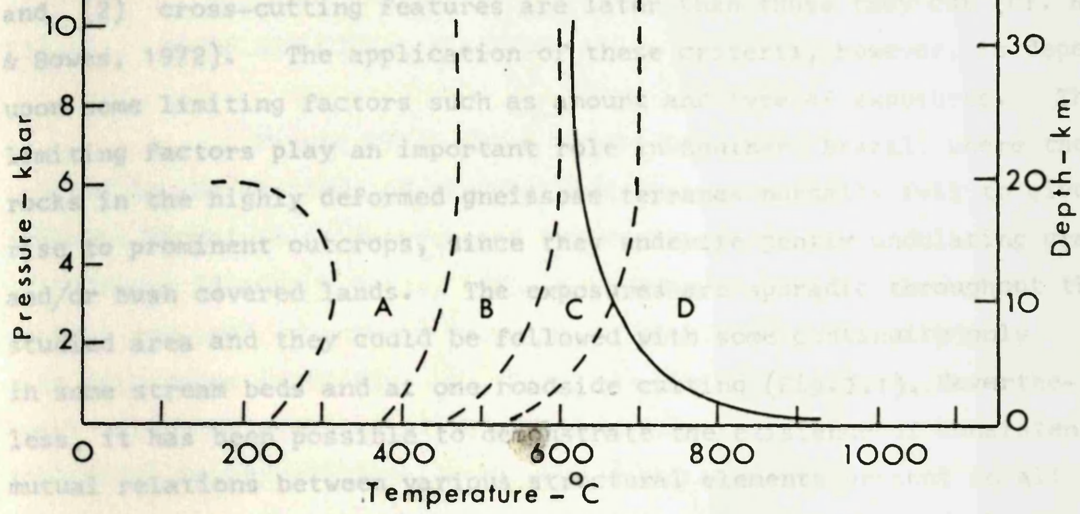

Pressure – kbar
10
8
6
4
2
0
200
400
600
800
1000
Temperature – °C
A
B
C
D
Depth – km
30
20
10
0

VII. STRUCTURE ANALYSIS

VII.1. INTRODUCTION

The criteria used in establishing a structure sequence are (1) deformed structures are older than those which deformed them, and (2) cross-cutting features are later than those they cut (cf. Hopgood & Bowes, 1972). The application of these criteria, however, is dependent upon some limiting factors such as amount and type of exposures. These limiting factors play an important role in Southern Brazil, where the rocks in the highly deformed gneissose terranes normally fail to give rise to prominent outcrops, since they underlie gently undulating grass and/or bush covered lands. The exposures are sporadic throughout the studied area and they could be followed with some continuity only in some stream beds and at one roadside cutting (Fig. I.1). Nevertheless, it has been possible to demonstrate the existence of consistent mutual relations between various structural elements present in all subareas. This has permitted the erection of a sequence of eleven deformational phases applicable to the whole region studied. These phases (cf. Hopgood 1980) are designated D_1, D_2, D_3, etc., and the equivalent fold sets produced by them are referred to as F_1, F_2, F_3, etc. Mesoscopic fold axes recorded on outcrops are designated as B_1, B_2, B_3, etc., whereas a fold axis determined statistically in stereoplots is represented by β (Turner & Weiss, 1963). Foliations or cleavages are designated by S_1, S_2, S_3, ... S_n, whereas lineations are represented by L_1, L_2, L_3, ... L_n. Deformational phases which post-date D_6 are grouped under D_{late} with individual phases designated by the strike of relevant axial planar cleavages, e.g., D_{010^o}, D_{150^o}, etc. As these cleavages are subvertical the notation also gives the axial trace direction of the folds of the particular phase.

The field work was based on the Brazilian Army Geographic Survey 1:50 000 sheet of Vila Nova and 1:25 000 air photographs. Detailed mapping of each subarea was carried out by using tape line and geologist's compass (Fig. VII.2 - VII.5)

The need for a versatile instrument capable of speeding up structural measurements and making them more accurate, gave rise to the development of a new version of the geologist's compass during the course of the field work. Details about this new instrument and its different field usages are presented as a separate paper, as an appendix of this Thesis.

VII.2. MAJOR STRUCTURAL FEATURES

Figure VII.1 shows on the basis of form lines related to the attitude of the dominant foliation (S_1) that the regional structure is represented by an alternating succession of non-cylindrical (Turner & Weiss, 1963) antiforms and synforms. The general regional structural trend as defined by the orientation of such structures is NE-SW. On a macroscopic scale the whole region looks quite homogeneous and this accounts for some of the misleading geological interpretations which have been presented by some workers.

In all subareas the major structure is represented by a NNE to NE-trending gneissose banding deformed by folds of varying style, size and orientation (Figs. VII, 2-4). Hence, in subarea IIIa the major structure is represented by a very open fold pair, with steeply plunging axis, which deform the gneissose banding (Fig.VII.4). Subarea IV (Fig. VII.5) forms the limb of a major fold, as indicated by the homoclinally dipping dominant foliation. This structural feature is also deformed by very open vertical folds (Fig.VII.30) apart from smaller and differently oriented folds. In addition, in this subarea the homoclinal feature can be demonstrated to be formed by a number of isoclinal to very tight folds so that the actual structural situation is that of folds deforming folds. Therefore, the regional structural "pattern" can only be interpreted in relation to polyphase deformation as will be demonstrated below. Figures VII.6,a,b which show the dispersion of poles to the gneissose banding S_1 and fold axes, respectively, recorded in all subareas supports the latter statement.

VII.3. DEFORMATIONAL PHASES

VII.3.1. Sequence and features

VII.3.1.1. Early features (Pre-D_1)

Early features are considered to be those which on the basis of field evidence are older than the earliest-recognized folds. These features include:

a) the presence of amphibolite layers with sedimentary parentage (Fig.V.11 and V.12);
b) quartzofeldspathic gneisses which originated either from pelites and/or semi-pelites or pelite-dolomite mixtures (Fig. V.11 and V.12);
c) layers of quartzite, within granitic gneisses, displaying a gross grading;
d) the reported occurrence of marble associated with gneisses which resemble those making up the rock assemblage in subarea IV, a few kilometers to the north of the latter (Picada & Lowatsky, 1962);
e) the occurrence of quartzofeldspathic and quartz vein neosomes.

The association of quartzites, paragneisses and para-amphibolites can be interpreted as representing a supracrustal unit. Thus, before the onset of the deformational processes which formed the first-recognized folds, the geological environment of the area was characterized by the deposition of sediments forming a pelite-psammite-carbonate association.

The quartzofeldspathic and quartz veins are likely the result of metamorphic segregation, a process commonly associated with a compressive stress system (cf. Bowes & Bhattacharjee, 1967; Halden, 1982). Whether this compressive stress was related to load generated by a thick lithological pile and the veins formed along the original layering (S_0) or whether they were related to pre-D_1 tectonism (such as thrusting) is a matter for conjecture. The association of layers with different composition with neosomes generated by metamorphic segregation gave rise to a gneissose banding which is hereafter designated as "original gneissose banding."

V.I 3.1.2. First deformational phase (D_1)

a) Folds

The earliest folds that can be placed in an overall sequence with confidence are isoclinal, intrafolial and rootless structures that deform quartzofeldspathic neosome in biotite-gneiss (Fig.VII.7.a, b, c,); blind quartz veins in micaceous bands (Fig.VII.8.a); and the original gneissose banding (Fig.VII.8.b). Such folds have, in general, very thick hinge zones compared to their limbs.

A characteristic feature of some of the quartzofeldspathic or quartz veins neosomes is that they are folded about F_1 axes without being accompanied by any other planar fabric (Fig.VII.7.a, b, c). This fact may suggest that the emplacement of these neosomes took place during late D_1 and were deformed by a continuing slip process, so that the foliation S_1 is axial planar to them.

As F_1 has been found always in flat 2D surfaces the determination of B_1 axes has been precluded.

b) Foliation

The deformation of the original gneissose banding by isoclinal folds was accompanied in the more mafic layers by the formation of a penetrative planar structure (S_1) which is marked by the dimensional orientation of biotite flakes and/or hornblende prisms (Fig.VII.7 and VII.8). Despite the effects of a number of superimposed phases of deformation this foliation can be recognized as such throughout the area with the layering and/or foliation, in practically every outcrop, involving the presence of S_1.

The original gneissose banding folded isoclinally about F_1 gave rise to a more complex compositional layering in which, apart from the original leucocratic and melanocratic alternating bands, there is a new structural element represented by the disrupted limbs of the F_1 folds. These disrupted limbs are seen normally as discontinuous quartzofeldspathic bands.

Except in fold hinges, the axial planar foliation to F_1 (S_1) parallels the compositional layering. This compositional layering is the most prominent feature relating S_1 throughout the area (Fig.VII. 9).

c) Lineation

Exposures do not permit measurements of the attitude of B_1 axes and no lineation which could with confidence be interpreted as being L_1 has been observed. However, in a three-dimensional exposure at the western end of subarea IV the southeastern limb of an F_2 fold which refolds F_1 there is a weakly expressed lineation which plunges gently NE (Fig. VII. 8.b). As F_2 plunges SW, this lineation cannot be L_2 and so the possibility exists that it represents L_1. If so, it can be concluded that B_1 and B_2 are not parallel.

VII.3.1.3. Second deformational phase (D_2)

a) Folds

F_2 folds deform the gneissose banding which parallels S_1 and refold F_1 folds (Figs. VII.8.b; VII.9 and VII.10). They vary from tight (Fig. VII.9 to isoclinal (Fig.VII.8.b) and some are intrafolial (Fig.VII.12.b).

In a single outcrop, as in subarea IV, they vary from very small folds with amplitudes of a few centimeters, deforming F_1 folds marked by very thin quartzofeldspathic veins (Fig.VII.10) to folds with an amplitude in excess of one meter, which deform F_1 folds marked by the composite gneissose banding (Figs. VII. 8.b and VII.9). In the latter situation the effects of younger deformations on F_2 are better expressed. Some F_2 folds in the western side of subarea IV are asymmetrical, having the SE limb stretched and parallel to their axial planes (Fig.VII.9.b). The nature of the hinges varies from angular (Fig.VII.9.a) to arcuate, (Fig.VII.8.b), and some display a thickened quartzofeldspathic layer in the outer part and a crumpled thinner layer of the same material in the inner part (Fig.VII.11).

Suitable exposures for measuring the attitudes of hinge line and axial plane are limited to the western side of subarea IV. There B_2 axes plunge at about $10^{\circ}/190^{\circ}-210^{\circ}$, the variation being the result of superimposed deformations. Except for the cases in which F_2 is affected by younger folds these structures are normally upright.

b) Foliations

In general, a prominent S_2 foliation marked by new mineral growth has not been observed. In places, however, a foliation axial planar to F_2 is evidenced by dimensionally oriented biotite flakes (Fig.VII.9b). When such a foliation is present in thin sections cut at high angle with regard to B_2, it is possible to see biotite flakes (S_2) cross-cutting the dominant foliation S_1 (Fig.VII.13). The development of S_2 was greatly controlled by the composition of the materials deformed. Thus, S_2 is never seen cross-cutting quartzofeldspathic layers or veins, being restricted to the more mafic bands of the deformed gneissose banding (Fig.VII.9b).

In the short limbs of asymmetrical F_2 folds, S_2 generally parallels S_1.

In places in subarea II, a mylonitic banding in which there are zones of concentration of very small detached F_2 hinges, makes up S_2 (Fig.VII.12).

c) Lineations

L_2 has only been recognized in subarea IV, and is represented by an intersection lineation which parallels B_2.

d) Igneous activity

A very prominent feature of subarea IV is the presence of tonalitic and trondhjemitic sheets varying in width from 15 to 35 cm emplaced generally parallel to F_2 axial planes (Fig.VII 9.a and VII.10.a). These igneous masses exhibit commonly pinch-and-swell features but they do not show any evidence of having been affected by F_2. The presence in such rocks of foliations making different angles with regard to F_2 axial planes indicates, however, they were disturbed by younger deformational phases. The identification of S_3 among the younger foliations allows one to conclude that the sheets were emplaced probably during late D_2.

The tonalitic-trondhjemitic sheets in subarea IV are cross-cut by a number of granodiotite veins, sometimes pegmatitic, of variable thickness, while in subarea IIIc they are seen truncated by a subhorizontal rock sheet. In addition, in subarea IV, the tonalite is seen cross-cut by a minor dioritic intrusion (transformed into amphibolite) in the eastern side of the outcrop. These cross-cutting relations, however, have not been observed with regard to the trondhjemites.

In the southern part of subarea I a large intrusion of tonalite is seen with a number of deformed xenoliths, of biotite schist oriented parallel to the dominant foliation.

Concordant tonalite sheets are also seen in different places in subarea II.

VII.3.1.4. Third deformational phase (D_3)

a) Folds

F_3 folds are by far the most abundant and prominent mesoscopic features throughout the area, and except for subarea IV they are readily recognizable. On account of this they can be used as key structures in the elucidation of the structural sequence. Together with other data, the distribution of F_3 axes as shown in figure VII.14 is an evidence that these folds developed on the limbs of major F_2 structures. As S_2 is weakly developed for the most part of the area, F_3 has deformed the compositional layering parallel to S_1. These folds are of variable style and size. Normally a particular style dominates in different places. Thus, the quartzite layers display very typical parallel folds in the middle part of subarea II (Fig.VII.15); symmetrical chevron folds are the characteristic feature of subarea IIIb (Fig.VII.16.a); close asymmetrical antiforms and tight synforms dominate in the southern end of subarea II (Fig.VII.16.b) and very appressed isoclinal folds are dominant in subarea IIIa (Fig.VII.17.a), the northern part of subarea II and in the middle part of subarea I. The size of these folds is related to their style. The chevron folds are small and have a wavelength and amplitude of a few centimeters, with a low amplitude/wavelength ratio as compared to the very appressed isoclinal folds which have also a wavelength of a few centimeters but the amplitude/wavelength ratio is very high; the close to tight folds have wavelength and amplitude between 1 and 2 meters with the amplitude/wavelength ratio of about 1.5.

The granitic veins exhibit open to close folds with very steep axes practically perpendicular to the earlier formed F_3 hinge lines. (Fig.VII.17.b)

The F_3 folds marked by transversal (in relation to S_1) quartzofeldspathic veins or granitic dykes, present characteristics somewhat different from the foregoing. The quartzofeldspathic veins are normally very thin, dip to opposite direction and intercept one another along a line which is perpendicular to the previously described F_3 axes. The axes of the folds formed by these veins plunge similarly either SW or NE but never to both directions in the same vein (Fig.VII.18). These folds differ from those F_3 which deform S_1 into two principal aspects, viz, (1) their dihedral interlimb angle is larger and (2) they plunge at steeper angles (Fig.VII.18). Some of these folds are symmetrical whereas others are asymmetrical, displaying a great difference in the length of two successive limbs.

In order to discriminate between the earlier formed F_3 axes and those displayed by the granitic dykes and the quartzo-feldspathic veins the notation F_{3b} and F_{3c}, respectively, is hereafter adopted and its meaning on genetic grounds will be discussed in section VII.3.4.

b) Foliation

An axial planar foliation to F_3 (S_3), marked by the dimensional alignment of biotite and/or hornblende, is normally well developed. This foliation can be seen normally cutting across S_1 (Fig.VII.19.a, b), and its expression is sometimes dependent upon variations in lithology. Thus, as shown in figure VII.15, when S_3 passes through the thickest of the quartzite layers it is refracted, becomes more spaced, and turns into fracture cleavage.

The most prominent examples of S_3 are related to zones in which the rocks are richer in biotite and/or hornblende (the mafic bands of the gneissose banding) and where there is evidence that slip took place (Figs.VII.15 and VII.19.a). Hence, the expression of S_3 is dependent upon both, type of lithology and intensity of strain.

In zones of high strain, F_3 folds are structurally transposed into a new compositional layering with the development of a feature which resembles an anastomosing mylonitic structure, very similar to that reported elsewhere by Collerson & Bridgewater (1979, Fig.11, pp220). Thus, in places, S_3 parallels a composite gneissose banding.

c) Lineations

The most conspicuous lineation L_3 is represented by a rodding formed by hinges of very appressed F_3 folds in quartzo-feldspathic material (Fig.VII.17.a). Where F_3 is represented by more open folds, with broad, rounded hinges (subarea II, southern part), L_3 is an intersection lineation, marked by the dimensional orientation of biotite and/or hornblende.

For the most part of the area, L_3 is seen plunging WSW but a reversal of plunge to ENE is seen in some places. The plunge of L_3, in general, varies from sub-horizontal to about 30^o; only in subarea I, middle part, in a zone in which F_3 is represented by very appressed folds, L_3 has been found plunging at an angle greater than 30^o.

d) Igneous activity

On the basis of cross-cutting relationships and particular structural features, a number of igneous masses varying in composition from granodiorite to adamellite, K-feldspar-rich pegmatite and a dyke of rhyolite, can be ascribed to different igneous activity developed during D_3. The granodiorites and adamellites form major intrusive masses or small veins.

The major granitic intrusions have been found always concordant with the dominant foliation, except for hinge zones of F_3 folds. They can be seen in places forming F_3 structures with a wavelength between 1 and 2 meters (Fig.VII.20), but in some instances the wavelength of these folds can be inferred to be in excess of 5 meters. Related to these major folds, large sub-horizontal sheets of granitic rocks have been found truncating the steep dominant foliation and, in some places, tonalitic sheets emplaced during D_2 (Fig.VII.21,a) In other places, thinner sheets moderately dipping to NW are seen folded about F_{3c} (Fig.VII.21.b). The general form of both types of intrusions is shown schematically in figure VII.22. In the southern part of subarea I a partly eroded antiform displays clearly the relationship between the structure and the igneous intrusions. There it is possible to see on the ground surface a sheet emplaced concordantly with the axial planar foliation to F_3 (S_3) and on a vertical section the same sheet connected to two other sheets of same composition separated by gneissic material making up the F_3 fold (Fig.VII.23).

On the surface of these folded granitic masses, apart from lineations related to younger deformational phases there is normally an L_3 lineation marked by the alignment of biotite flakes. In places where weathering and erosion have deeply affected the gneissic host rocks and masking their structures, remnants of folded inclined granitic sheets are of relevant value because their lineations L_{3c} are the only information about the attitude of F_{3c} axes (Fig.VII.21.b)

The granitic veins can be either concordant or discordant in relation to the dominant foliation and, in places, some of them are partly concordant and partly discordant (Fig.VII.24.a). The discordant thin veins, emplaced approximately perpendicularly to the dominant foliation normally display the effects of folding about F_{3c} axes, showing folds with thick hinges and thin limbs (Fig.VII.24.b). Some of these veins exhibit parasitic folds with appressed hinges and have the limbs boudinaged (Fig.VII.25.a). In some cases these veins are found as intrafolial folds exhibiting thick hinges with a lobate-type contact with the host gneissic rock in the concave side. The cusps formed by the deformation of the interface vein/gneiss point towards the vein (Fig.VII.25.b). On the other hand, the thicker discordant veins, as referred to above display open folds with steep F_3 axes.

The dyke of rhyolite is seen cross-cutting at a high angle the axial planar foliation of the F_3 chevron folds in subarea IIIc (Fig.VII.26.a). It displays a prominent intersection lineation trending SE in the range 110°-160° with a less variable plunge averaging 40°, the variation being the result of superimposed deformations (Fig.VII.26.b). In addition, this dyke is disturbed by very open folds whose axes plunge very steeply northward (F_{3b}), and display in the subvertical surface of the outcrop figures of interference reproducing a dome-and-basin pattern (Fig.VII.27.a, b). The folding of this dyke about the steeply plunging axes gave rise to the formation of a prominent fracture cleavage which intersects the subvertical surface of the outcrop parallel to the F_{3b} axes. An interesting feature displayed by this cleavage is its rotation (accompanied by the F_{3b} axes) about an axis parallel to its strike (030^{o}). This dyke displays also a primary structure represented by an isoclinal fold, which plunges SE and is marked by flow banding, in the contact zone with the gneissic host rock (Fig.VII.28). This folded zone is about 40 cm wide and no other similar folds have been found farther away from the contact with the country rock.

The K-feldspar-rich pegmatites form concordant sheets and are seen either in the limbs or restricted to the hinges of F_3 folds. Those emplaced along the limbs of the folds are normally boudinaged and deformed by very open folds related to subvertical late axes (Fig.VII.29.a).

The association of agmatite with the igneous activity developed in this deformational phase is extremely rare. Only in the southern part of subarea I a small occurrence has been found (Fig.VII.29.b). A breccia formed by fragments of granodiorite exhibiting rounded corners and cut across by folded veins of the same material has been found in subarea IIIb. The folded veins associated with this breccia display, as do similar veins in the area, thick hinges and thin limbs.

VII.3.1.5. Fourth deformational phase (D_4)

a) Folds

Evidence of folded features related to the fourth deformational phase are not so widespread as those of the earlier phases. They are rather limited and only in subareas II and IV a few structural features representing F_4 have been found. They are best developed in subarea IV where they deform the gneissose banding which parallels S_1, in the limbs of F_2 folds (Fig.VII.30.a). There, in places where tonalite sheets were involved in the deformations, the interface with the biotite-gneiss, which constitutes the country rock, developed mullion features (Fig.VII.30.a). In this surface there is a weak lineation which makes an angle of about 40^o with B_4 and is deformed by it. This lineation is L_3 and in figure VII.30.a its general trend parallels the orientation of the pencil. These F_4 folds have a dextral asymmetry,axes plunging gently towards SW, and axial planes steeply inclined to the NE.

In the northern part of subarea II, F_4 folds are also seen as structures with dextral asymmetry but in contrast to the previous example, they exhibit steeply plunging axes. These are related to axial planes whose traces on a horizontal surface trend 030^o.

A geometrical characteristic of the F_4 folds is the tendency of the folded layers manifest to maintain their thicknesses all over the folded structure. A schematic relationship of B_4 with other fold axes is given in figure VII.30.b.

b) Foliations

The most prominent planar structure related to F_4 is a very closely spaced cleavage which is seen cross-cutting the F_3 folds (subarea II, middle part), and is parallel to the F_4 axial planes (subarea IV).

c) Lineations

Apart from the lineation represented by the mullion features there is an intersection lineation trending 030° parallel to the axial planes of these structures.

VII.3.1.6. Fifth deformational phase (D_5)

a) Folds

Open to very open, symmetrical F_5 folds have been found throughout the area (Fig.VII.31.a, b). They deform S_1 in the limbs of F_2, F_3 and F_4 folds. They have subhorizontal axial planes and gently plunging axes trending ENE. Their wavelength varies from a few centimeters up to three meters.

b) Foliations

There is no prominent foliation associated with F_5. A weakly developed foliation marked by the orientation of small biotite flakes has been found in places, parallel to the axial planes of these structures.

c) Lineations

There is a conspicuous crenulation lineation parallel to B_5 in the biotite-gneisses of subarea IV (Fig.VII.31.b). This is the only expression of L_5 which has been observed.

VII.3.1.7. Sixth deformational phase (D_6)

a) Folds

F_6 folds deform the gneissose banding (S_1) generally as relatively large open folds with subvertical axial planes and very steeply plunging axes. On account of this, sometimes they are not readily recognized at an outcrop. For instance, the major structure in subarea IIIa is represented by an F_6 fold which is apparent only when the attitude variation of the gneissose banding is put on a map (Fig.VII.4). Similarly, the general attitude of B_6 in subarea IV was determined from a β diagram (Fig. VII.32). The most prominent expression of F_6 in a mesoscopic scale is in F_5-F_6 interference features (Fig.VII.33.a, b). On account of that, and at this scale, the attitude of the F_6 fold axes is controlled by the attitude of the previous surfaces (Fig.VII.33, a) and they plunge NW or SE at steep to moderate angles.

The practically perfect intersection in one point (Fig.VII.32) of the several S_1 planes recorded in subarea IV indicates the high cylindrical character of F_6, at least in this subarea. The effect of F_6 on earlier formed folds was significant, as indicated by the strong dispersion displayed by F_2, F_3, F_4 and F_5 in figure VII.34.

b) Foliations

No mineral growth has been found related to F_6 but a fracture cleavage (S_6) parallel to the axial planes of these structures is quite evident (Figs. VII.9.b and VII.33.b). Along these planes the crystallization of secondary quartz or carbonate was very common.

c) Lineations

The only linear element which has been found representing L_6 is the trace of S_6 on different surfaces. On account of the secondary crystallization which took place along S_6, "L_6" is readily recognized by the presence of white lines (secondary minerals), trending 130^o and cross-cutting the gneissose banding at high angles.

V.II.3.1.8 Late deformational phases (D_{Late})

A number of structural features occur which post-date the D_6 structures. They are expressed as open or asymmetrical folds, shear or fracture cleavages and healed cleavages which deform the S_1 gneissose banding and their mutual relationships cannot be demonstrated inequivocally. They are described below and an assessment of possible order of development is given in section VII.3.2. The most convenient way to refer to them is to use the trend of the traces they make on horizontal surfaces.

VII.3.1.8.1. Phases D_{010^o}- D_{110^o}

These two sets form kink structures which appear to be conjugate and are described together. Folds of the D_{110^o} phase are sinistral asymmetrical kinks (Fig. VII.35.a) whereas folds of the D_{010^o} are expressed by dextral asymmetrical kinks (Figs. VII.35.b and VII. 36.a). Where both sets of kinks occur together they result in the development of box folds (Fig.VII.36.b). The obtuse angle between both sets of cleavages is similar to that given by Anderson (1974) as the mean value found in the deformation of slates in experimental work, and to that observed in naturally occurring kink bands (Park, 1981).

No mineral growth has been found associated with these deformational phases, and the planar elements S_{010^o} and S_{110^o} represent normally fracture cleavages. The intersection of the gneissose banding by either S_{010^o} or S_{110^o} gave rise to strong lineations (Fig. VII.37.a). These lineated features are greatly dependent upon the angle of incidence of the sun on the rock surface to be discernible, and, on account of the large angle that exists between S_{010^o} and S_{110^o}, normally only one of the traces is observed in a certain rock surface. In addition, the intersection lineations in general have not been observed in the same outcrop together with kink bands.

VII.3.1.8.2. Phase D_{080^o}

Small, asymmetrical sinistral folds with subvertical axial planes striking 080^o are seen in subarea IIIa (Fig.VII.4).

The character of D_{080^o} as manifested by planar structures is variable. In places, as in the southern part of subarea I, S_{080^o} is represented by a foliation marked by the alignment of biotite flakes in a granodiorite sheet. In other places S_{080^o} is expressed by strongly developed shear planes, which, sometimes pass into mylonite zones (subarea II, middle part figures VII.3 and VII.7.b).

VII.3.1.8.3. Phase D_{150^o}

F_{150^o} structures are seen for the most part as very open folds with steeply plunging axes deforming the compositional layering. In places these warps are well marked by deformed granitic pegmatites emplaced in the limbs of F_3 folds (Fig.VII.29.a). In the northern end of subarea II a small F_{150^o} fold have been found deforming the southern limb of an F_3 fold in granitic neosome (injected gneiss) (Fig.VII.38.a)

A steeply dipping, spaced fracture cleavage is axial planar to such folds but it is also seen where no corresponding folds have been observed.

In subarea IIIa the most prominent feature with the 150^o orientation is represented by a set of spindle-shaped quartz veins (Fig.VII.4).

VII.3.1.8.4. Phase D_{170^o}.

This structural direction is represented only by cleavage planes. These are dominantly spaced fracture cleavage but the off-set of an adamellite vein by a granitic pegmatite emplaced along S_{170^o} in subarea IIIa (Fig.VII.4) indicates that shear displacement with a dextral horizontal component took place along these planes.

The most characteristic feature relating the 170^{o} orientation is expressed by a set of underformed granitic pegmatites cutting across the gneissose banding at high angles in places where the gneissose banding has not been affected by F_6 (Fig.VII.4). As a general rule these veins are much less affected by weathering than the host rocks so that they are readily identified in the field as prominent dykes positioned at high to moderate angles to the compositional layering. In places, instead of pegmatites, there are thin pink coloured bands due to enrichment in K-feldspar marking the $S_{170^{o}}$ planes. These feldspathized bands also resist more the effects of weathering and erosion than the host biotite-gneisses, forming parallel, elongate prominences on the ground (Fig.VII.38.b).

VII.3.1.8.5. Phase $D_{180^{o}}$

Asymmetrical, dextral $F_{180^{o}}$ folds related to subvertical axial planes striking 180^{o} occur in subarea IIIa (Fig.VII.4). A weakly developed foliation marked by biotite is associated with these folds in the northern part of subarea II.

However, the dominant planar structure associated with $D_{180^{o}}$ is shear cleavage. The distance between these planes varies throughout the area depending on the type of lithology which is affected by them. In subarea IV the shear nature of the observed $S_{180^{o}}$ planes is evidenced by the crenulation of planar elements representing $S_{080^{o}}$.

VII.3.2. <u>Evidence for sequential development of D_{Late} features</u>

As referred to earlier, there is no direct evidence in the field allowing one to place all the late deformational phases in a complete chronological sequence. However, on the basis of both mutual relations that are apparent in some places and mineral growth associated with some foliation development, an attempt can be made to achieve a reasonable chronological ordering of these phases. In this respect, the geological features represented in figure VII.4 are of great relevance. If the area represented in this figure is considered in the whole, it is possible to see that the overall structural pattern is that of a large F_6 fold. On the other hand, if this area is divided into smaller domains (Turner & Weiss, 1963) on the basis of the variation of the trend of the trace of the dominant foliation, it can be seen that structures of same generation maintain their attitudes irrespective of the domain in which they are found. This is reliable evidence showing that actually all structural features grouped as D_{late} are younger than F_6. In addition, it can be seen in the same figure that a pegmatite oriented to 170° in domain C is cut by a S_{150^o} cleavage showing readily the chronological relationship between these two deformational phases.

As referred to earlier, S_{010^o} and S_{110^o} have been considered as forming a conjugate set of shear planes and the absence of interference patterns where the two sets appear together supports this opinion. In domain D a pegmatite emplaced along a S_{170^o} cleavage plane, off-setting dextrally an adamellite vein, is cutting-across F_{110^o} folds so that another relation can be established.

The relation between the phases referred to above and phases D_{080^o} and D_{180^o}, however, are not conclusive on the basis of the evidence presented in figure VII.4. Nevertheless, as has been shown in subarea IV, S_{180^o} has crenulated S_{080^o}, which allows another relationship to be established. The only problem left is, therefore, to relate D_{180^o} to some of the other deformational phases.

Taking into account that among the late phases, mineral growth has been recognized only in relation to the development of S_{080^o}

and S_{180}o, and, in addition, assuming that the late tectonic evolution of the area was marked by continuously declining metamorphic conditions, D_{180}o can be considered as having taken place before the development of the conjugate set D_{010}o - D_{110}o. This conclusion, therefore, allows to establish a complete chronological sequence for the late deformational phases as shown in Table X, in which the age decrease from D_{080}o to D_{150}o.

VII.3.3 Discussion

On the basis of the available data the deformational sequence history of the area can be summarized as shown in Table XI.

The division of the structural sequence into phases does not imply that the orogenic deformation was episodic in character since, on the contrary it may have been a continuous and progressive response to a long-applied regime of compression with intensity varying in both time and space.

Pre-D_1: As has been presented in the section VII.3.1.1. the geological conditions prevailing before the onset of D_1 represented an environment in which sedimentation and volcanism took place. There is no evidence suggesting that deformational processes were operative during this early phase of the whole sequence. It is, therefore, assumed that the metamorphic segregations represented by quartzofeldspathic and quartz veins resulted from the compression exerted by a thick supracrustal pile. This metamorphic redistribution of certain elements in the original layering gave rise to the earliest gneissose banding (original gneissose banding) of the rock sequence making up the Vila Nova Complex. In the absence of evidence of deformation during this early phase, the original gneissose banding is considered as subhorizontal before the onset of D_1.

D_1: The intrafolial, isoclinal, rootless nature of F_1 folds is indicative of a significant degree of flowage manifested by the materials during deformation. This deformation gave rise to the strongest planar fabric (S_1) recognized throughout the area under P-T conditions compatible with amphibolite facies metamorphism. The thin veins of neosome deformed isoclinally, during late D_1 constitute an evidence of the low viscosity of the rocks by the time they were emplaced (Fig.VII.7) However, on the basis of the evidence that all rocks which display F_1 represent elements of a supracrustal pile it can be concluded that the low viscosity of the different materials is not necessarily a result of metamorphic conditions. On these grounds, it is possible to interpret the metamorphic fabrics as developed during late D_1, mimectically in relation to the slip planes, with the neosome being intruded into the rock sequence undergoing flowage. This fact could be an explanation for the absence of deformed fabrics around F_1 hinges in deformed quartz and quartzofeldspathic veins.

The strong flowage undergone by the rocks during D_1, which is expressed by the extremely strained features that can be observed everywhere in exposures of D_1 elements, allows one to deduce that this phase of deformation gave rise to large sub-horizontal rock sheets parallel to S_1.

D_2: On the basis of geometrical features, such as crumpling of the layers in the hinge zones and thinning along the limbs (Fig.VII.11) the formation of F_2 folds is interpreted as due to buckling accompanied by layer-parallel shortening (cf. Ramberg & Ghosh, 1968). As the expected effect of a subhorizontal compression on a layered sequence lying subhorizontally is the initial formation by buckling of folds with subhorizontal axes, then a subhorizontal disposition of S_1, before the onset of D_2 appears very likely. As the deformational process continued these folds progressively tightened. This is likely to have been associated with a marked increase in the amplitude of the folds accompanied by rotation of the F_2 axial planes, in places, until very inclined positions were achieved.

These features indicate that at the onset of D_2 the rocks were still very ductile.

Under the effect of the compressive stress-system the rocks progressively would behave in a less ductile fashion.

Evidence of such a change in the mechanical behaviour of the rocks during D_2 is provided by the existence of zones of intense movement parallel to F_2 planes, some of which are now represented by mylonite (Fig.VII.12.a,b) but most of which are represented by S_2 schistosity. These zones developed where F_2 folds were tight rather than isoclinal and they represent zones where there was release of pressure built up within a system in which adjustment by tightening of the folds was no longer possible. Had the rock sheet remained as ductile as it had been during the initial stage of this deformation then isoclinal folds would have developed instead of the zones of shear movement.

The control exerted by S_2 on the emplacement of the tonalite sheets and the evidence that they were not folded about F_2, but remained unfolded until the onset of D_3, indicate that (1) pressure release along the shear planes assisted magma injection, and (2) this took place very late in D_2. The latter conclusion is important for any future geochronological studies which could utilize the tonalites as time markers of late D_2 and indirectly indicate the time of major thrusting development. As younger structures commonly deform the limbs of F_2 folds, the latter are considered as possibly making up the major regional structures (Fig.VII.39). The mesoscopic example of F_2 may represent, therefore, parasitic folds relating large structures of same generation.

D_3: The superimposition of F_3 folds on F_2 structures is clearly brought out by the very distinct orientation of F_3 axes recorded in subarea II (Fig.VII.14). The relatively similar orientations of S_2 and S_3 may be interpreted as indicating that the overall compressive stress-system did not change its disposition between D_2 and D_3. However, different features relating these phases point to significant changes in the response of the rocks to the operating stresses. For instance, the strong pervasive character of S_3, well marked by the alignment of biotite and/or hornblende, together with a return to deformation being expressed as folds rather than as shear cleavages and mylonite formation, are indicative of important changes in P-T conditions.

The variation in F_3 style from one subarea to another (Fig.VII.15; VII.16 and VII.17) was related to differences in the rheological properties of the rocks from place to place together with differences in strain intensity and mechanism of deformation. Such variations lend support to the use of the consistent orientation of axial planes and linear metamorphic mineral growths, together with P-T conditions rather than fold style, in the characterization of successive phases of deformation (cf. Skinner et al., 1969). In addition, the variation in style of F_3 folds is dependent upon the degree of finite strain of the part of the tectonic zone in which the rocks were deformed. For example, the very appressed isoclinal folds with a high amplitude/wave-length ratio in the quartzofeldspathic layers in subarea IIIa (Fig.VII.17.a) whose hinges give rise to the prominent L_3 rodding, are the result of high strain concentration due to the intrusion of major granitic bodies (Fig.VII .4). There, as in other zones of high strain concentration, S_3 became very steep parallel to S_1, and F_2 folds were completely masked. Due to the strong transposition of S_1 by S_3 it is likely that there are intrafolial, rootless folds representing F_3 hinges which are indistinguishable from F_1 folds. The differences in mechanisms of deformation is expressed by the existence of such contrasting features as parallel folds and rootless folds with very thick hinges and thin limbs. In terms of the rheological properties of the rocks, D_3 is also characterized by other examples of contrasting features as those represented by either extension fractures (granitic dykes) or shear planes (quartzofeldspathic veins). This may be envisaged as due to a very active tectonic behaviour of the crust so as to change the physical conditions of the geological environment in a relatively short time-span or, alternatively, as a consequence of a long-lasting period of deformation. Although a long-lasting deformation (cf. Hopgood

& Bowes, 1978) was very likely an important factor influencing the mechanical behaviour of the rocks, the igneous activity which supplied the crustal rocks with heat at different stages during D_3, and generated very steep thermal gradients, is a reasonable cause for local variations in the rheological properties of the rocks. The overall deformational pattern of D_3 is consistent with a long-lasting progressive deformational process which can be divided into three main subphases which, in turn, can be subdivided into differnt stages, as follows:

1. Initial subphase - preceeds the igneous activity and is characterized by two stages, viz. (a) the formation of parallel F_3 folds, and (b) the formation of conjugate shear planes with metamorphic segregation of quartzofeldspathic material (quartzofeldspathic veins);
2. Intermediate subphase - is represented by the stage in which the major granitic intrusions were emplaced generating zones of high strain which deformed the previous F_3 folds to very appressed isoclinal features. The granitic material was also folded about F_3 axes.
3. Late subphase - characterized by (a) the intrusion of granitic sheets along transversal extension fractures and the opening of some shear planes with emplacement of inclined granitic sheets; (b) strong compression perpendicular to the compositional layering leading to flattening of the rock assemblage and folding by buckling of the transversal veins about F_{3b}; (c) superimposition of slip along S_1, on certain zones, affecting some of the buckled structures, generating similar-type F_{3c} folds. These features are described in more detail in section VII.3.4

D_4: The characteristics displayed by F_4 folds suggest they were developed by flexural slip along planes making up the compositional layering (Fig. VII.30.a). The mullion features developed in the biotite-rich layer underlying a tonalite-sheet, as shown in figure VII.30.a support such a conclusion, as does the absence of obvious variation in the thickness of the tonalite from the hinge to the limbs of this structure. The difficulty in observing effects of F_4 on earlier-formed lineations is likely a result of the small angular difference between them and F_4 hinges. A similar difficulty in polyphase deformed terrane elsewhere has been reported by Park (1969).

D_5: On the basis of the constant thickness of the folded materials as measured perpendicular to the compositional layering, along F_5 folds, it is suggested that flexural slip was also a major mechanism in the formation of these structures. However, the existence of a prominent L_5 crenulation lineation suggests that there was a certain amout of slip during D_5. As F_5 folds deform steeply dipping S_1 in the limbs of earlier-formed major structures (Fig.VII.31.a,b) the process of layer parallel compression which led to the initiation of F_5 folds by buckling may be considered as having been greatly enhanced by gravity (cf. Ramberg & Ghosh, 1968).

D_6: A general evidence of the effects of F_6 on older structures is a strong dispersion shown by the earlier-formed fold axes when plotted on a stereonet (Fig.VII.34). The pattern of dispersion exhibited by axes older than F_6, during D_6, is consistent with a deformation which took place under the influence of a stress-system whose principal compressive component acted along a NE-SW direction with the direction of "tectonic transport" (Sander, 1930; Turner & Weiss, 1963) or the "slip line" (Hansen, 1971) practically horizontal and trending 130°. This deformation, therefore, took place under the influence of a stress-system with an orientation rotated practically 90° in relation to the overall compressive system which prevailed until D_5.

D_{Late}: The contrasting features displayed by D_{080^o}, i.e. the presence of a foliation S_{080^o} marked by dimensional orientation of biotite, F_{080^o} asymmetrical folds and S_{080^o} shear cleavages may be interpreted on the grounds of variation in conditions favouring folding and mineral growth to conditions dominated by shear movements, including the formation of mylonitic bands. The same situation is observed relating D_{180^o} except for the absence in this case of zones of high concentration of strain as marked by mylonitic bands. The features representing these deformational phases are so similar that they could be considered as forming a conjugate set in the absence of the evidence that $S_{180}o$ crenulates $S_{080}o$ (subarea VI). The association of shear planes with features relating folds and foliations can be explained in the same way as similar features formed during D_2. The shear movements are the result of a different response of the rocks to the continuing compressive stress-system which initiated the folding. The weakly developed foliation $S_{180}o$ appears to represent the effects of a declining metamorphic grade. The deformational phases younger than $D_{180}o$ exhibit features compatible with a crustal behaviour progressively more brittle than that existing earlier. Thus, the emplacement of pegmatites and quartz veins along $S_{170}o$ and $S_{150}o$ planes, respectively, point to a crustal behaviour in which extensional mechanisms may have played a significant role.

The overall deformational sequence which has been discussed above closely resembles those set out by Hopgood (1973) for Precambrian crustalline terranes in Scotland, Greenland, Australia, Uganda and India particularly in the following ways: (1) the first fold set is isoclinal, intrafolial, rootless and represent remnants of structures formed under conditions of intense deformation, where flowage of the materials played a very significant role, and (2) the latest folds are open to broad warps that are generally upright and associated with axial planar quartz veins and fractures.

However, as pointed out by Hopgood (1973) despite the number of similarities which can be found relating different terranes in an overall general deformational pattern there are differences which make each set of structures distinctive for every particular orogen.

VII.3.4. Kinematics and strain analysis

VIII.3.4.1. Folding mechanism

In terms of folding mechanisms it seems that flexural slip played a very important role, and even the most similar-looking structures (eg. F_2 in subarea IV) when observed in closer detail reveal characteristics of parallel folds. Hence in figure VII.11 it is possible to see in the hinge zone of an F_2 fold a thinner layer crumpled by small flexure folds, adjacent to a thicker layer displaying a larger wavelength. Therefore, the folds which show geometrical features resembling those of similar type, must have acquired such features on account of further compression after being generated by a flexural mechanism. In other words, flattening (pure shear) of earlier formed flexural folds seems to be the real process leading to the generation of some structures that resemble similar folds, since this process results in modification of the constance of thickness of the folded layers, which become thickened in the hinge zones.

It has been claimed that a strong compression was imposed on the rocks throughout the deformational history of the area, but it is particularly well evidenced during phases D_2 and D_3. If it is assumed that this compressive process was not uniform, so as to give rise to a differential flattening of the rocks in both kinematic planes "ac"and "bc", it is possible to realize that a complex geometrical folding pattern has resulted (Ramsay, 1962). An important consequence of such a process of deformation is the reversal of plunge manifested by fold axes. In figure VII.40 it can be seen that the F_3 fold axes in subarea I as a whole manifest a tendency to be dispersed along a girdle oriented ENE-SSW what, actually, can be accounted for differential flattening. Furthermore, if this mechanism is envisaged as having been active in a macroscopic scale, as well, it might be an account for the formation of elongate dome-and-basin structures by the alternating distribution of acylindrical antiforms and synforms (Fig.VII.1). It must be pointed out, however, that this reversal of plunge of fold axes could also be related to pre-existing variations in attitude of the very steep foliation planes represeting S_1, S_2 and, perhaps S_3. Thus the reversal of plunge of F_3 axes from ESE to SW, along F_3 axial planes is more likely to have resulted from the superimposition of the D_3 deformation on the limb of F_2 folds (Fig.VII.14).

VII.3.4.2. Progressive deformation

Throughout the area there is evidence of progressive deformation and the various features of D_3 are particularly significant as indicative of a whole series of deformed states. In this progressive deformational process it is significant that deformation started with the formation of parallel folds and ended with the dominance of slip along S_1 planes. On kinematic grounds this fact is reflecting the effect of a continuously acting compression on rocks whose mechanical behaviour changed with time.

At the beginning of the deformation the compositional layering behaved actively in face of the compressive stresses and parallel folds developed. With the continuing of the compression the folds were progressively tightened. In zones where the rocks could no longer adjust to the stresses by tightening slip took place parallel to the S_3 axial planar foliation. The effects of slip are best seen in transversal, thin quartzofeldspathic and/or pegmatite veins. The attitudes of F_{3c} axes in quartzfeldspathic veins strongly suggest that such veins may be related to a previously formed conjugate set of shear planes. On the other hand, the attitudes of the granitic dykes folded about F_{3b} suggest they were emplaced along transversal fractures, in relation to F_3 axes ("ac" fractures, cf. Price, 1966).

The attitudes of the conjugate shear planes lead to the conclusion that a principal compressive stress (σ_1) must have acted vertically when they were formed. This conclusion is, however, puzzling if it is taken into account that such planes are considered as having been formed in accordance with the overall D_3 subhorizontal compressive stress-system. However, if before the formation of these planes, the granitic magma was already in existence at some depth in the crust, it is possible to conceive that this magma was also under the effect of the overall compressive stress. On the account of its "liquid" behaviour, the magma was under hydrostatic-type stress and transmitted pressure to the surrounding rocks. Therefore, it can be inferred that the rocks above the "magma chamber" were subjected to a pressure directed upward and proportional to the overall lateral compression. This upward directed pressure generated by the magma increased with time and was responsible for the rotation of the principal compressive stress from a subhorizontal position to a subvertical direction. At the onset of the development of the conjugate shear planes, the deformation took place in a ductile fashion and the pressure release accompaning shearing was too small to enhance upward movement of the magma but sufficient to promote the formation of quartzofeldspathic veins by metamorphic segregation. Later on, perhaps on account of an ever increasing vertical compressive stress, the rocks were subjected to tension laterally, so that magma intrusion along planes parallel to the dominant foliation took place. As a consequence of this magma intrusion the vertical compressive stress was released, the lateral tension regime vanished and a quick reorientation of the overall stress system succeeded, with a principal compressive stress acting again along a subhorizontal direction. This stress-system was responsible by the deformation of the granodiorite sheets about F_3 axes and enhanced the mineral growth marking the lineation L_3 seen in these rocks. The intrusion of the granodioritic sheets, added material to the compositional layering and made the rock assemblage thicker, and likely more resistent to compression. It appears that the effects of this stress-system lasted until the latest stage in D_3 when the rocks behaving in a more brittle state than in the earlier subphases gave rise to the formation of transversal fractures parallel to σ_1 (extension fractures), and opened some of the shear planes, promoting the intrusion of new granitic material. These intrusions are represented by the granitic dykes (Fig. VII.17.b), granitic pegmatites and a dyke of rhyolite (Fig.VII.26). Such rocks in the continuing of the compressive process were buckled, forming folds with F_{3b} axes and, in some places, influenced by late slip parallel to S_3. This stage of slip is responsible for the occurrence of F_{3c} folds and L_{3c} lineations, as well. This sequence of events is particularly well exhibited by the dyke of rhyolite in subarea IIIb. As this dyke cuts across F_3 folds and displays dome-and-basin interference pattern on its sub-vertical surface (Fig.VII. 27.a, b), at first sight the interference figures seem to be related to events younger than D_3. A closer examination of the structural elements that it displays, however, shows that its deformational history is, indeed, very complex. This complexity is quite apparent when the linear elements it displays on its sub-vertical surface are plotted on a stereonet together with some fracture cleavage planes (Fig.VII.41). These data interpreted on kinematic grounds can be properly ordered and an overall deformational process established.

The earliest structure recognized in this dyke is represented by an isoclinal fold plunging southeastward and marked by flow bands (Fig.VII.28). This structure is considered to have been formed as a result of differential flow when the magma uprise took place. The delay caused to the moving system by the contact with the host rock generated the differential flow forming the fold. This is consistent with the absence of primary folds in the dyke away from the zone of contact with the host gneiss. Apart from this "primary" structure, there are other features undoubtedly related to tectonic processes and that can be discussed on the basis of the observation of three distinct features (Fig.VII.41) as follows:

1) the traces of the fracture cleavages on the dyke's surface and the very steep F_{3b} fold axes are dispersed towards NW:
2) the dispersion exhibited by both, the southeastward plunging intersection lineation L_{3c} and the F_3 hinges, observed in the host rock:
3) the gradual change in dip that the fracture cleavage planes display from very steep, in the

middle part of the outcrop, to relatively gently close to the SE and NW ends (Fig.VII.27.a)

The fracture cleavage which parallels the steeply plunging axes F_{3b} is seen fanning in relation to the axial plane of these folds, giving rise to a convergent pattern which intersects in F_{3b} (Fig. VII.41). On this basis it can be envisaged as an initial stage of deformation in which a compression parallel to the length of the dyke gave rise to longitudinal shortening, followed by buckling of the dyke about steeply plunging axes F_{3b}, related to an axial plane striking 030°. This stage is considered to relate to the flattening stage of the late subphase which has been inferred as the cause of an overall buckling of transveral intrusive bodies, in relation to the dominant foliation (S_1).

After the buckling stage, slip took place and the superimposition of the two deformations gave rise to the dome-and-basin interference pattern. The perfect domal or basin-like shapes of these interference features is accounted for the intersection of the slip planes with the axial plane of the F_{3b} folds in such a way that the axis B_{3b} acted practically as pole to the slip plane. If figure VII,41 is examined with care it can be seen that the plane of best fit to the great majority of the L_{3c} lineations generated by the slip mechanism, practically, has the axis B_{3b} as its pole.

By comparing figure VII.14 with figure VII.41 it is possible to see that the plane of best fit to the lineations generated by slip (L_{3c}) has the same attitude of the axial planar foliation to F_3 folds in subarea II. In addition, the characteristic features of a shear plane as manifested by the latter is quite obvious. Also of significance is the fact that in figure VII.41 the lineations representing F_3 hinge lines in the banded gneiss cut-across by the dyke, fall along the same plane. The conclusion to be drawn, therefore, is that the generation of the interference figures in the dyke's surface was caused by the superimposition of slip along S_3 planes on previously formed F_{3b} folds.

The distribution of the F_3 fold axes on the diagram shown in figure VII.41, suggests some dispersion along the plane S_3, which is also manifested by the lineation L_{3c}. This indicates that the kinematic axis "a" must have been positioned between both types of lineations on the S_3 plane. On the basis of the geometrical relationships between B_{3b} and the slip plane S_3, "a" must have been very close to the intersection of the F_{3b} axial plane and S_3. For practical purposes "a" may be considered as actually representing the intersection of these two planes.

The dispersion of F_{3b} and L_{3c} along an averaged NW-SE girdle is accounted for a rotation undergone by all planar elements about an horizontal axis trending 030^o. This rotation can be understood as a consequence of an unbalanced shear couple acting parallel to the dyke, in such a way that the southeastern end was bent upwards and the northwestern end was bend downward. The movement must have been in its overall pattern, controlled by the attitude of the regional dominant foliation, and was related to a steeply inclined principal compressive stress. The effects of this rotation can be observed on the dyke's surface mainly by the attitude of the prominent fracture cleavage, but also by the bending of the intersection lineation L_{3c}, and the rotation of the dome-and-basin features (Fig.VII.27.a).

The dyke is also cut-across by S_4 fracture cleavages which is some places are seen as axial planar to F_4 folds (Fig.VII. 27a, bottom left). These D_4 structural elements <u>were not</u> affected by the rotational event. This is a strong evidence favouring the interpretation that all other structural features displayed by the dyke, and discussed so far, were acquired during D_3.

In the absence of evidence which could lead one to think of oriented xenoliths within a tonalite body occurring in the southern part of subarea I (Fig.VII.42) as being related to some shear zone, the conclusion to be drawn is that the deformation and orientation of the xenoliths was also the result of the strong compressive regime which acted during D_3.

The characteristics of D_3 in terms of fold style and deformational mechanism during stage (c) of subphase III closely resemble those reported by Hopgood et al. (1976) as representing the phase D_b in the polyphase deformed migmatites of the Skaldö region, Finland. Park (1969) has criticized correlations based upon style similarities. However, similar rock assemblages subjected to similar tectonic environments (P-T conditions, stress-systems, etc.) will exhibit similar structural features. As a corollary it can be said that similar rock sequences displaying structures which are in close resemblance may be conceived as having been subjected to similar deformational conditions. Thus, a significant outcome of the analysis of phase D_3 is the possibility of comparing the deformational mechanisms which were in existence by that time in the Sulriograndense Shield with those controlling the development of the structures in the migmatites of the Skaldö region during the time-span of the phase D_b of Hopgood et al. (1976).

VII.3.4.3. Features resulting from layer parallel extension

Some structures are clearly the result of the heterogeneity of the rock assemblage, subjected to a compressive stress-system. These latter features are related to competence difference between materials undergoing deformation. Subarea IV is particularly suitable for an analysis on these grounds on account of the layered inhomogenous nature of the materials which crop out. In this subarea a number of features resulting from extension can be distinguished when an analysis of two-dimentional finite strain is carried out. The most prominent of such structures are pinch-and-swell features exhibited by tonalite and/or trondhjemite sheets, inserted in the gneissic host rock (Fig.VII.43). As the more competent leucocratic layers are seldom separated into a number of pieces, it can be said that real boudins are not common. Furthermore, this fact leads to the conclusion that the difference in ductility between host rock and intrusive material, was not sufficient to enhance a very contrasting behaviour during the deformation. Nevertheless, some features do exist that can be regarded as "rotated"boudins (cf. Ramsay, 1967) (Fig.VII.44.a).

A fundamental characteristic of a rotated boudin is the lack of concordance between the orientation of the foliation of the matrix and that of the enclosed, more competent, material, at the zone which separates one boudin from another. In figure VII.44,a, this feature is extremely well represented and the high angle which exists between the foliation in the upper part of the leucocratic vein and the foliation in the matrix exhibits the effects of flowage. This phenomenon may be envisaged as resulting from faulting in the more competent material accompanied by simutaneous flowage of the more ductile surrounding material. According to Ramsay (1967), this is a common feature of rocks which have been boudinaged under conditions in which the competent material is not aligned parallel to a principal extension direction of the strain ellipse. On account of the asymmetrical arrangement of the foliation of the whole (host rock and competent layer) in relation to the strain ellipse (since deformation is considered in two dimensions) there is a differential rotation with the competent material rotating less than the more ductile matrix.

It must be pointed out that despite the fact that the conclusions drawn hitherto have been based on two-dimensional finite strain analysis, the deformations were not necessarily plane strain. As a matter of fact, if the pinched feature shown by a trondhjemite sheet in bottom right of figure VII.43.a, is actually, perpendicular to similar features seen in the subhorizontal surface of the outcrop, rather than a projection of those features on a subvertical plane, it is to be concluded that extension took place along the Y axis of the strain ellipsoid, as well. If such an assumption holds true the conclusion that can be drawn is that all directions within the rock sheet must have suffered extension during the process of deformation concerned. Therefore, this strain regime could, to some extent account for the presence of very disrupted folds lying parallel to the plane of the dominant foliation (S_1).

In the situation shown in figure VII.44.b, the development of the boudins was not restricted to the layer of amphibolite. The quartzofeldspathic injected gneiss which encloses the amphibolite was boudinaged, as well. A similar feature has been reported elsewhere by Findlay (1970) who considers that the development of boudins within boudins, is the result of different scales of competency contrasts controlling boudin generation, involving complex lithological assemblages. In the case dealt with here, the amphibolite contrasted in behaviour with the injected gneiss which, in turn, contrasted with the regional biotite-gneiss. It is also apparent from figure VII.44.b that an F_{3c} fold exhibits one of its limbs pinched by flow along the boudin's necking-zone. This feature indicates that the formation of some amphibolite lenses can be related, at least, to the very end of phase D_3 when the rocks, having achieved a limit for contracting perpendicular to their strike, yielded by layer-parallel extension. This period of deformation may represent that just predating the onset of extension fracture development. If so, it could represent the latest period in which rock flowage took place within D_3.

VII.3.4.4. Shear zones

On the basis of what has been said in the discussion of the evolution of the structural sequence, a feature which is problematical is the existence of zones of highly sheared rocks between zones of much less deformation. This outstanding tectonic characteristic of the area is very similar to tectonic patterns reported elsewhere by some workers (eg. Ramsay & Graham, 1970; Hopgood et al., 1976). These zones of movement, which influenced to a great extent the mechanical behaviour of the rocks, persisted until the time that D_{Late} deformations took place and were responsible by the formation of some asymmetrical fold sets in zones where the general behaviour was essentially brittle.

Some folds developed in transversal veins were, later on, subjected to a process of flattening, resulting from simple shear rather than pure shear. Rotated S_1 along with F_1 rootless folds, can be seen in some places in accordance with a deformational event related to a sinistral couple (Fig.VII.45.a). Evidence of dextral shear zones may be seen throughout the area, as for example in the southern part of subarea I (Fig.VII.45.b). These zones are considered to be related to a compressive stress-system which acted along a direction ENE-WSW.

The effects of this particular deformational process can be seen varying as a function of the position of the elements of the earlier formed structures in relation to the orientation of the principal axes of deformation. Hence, in figure VII.46.a a grandiorite vein folded about F_{3c} displays clear extension along one of the limbs and contraction along the other one. The strain ellipse inset in this figure is a possible interpretation of the finite strain displayed by the vein. The undeformed layers of tonalite between the limbs of the fold are considered to be parallel to lines of no finite longitudinal strain. The overall pattern of deformation is related to a shear zone generated by a dextral couple acting parallel to the compositional layering (S_1),

The shear strain which corresponds to the strain ellipse shown in figure VII.46.a is about 0.35 and X/Z = 2.0. On the other hand, the analysis of the rotated boudin leads to the conclusion that a compressive stress-system with a direction SSE-NNW was responsible for the sinistral displacement which can be deduced from this structure. The strain measured in the latter is about 40 and X/Z = 6.5 (Fig.VII.46.b).

The conspicuous colour striping displayed by the host gneisses close to the contact with the trondhjemite sheet forming the rotated boudin (Fig.VII.44.a and VII.46.b) may be accounted for differentiation of the more mobile minerals (quartz and plagioclase) as a result of the rock movement. Thus, it may be inferred that in such zones of displacement, apart from simple shear, a certain amount of volume change may have taken place, as well (cf. Ramsay, 1980).

Gash veins filled with carbonate and also related to a sinistral shear movement, may represent a final stage in this deformational event (Fig.VII.47).

In both types of shear zones described, the orientation of the planes of movement was controlled by the strong anisotropy of the rocks, due to the existence of the compositional layering or the dominant foliation S_1, along which all the displacements took place. This fact, might explain the absence of sigmoidal schistosities with varying displacement gradient profiles within the shear zones, as reported elsewhere (cf. Ramsay & Graham, 1970; Beach, 1974; Ramsay, 1980; Park, 1981).

Very interesting examples of shear movement can also be seen on a microscopic scale as represented by features other than granulation or cataclases. Thus, in figure VII.48.a is shown an aggregate of chlorite bending under the influence of a dextral couple, whereas in figure VII.48.b a porphyroblast of plagioclase, dimensionally oriented parallel to a shear plane, in which sinistral movement took place, exhibits a set of fractures filled with albite and displaying some effects of progressive deformation (as manifested by a tendency to a sigmoidal shape). These features may be considered as the microscopic equivalents of tension gashes.

The two episodes of shear movements described above may be related to tectonic conditions which induced stress absorption during deformation to be accomplished by wrench-like movements.

VII.3.4.5. Viscosity contrasts

Unlike materials emplaced concordantly with the compositional layering, discordant veins or pegmatites provide evidence of contraction during deformation. The pegmatites and veins that have thickness greater than 30 cm form open folds or warps as a result of compression parallel to their length, as discussed above. The thinner quartzofeldspathic veins, however, develop tighter folds. These features are in accordance with theoretical and experimental evidence which shows that the dominant wavelength of a buckled material of viscosity μ_1 within another one with viscosity μ_2, being $\mu_1 > \mu_2$ is directly proportional to its thickness "t" (cf. Biot, 1961; Ramberg, 1959, 1963). The position of the cusps formed in the interface host rock/vein (Fig.VII.25.b) pointed to the deformed granitic veins leads to the conclusion that the viscosity of the intruded vein was higher than that of the host gneissic rock when their deformation took place (cf. Park, 1983). This conclusion shows that a certain time elapsed between the intrusion of the igneous masses and their deformation. If it is taken into account that the intrusion of the transversal veins was enhanced by the brittle behaviour of the rocks that would preclude any deformation by slip (flow). The latter conclusion is consistent with time-related changes in the crust, which put the rocks again under ductile conditions.

VII.3.5. Stress-system analysis

On the basis of the average strike of S_1 being 060° and the axial trends of F_2 to F_4 being within 20-25° apart of one another, it can be considered that the principal compressive stress before D_6 was approximately NW-SE. This assumes that D_1 was oriented at right angles to the XY plane, an assumption which may be invalid. During D_5, although maintaining a similar trend, this compressive stress was disposed steeply, tending to become vertical. However, from D_6 onwards, the evidence points to it acting at low angles and NE-SW, i.e., almost at right angles to the previous disposition. As an evidence of the orientation of this late principal compressive stress the bisectrix of the obtuse angle formed by the conjugate planes $S_{010^{\circ}}$ and $S_{110^{\circ}}$ has a trend 060°. In addition, the geometry of this conjugate set of planes is comparable to that of reverse kink bands (Dewey, 1965). This indicates that the formation of these structures was unrelated to the stress system responsible for the previous buckling of the rocks because then they would be expected to display a geometry corresponding to that of normal kink bands (Dewey, 1965). Thus, the geometry of $D_{010^{\circ}}$-$D_{110^{\circ}}$ kink structures implies a principal compressive stress at low angle, or parallel to, the dominant fabric S_1 (cf. Cobbold et al., 1971).

A compressive stress acting along a NE-SW direction is also consistent with the dextral movements associated with $S_{170^{\circ}}$ and $S_{180^{\circ}}$, and with the sinistral displacements along $S_{080^{\circ}}$.

Analysis of boudinaged veins, rotated boudins and gash veins, indicates the effects of two distinct stress-systems which were responsible for shear movements parallel to the dominant fabric S_1. One of these is related to sinistral displacements and its orientation is consistent with that of the stress-system which accounts for D_6 and D_{late} phases. On the other hand, the other stress-system, which led to extensive dextral shear along planes making up a very anisotropic rock assemblage, cannot be related to that associated with the development of phases D_2 to D_5. On the basis of the experimental work carried out by Donath (1961) concerning the development of shear failure in anisotropic rocks, it can be concluded that the compression related to the dextral couple was oriented in the range 060^o-090^o. On the same basis, the compressive stress related to the sinistral couple can be considered as having acted in the range 030^o-060^o.

As dextral couples relating the approximately E-W compressive stress-system are seen affecting structures older but not younger than those of D_6, it is assumed that the sinistral shear zones are younger than the dextral ones. This conclusion is significant in establishing an overall tectonic evolution for the area which from a dynamic point of view can be summarized as follows:

1) a first episode which includes deformational phases up to D_5 and had an overall compressive stress system with general direction NW-SE (σ_{1A}). Early orogenic stage.
2) an "intermediate" episode related to the development of shear zones parallel to the dominant composite foliation (S_1) characterized by dextral displacements and moderate strain. Stress-system σ_{1B}.
3) a late episode characterized by the development of sinistral displacements along shear zones parallel to the dominant composite foliation (S_1), accompanied by high strains, apart from all the deformations under the heading D_{late}. Stress-system σ_{1C}. Late orogenic stage.

As illustrated in figure VII.49, the overall pattern of compression in the rocks making up the Vila Nova Complex could be interpreted as representing a continuous (and long lasting ?) deformational process, accounted for the counterclockwise rotation of the principal compressive stress-system. The significant change in the orientation of σ_{IC} as compared to that of σ_{1A} could also, be related to the development of a distinct orogenic episode. However, the continuation of the metamorphic conditions until D_{180^o} and their progressively declining characteristic onwards, in addition to the similar evolution manifested by igneous events, which appear to have started early in the first orogenic stage and ended when the crust achieved stabilization in $D_{150^{o}}$, point to a long-lasting progressive deformational history within a single major orogenic episode.

TABLE X. FEATURES RELATED TO THE LATE DEFORMATIONAL PHASES (D_{Late})

PHASE	FOLDS	FOLIATION	MINERAL GROWTH	INTRUSIONS
D_{150^o}	---	Fracture cleavage	---	Quartz veins
D_{170^o}	---	---	---	Pegmatites
D_{010^o}-D_{110^o}	Kink bands, box folds	Shear cleavage	---	---
D_{180^o}	Asymmetrical dextral kinks	Foliation and shear cleavage	Biotite	---
D_{080^o}	Asymmetrical sinistral kinks	Foliation and shear cleavage	Biotite	---

TABLE XI. OUTLINE OF A SEQUENCE OF DEFORMATIONAL EVENTS AND PRINCIPAL IGNEOUS ACTIVITY IN THE VILA NOVA COMPLEX

9. Late deformations (D_{Late}) which took place in a crust less ductile than that affected by the older deformations, so that the main features related to them are fracture cleavages. In places, some warps and small asymmetric folds, related to zones of more intense strain, can also be seen. These phases are represented by a heading where is indicated the trend of the related cleavages and the chronological succession appears to be: D_{010}o-D_{110}o (conjugate set); D_{080}o; D_{180}o; D_{170}o and D_{150}o according to their decreasing age.

8. Deformation D_6, characterized by very open F_6 folds, with steep dipping axial planes and, more frequently, by fracture cleavage trending 130°. From the superimposition of F_6 on F_4 well formed figures of interference of basin-and-dome type.

7. Deformation D_5, characterized, normally, by symmetric F_5 folds with subhorizontal axial plane. These folds can be identified throughout the area. Strong axial planar foliation is not prominent, so that the identification of this fold set depend on its style. In places a strong crenulation lineation L_5 parallels B_5.

6. Deformation D_4, characterized by asymmetrical folds with axes displaying a variety of plunges, depending upon the part of the older structures where they developed. The fold have steep dipping axial planes, and an axial planar foliation is not prominent. Their occurrence throughout the area is very limited.

5. Deformation D_3, probably involving a considerable time-span and constituted by three sub-phases, namely, (1) initial sub-phase, which is characterized by formation of folds by flexural mechanism and conjugate sets of shear planes accompanied by metamorphic segregation of quartzofeldspathic material. This sub-phase preceeds any D_3 igneous activity; (2) intermediate sub-phase, represented by major granitic intrusions, which generated, in places, zones of high strain in which the previous F_3 folds were deformed to very appressed isoclinal folds; (3) late sub-phase, which is characterized by (a) the intrusion of granitic sheets along either transversal extension fractures or some of the conjugate shear planes, (b) flattening of the rock-assemblage causing buckling of the transversal veins or dykes, (c) superimposition of slip on earlier-formed D_3 structures generating, in places, dome-and-basin interference figures or similar-type folds, depending on the orientation of the previous structures in relation to the direction of slip.

4. Intrusions of tonalitic magma along zones of high movement developed in late D_2.

3. Deformation D_2, deforming the composite foliation S_1 and refolding F_1, about F_2 axes. Intense movement, in a late event, along planes parallel to the axial planes of the F_2 folds, but mainly localized along the limbs, giving rise to the formation of some intrafolial folds.

2. Deformation D_1, leading to the formation of a strongly transposed gneissose banding lying subhorizontally, and of the present isoclinal intrafolial rootless folds (F_1). This phase seems to be responsible for the main gneiss-forming event, and is characterized by very strong deformation. The formation of a composite gneissose banding is assumed as having taken place during the movement of a very large lithological layered sheet.

1. Deposition of a supracrustal pile composed of semi-pelites or pelites, pelite-dolomite mixtures, dolomites (to the north of the studied area, Picada & Lowastky, 1962) and quartzites. Metamorphic seggregation of quartz or quartzofeldspathic material, and formation of an original gneissose banding.

FIGURES VII.6 TO VII.49

Figure VII.6.a	Plots of poles to S_1 for the whole area (equal area net).
Figure VII.6.b	Plots of folds axes of different generations for the whole area (equal area net).

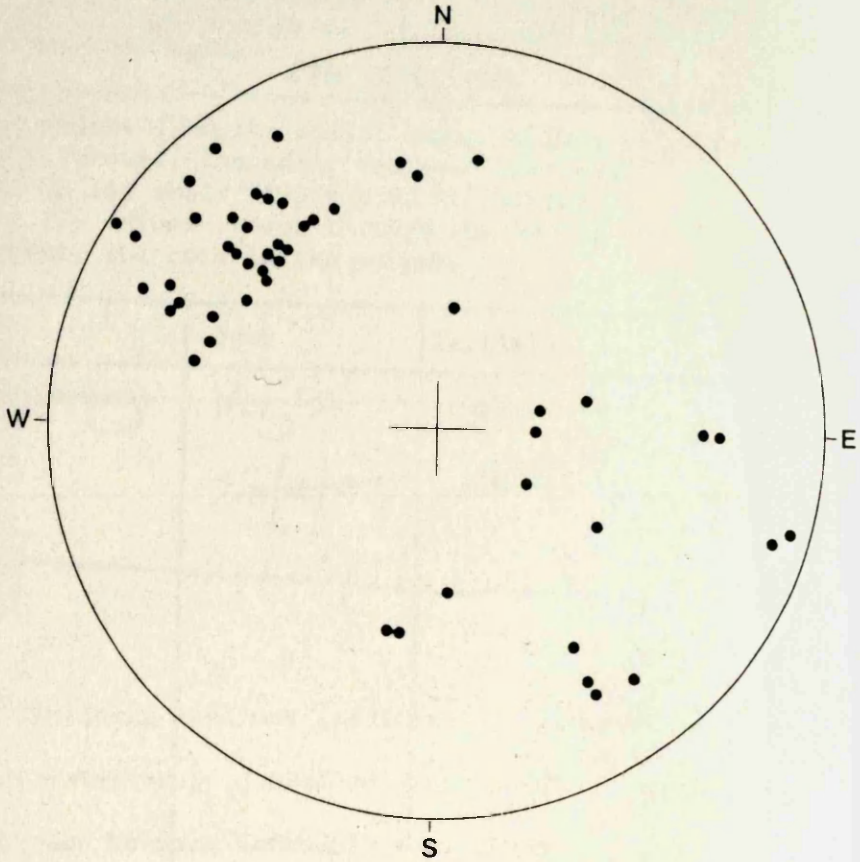

(a)

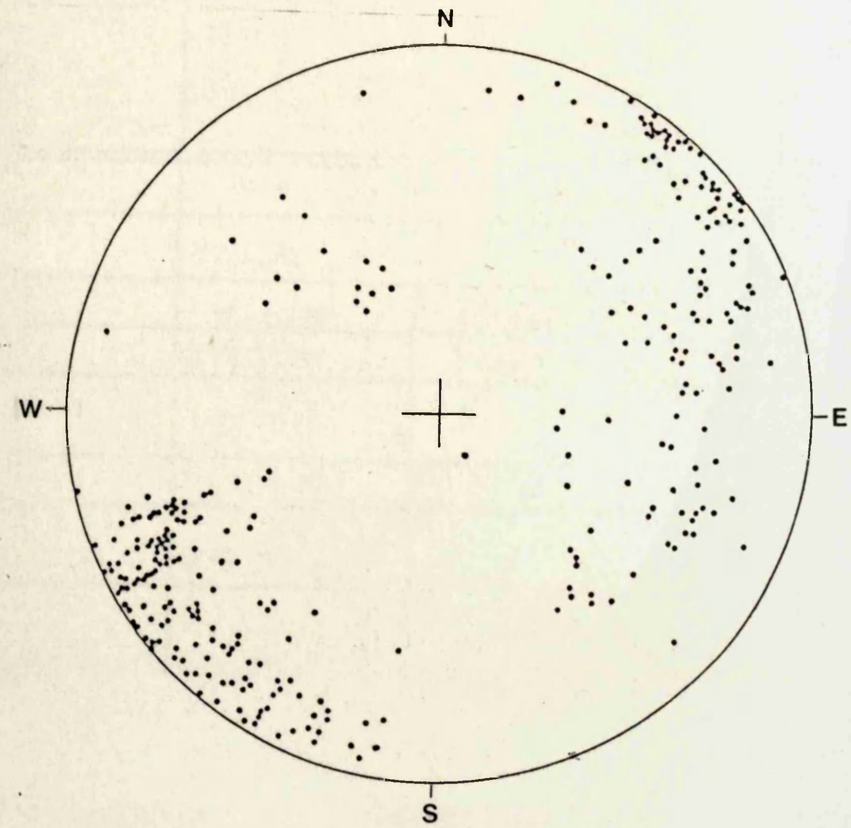

(b)

Figure VII.7.a,b,c. Intrafolial, rootless isoclinal F_1 folds shown by late D_1 quartzofeldspathic veins, in a micaceous band of quartzofeldspathic dioritic gneiss; subarea IV, eastern end (drawings from photographs).

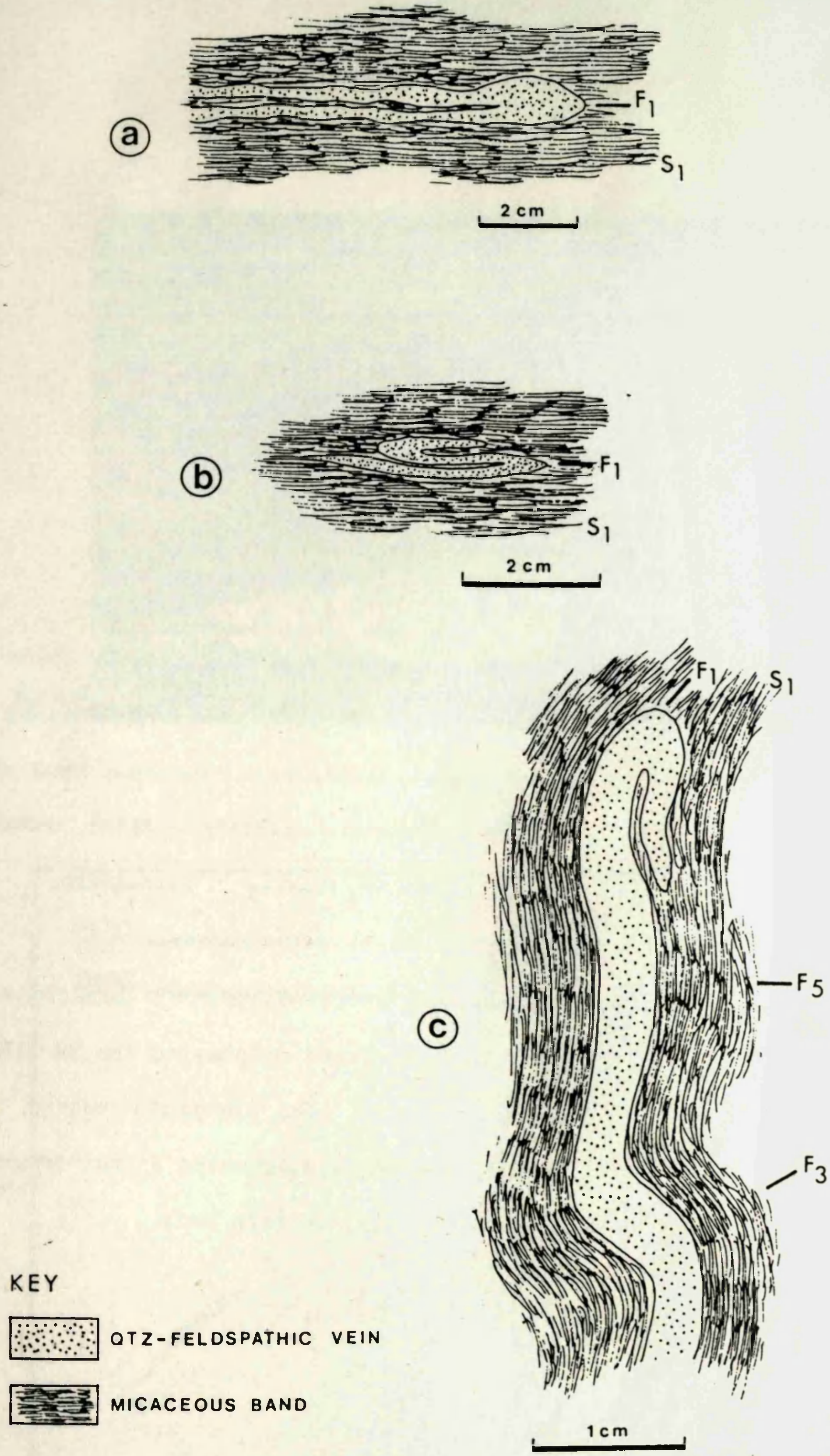
a
F_1
S_1
2 cm
b
F_1
S_1
2 cm
c
F_1
S_1
F_5
F_3
1 cm
KEY
QTZ-FELDSPATHIC VEIN
MICACEOUS BAND

Figure VII.8.a Intrafolial, rootless, isoclinal F_1 folds shown by a blind quartz veins, exhibiting a very thick hinge, in a micaceous band of quartzofeldspathic dioritic gneiss; subarea IV, eastern end; looking southeast.

Figure VII.8.b F_2 refolding isoclinally an F_1 intrafolial isoclinal fold, and displaying the SE limb affected by F_5. The plunging lineation seen in the inner surface of F_2 may represent L_1; subarea IV, western end.


CRT
S1

a

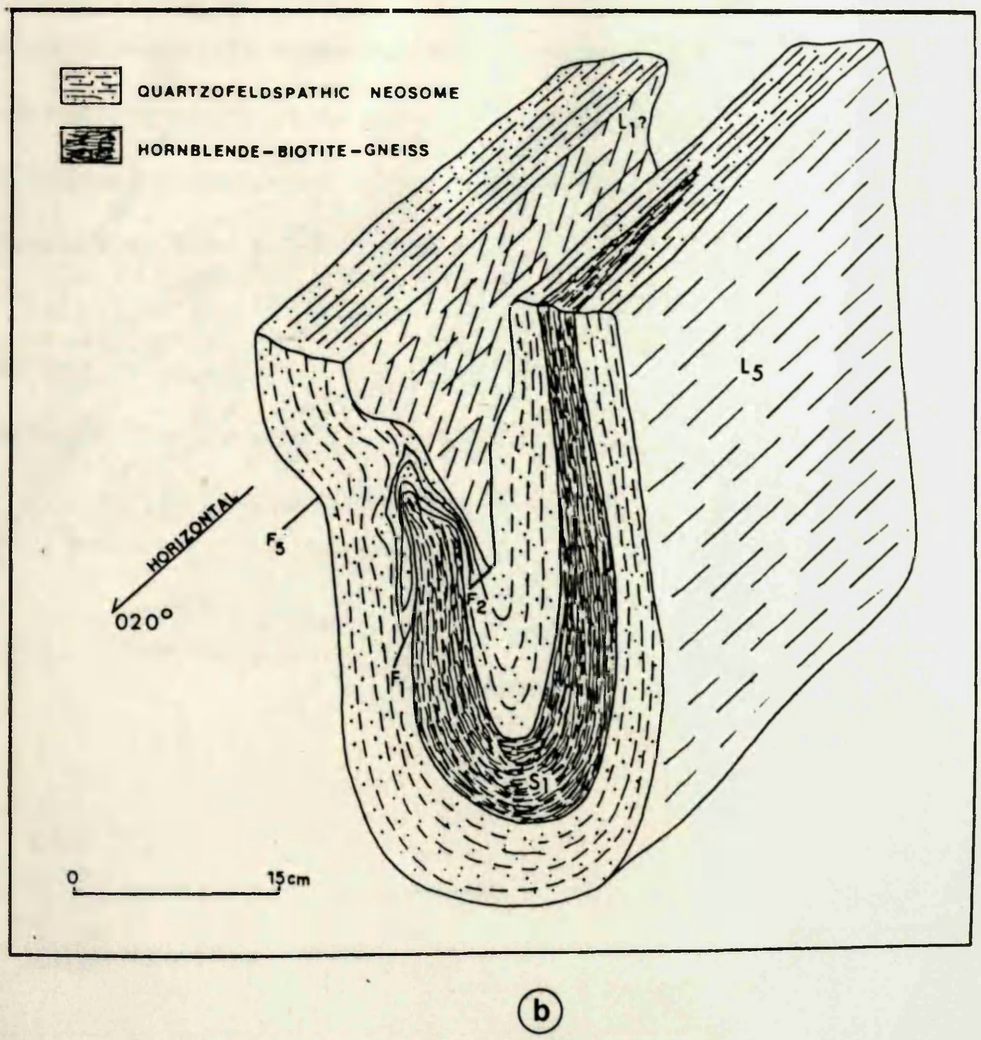
QUARTZOFELDSPATHIC NEOSOME
HORNBLENDE-BIOTITE-GNEISS
L1?
L5
HORIZONTAL
020°
F5
F2
F1
S1
0
15cm

b

Figure VII.9.a F_2 tight folds deforming the gneissose banding and parallel, S_1 (except for the F_1 hinges) and refolding F_1. Tonalite sheets (T) are seen emplaced parallel to F_2 axial planes; subarea IV, western end (Photograph D.R. Bowes).

Figure VII.9.b Detail of the structure illustrated in figure VII.9.a., showing an F_1 fold refolded by F_2, and the development of a foliation (marked by the dimensional alignment of biotite flakes) parallel to the F_2 axial planes (S_2). Some deformational features younger than D_2 are also shown; subarea IV, western end (drawing from a photograph).


T
N
T
S1
F2

a

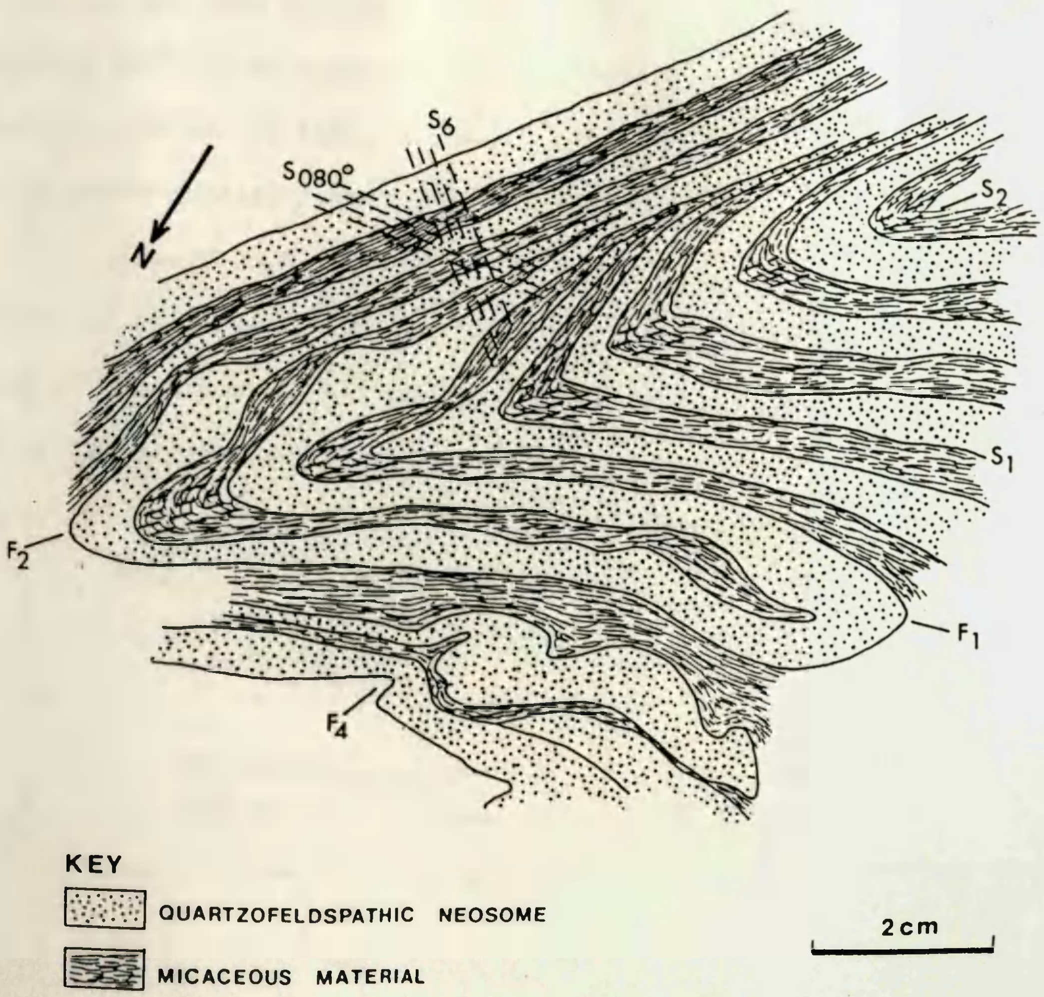
S6
S080°
N
S2
S1
F2
F1
F4
KEY
QUARTZOFELDSPATHIC NEOSOME
MICACEOUS MATERIAL
2cm

b

Figure VII.10.a Compositional layering parallel to S_1 deformed by F_2 folds. The complexity displayed by the F_2 folds below the hand-lens is due to the crumpling of the quartzofeldspathic veins in the hinge zones, together with the presence of F_1 folds. In the upper part of the photograph a late D_2 tonalite sheet (T) is seen emplaced parallel to the F_2 axial planes; subarea IV, eastern end (Photograph D.R. Bowes).

Figure VII.10.b Detail of the encircled area shown in figure VII.10.a., showing the deformation of F_1 folds, displayed by quartzofeldspathic veins, in the hinge zones of F_2 folds.

Z
T
S_1

(a)

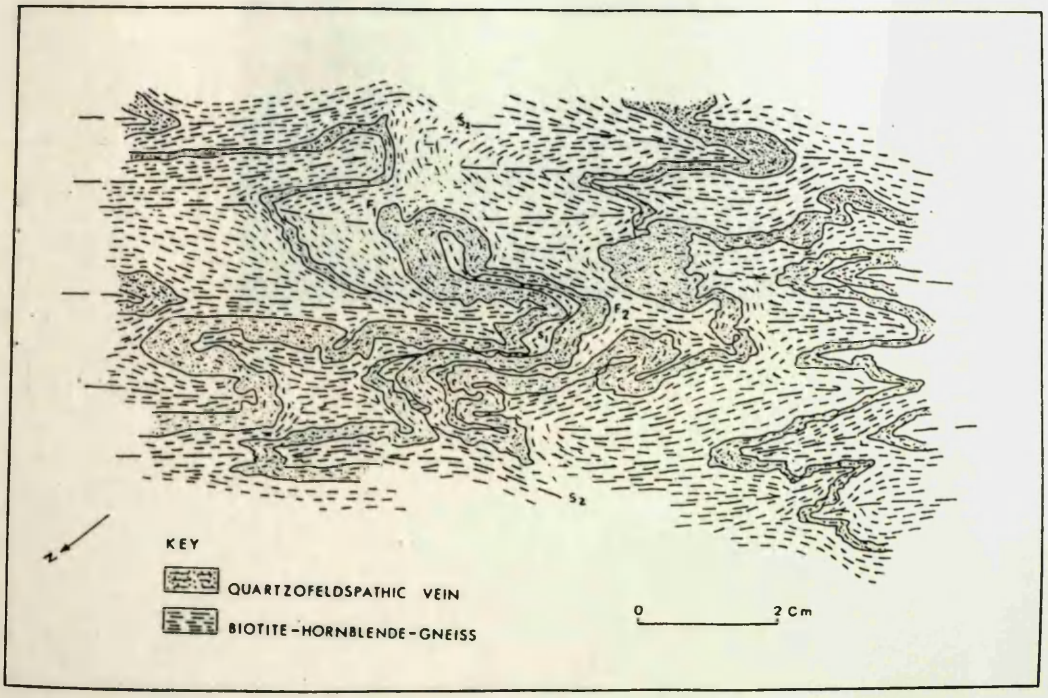

KEY
QUARTZOFELDSPATHIC VEIN
BIOTITE-HORNBLENDE-GNEISS
0
2 Cm

(b)

Figure VII.11 An F_2 fold deforming the gneissose banding (S_1) in banded quartzofeldspathic gneiss and showing thickening of the hinge zone in the outer layer of neosome and crumpling of the layer situated below; subarea IV, western end; looking south-east.

Figure VII.12.a Mylonitic banding making up S_2 cutting-across the dominant gneissose banding S_{o-1}; subarea II, middle part (Photograph D.R. Bowes); looking south.

Figure VII.12.b Detail of the mylonitic banding shown in figure VII.12.a. In the central part of the photograph there is a band made up by detached, very small F_2 hinges (Photograph D.R. Bowes).

(a)

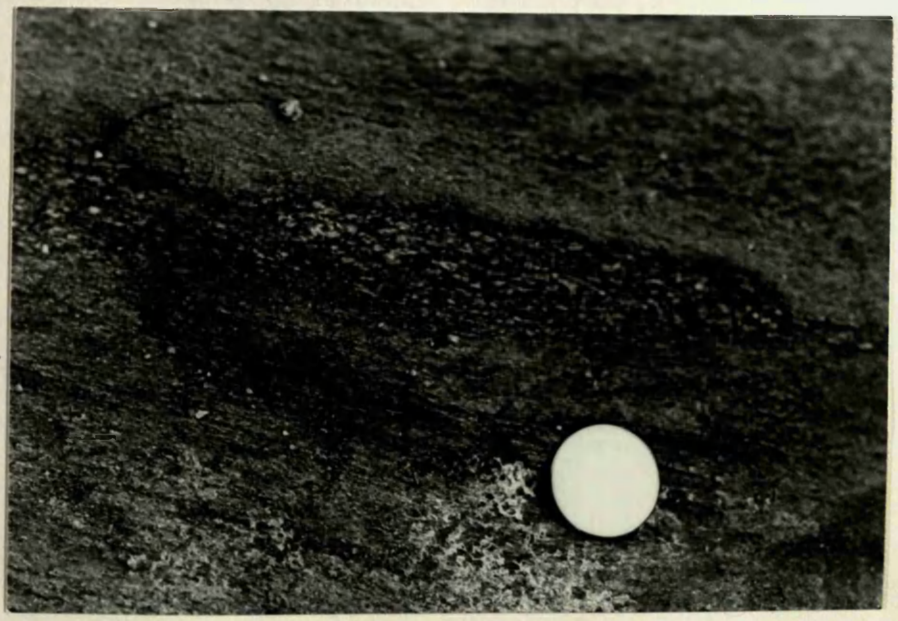

(b)

Figure VII.13 Photomicrograph of a quartzofeldspathic granitic gneiss showing an S_2 fabric marked by biotite cutting-across the S_1 fabric at a small angle; subarea II, middle part (XN, X 25)

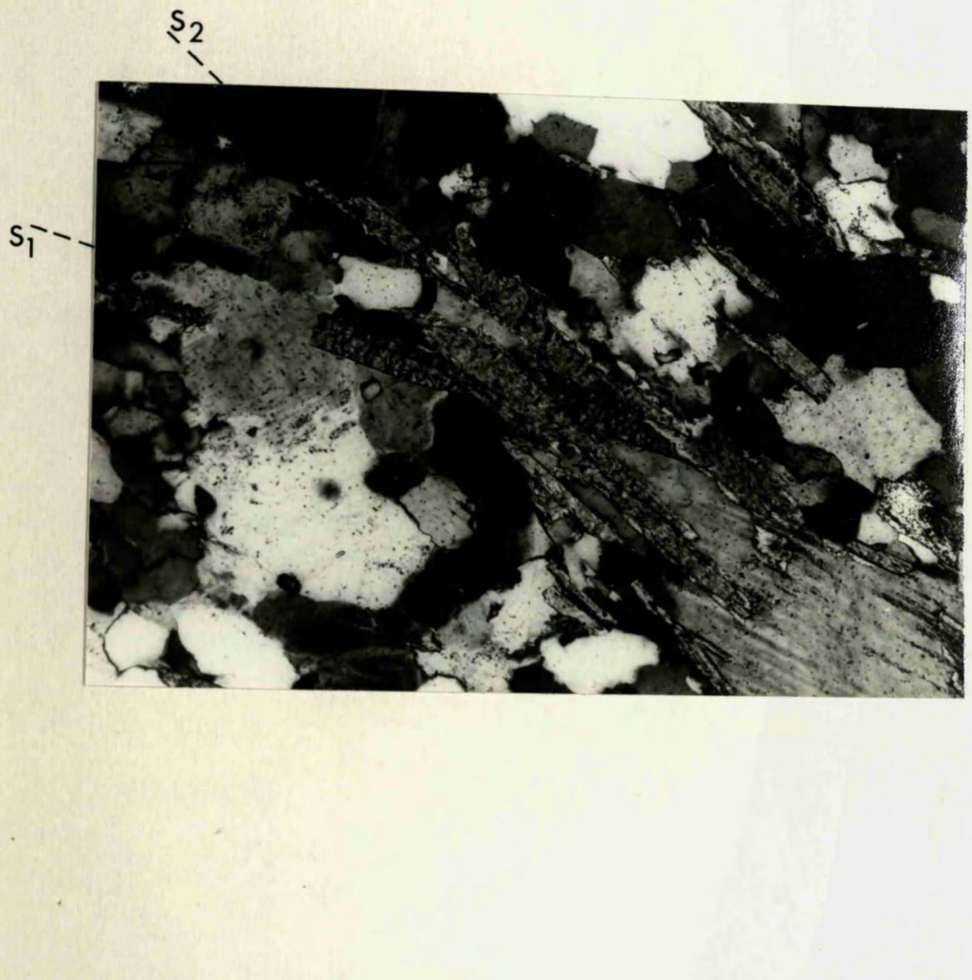
S_2
S_1

Figure VII.14. Equal area projection of F_3 axes, the average attitude of S_3 and two distinct attitudes of S_1, as determined in subarea II.

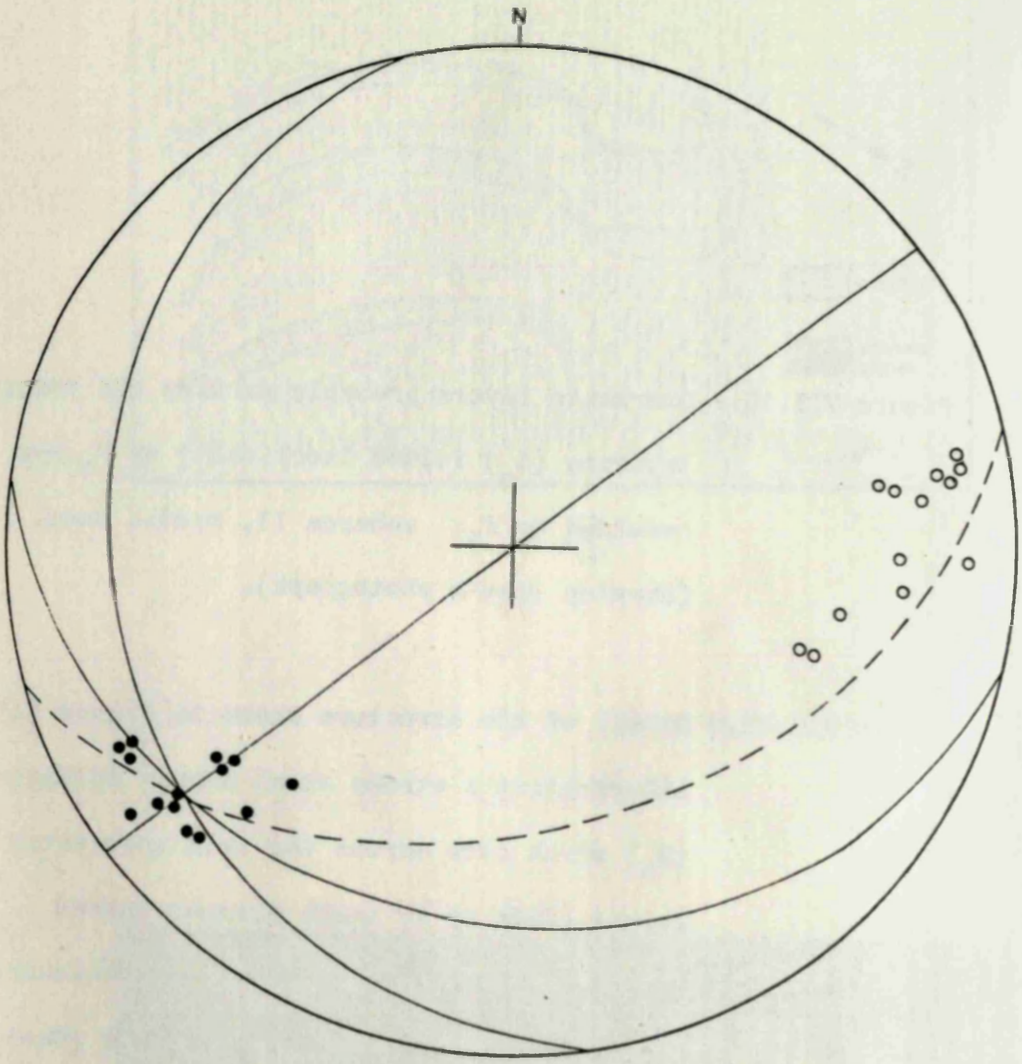

Subarea II

● F_3 axes in southern part
○ F_3 axes in northern part
——— S_1
- - - - F_3 axial plane

Figure VII.15.a Quartzite layers probably marking the original layering (S_o) folded isoclinally by F_1 and refolded by F_3; subarea II, middle part. (Drawing from a photograph).

Figure VII.15.b Detail of the structure shown in figure VII.15.a illustrating a strong axial planar foliation (S_3) which cuts across the thin quartzitic layers (made up by small diamond-shaped fragments) but is refracted by the thicker ones, except in the hinge zone of the fold (Photograph D.R. Bowes).

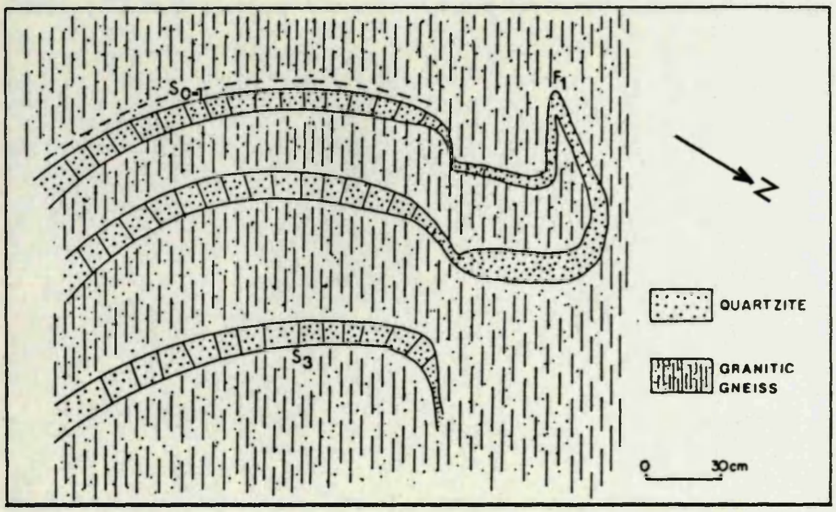

a

b

Figure VII.16.a Small F_3 folds deforming the gneissose banding (which parallels S_1) and displaying a chevron-like style; subarea IIIb.

Figure VII.16.b F_3 deforming the gneissose banding (S_1) and forming relatively open antiforms and tight synforms; subarea II, eastern end (Photograph D.R. Bowes).

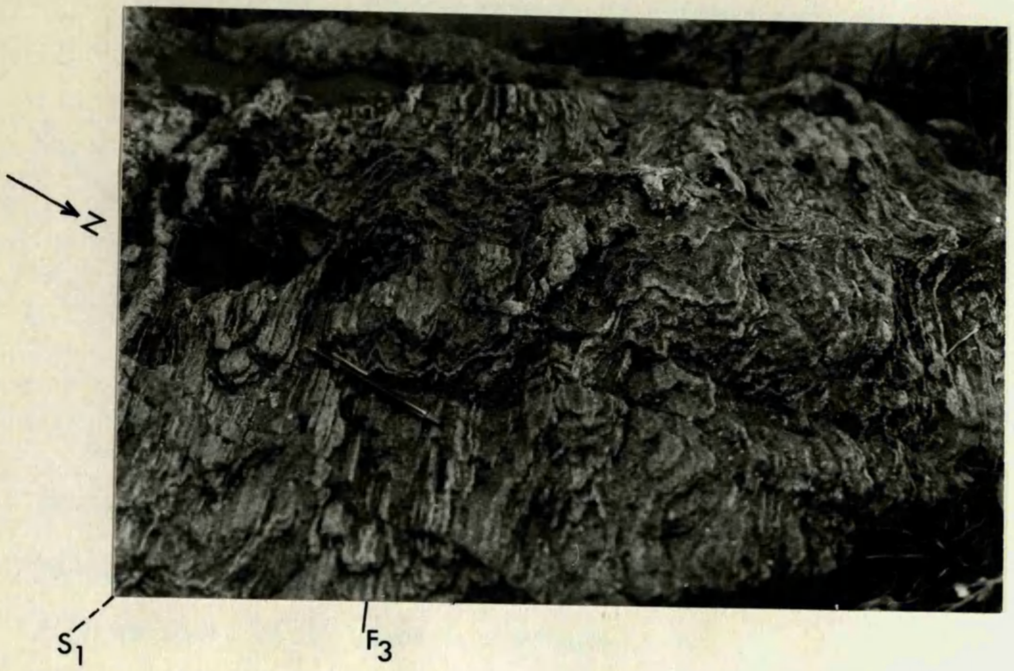
Z
S_1
F_3


Z

Figure VII.17.a Very appressed isoclinal F_3 folds, marked by quartzofeldspathic neosome, giving rise to a prominent rodding (L_3); subarea IIIa (Photograph D.R. Bowes).

Figure VII. 17.b Granitic dyke emplaced into quartzofeldspathic tonalite gneiss approximately perpendicular to the dominant foliation and deformed by length-parallel compression, originating open folds with steeply plunging axes (F_{3b}); subarea I, middle part.

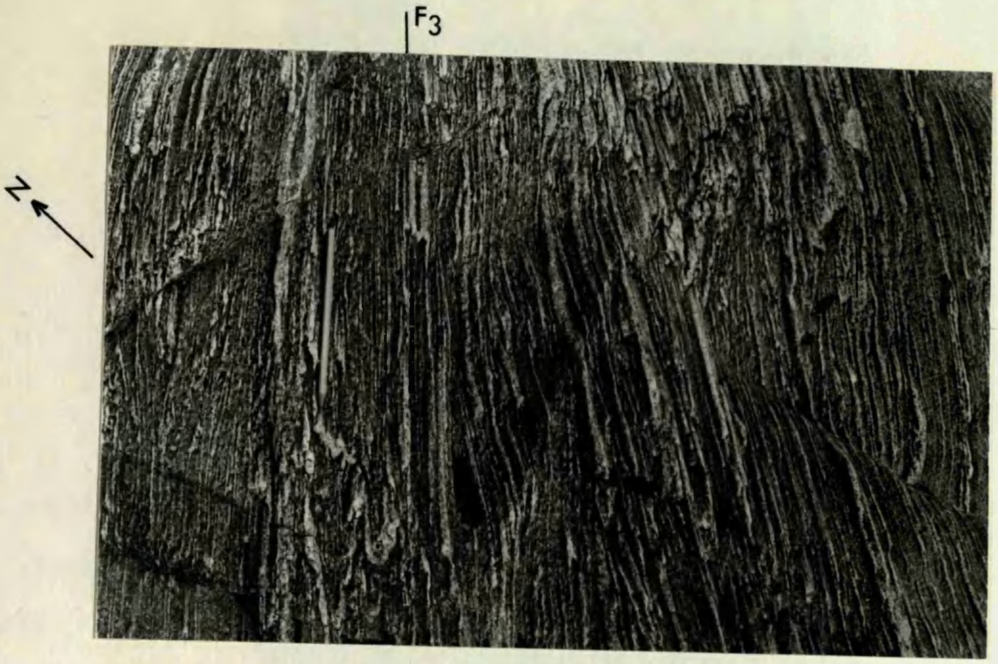

(a)

(b)

Figure VII.18.a Late D_3 quartzofeldspathic vein deformed by slip parallel to S_1 giving rise to axes which plunge steeply to NE (F_{3c}); subarea I, middle part. (Photograph D.R. Bowes).

Figure VII.18.b Late D_3 quartzofeldspathic vein deformed by slip parallel to S_1, showing axes (F_{3c}) plunging steeply to SW. Note the large interlimb angle of F_{3c} as compared to that of F_3; subarea I, middle part. (Photograph D.R. Bowes).

(a)

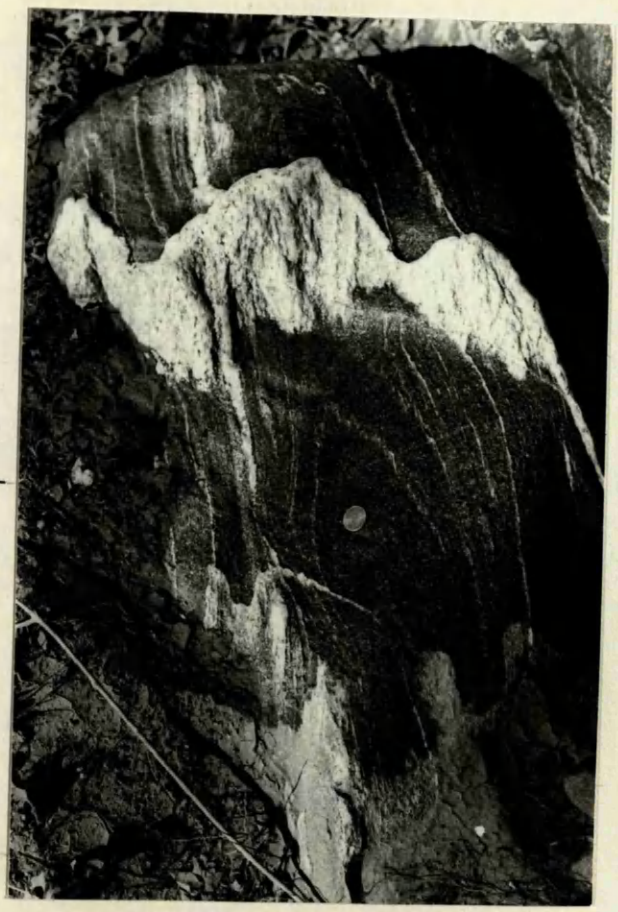

(b)

Figure VII.19.a Photomicrograph of a concordant fine-grained amphibolite showing the S_3 fabric marked by biotite (grey) cutting across the S_1 fabric, marked by biotite (grey) and hornblende (dark), at small angle; subarea II, southern end. (XN, X 10).

Figure VII.19.b Photomicrograph of a quartzofeldspathic granitic gneiss showing S_3 (marked by biotite) at high angle to S_1 in the hinge zone of an F_3 fold; subarea II, southern end. (OL, X 10).

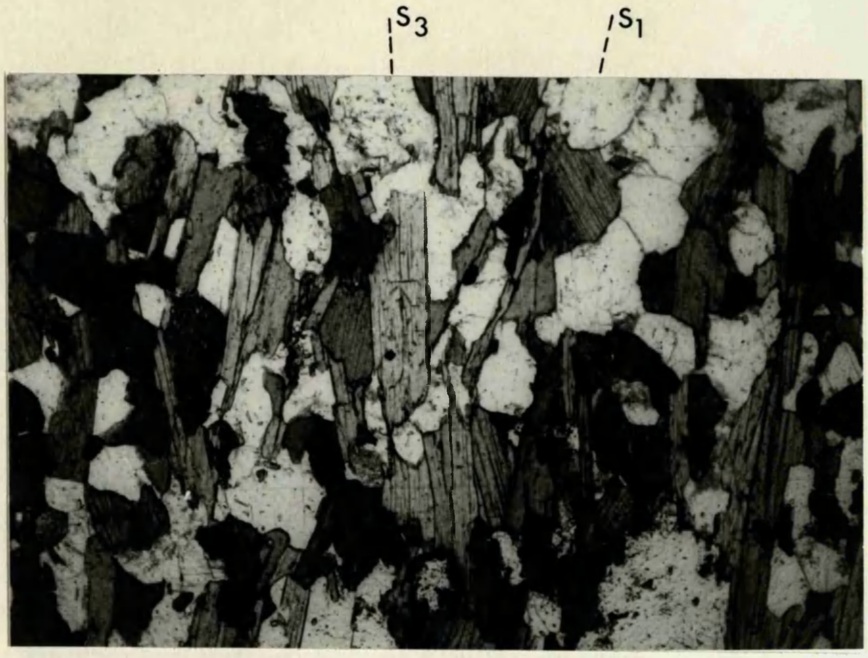

(a)

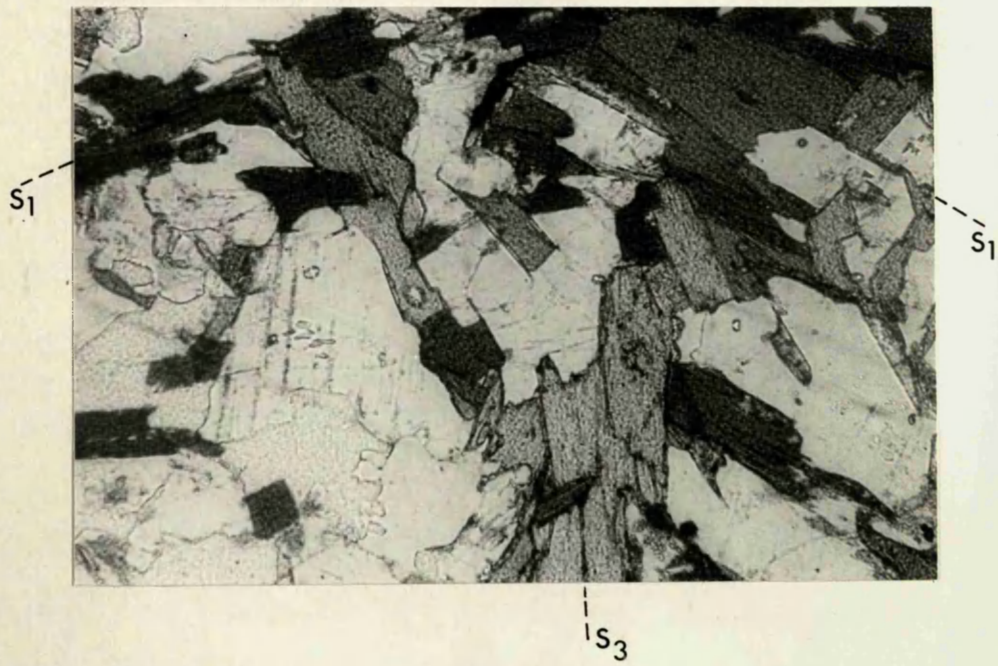

(b)

Figure VII.20 Large mass of granodiorite (G) cutting-across the dominant foliation (S_3) in the hinge zones of small F_3 folds; subarea I, middle part.


G
Z

Figure VII.20 Large mass of granodiorite (G) cutting-across the dominant foliation (S_3) in the hinge zones of small F_3 folds; subarea I, middle part.


G
Z

Figure VII.21.a Subhorizontal adamellite (A) sheet, probably representing part of a large late F_3 fold, truncating the gneissose banding with a concordant tonalite sheet (T) related to late D_2; subarea IIIc. (Photograph D.R. Bowes).

Figure VII.21.b Remnant of an eroded F_{3c} fold formed by a granitic sheet emplaced along a southwestward dipping fracture; subarea I, southern part.

(a)

(b)

Figure VII.22. Schematic representation of concordant and discordant D_3 granitic sheets, in relation to earlier-formed D_3 features.

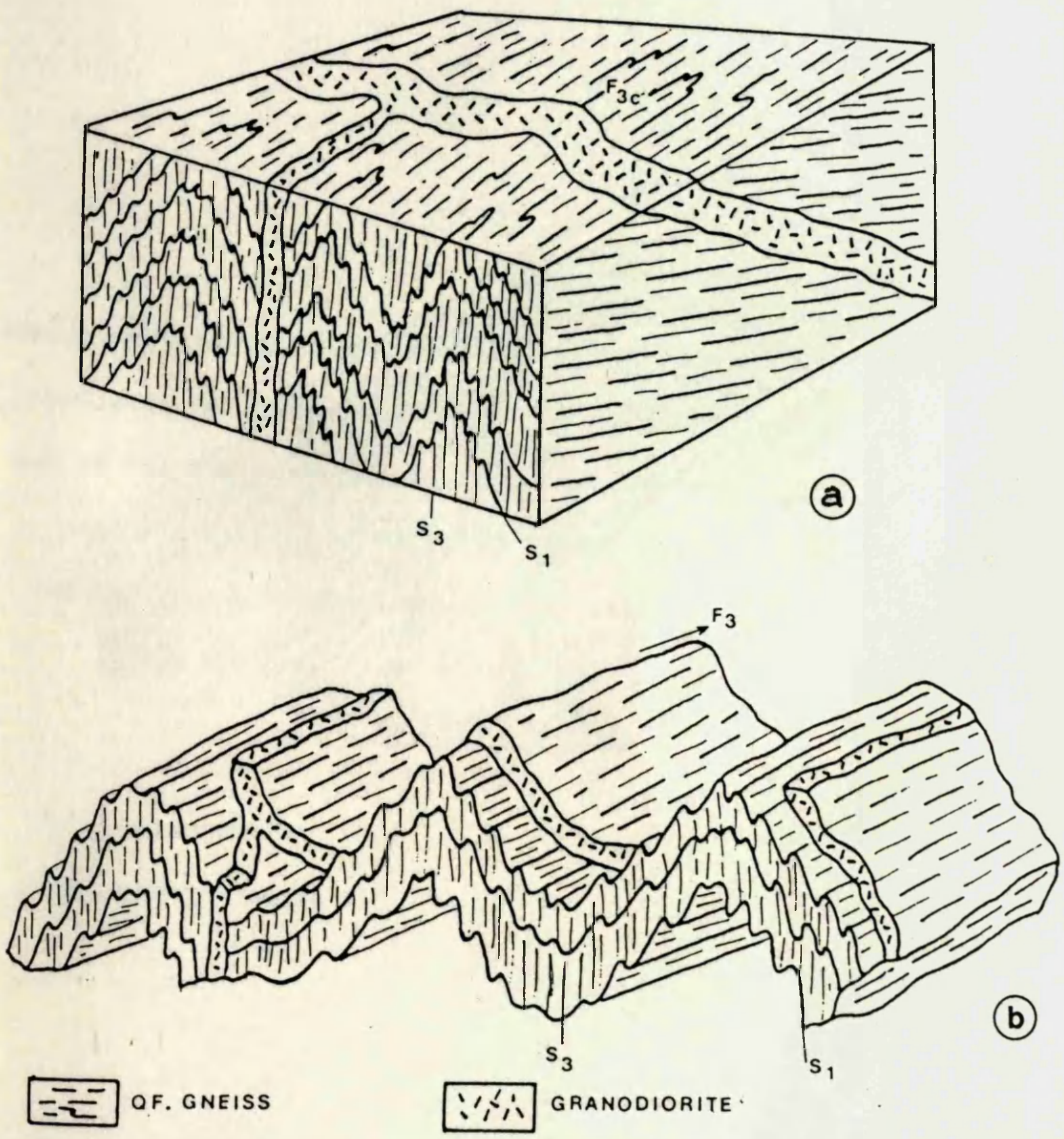

F3c
S3
S1
a
F3
S3
S1
b
QF. GNEISS
GRANODIORITE

Figure VII.23. Schematic representation of an antiform formed by D_3 granitic sheets, showing the relationship between the material emplaced parallel to the axial planar foliation to F_3 (S_3) and the material forming the limbs of the structure.

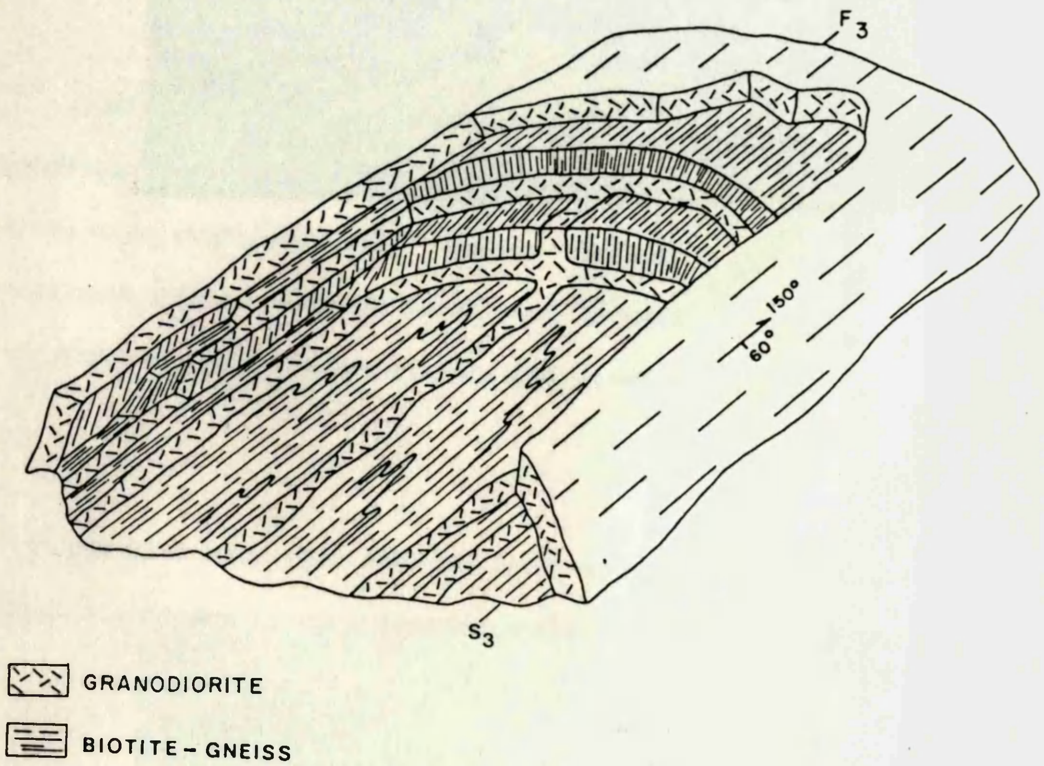

F3
150°
60°
S3
GRANODIORITE
BIOTITE - GNEISS

Figure VII.24.a Partly concordant and partly discordant granodiorite sheet intruded in quartzofeldspathic dioritic gneiss. The concordant part of the igneous body shows pinch-and-swell features; subarea IV, eastern end. (Photograph D.R. Bowes).

Figure VII.24.b Transversal granodiorite vein deformed by F_3, displaying very thick hinge and thin disrupted limbs; subarea I, middle part.

a

b

Figure VII.25.a Pegmatitic granodiorite vein showing bulging and boudinage, perpendicularly and parallel to the gneissose banding, respectively; subarea IV, eastern end.

Figure VII.25.b Granite vein folded about F_{3c} showing thickening of the hinge zone and thinning of the limbs. Note the lobate shape of the interface between the vein and the host gneiss in the concave side of the hinge zone, subarea II, northern end. (Photograph D.R. Bowes).

65°
040°

a

75°
065°

b

Figure VII.26.a Dyke of banded rhyolite cutting-across both the dominant foliation (S_1) and F_3 hinges; subarea IIIb. (Photograph D.R. Bowes)

Figure VII.26.b Strong intersection lineation (L_{3c}) on the surface of the dyke of rhyolite shown in figure VII.26.a.; subarea IIIb, northern end, looking southwest.

(a)

(b)

Figure VII.27.a Dyke of banded rhyolite displaying a number of dome-and-basin interference figures; a fanning fracture cleavage with dip decreasing to the left side of the photograph, and a transversal cleavage (S_4) whose trace on the dyke's surface is seen inclined to the left (see text for explanation); subarea IIIb, middle part; looking southwest.

Figure VII.27.b Detail of the photograph shown in figure VII.27.a. illustrating the small dome-and-basin interference features and an intersection lineation steeply inclined to the right; (Photograph D.R. Bowes).

(a)

(b)

Figure VII.28. Map view of the dyke of rhyolite showing an isoclinal fold, marked by the flow bands, along the zone of contact with the host quartzofeldspathic gneiss, deformed about steeply plunging axis (F_{3b}); subarea IIb. (Drawing from a photograph).

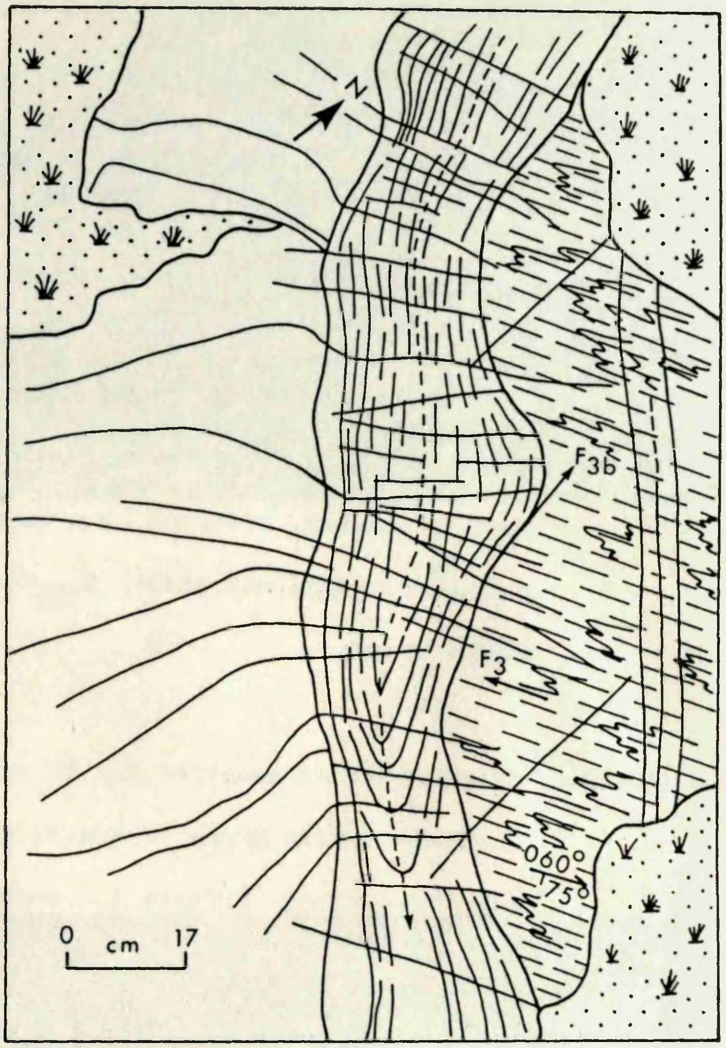

COVERED-SOIL
HOMOGENEOUS RHYOLITE
FLOW-BANDED RHYOLITE
BANDED QUARTZOFELDSPATHIC GNEISS
FRACTURE CLEAVAGE
F3 FOLD AXIS
AXIAL PLANE
ATTITUTE OF FOLIATION

Figure VII.29.a Granitic pegmatite emplaced parallel to the limb of an F_3 fold, formed by quartzofeldspathic granitic gneiss, deformed by a warp related to a late deformational phase (D_{1} 50^{o}); subarea II, southern end.

Figure VII.29.b Development of agmatite due to the intrusion of granodioritic magma in quartzofeldspathic dioritic gneiss; subarea I, southern part.

a

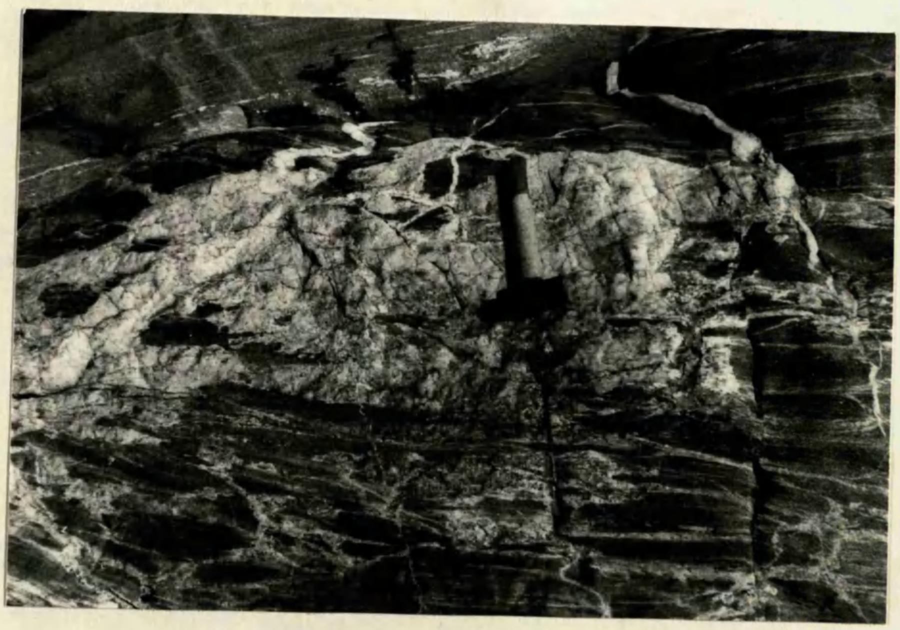

b

Figure VII.30.a F_4 folds formed by tonalite sheet and small mullions generated at the interface tonalite/host quartzofeldspathic gneiss. A weak lineation (L_3) can be seen parallel to the pencil, and making up a moderate angle with B_4. It is also shown by this photograph the deformation of the gneissose banding (S_1) by very open folds related to steeply plunging axes (F_6); subarea IV, western end. (Photograph D.R. Bowes).

Figure VII.30.b Schematic representation of the mutual relationship between D_3, D_4 and D_6 as shown by a tonalite sheet; subarea IV, western end.

(a)

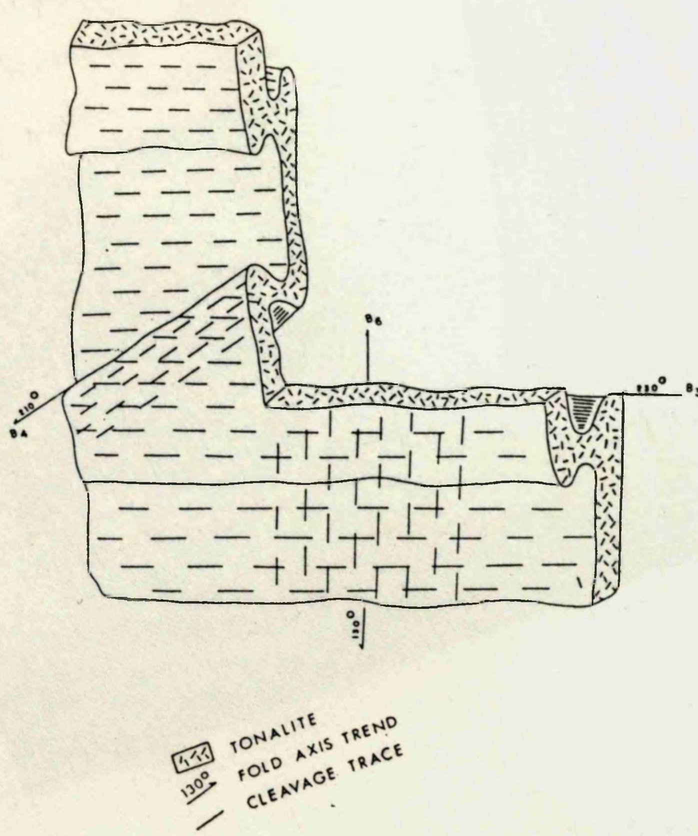

(b)

Figure VII.31.a Gneissose banding (S_1) in quartzofeldspathic dioritic gneiss deformed by a symmetrical, open F_5 fold, with sub-horizontal axis and axial surface moderately dipping to NE; subarea IV, western end.

Figure VII.31.b. Very open F_5 fold and a crenulation lineation (L_5) parallel to B_5, deforming the gneissose banding (S_1) in quartzofeldspathic dioritic gneiss; subarea IV, middle part. (Photograph D.R. Bowes).

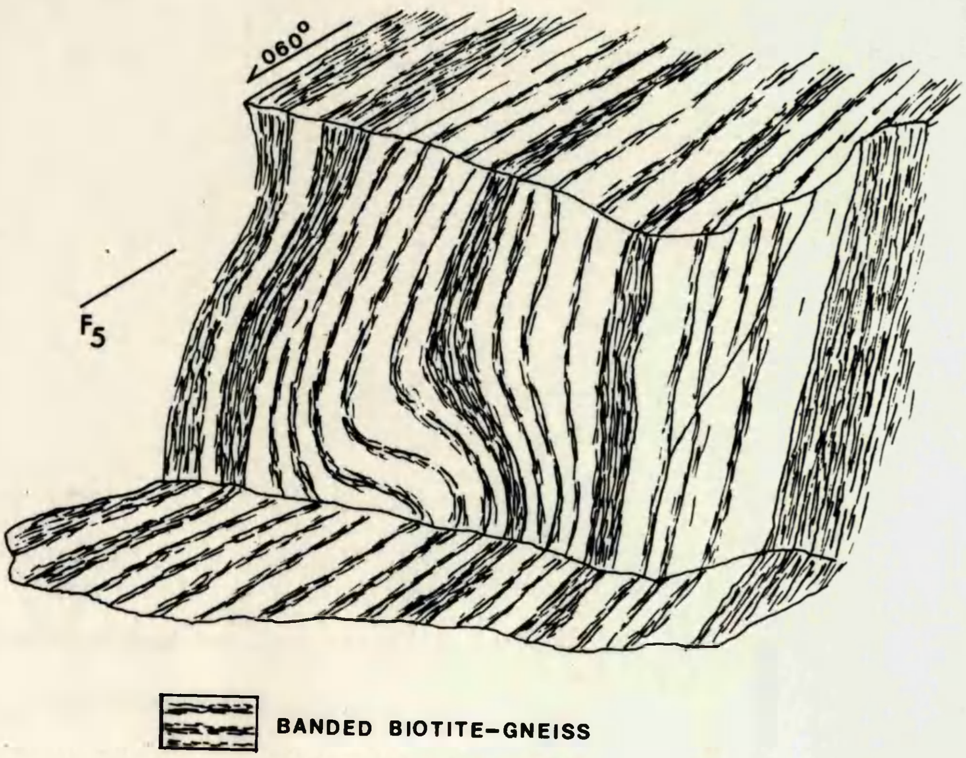

(a)

(b)

Figure VII.32. β diagram illustrating the high cylindricity and the plunging-upright character of F_6 folds in subarea IV.

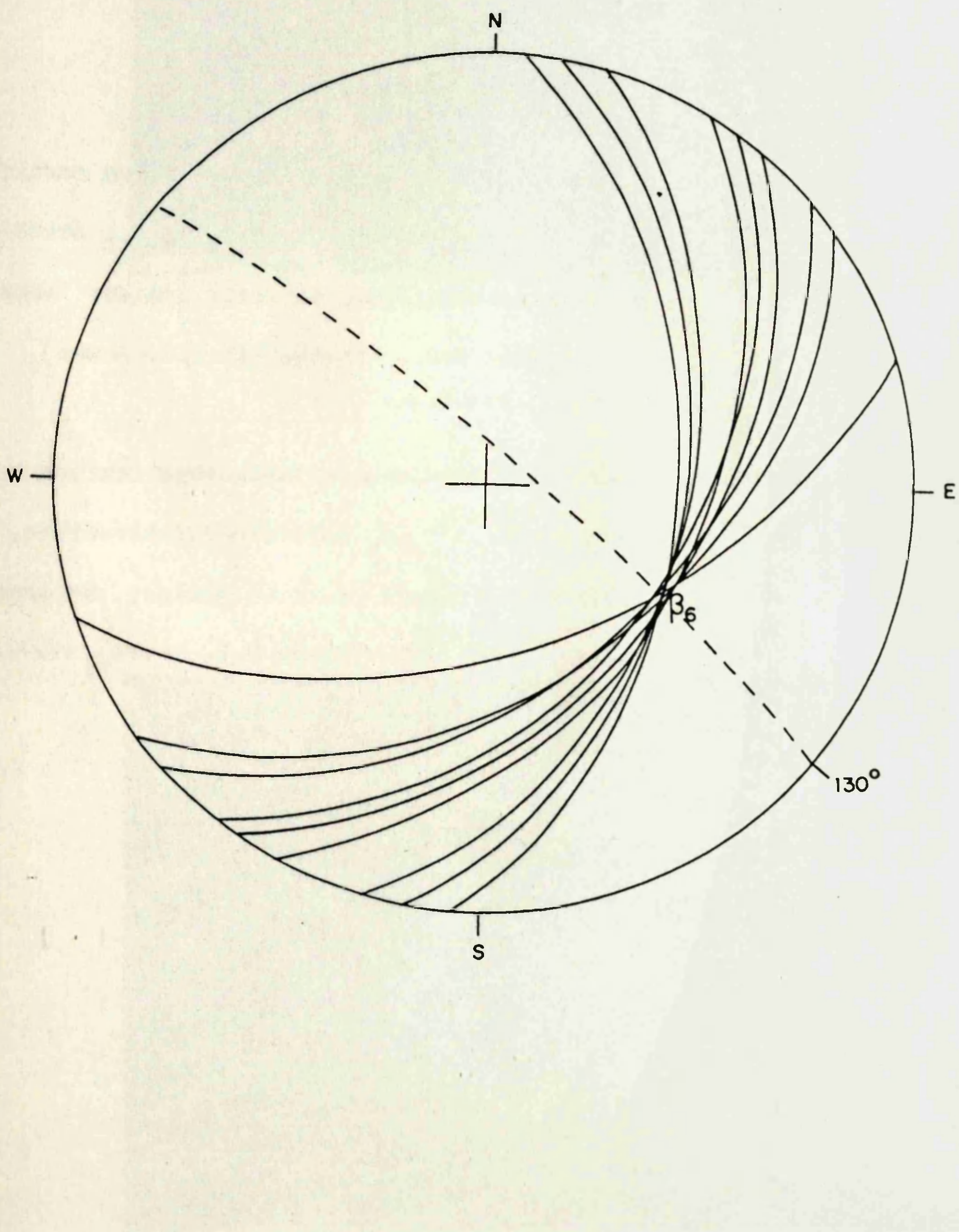
N
W
E
S
130°
β_6

Figure VII.33.a Dome-and-basin interference pattern resulting from the superimposition of F_6 on F_5, developed in quartzofeldspathic dioritic gneiss; subarea IV, western end. (Photograph D.R. Bowes); looking southeast.

Figure VII.33.b Detail of an elongate basin-type feature related to an F_6-F_5 interference structure, in quartzofeldspathic dioritic gneiss; subarea IV western end. (Photograph D.R. Bowes); looking southeast.

(a)

(b)

Figure VI.34 Dispersion of earlier-formed fold axes by F_6 in subarea IV.

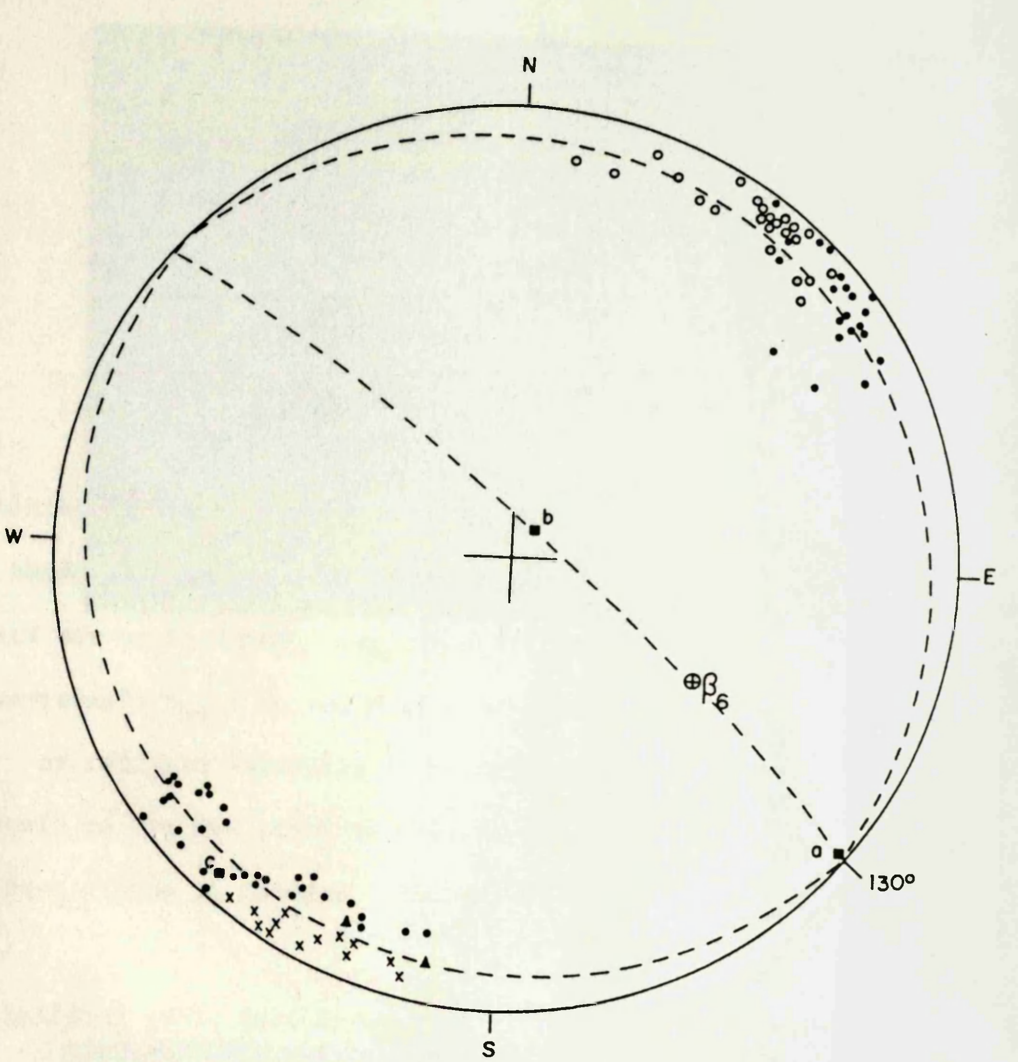

F2 ▲

F3 •

F4 - x

F5 o

a,b,c : Kinematic axes

Figure VII.35.a Gneissose banding in quartzofeldspathic tonalitic gneiss deformed by kink bands parallel to S_{110}o. Parallel to the kink bands there is a set of S_{110}o cleavages. A second set of cleavages parallel to S_{010}o can also be seen, but not so clearly as the former set; subarea I, middle part, looking south.

Figure VII.35.b Dextral kink, with kink plane parallel to S_{010}o deforming the gneissose banding ($S_1 = S_3$) in quartzofeldspathic granodioritic gneiss; subarea IIIa.

(a)

(b)

Figure VII.36.a Dextral kink with kink plane parallel to S_{010}o, deforming the gneissose banding in quartzofeldspathic gneiss, subarea III.b.

Figure VII.36.b Conjugate kink folds formed by the deformation of the gneissose banding in quartzofeldspathic granodioritic gneiss, by planes parallel to S_{010}o and S_{110}o; subarea IIIa, (Photograph D.R. Bowes).

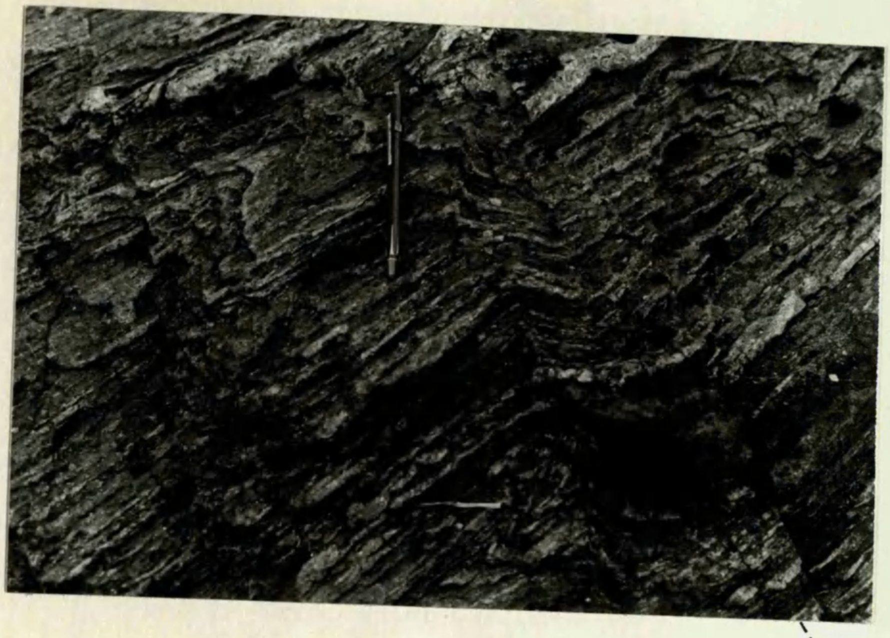

(a)

(b)

Figure VII.37.a Strong lineation marked by the intersection of the outcrop surface by S_{010^o} cleavage planes; subarea II, southern end. (Photograph D.R. Bowes).

Figure VII.37.b Trace of S_{080^o} on the outcrop surface (quartzofeldspathic granitic gneiss) obliquely oriented in relation to the axial planar foliation to an F_3 fold (S_3); subarea II, middle part.

(a)

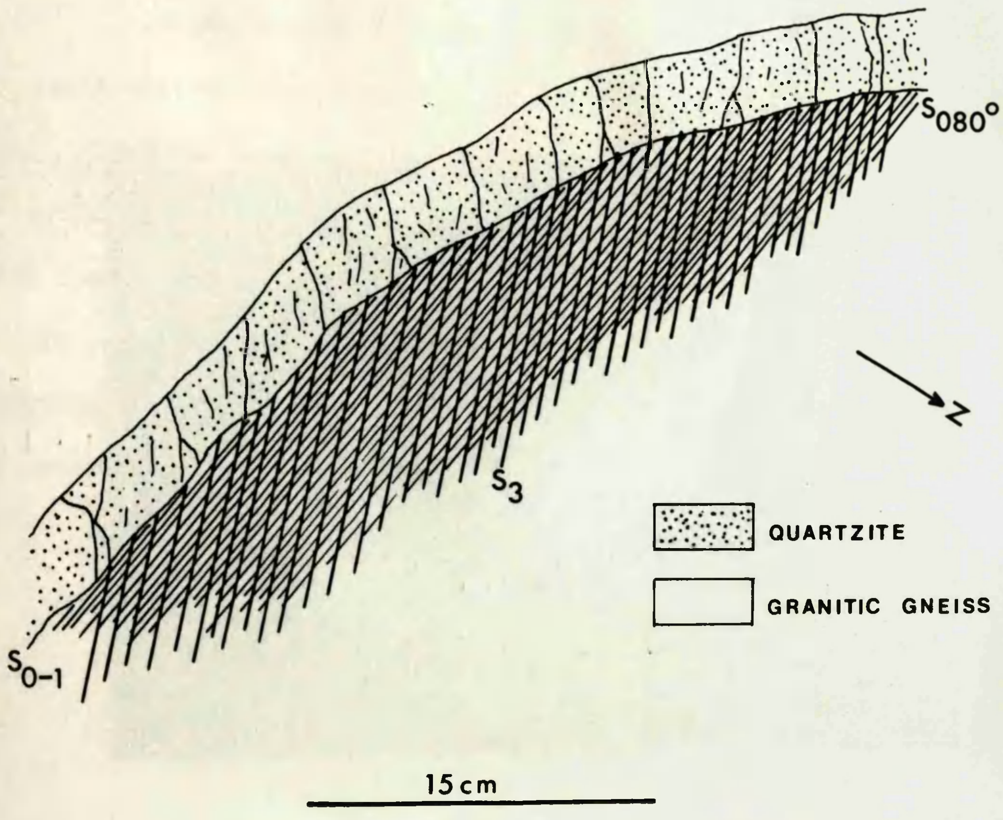

(b)

Figure VII.38.a Steeply plunging F_{150^o} fold deforming the southern limb of an F_3 fold, with sub-horizontal axis and moderately dipping axial plane to SE, in injected granitic gneiss; subarea II, northern part.

Figure VII.38.n Late S_{170^o} cleavage planes readily evidenced by the transversal relief lines in relation to the gneissose banding. The relief is caused by feldspatization along the S_{170^o} planes. Note that it is not seen when the cleavages cut across a layer of quartzite (Q) intercalated with the quartzo-feldspathic gneiss; subarea II, northern part. (Photograph D.R. Bowes).

(a)

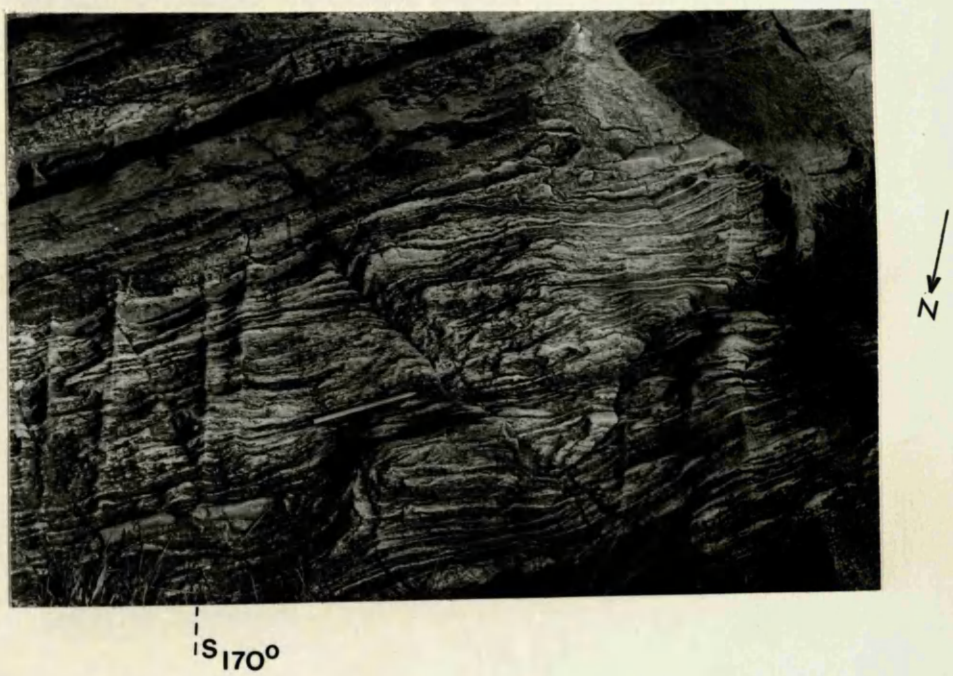

(b)

Figure VII.39 Schematic representation of the relationship between the major F_2 structures and younger structural elements.

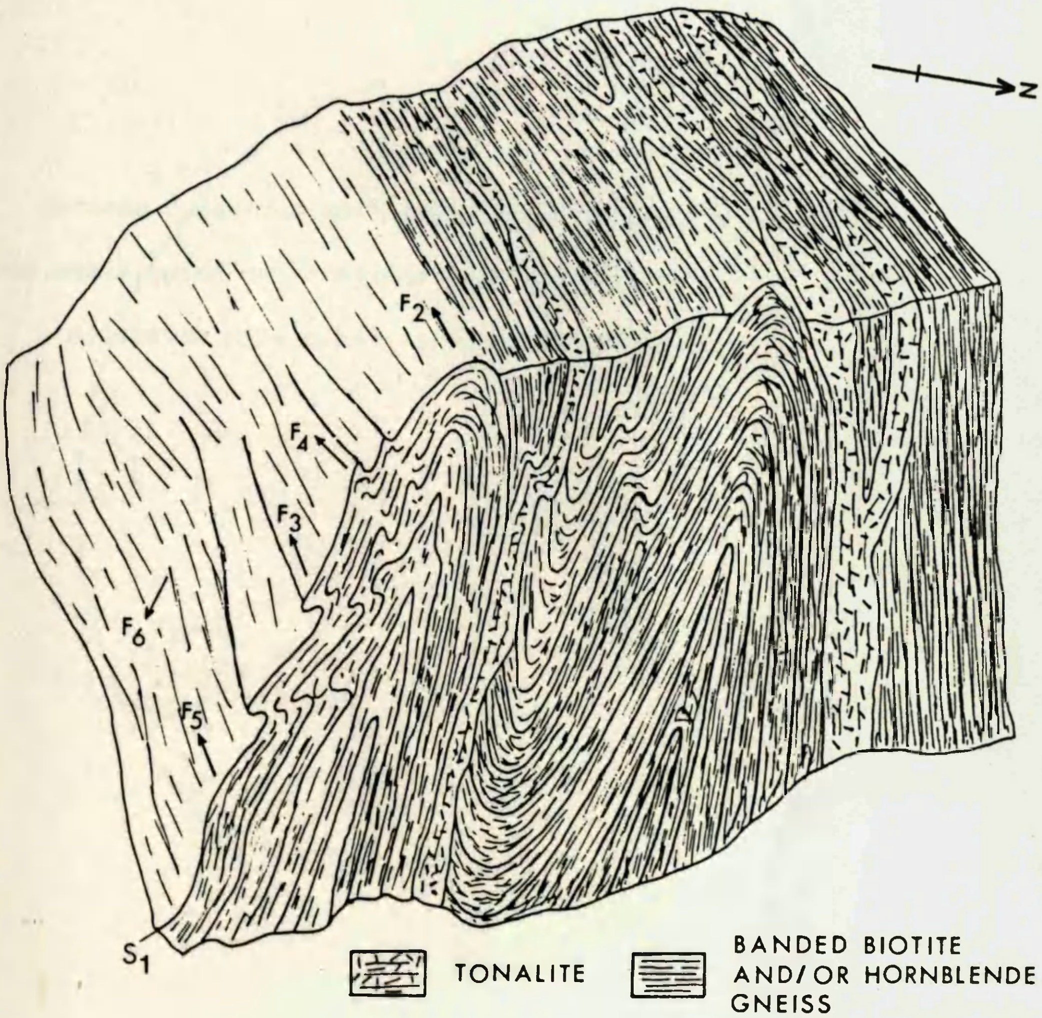
N
F_2
F_4
F_3
F_6
F_5
S_1
TONALITE
BANDED BIOTITE AND/OR HORNBLENDE GNEISS

Figure VII.40 Stereoplot of F_3 axes from subarea I showing the tendency they manifest for being dispersed along a subvertical girdle with direction NE-SW.

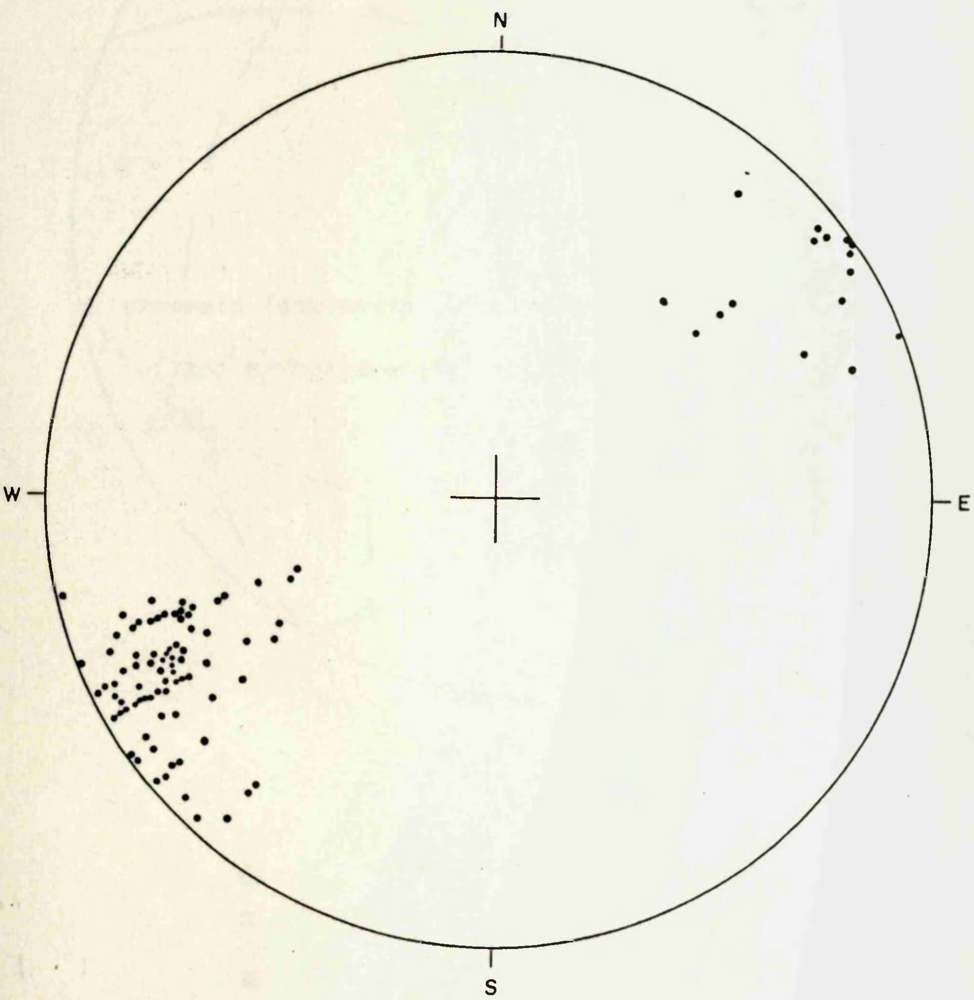

SUBAREA I

● F_3

Figure VII.41. Stereoplot of D_3 structural elements in subarea IIIb (explanation in text).

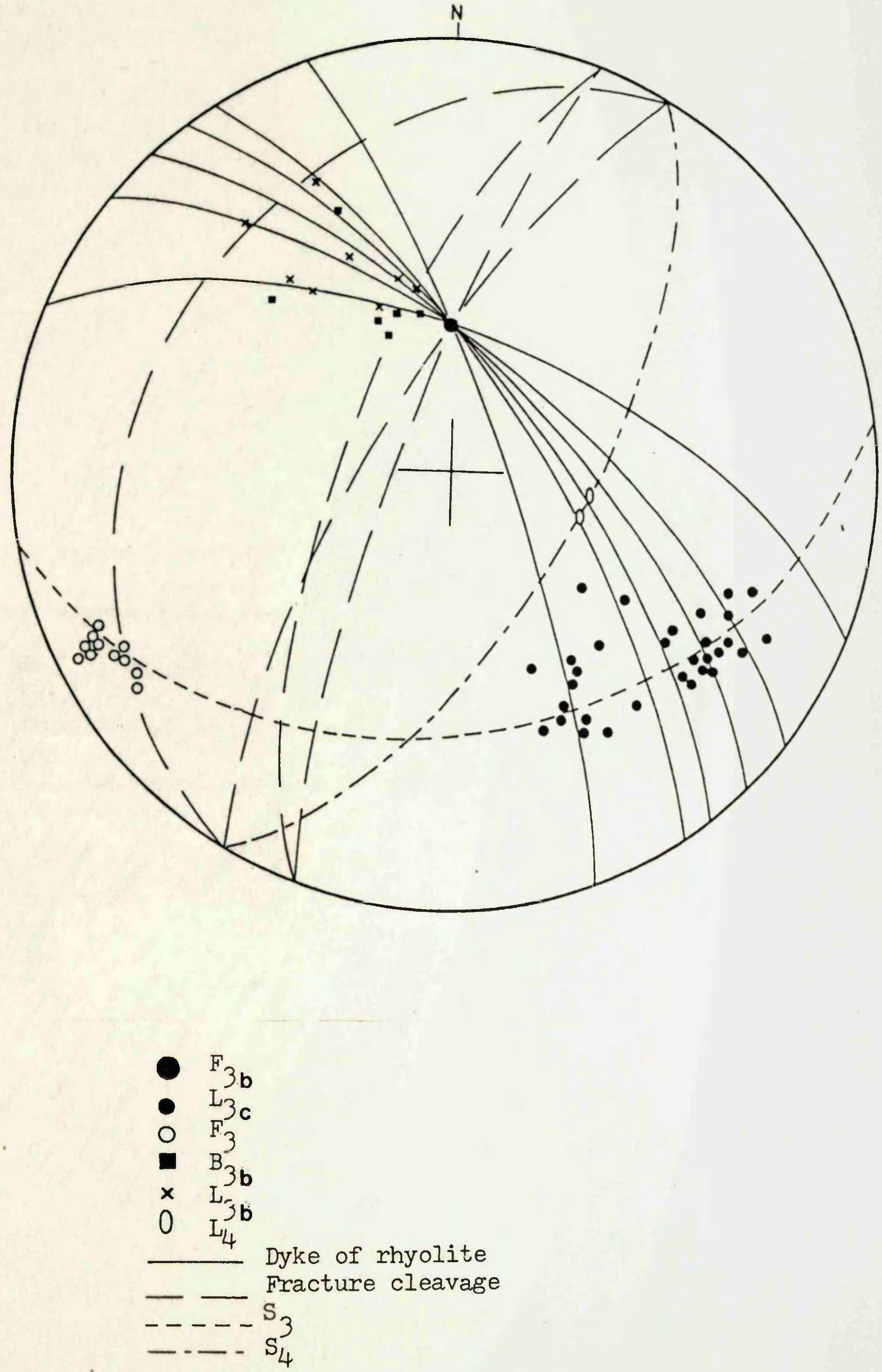
N
F_{3b}
L_{3c}
F_3
B_{3b}
L_{3b}
L_4
Dyke of rhyolite
Fracture cleavage
S_3
S_4

Figure VII.42. Deformed xenoliths of biotite schist within a tonalite sheet, showing a tendency for lying parallel to the foliation (S_3) of the igneous body; subarea I, southern part (Drawing from a photograph).


N
30 cm
FOLIATED TONALITE
BIOTITE SCHIST

Figure VII.43.a Concordant, banded trondhjemite sheet, emplaced in quartzofeldspathic dioritic gneiss, displaying pinch-and-swell feature. Note in the bottom right of the photograph a thin tonalite sheet exhibiting a similar feature on a plane representing a sub-vertical section of the outcrop; subarea IV, middle part. (Phtograph D.R. Bowes).

Figure VII.43.b Concordant trondhjemite sheet, emplaced in quartzofeldspathic dioritic gneiss, displaying quartz segregation in the necking-zone of a pinched feature; subarea IV, eastern end.

a

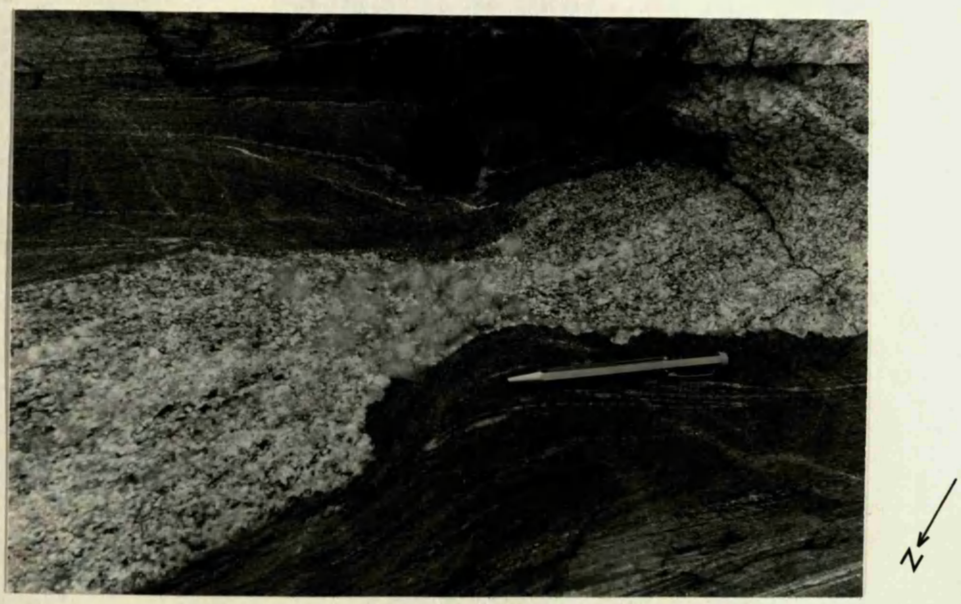

b

Figure VII.44.a Trondhjemite sheet, emplaced concordantly in quartzofeldspathic dioritic gneiss, displaying a rotated boudin; subarea IV, middle part. (Photograph D.R. Bowes).

Figure VII.44.b Boudinaged amphibolite lense, parallel to the gneissose banding, deformed together with granodiorite neosome, intruded into quartzo-feldspathic dioritic gneiss, and F_{3c} folds; subarea I, southern part. (Drawing from a photograph).

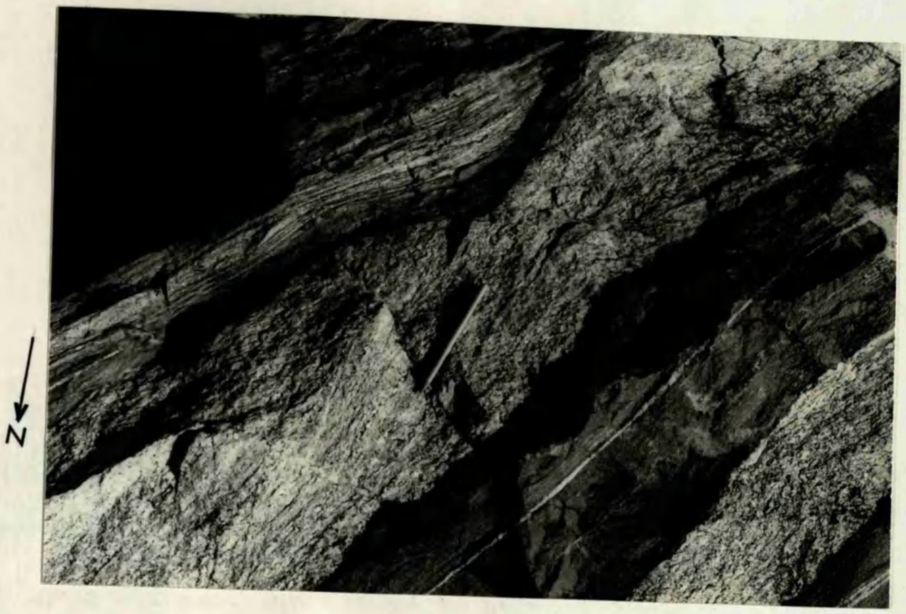
N

(a)

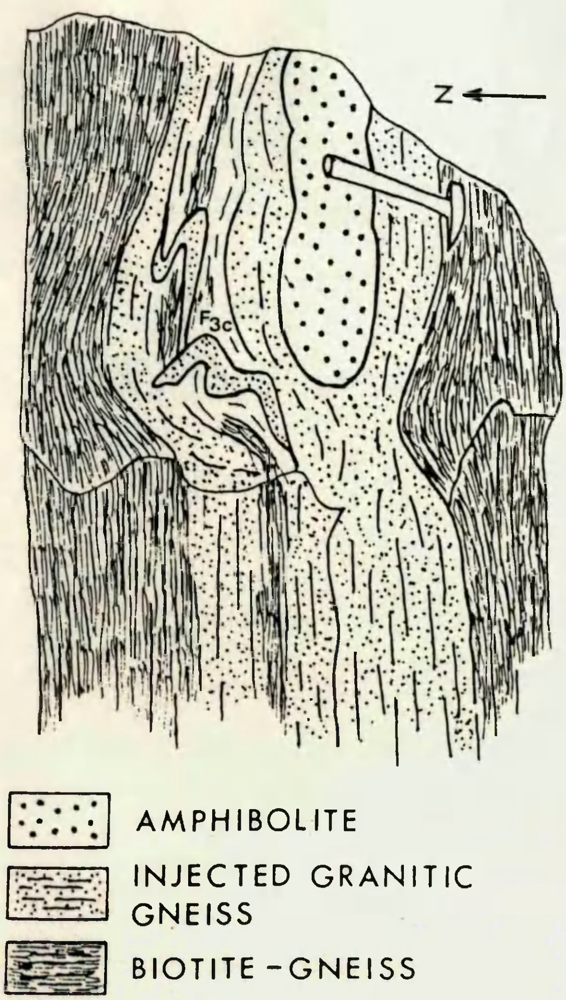
Z
F3c
AMPHIBOLITE
INJECTED GRANITIC GNEISS
BIOTITE-GNEISS

(b)

Figure VII.45.a Isoclinal, rootless F_1 folds formed by quartzofeldspathic material, in biotite-gneiss, deformed in a sinistral shear zone; subarea I, southern part. (Drawing from a photograph).

Figure VII.45.b Isoclinal, rootless F_1 folds formed by quartzofeldspathic material, in biotite-gneiss, deformed in a dextral shear zone; subarea I, southern part. (Drawing from a photograph).

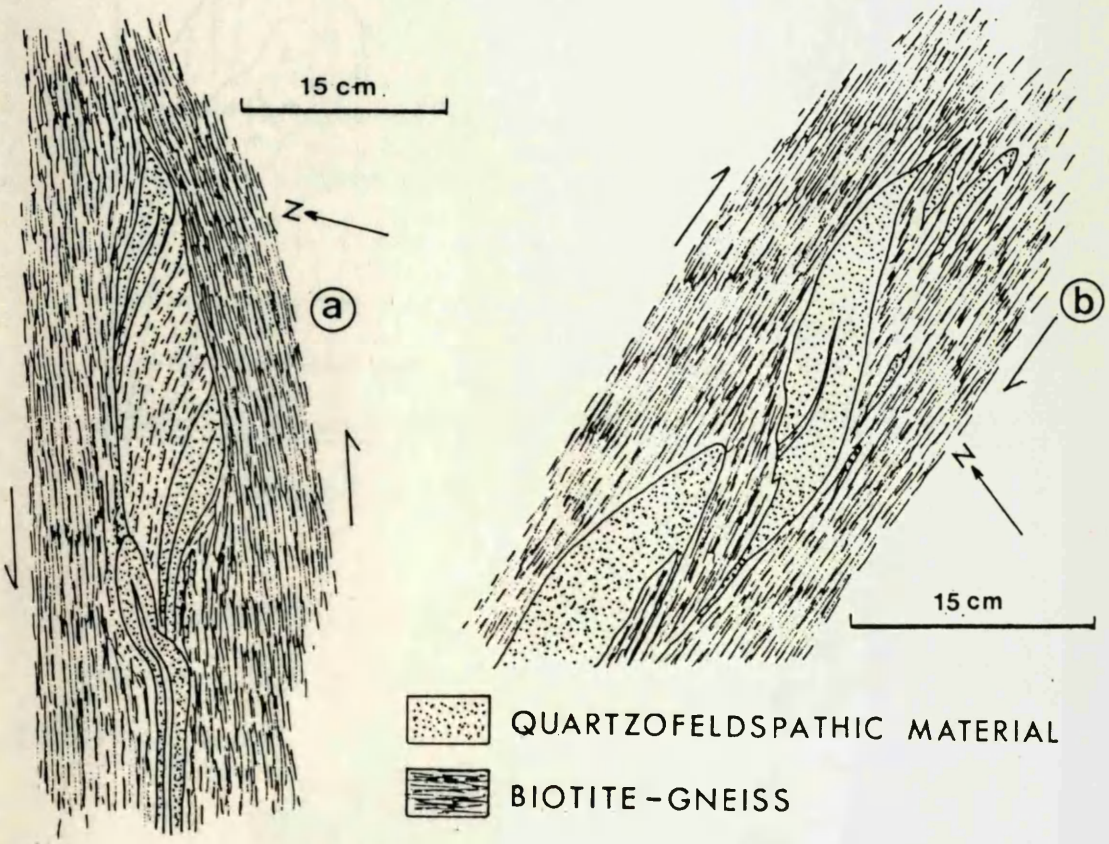
15 cm
Z
a
b
Z
15 cm
QUARTZOFELDSPATHIC MATERIAL
BIOTITE-GNEISS

Figure VII.46.a Folded transversal granodiorite vein, emplaced in quartzofeldspathic dioritic gneiss, displaying effects of compression in one of the limbs and extension in the other, as a result of deformation by a dextral shear couple; subarea IV, middle part (Drawing from a photograph).

Figure VII.46.b Strain analysis of the trondhjemite sheet displaying a rotated boudin as shown in figure VII.44. (Drawing from a photograph).

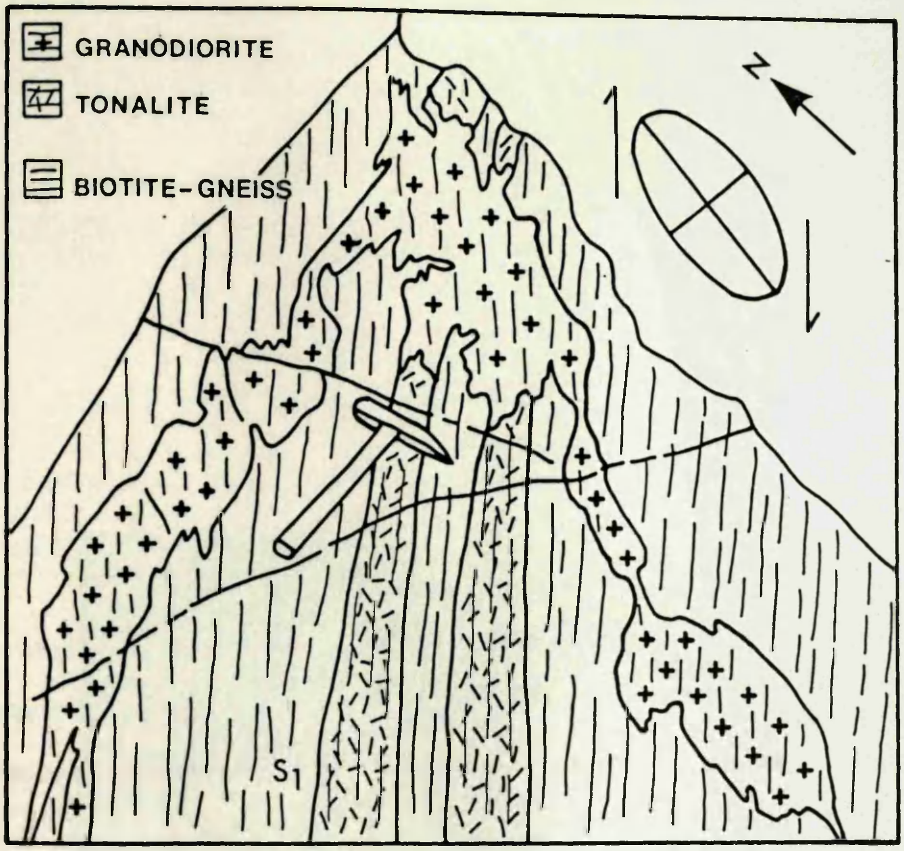
GRANODIORITE
TONALITE
BIOTITE-GNEISS
N
S1

(a)

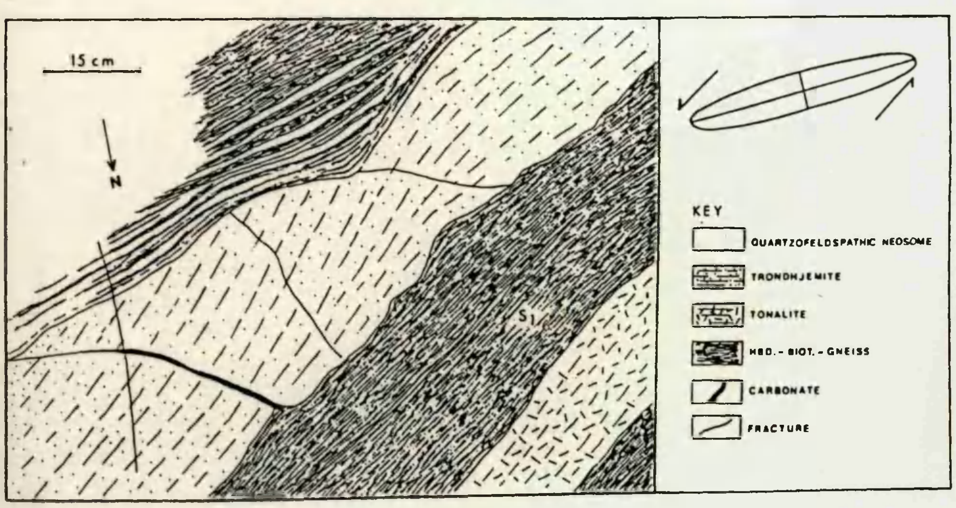
15 cm
N
S1
KEY
QUARTZOFELDSPATHIC NEOSOME
TRONDHJEMITE
TONALITE
HBD. - BIOT. - GNEISS
CARBONATE
FRACTURE

(b)

Figure VII.47 Banded quartzofeldspathic dioritic gneiss displaying gash veins filled with carbonate, related to a sinistral shear zone; subarea IV, eastern end.


N

Figure VII.48.a Photomicrograph of a quartzofeldspathic dioritic gneiss, showing an aggregate of chlorite with sigmoidal shape due to movement along a dextral shear zone; subarea I, southern part. (OL,X 20)

Figure VII.48.b Drawing from a photomicrograph of a quartzofeldspathic dioritic gneiss showing a porphyroblast of andesine displaying fractures filled with albite, and related to displacements in a sinistral shear zone; subarea I, southern part.

(a)

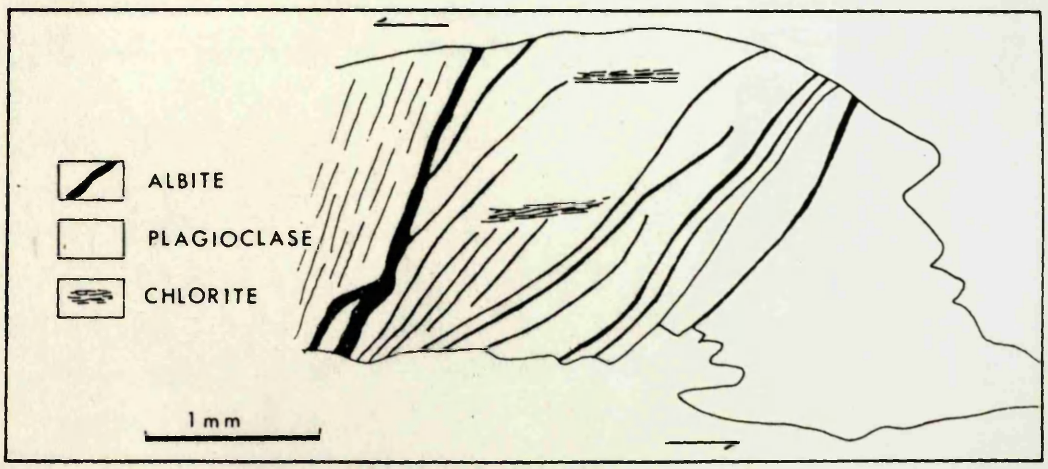

(b)

Figure VII.49. Variation with time of the principal compressive stress-system as inferred from the progressive development of different planar structural elements.

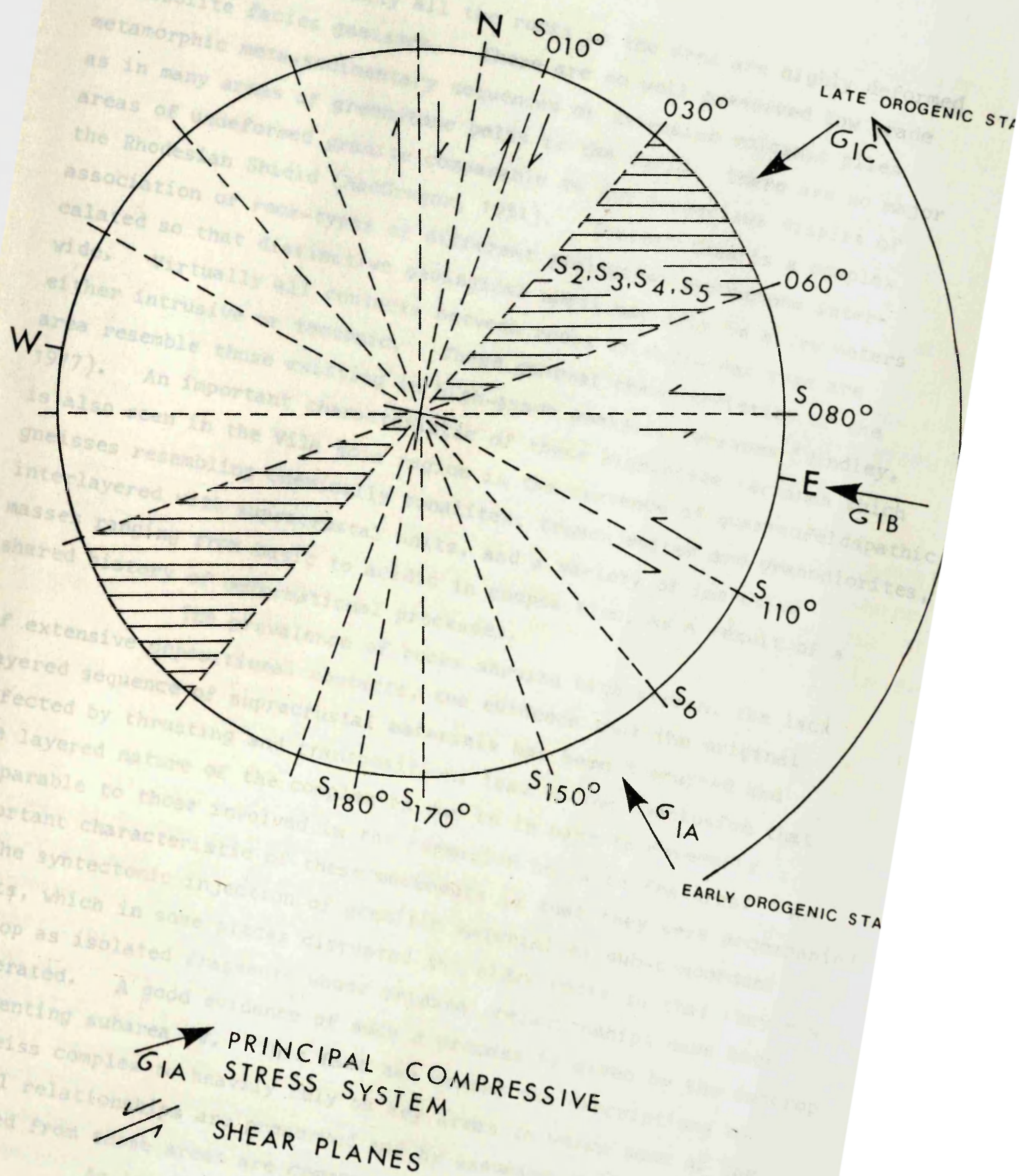
N
S 010°
030°
LATE OROGENIC STA
G IC
S2,S3,S4,S5
060°
W
S 080°
E
G IB
S 110°
S6
S 180°
S 170°
S 150°
G IA
EARLY OROGENIC STA
G IA
PRINCIPAL COMPRESSIVE STRESS SYSTEM
SHEAR PLANES

VIII. TECTONIC SETTING

Virtually all the rocks in the area are highly deformed amphibolite facies gneisses. There are no well preserved low grade metamorphic meta-sedimentary sequences or extensive volcanic piles as in many areas of greenstone belts in the world. There are no major areas of undeformed granite comparable to the gregarious diapirs of the Rhodesian Shield (MacGregor, 1951). Instead there is a complex association of rock-types of different geological provenance intercalated so that distinctive geological units may only be a few meters wide. Virtually all contacts between rocks of different type are either intrusive or tectonic. These general characteristics of the area resemble those existing in high-grade gneissic terranes (Windley, 1977). An important characteristic of these high-grade terranes which is also seen in the Vila Nova region is the presence of quartzofeldspathic gneisses resembling chemically tonalites, trondhjemites and granodiorites, interlayered with supracrustal units, and a variety of intrusive masses ranging from basic to acidic in composition, as a result of a shared history of deformational processes.

The prevalence of rocks showing high strain, the lack of extensive depositional contacts, the evidence that the original layered sequence of supracrustal materials has been disrupted and affected by thrusting and transposition, lead to the conclusion that the layered nature of the complex is due to in part to movements comparable to those involved in the formation of nappe features. An important characteristic of these movements is that they were accompanied by the syntectonic injection of granitic material as sub-concordant sheets, which in some places disrupted the older rocks so that they now outcrop as isolated fragments whose original relationships have been obliterated. A good evidence of such a process is given by the outcrop representing subarea IV. This fact has caused the descriptions of the gneiss complex to heavily rely on key areas in which some of the original relationships are preserved and by assuming that the phenomena described from these areas are common to the rest of the complex.

An important feature to consider when trying to interpret the tectonic evolution of the area is the presence of the tonalite-trondhjemite suite.

According to Barker (1979) tonalitic-trondhjemite suites are found in four principal geologic setting, as follows:

1) Archean grey gneisses terranes. This is the situation in which these suites are most developed, occurring through huge areas. The predominance is of intrusive bodies, but some volcanics may also exist. There is a common association with younger K-rich granitoids.

2) Peripheries of Archean greenstone belts formed by intrusions related to the deformation of those belts and also associated with intrusions of granitic rocks.

3) Along margins of Proterozoic and Palaeozoic continental margins. These may be related to subduction zones or to subsidiary back-arc spreading, and are typically accompanied by the quartz-diorite-tonalite-granodiorite granite suite.

4) Along margins of Mesozoic and Cenozoic continental margins. These are almost certaly related to subduction zones and are of relatively small volumes.

Arth (1979) has divided trondhjemitic rocks on the basis of their Al_2O_3 content into (1) continental (trondhjemites of high-Al_2O_3-type) and, (2) oceanic (low-Al_2O_3-type trondhjemites). The discrimination between both types of trondhjemitic rocks is enhanced by other chemical differences in both major and trace elements other than Al_2O_3. Thus figure VIII.1 and figure VIII.2 illustrate plots of Rb against S_r and K_2O against SiO_2, respectively, in which different fields of various rocks, according to Coleman & Peterman (1975), have been included for comparison. It is apparent from these figures that the trondhjemites plot within the field corresponding to continental trondhjemites. In terms of REE, figure VIII.3 shows examples of the chondrite normalized patterns for trondhjemites and chemically equivalent dacites from four distinct tectonic settings (Arth, 1979).

Trondhjemites from oceanic regions are characterized by flat or LREE depleted patterns with chondrites normalized values greater than 10 and negative Eu anomalies. On the other hand, continental trondhjemites have high fractionated patterns, showing chrondrite normalized HREE values less than 5, and small positive Eu anomalies. The correspondence of the Vila Nova trondhjemitic rocks with similar lithologies from continental environments is quite apparent from this figure.

As pointed out by Arth (1979) REE appears to be the most reliable of the elements used in studies of trondhjemite genesis and paleo-tectonic setting. According to this author low HREE contents are characteristic of trondhjemitic liquids originated at continental margins.

In figure VIII.4 the average La, Ce and Y contents of the Vila Nova tonalites and trondhjemites are compared with those of trondhjemitic rocks from New Mexico and Colorado, USA (cf. Barker et al., 1976). The tonalites closely resemble the Pitts Meadow granodiorite from Colorado whereas the trondhjemites despite a very close similarity in terms of LREE are much more depleted in HREE. According to Barker et al (1976) the Pitts Meadow granodiorite is produced from liquids formed by melting at 55 to 65 km depth. On the basis of the evidence provided by figure VIII.1, however, the trondhjemites may be deduced to have been produced at crustal levels about 15-20 km. It is apparent from figure VIII.1 that the tonalites tend to plot in a field of greater depths than the trondhjemites, followed by the diorites.

On the basis of the foregoing evidence it might be assumed that the Vila Nova Complex was formed in a tectonic setting of continental margin type.

However, some aspects of the Vila Nova Complex need to be analysed in more detail, as they differ from the general characteristics displayed by complexes formed along destructive plate margins. Following McGregor (1979) the Vila Nova rocks when compared with the classical calc-alkaline sequence from Western North America present distinctive characteristics as follows:

1) As illustrated in figure V.8 the trend of the Vila Nova rocks differs markedly from the normal calcalkaline trend of Nockolds & Allen (1954).

2) The intrusions are controlled by movement planes and do not form diapiric masses.

3) The tonalitic rocks are richer in SiO_2 as compared to similar rocks in the Southern California batholith, according to data from Larsen (1948, in McGregor, 1979).

4) Granodiorites in the Coast Plutonic Complex of British Columbia, Canada, have an average SiO_2 content of 63% (Roddick & Hutchison, 1974 in McGregor, 1979) and tonalites have 59% SiO_2, while in Vila Nova these rock types have 71 and 65% SiO_2, respectively.

5) In addition to being more silicic than the corresponding rocks in the Western North American batholith, the Vila Nova rocks are more sodic, as shown in figure V.8.

The sheet-like, thrust-controlled emplacement of granitic sheets in the Vila Nova Complex is more in accordance with the situation reported by McGregor (1979) in relation to the formation of the Nuk gneisses in the Greenland Archean. In fact, McGregor (1979) has emphasized the very different form of the Nûk gneisses as compared to calc-alkaline batholiths associated with convergent plate margins, since the former were intruded mostly as sub-concordant sheets rather than globular masses forcibly intruded into denser crust. According to him, the reason for this difference must be sought in the tectonic conditions that prevailed during the intrusion of the Nûk magmas. These, according to Bridgewater et al. (1974) were intruded during a period of very intense horizontal movements and McGregor (1979) has pointed out that these intrusions accompanied deformation as demonstrated by many sheets intruded along active movement planes.

Inclusions of supracrustal rocks, mainly amphibolites, ultramafic rocks and dioritic gneisses are common within the Nûk gneisses. These are characterized by a number of different gneiss phases and where the sequence is less deformed it is clear that the different phases have intruded one another and that the more biotite-rich members are older than the more leucocratic. Hence the trondhjemites are younger than the tonalites, and the granodiorites are the youngest members of the sequence (McGregor, 1979).

This rock succession is much the same that described as making up the suite which is younger than the suprecrustals in the Vila Nova area.

On chemical grounds, the features of the Vila Nova rocks which compare with those of the Nûk gneisses, are (1) considerable scatter of points on plots of SiO_2 against Al_2O_3; (2) high contents of Na_2O, K_2O, Sr and Ba and low contents of TiO_2, as compared with many other calc-alkaline sequences with similar SiO_2 contents; (3) very low concentrations of Y, suggesting that the rocks are depleted in heavy rare earths; (4) a marked decrease in Ni with increasing SiO_2.

In the Nûk gneisses assemblage in the Buksefjorden region, Greenland (McGregor, 1979) the trondhjemitic gneisses have REE patterns that are consistent with an origin by hornblende fractionation of dioritic or tonalitic magmas, or by a large fraction of partial melting of amphibolites. The association of the trondhjemitic rocks, as minor phases, with tonalitic gneisses favours the former possibility, as have been the conclusion in relation to the Vila Nova suite.

In relation to these characteristics of the Greenland Archean, Myers (1976) has suggested that the sheet-like granitoid intrusions might have been generated at a Himalayan-type convergent plate margins. This fact could have provided an extensive environment in which thrust tectonics was associated with the production of granitoid rocks and crustal thickening. The relatively high proportion of adamellites found in the Vila Nova area is consistent with the granitic rocks expected to be generated in such an environment.

In addition the rotation of the fold axial planes with time from a position subvertical (D_2) to a subhorizontal attitude

(D_5), is compatible with a deformational process in which the forces acting on the rocks were, at first, dominantly compressional with the main direction of relief positioned vertically, but changed later on to a couple with a subhorizontal direction of relief. This evolution can be explained on the basis of the deformation of the supracrustal pile having taken place by the closure of the depositional site, under the influence of crustal blocks which approached relative to one another on account of plates motion. It appears to be significant the dramatic change in the orientation of the overall compressive stress-system, from D_6 onwards. This may indicate that when the approaching blocks (continents?) achieved a certain limit of movement along the NW-SE direction the continued driving force originated components which caused the counterclockwise rotation of the crustal elements about a vertical axis. This rotation was enhanced by the irregular boundaries of the crustal elements involved in this deformational process.

On the other hand, the time-related generation of K_2O-rich acidic magmas if found to be the result of partial melting of crustal rocks, could be the result of the thickening of the crust caused by such a type of collision.

FIGURES VIII.1 TO VIII.4

Figure VIII.1 Plot of Rb against Sr for the intrusive rocks of the Vila Nova Complex. The ringed fields are as follows: (A) Continental tronghjemites and quartz diorites; (B) Continental granophyres and Iceland rhyolites; (C) Red Sea granophyres (after Coleman & Peterman, 1975). The dashed lines separating distinct fields of depth of magma generation are from Condie (1973).

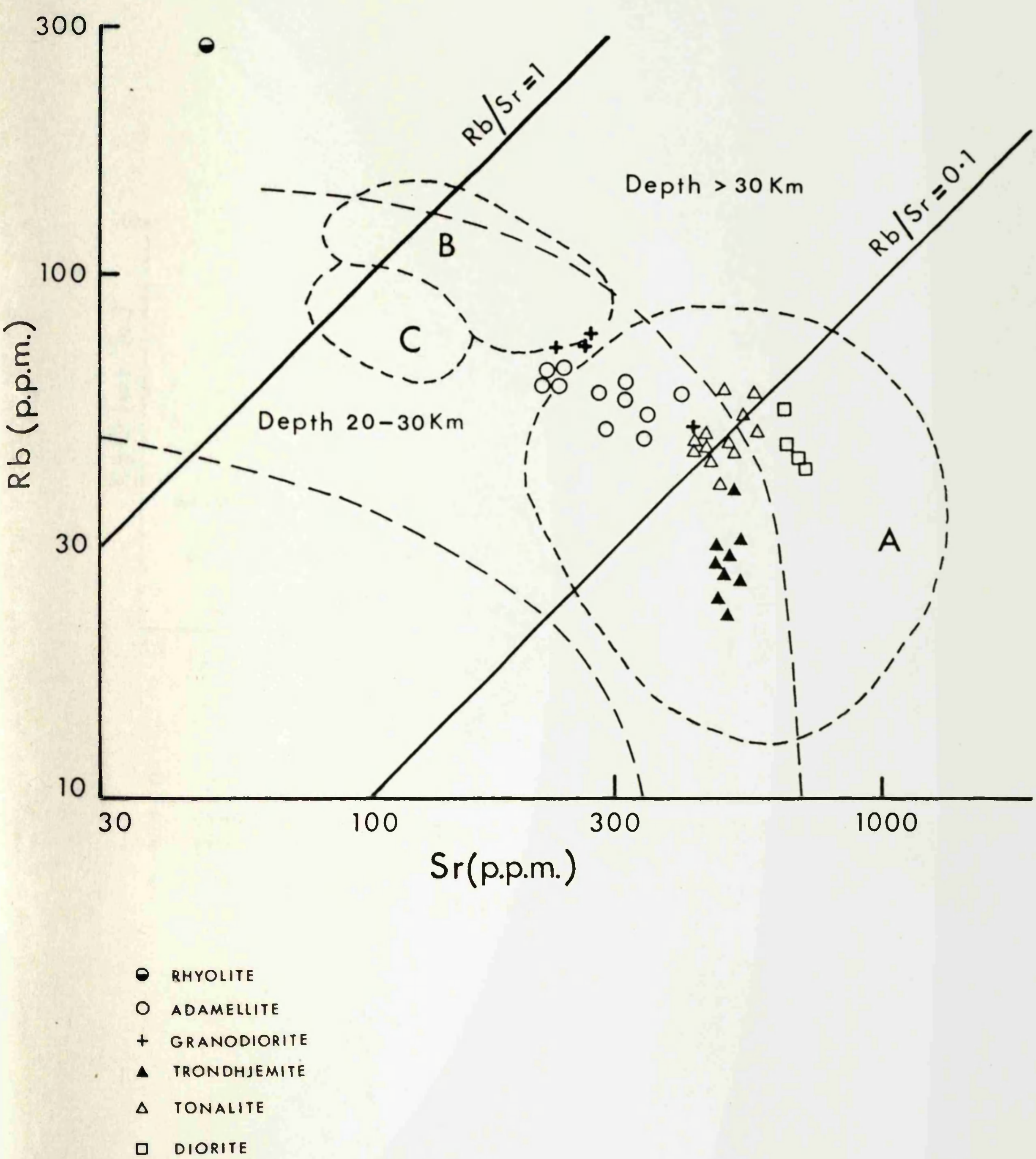
300
100
30
10
Rb (p.p.m.)
30
100
300
1000
Sr(p.p.m.)
Rb/Sr =1
Rb/Sr =0·1
Depth > 30 Km
Depth 20–30 Km
A
B
C
RHYOLITE
ADAMELLITE
GRANODIORITE
TRONDHJEMITE
TONALITE
DIORITE

Figure VIII.2 Plots of K_2O against SiO_2 for the intrusive rocks of the Vila Nova Complex compared to fields from Coleman & Peterman (1975) as follows: (A) Continental trondhjemites; (B) Continental granophyres.

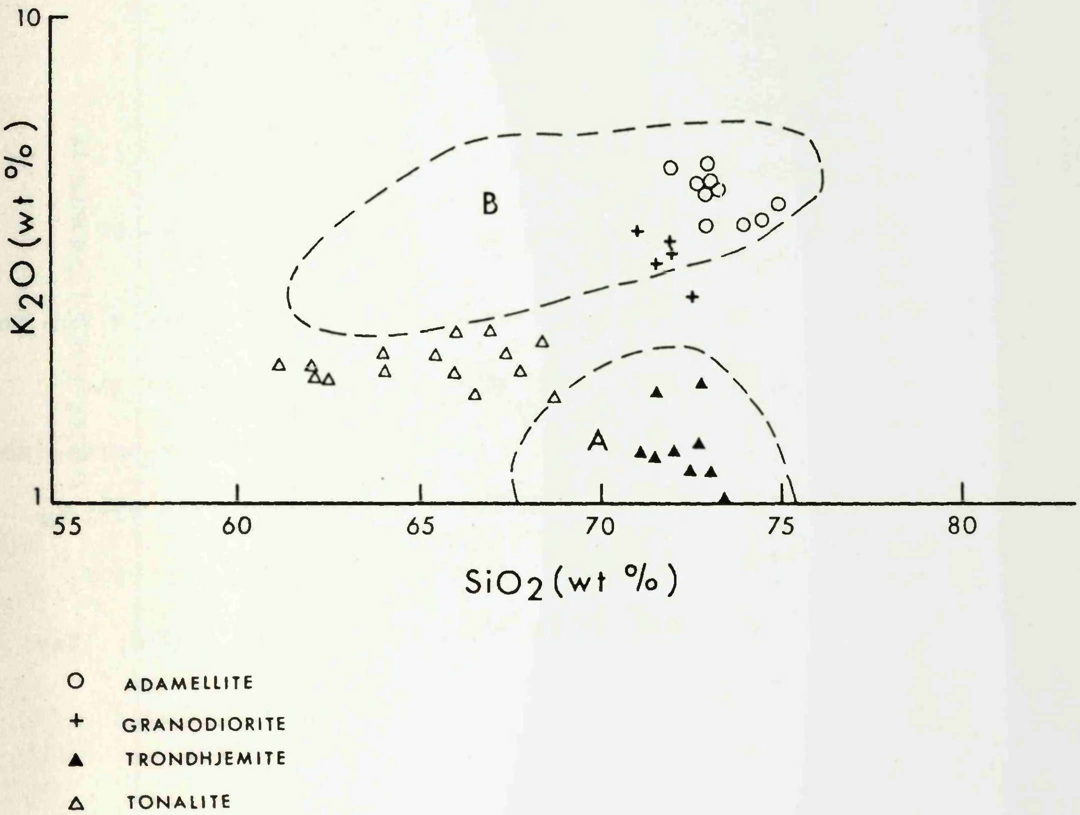
10
1
K_2O (wt %)
55
60
65
70
75
80
SiO_2 (wt %)
B
A
ADAMELLITE
GRANODIORITE
TRONDHJEMITE
TONALITE

Figure VIII.3 Range of chondrite-normalized La, Ce and Y for the diorites, tonalites and trondhjemites of the Vila Nova Complex compared to chondrite-normalized rare earth plots for trondhjemites from various tectonic settings (after Arth & Hanson, 1972; Arth & Barker, 1976; Barker *et al.*, 1976; Kay & Senechal, 1976 in Arth, 1979).

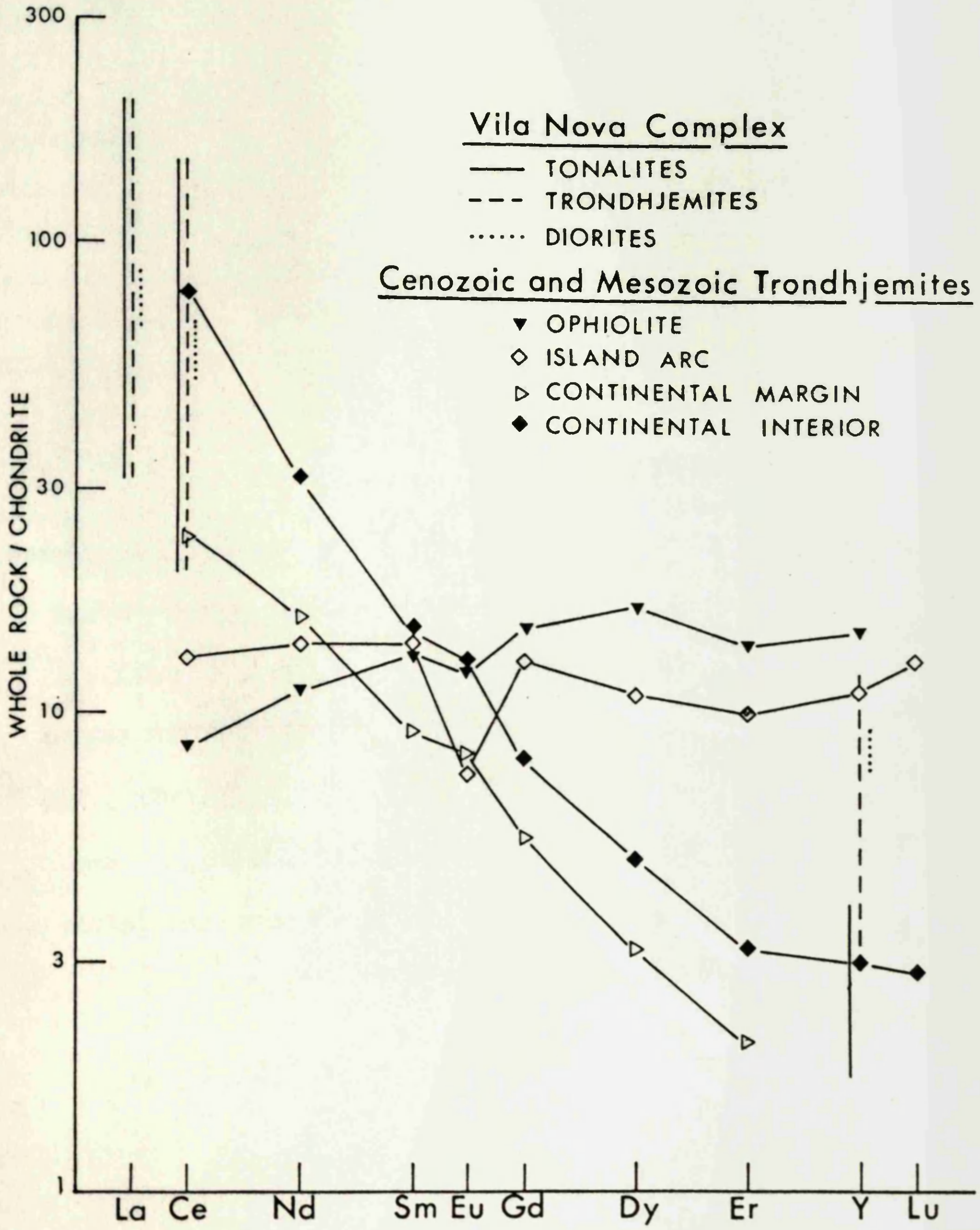

Vila Nova Complex
TONALITES
TRONDHJEMITES
DIORITES
Cenozoic and Mesozoic Trondhjemites
OPHIOLITE
ISLAND ARC
CONTINENTAL MARGIN
CONTINENTAL INTERIOR
WHOLE ROCK / CHONDRITE
300
100
30
10
3
1
La Ce Nd Sm Eu Gd Dy Er Y Lu

Figure VIII.4 Chondrite-normalized La, Ce and Y (considered as a HREE) for the diorites, tonalites and trondhjemites of the Vila Nova Complex, compared to chondrite-normalized REE trends of the Twilight gneiss (Colorado, USA), Rio Brazos trondhjemite (New Mexico, USA) and Kroenke grandiorite (Colorado, USA) (after Barker _et al._, 1976).

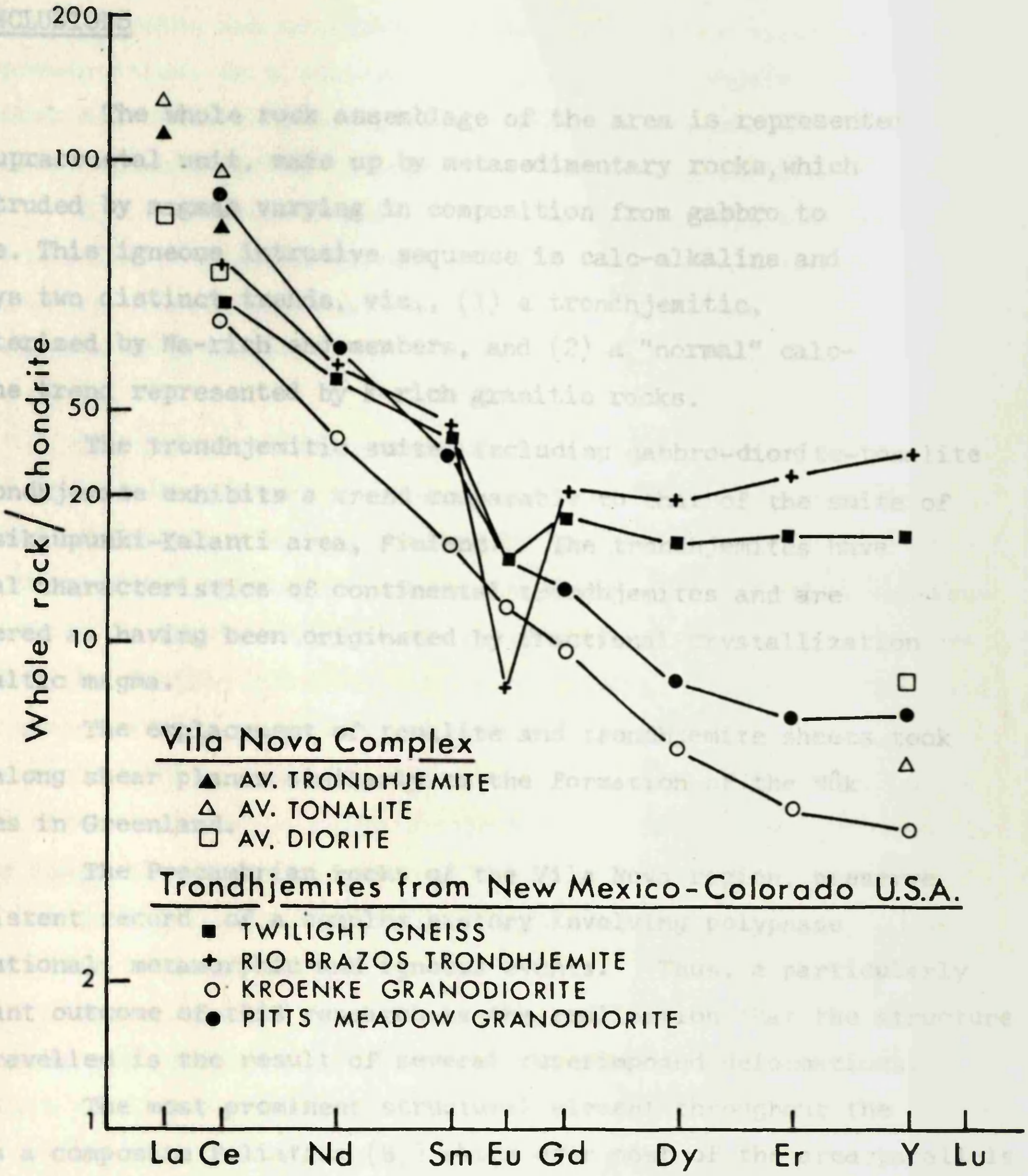
Whole rock / Chondrite
200
100
50
20
10
2
1
La Ce Nd Sm Eu Gd Dy Er Y Lu
Vila Nova Complex
AV. TRONDHJEMITE
AV. TONALITE
AV. DIORITE
Trondhjemites from New Mexico-Colorado U.S.A.
TWILIGHT GNEISS
RIO BRAZOS TRONDHJEMITE
KROENKE GRANODIORITE
PITTS MEADOW GRANODIORITE

IX. CONCLUSIONS

The whole rock assemblage of the area is represented by a supracrustal unit, made up by metasedimentary rocks, which was intruded by magmas varying in composition from gabbro to granite. This igneous intrusive sequence is calc-alkaline and displays two distinct trends, viz., (1) a trondhjemitic, characterized by Na-rich end-members, and (2) a "normal" calc-alkaline trend represented by K-rich granitic rocks.

The trondhjemitic suite, including gabbro-diorite-tonalite and trondhjemite exhibits a trend comparable to that of the suite of the Uusikaupunki-Kalanti area, Finland. The trondhjemites have chemical characteristics of continental trondhjemites and are considered as having been originated by fractional crystallization of basaltic magma.

The emplacement of tonalite and trondhjemite sheets took place along shear planes similarly to the formation of the Nûk gneisses in Greenland.

The Precambrian rocks of the Vila Nova region, preserve a consistent record of a complex history involving polyphase deformational, metamorphic and igneous events. Thus, a particularly important outcome of this research is the realization that the structure now unravelled is the result of several superimposed deformations.

The most prominent structural element throughout the area is a composite foliation (S_1) which over most of the area parallels a lithological layering, mostly resulting from both extensive metamorphic differentiation and igneous activity. The extremely transposed nature of this foliation and the very common occurrence of intrafolial, rootless, isoclinal folds are evidence of a regime of strong deformation, in which flowage played the most outstanding role.

Despite the extensive tectonic overprinting the dominant foliation (S_1) has retained its identity and, in some places, even remnants of the original layering (S_0) can be found.

Some of the structural complexity of the area, considered so far as resulting from ptygmatic folding, is the result of polyphase deformation.

F_2 folds are considered as making up major structures with representatives on a regional scale, forming elongate non-cylindrical features in whose limbs F_3 developed forming the largest structures mapeable within the domain represented by the studied area.

D_3 is the most important deformational phase because, apart from being recognized everywhere, it gave rise to structural features which provide information leading to the reliable interpretation of a progressive, and likely long-lasting deformational history.

The different deformational phases were identified on the basis of their mutual relationships in the field and they have been considered as making up a single orogenic episode related to three general compressive stress-systems. The first of these stress-systems is considered as responsible for the generation of structural features essentially by ductile flow, during an early orogenic stage. The late general stress-system is related to deformational processes taking place in rocks with a predominant brittle behaviour. The orientation of these stress-systems is quite distinct from one another and there is evidence suggesting that the orientation of the principal compression rotated counterclock-wise with time from NW-SE (early orogenic stage) to NE-SW (late orogenic stage).

The structural and geochemical characteristics exhibited by the whole rock-sequence suggest that the orogenic episode was caused by a continent-continent collision.

On the basis of the lithological and structural complexity which has been unravelled for the studied area, and for considering either "Cambai Formation" or "Cambai Group" as inadequate terms to designate the rock assemblage dealt with, the designation "Vila Nova Complex" is suggested to replace the previous terms.

X. REFERENCES

ANDERSON, T.B. 1974 The relationships between kink bands and shear fractures in the experimental deformation of slate. J.Geol. Soc. London, 130: 367-82.

ARTH, J.G. 1976 A model for the origin of the Early Precambrian Greenstone-Granite Complex of Northeastern Minnesota. In: B.F. Windley, Ed. The early history of the Earth, Wiley, New York, p. 299-302.

ARTH, J.G. 1979 Some trace elements in trondhjemites. Their implications to magma genesis and plate tectonic settings. In: F. Barker, Ed. Trondhjemites, dacites and related rocks. Developments in Petrology, 6. Elsevier, Amsterdam. p. 123-32.

ARTH, J.G. & BARKER, F. 1976 Rare-earth partitioning between hornblende and dacitic liquid and implications for the genesis of trondhjemitic-tonalitic magmas. Geology, 4: 534-36.

ARTH, J.G. & HANSON, G.N. 1975. Geochemistry and origin of the early Precambrian crust of northeastern Minnesota. Geoch. Cosmoch. Acta, 30: 325-62.

ARTH, J.G.; BARKER, F.; PETERMAN, Z.E.; FRIEDMAN, I. & DESBORANGE, G.A. 1974 Geochemistry of the gabbro, diorite, tonalite, trondhjemite suite of the Kalanti area, Southwest Finland. Geol. Soc. Am. Bull, 65:637-38.

BARKER, F. 1979 Trondhjemite: definition, environment and hypothesis of origin. In: F. Barker, Ed. Trondhjemites, dacites and related rocks, Developments in Petrology, 6. Elsevier, Amsterdam, p.1-12.

BARKER, F. & ARTH, J.G. 1976 Generation of trondhjemitic-tonalitic liquids and Archean bimodal trondhjemite-basalt suites. Geology, 4: 596-60.

BARKER, F.; ARTH, J.G. & MILLARD, Jr. H.T. 1979 Archean trondhjemites of the southwestern Big Horn Mountains, Wyoming: a preliminary report. In: F. Barker, Ed. Trondhjemites, dacites and related rocks, Developments in Petrology, 6. Elsevier, Amsterdam. p. 401-14.

CARVALHO, P.F. 1932 Reconhecimento geológico do Estado do Rio Grande do Sul. Instituto Geológico e Mineralógico do Brasil, Rio de Janeiro, Boletim 66.

CHENEY, E.S. & STEWART, R.J. 1975 Subducted graywacke in the Olimpic Mountains, USA - Implications for the origin of Archean sodic gneisses. Nature, 258:60-1.

CHURCH, B.N. 1975 Quantitative classification and chemical comparison of common volcanic rocks. Geol.Soc.Am.Bull., 86:257-63.

COBBOLD, P.R.; COSGROVE, J.W. & SUMMERS, J.M. 1971 The development of internal structure in deformed anisotropic rocks. Tectonophysics, 12: 23-53.

COLEMAN, R.G. & PETERMAN, Z.E. 1975 Oceanic plagiogranite. J.Geophys.Res., 80:1099-108

COLLERSON, K.D. & BRIDGWATER, D. 1979 Metamorphic development of early Archean tonalitic and trondhjemitic gneisses: Saglek area, Labrador. In: F. Barker, Ed. Trondhjemites, dacites and related rocks. Developments in Petrology, 6. Elsevier, Amsterdam p. 205-73.

CONDIE, K.C. 1973 Archean magmatism and crustal thickening. Geol.Soc.Am.Bull., 84: 2981-92.

COX, K.G.; BELL, J.D. & PARKHURST, R.J. 1979 The interpretation of igneous rocks. George Allen & Unwin, London. 450 p.

DASH, B. 1969 Structure of the Lewisian rocks between Strath Dionard and Rhiconich, Sutherland, Scotland. Scot. J.Geol., 5: 347-74.

DEWEY, J.F. 1965 Nature and origin of kink bands. Tectonophysics, 1: 459-94.

DIETRICH, R.V. & MEHNERT, K.R. 1960 Proposal for the nomenclature of migmatites and associated rocks. In: Inter.Geol.Cong., 21, Copenhagen, Report Session, Supp.Vol.Sect. 1-21: 56-67.

DONATH, F.A. 1961 Experimental study of shear failure in anisotropic rocks. Geol.Soc.Am.Bull., 72: 985-90

EHLERS, E.G. & BLATT, H. 1980 Petrology. Igneous, sedimentary and metamorphic. W.H. Freeman, San Francisco. 732p.

ESKOLA, P. 1939 Die metamorphen Gesteine. In: T.F.W. Bartte, C.W. Correns & P. Eskola, Eds. Die Entstehung der Gesteine. Julius Springer, Berlin, p263-407.

EVANS, B.W. & LEAKE, B.E. 1960 The composition and origin of the striped amphibolites of Connemara, Ireland. J. Petr., 1(3): 337-63.

FINDLAY, D. 1970 Studies of fold tectonics in the Lewisian of the Durness region, Sutherland. Ph.D. Thesis, University of Glasgow, (Unpublished).

GOLDSCHMIDT, V.M. 1922 Stammestypen der Eruptivgesteine, Vidensk. Sksifter, Kristianic., I. Mat.Na.Klasse, 10:1-12.

GONI, J.C. 1962 Origine des roches ultrabasiques et serpentineuses du pré-Cambrien de Rio Grande do Sul (Brésil). Mode de gisement et minéralization Bol.Esc.Geol.Porto Alegre, 12: 1-89.

GONI, J.C., GOSO, H. & ISSLER, R.S. 1962 Estratigrafia e geologia economica do Pré-Cambriano e Eopaleozoico uruguaio et sul-riograndense. Avulso Esc.Geol.Porto Alegre, 3.

GREEN, T.H. & RINGWOOD, A.E. 1966 Origin of calc-alkaline igneous rock suite, Earth Planet.Sci.Letters, 1: 307-16.

GREEN, T.H. & RINGWOOD, A.E. 1968 Genesis of calc-alkaline igneous rock suite. Contr.Miner.Petro., 18: 105-62.

HALDEN, N.M. 1982 Structural, metamorphic and igneous history of migmatites in the deep levels of a wrench fault regime, Savonranta, Eastern Finland. Trans.Royal Soc.Edinburgh, Earth Sciences, 73: 17-30.

HANSEN, E. 1971 Strain facies. Springer Verlag, Berlin. 207p

HANSON, G.N. & GOLDISH, S.S. 1972 Early Precambrian rocks of the Saganaga Lake - Northern Light Lake area, Minnesota-Ontario. Part II: Petrogenesis. Geol.Soc.Am.Memoir, 135: 179-92.

HARPUM, J.R. 1963 Petrographic classification of granitic rocks in Tanganyika by partial chemical analysis, Records Geol.Surv. Tanganyika, 10: 80-88.

HATCH, F.H.; WELLS, A.K. & WELLS, M.K. 1972 Petrology of the igneous rocks. George Allen & Unwin, London. 550p.

HIETANEN, A. 1943 Über das Grundgebirge des Kalantigebietes im Südwestlichen Finnland. Bull.Comm.Geol.Finlande, 130: 1-250.

HOLLOWAY, J.R. 1971 Composition of fluid phase solutes in a Basalt-H_2O-CO_2 system. Geol.Soc.Am.Bull., 82: 233-38

HOPGOOD, A.M. 1971a Structure and tectonic history of Lewisian gneiss. Isle of Barra, Scotland. Krystalinikum, 7: 27-60.

HOPGOOD, A.M. 1971b Correlation by tectonic sequence in Precambrian gneiss terrains. Spec.Pub.Geol.Soc.Australia, 3: 367-76.

HOPGOOD, A.M. 1973 The significance of deformational sequence in discriminating between Precambrian terrains. Sp.Pub.Geol.Soc. South Africa, 3: 45-52.

HOPGOOD, A.M. 1980 Polyphase fold analysis of gneisses and migmatites. Trans. Royal Soc.Edinburgh, Earth Sciences, 71: 55-68.

HOPGOOD, A.M. & Bowes, D.R. 1972 Application of structural sequence to the correlation of Precambrian gneisses, Outer Hebrides, Scotland. Geol.Soc.Am.Bull., 83: 107-28.

HOPGOOD, A.M. & BOWES, D.R. 1978 Neosomes of polyphase agmatites as time-markers in complexly deformed migmatites. Geol.Rundsc., 67: 313-30.

HOPGOOD, A.M.; BOWES, D.R. & ADDISON, J. 1976 Structural development of migmatites near Skaldö, Southwest Finland. Bull.Geol.Soc.Finaland. 48: 43-62.

HUGHES, C.J. 1982 Igneous Petrology. Developments in Petrology, 7 Elsevier, Amsterdam. 551p.

JAMES, R.S. & HAMILTON, D.L. 1969 Phase relations in the system $NaAlSi_3O_8$-$CaAl_2Si_2O_8$-SiO_2 at 1 kilobar water vapour pressure. Contr.Miner.Petro., 21:111-41.

JOST, H. & VILLWOCK, J.A. 1966 Contribuição à estratigrafia do Pré-Cambriano do Rio Grande do Sul. Notas e Estudos Esc.Geol. Porto Alegre, 1(1): 13-26.

JOUBERT, P. 1971 The regional tectonism of the gneisses of part of Namaqualand. Precambrian Research Unit Bull., Chamber of Mines, Univ. of Cape Town, 10: 220.p.

KLEEMAN, A.W. 1965 The origin of granitic magmas. J. Geol.Soc. Australia, 12: 35-52.

KOISTINEN, T.J. 1981 Structural evolution of an early Proterozoic strata-bound Cu-Co-Zn deposit, Outokumpu, Finland. Trans.Royal Soc.Edinburgh, Earth Sciences, 72(2): 115-58.

LAMBERT, I.B. & WYLLIE, P.J. 1970 Melting inthe deep crust and upper mantle and the nature of the low-velocity zone. Phys. Earth Planet.Interiors, 3: 316-22.

LAMBERT, R. St.J. & HOLLAND, J.G. 1974 Yttrium geochemistry applied to petrogenesis utilizing calcium-yttrium relationships in minerals and rocks. Geoch.Cosmoch.Acta, 38: 1393-414.

LEAKE, B.E. 1964 The chemical distinctions between ortho- and para-amphibolites. J. Petrol., 5(2): 238-54.

LUTH, W.C.: JAHNS, R.H. & TUTTLE, O.F. 1964 The granitic system at 4 to 10 kilobars, J.Geophys.Res., 64:759-73.

MacGREGOR, A.M. 1951 Some milestones in the Precambrian of Southern Rhodesia. Proc.Geol.Soc.South Africa, 54: 27-71.

MARJORIBANKS, R.W.; RUTLAND, R.W.R.; GLEN, R.A.& LAING, W.P. 1980 The structure and tectonic evolution of the Broken Hill region, Australia, Precambrian Res., 13: 209-40.

MASON, R. 1978 Petrology of the metamorphic rocks. George Allen & Unwin, London. 254p.

McGREGOR, V.R. 1979 Archean grey gneisses and the origin of the continental crust: evidence from the Godthab region, West Greenland. In: F. Barker, Ed. Trondhjemites, dacites and related rocks, Developments in Petrology, 6. Elsevier, Amsterdam. p 169-204.

MEHNERT, K.R. 1968 Migmatites and the origin of granitic rocks. Developments in Petrology, 1. Elsevier, Amsterdam. 405 p.

MIYASHIRO, A. 1961 Evolution of metamorphic belts. J.Petro., 2: 277-311.

MIYASHIRO, A. 1973 Metamorphism and metamorphic belts. George Allen & Unwin, London. 492 p.

MYERS, J.S. 1976 Granitoid sheets, thrusting and Archean crustal thickening in West Greenland. Geology, 4: 265-68.

NAHA, K. & HALYBURTON, R.V. 1977 Structural pattern and strain history of a superimposed fold system in the Precambrian of central Rajasthan, India. I: Structural pattern in the "Main Raiah Syncline", Central Rajasthan. Precambrian Res., 4: 39-84.

NOCKOLDS, S.R. & ALLEN, R. 1953 The geochemistry of some igneous rocks series. Geoch.Cosmoch.Acta, 4: 105-42.

NOCKOLDS, S.R.: KNOX, R.W. & CHINNER, G.A. 1978 Petrology for students, Cambridge Univ. Press, Cambridge. 435p

O'CONNOR, J.T. 1965 A classification for quartz-rich igneous rocks based on feldspar rations. U.S.Geol.Surv.Prof.Pap. 525-B: 79-84.

ORVILLE, P.M. 1969 A model for metamorphic differentiation origin of thin-layered amphibolites. Am.J.Sci., 267: 64-86.

PARK, R.G. 1969 Structural correlation in metamorphic belts. Tectonophysics, 7(4): 323-38.

PARK, R.G. 1981 Shear-zone deformation and bulk strain in granite-greenstone terrain of the western Superior Province, Canada. Precambrian Res., 14: 31-47.

PARK, R.G. 1983 Foundations of structural geology. Blackie, London. 135p

PAYNE, J.G. & STRONG, D.F. 1979 Origin of the Twillingate trondhjemite, north-central Newfoundland: partial melting in the roots of an island arc. In: F. Barker, Ed. Trondhjemites, dacites and related rocks, Developments in Petrology, 6. Elsevier, Amsterdam. P 489-516.

PETERMAN, Z.E. 1979 Strontium isotope geochemistry of late Archean to late Cretaceous tonalites and trondhjemites. In: F. Barker, Ed. Trondhjemites, dacites and related rocks, Developments in Petrology, 6. Elsevier, Amsterdam. p133-47.

PHILPOTTS, J.A. 1974 Redox estimation from a calculation of Eu^{+2} and Eu^{+3} concentrations in natural phases. Earth Planet, Sci. Letters, 9: 257-68.

PICADA, R.S. & LOWATSKY, R. 1962 Geologia da Faixa VII, Folha de Vila Nova, São Sepe. Trabalho de Graduação, Escola de Geologia de Porto Alegre (Unpublished).

POLDERVAART, A. & GILKEY, A.K. 1954 On clouded plagioclase Am. Miner., 39: 75-91.

PRICE, N.J. 1966 Fault and joint development in brittle and semi-brittle rock. Pergamon Press, New York. 176 p.

RAMBERG, H. 1959 Evolution of ptygmatic folding. Norsk.Geol. Tidsskr., 39: 99-151

RAMBERG, H. 1963 Fluid dynamics of viscous buckling applicable to folding of layered rocks. Am.Assoc.Petrol.Geol.Bull., 47: 484-505.

RAMBERG, H. & GHOSH, S.K. 1968 Deformation structures in the Hovin Group Schists in the Hommelvik-Hell region (Norway). Tectonophysics, 6(4); 311-30.

RAMSAY, J.G. 1962 Interference patterns produced by the superimposition of folds of similar type. J.Geol., 70: 466-81.

RAMSAY, J.G. 1967 Folding and fracturing of rocks. McGraw Hill, New York. 568 p.

RAMSAY, J.G. 1980 Shear zone geometry: a review. J.Struct.Geol., 2: 83-99.

RAMSAY, J.G. & GRAHAM, R.H. 1970 Strain variation in shear belts. Canad.J.Earth Sci., 7: 786-813.

RIBEIRO, M.; BOCCHI, P.R.; FIFUEIREDO F°, P.M. & TESSARI, R.I. 1966 Geologia da quadricula de Caçapava do Sul, RS, Brasil. DFPM, DNPM, Rio de Janeiro, Boletim, 127: 1-200.

SANDER, B. 1930 Geflügekunde der Gesteine. Springer-Verlag, Berlin. 352 p.

SKINNER, W.R.; BOWES, D.R.; KHOURY, S.G. 1969 Polyphase deformation in the Archean basement complex, Beartooth Mountains, Montana and Wyoming. Geol.Soc.Am.Bull., 80: 1053-60.

TARNEY, J.; WEAVER, B.& DRURY, S.A. 1979 Geochemistry of Archean trondhjemite and tonalitic gneisses from Scotland and East Greenland, In: F. Barker, Ed. Trondhjemites, dacites and related rocks, Developments in Petrology, 6 Elsevier, Amsterdam. p. 275-99.

TURNER, F.J. & VERHOOGEN, J. 1960 Igneous and metamorphic petrology McGraw Hill, New York. 694 p.

TURNER, F.J. & WEISS, L.E. 1963 Structural analysis of metamorphic tectonites. McGraw Hill, New York. 545p.

TUTTLE, O.F. & BOWEN, N.L. 1958 Origin of granite in the light of experimental studies in the system $NaAlSi_3O_8$-$KAlSi_3O_8$-SiO_2-H_2O. Geol.Soc.Am.Memoir, 74: 1-153.

VERHOOGEN, J.; TURNER, F.J.; WEISS, L.E. & WAHRFAFTIG, C. 1970 The Earth. Holt, Rinehart & Winston, New York. 748 p.

WHITE, A.J.R. & CHAPPELL, B.W. 1977 Ultrametamorphism and granitoid gneisses, Tectonophysics, 43: 7-22.

WINDLEY, B.F. 1977 The evolving continents. Wiley, New York. 385 p.

WINKLER, H.G.F. 1967 Petrogenesis of metamorphic rocks. Springer-Verlag, Berlin. 218 p.

WINKLER, H.G.F. & von PLATEN, H. 1961 Experimentelle Gestein-metamorphose: IV- Bildung anateklischer Schmelzen aus metamorphisierten Grauwacken. Geoch, Cosmoch.Acta, 24: 48-69.

YODER, H.S. & TILLEY, C.E. 1962 Origin of basalt magmas; an experimental study of natural and synthetic rock systems. J.Petro., 3: 342-52.

XI. APPENDIX

A NEW MODEL OF "UNIVERSAL COMPASS"

Breno Correa da Silva Filho+

ABSTRACT

This paper introduces a new instrument which has been designed for geological mapping, whose greatest usefulness is achieved when the work is concerned with structural analysis and a great deal of attitudes of both planar and linear structures are to be determined.

The instrument allows the determination in a single operation of the strike and dip of a planar rock surface, as well as, the rake of any lineation it contains.

The classical drawback posed by steeply plunging lineations, as far as trend measurements are concerned, is easily overcome by using this true "universal compass".

INTRODUCTION

In the course of any geological mapping the determination of attitudes of both, planar and linear structures is a task with which a field geologist is very much concerned. The aim of such a field procedure varies depending on the type of structures dealt with (viz. primary or secondary structures) but

---

+ Federal University of Rio Grande do Sul
Department of Geology
Porto Alegre, RS - Brazil

the position in space of the latter, whatever the origin they have, is determined with the aid of a compass which is known as the "geologist's compass". The performance of this compass is, however, unsatisfactory in many circumstances. As a matter of fact frequently the geologists has to use the compass together with a board, his note-book, or a pencil, in order to overcome difficulties related to the determination of attitudes of planes or lineations.

On the grounds of structural analysis this problem takes up a great importance on account of the amount of readings that must be taken, and because it has a high effect on the precision of the measurements.

In the past, geological maps used to display dominantly the distribution of rock units, i.e. they used to be essentially lithological maps. In fact, prior to the structural approach initiated by SANDER (1930) workers were by far more concerned with Stratigraphy and Petrology. The importance of Sander's work was such that a new branch of geology dealing with the detailed study of structures came up. This field of geological research was put forward by SANDER (op.cit.) under the name of "Gefügekunde" and after being introduced to English-speaking geologists by KNOPF (1933) it has been translated into English as "petrofabrics", "structural petrology", and ultimately, as "structural analysis". This latter term is the preferable, according to TURNER & WEISS (1963), for it does not carry the connotation of microscopic study, as is the case in relation to the first two terms.

Structural analysis as conceived at present, particularly after HOPGOOD (1980) set out his methodology for studying gneissose and migmatitic terranes is founded upon the determination in the field of the mutual relations between foliation planes and lineations of distinct generations. These relations are evidenced after the position in space of the different structural elements involved has been established and it is not uncommon that distinct foliation planes are found to be just a few degrees apart. The same kind of relation can be shown by different lineations lying on the same rock surface. In either case errors in the measurements must be brought to a minimum.

As far as attitudes of planar structures are concerned the field procedure for measuring them is, normally, a simple task. Lineations, however, in some instances pose difficulties to the worker, attending the use of the common geologist's compass. This problem was reviewed by the author in an earlier paper (SILVA FILHO, 1979) where an special device, to be used in connection with the ordinary compass, was presented with the main purpose of overcoming difficulties related to measurements on steeply plunging lineations. Such device has been improved since then and its more recent design makes up the subject of this paper.

The idea of developing an instrument capable of giving the trend and plunge of lineations directly, without need of nomograms or net construction, actually is not new. In fact, BLAAS (1903) described a clinometer to fullfil these requirements, and INGERSON (1942) presented a clinometer of a somewhat different design with the same purposes. This latter instrument became known as "Ingerson's universal compass". Recently, basically a copy of Ingerson's compass was manufactured in Japan (see BARNES, 1981, fig. 2.6, pg. 19) and advertised as an universal compass. However, either instrument, the original of INGERSON (op.cit.) or the modern Japanese copy, has as a great disadvantage the fact that any reading must always to be performed with the instrument positioned vertically. In other words, this sort of instrument does not allow the determination of the "rake of any lineation",which constitutes a serious constraint, since under certain situations a geologist has to deal with rake rather than plunge to determine the position in space of a linear element.

In contrast, the instrument which is being presented can operate in any position and to determine the attitude of either planar or linear elements whatever the natural situation found at any outcrop. On account of this such an instrument indeed fullfils the requirements for being thought of as univeral compass.

INSTRUMENT CHARACTERISTICS

The instrument here dealt with is made up by two main pieces, viz. (1) a base plate, and (2) a case which contains a compass. Both pieces are to be manufactured in resistent transparent plastic material, and their characteristics are shown in figures 1 and 2. In relation to the base plate it is worth mentioning the following:

(a) The line parallel to the width is intended to represent any linear element whose attitude is to be determined. This line, on account of that, is hereafter referred to in the text as "parallel line". It is to be represented in black in the instrument's surface.

(b) The line parallel to the length is intended to represent the normal to the linear element in the field and is hereafter termed simply "normal line". It is to be represented in red on the surface of the instrument.

(c) The inner scale of the protractor is to be black whereas the outer one is to be red.

The case, which is the compass housing, represents what can be termed the "measuring device" of the instrument. It is connected to the base plate through an axis, about which it can be rotated. The compass is attached to the case lid and it's dial, scaled from 0 to 360°, can be turned upon the rotation axis of the magnetic needle.

The "horizontal" and "dip" lines marked on the bottom of the case, are to be represented in black and red, respectively.

INSTRUMENT USAGE

For the sake of clarity it must be pointed out that in the following text the term "lineation" is used in it's broadest meaning, as defined by CLOOS (1946): "Lineation is a descriptive and nongenetic term for any kind of linear structure within or on a rock. It includes all linear structures without regard to origin, such as slickensides, fold axes, flow-lines, stretching, elongate pebbles or ooids, wrinkles streaks, intersection of planes, linear parallelism of minerals or components".

All the readings with the instrument are founded upon the geometric property whereby the angle between two lines is equal to the angle formed by the normals to them. Therefore, the readings referring to rakes and/or plunges of lineations can be taken with the aid of either the "parallel line" or the "normal line", of the base plate, in combination with the "horizontal" or "dip" lines of the "measuring device", paying attention to the fact that whatever the line choosen it must be in accordance with the scale of the protractor,which is achieved by taking readings always with elements of the same color.

The instrument has been designed so as to make readings easier when the "dip line" is positioned to the right (clockwise) of a person viewing parallel to the strike line. The manners whereby it is used, depends on the kind of problem with which a geologist is concerned, as follows:

(1) Direct determination of the attitude of planar structures

a) The instrument is placed with the base plate against the rock surface (bedding plane, cleavage, etc.);

b) After opening the case the lid with the compass is brought to horizontality by rotating both, the "measuring device" as a whole, and the lid itself about its own axis. In such a position the "horizontal line" materializes the strike line of the planar element.

c) By rotating the compass dial until the "orienting arrow" fits the magnetic needle, the bearing of the strike line is determined. On account of the suitable size of the instrument, while the base plate is held firmly against the rock surface with one hand, the other can easily rotates the compass dial.

d) With the lid in the horizontal position, the dip is read out on the "dip scale".

e) The attitude of the planar element may be represented into two different ways, namely:

i) writing down the bearing of the strike line by the angle of dip;

ii) by indicating the bearing of the "dip line direction" and the value of the dip.

(2) Direct determination of the attitude of lineations

a) The case is open and the angle between the lid and the bowl is set at 90^{o}, with the aid of the "dip scale clamp release" (figure 2).

b) The instrument is placed with the lower (or upper, in overhanging situation) edge of the base plate parallel to the lineation and the lid is brought to horizontality.

c) The angle between the "horizontal line" and the "parallel line" or alternatively, the angle between the "dip line" and the "normal line" represents the plunge of the lineation.

d) The orientation of the "direction arrow" (figure 2) represents the trend of the lineation.

(3) Indirect determination of the attitude of lineation

The direct determination of the attitude of a lineation has become along the years, the normal procedure for field geologists. Nevertheless, on account of factors such as type of rock exposure and type and position in space of lineations, in some instances ir fails to be used.

The reason for the popularity of the "plunge method" rests upon the fact that working with an ordinary geologist's compass, the determination of the attitude of a lineation by the "rake method" is a relatively time-consuming task, and under certain circustances is impossible to be carried out only by one person. However, situations do exist when the rake method is the only one capable of allowing readings to be performed.

In such cases the procedure is as follows:

a) The base plate is placed with its lower (or upper) edge parallel to the lineation, and held at any angle in relation to the horizontal.

b) The lid of the case is brought to horizontality.

c) The angle between the "horizontal line" and the "parallel line" (or the equivalent angle) represents the rake of the lineation on the plane materialized by the base plate which is called "auxiliary plane".

d) The orientation of the "strike line" and the dip read out the "dip scale", give the attitude of the "auxiliary plane" (base plate).

e) The position of the lineation in space, in terms of its plunge and trend can be easily drawn in the field from the nomograms presented by SILVA FILHO (1979, figs. 9 and 10) or alternatively by plotting the attitude of the auxiliary plane with the lineation on a stereonet.

f) The field notation of the readings performed in this case is here suggested to be represented by the normal notation used for any planar structure, followed by the rake value within brackets. The rake is given a sign positive or negative depending on the lineation (parallel line) deviates from the "horizontal line" in a clockwise or counter clockwise sense. The signs "+" or "-" on the base plate allow a direct determination of the positive or negative value of the rake. When the nomogram presented elsewhere (SILVA FILHO, 1979) is used to establish the attitude of a lineation it must be borne in mind that the orientation of the latter is given in relation to that of an auxiliary plane. This relatioship is represented by the angle between the strike line of the auxiliary plane and the lineation, as seen on a horizontal plane. In other words, the nomogram does not give directly the bearing of the horizontal projection of the lineation. Thus, terming "deviation" the angle referred to above, the following relations hold:

i) when the rake is positive, the "deviation" must be added to the bearing of the strike line of the auxiliary plane to represent the trend of the lineation;

ii) when the rake is negative the lineation's trend is got by subtracting the value of the "deviation angle" from the bearing of the opposite side of the arrowed part of the strike base.

iii) when the rock surface is over-hanging the bearing of the strike line of any plane must be read in relation to the non-arrowed side of the strike line. Therefore, in such situations a positive rake has to be written down as negative and vice-versa, so that what is said in items "i" and "ii" hold. This inversion in the signs of the rake is dictated by the fact that the sense of rotation of a line in a plane is here determined with regard to the lower hemisphere of a sphere of projection.

(4) Indirect determination of the attitude of a planar structure

The procedure in this case rests upon the geometric property whereby a plane may have its position in space determined if the attitudes of at least two lines belonging to it, are known. Therefore, what is to be done in this situation is to determine the attitudes of two intersection lineations referred to the same planar structure, as outlined under the headings 2 and 3, and to plot them in a stereonet. The great circle passing through both lineations materializes the planar structure which one is dealing with.

CONCLUSION

From the foregoing it can be concluded that this new instrument for field work in geology, when compared with the traditional geologist's compass, is far more versatile. In addition, on account of its characteristics, readings of the parameters which allow the position in space of both planar and linear structures to be understood are very much more accurate. This fact is of great importance if it is taken into account that in some polyphase deformed areas there exist foliations positioned at very small angles apart.

It is a well known fact that normally parallelism of either foliation or lineation is understood on the basis of a statistical concept. Thus, even when "parallel" structural elements are being dealt with a certain amount of dispersion, as manifested by the readings performed, is to be expected. This condition precludes distinction between elements of different generations and similar orientation to be made on the basis of data plotted on a stereonet. If to this natural drawback is added the inaccuracy of readings, the problem obviously become enlarged. So, if errors in readings are minimized the area occupied by points representing a particular lineation on a stereonet will be also reduced, so as to enhance a better discrimination of such lineations in relation to another set having an orientation statistically similar.

A fundamental characteristic of this instrument is that whatever the structural element one is concerned with, it is positioned on the rock surface only once to allow readings to be performed. Even when the situation of a planar element containing a lineation is considered, all the readings, including strike and dip of the plane, value and sense of rake, are carried out consecutively, without need of moving the instrument from one position to another, as would be the case if an ordinary compass were used. In addition, as it is not necessary to make any mark on the rock surface for readings to be performed even under wet conditions measurements can be carried out accurately. A factor which contributes to the high degree of accuracy of the readings when using this instrument, is that one does not have to deal with imaginary projections of lines on imaginary planes. Whatever the sort of measurements which one is concerned with, lines and/or planes are always materialized by the instrument. On teaching grounds, this fact is of upmost importance when one take into consideration how difficult it is for students to realize the position in space of planar and, principally, linear structures, and how misleading is for the great majority of them the determination of the sense of the rake.

Finally, it is worth mentioning that besides its great versatility in the field, this instrument is very useful for laboratory studies of mesoscopic fabric elements (TURNER & WEISS, 1963) carried out on oriented samples. The dip scale clamp release allows one to set the instrument in the position which represents the true situation of the oriented surface in the field. To bring the specimen to its right position in space is just a matter of fitting it to the pre-set attitude of the instrument.+

+ Patent pending

REFERENCES

BARNES, J.W. 1981 Basic geological mapping. Geological Society of London, Handbook Series.

BLAAS, J. 1903 Der Klinocompass. Jahrbuch d. Kaiserlich-Königl. Geologischen Reichsanstalt, 53(3):453-58.

CLOOS, E. 1946 Lineation. Geological Society of America, Memoir, 18, 122 p. illust.

HOPGOOD, A M. 1980 Polyphase fold analysis of gneisses and migmatites Trans.Royal Soc.Edinburgh, Earth Sciences, 71:55-68.

INGERSON, E. 1942 Apparatus for direct measurements of linear structures. American Mineralogist, 27(11):721-25.

KNOPF, E.B. 1933 Petrotectonics. American Journal of Science, 25:433-70.

SANDER, B. 1930 Gefügekunde der Gesteine. Julius Springer, Wien. 352 p. illust.

SILVA FILHO, B.C. 1979 Determinação da atitude de estruturas lineares. Acta Geologica Leopoldensia, São Leopoldo, 3(6):1-28.

TURNER, F.J. & WEISS, L.E. 1963 Structural analysis of metamorphic tectonites. McGraw Hill, New York, 545 p.

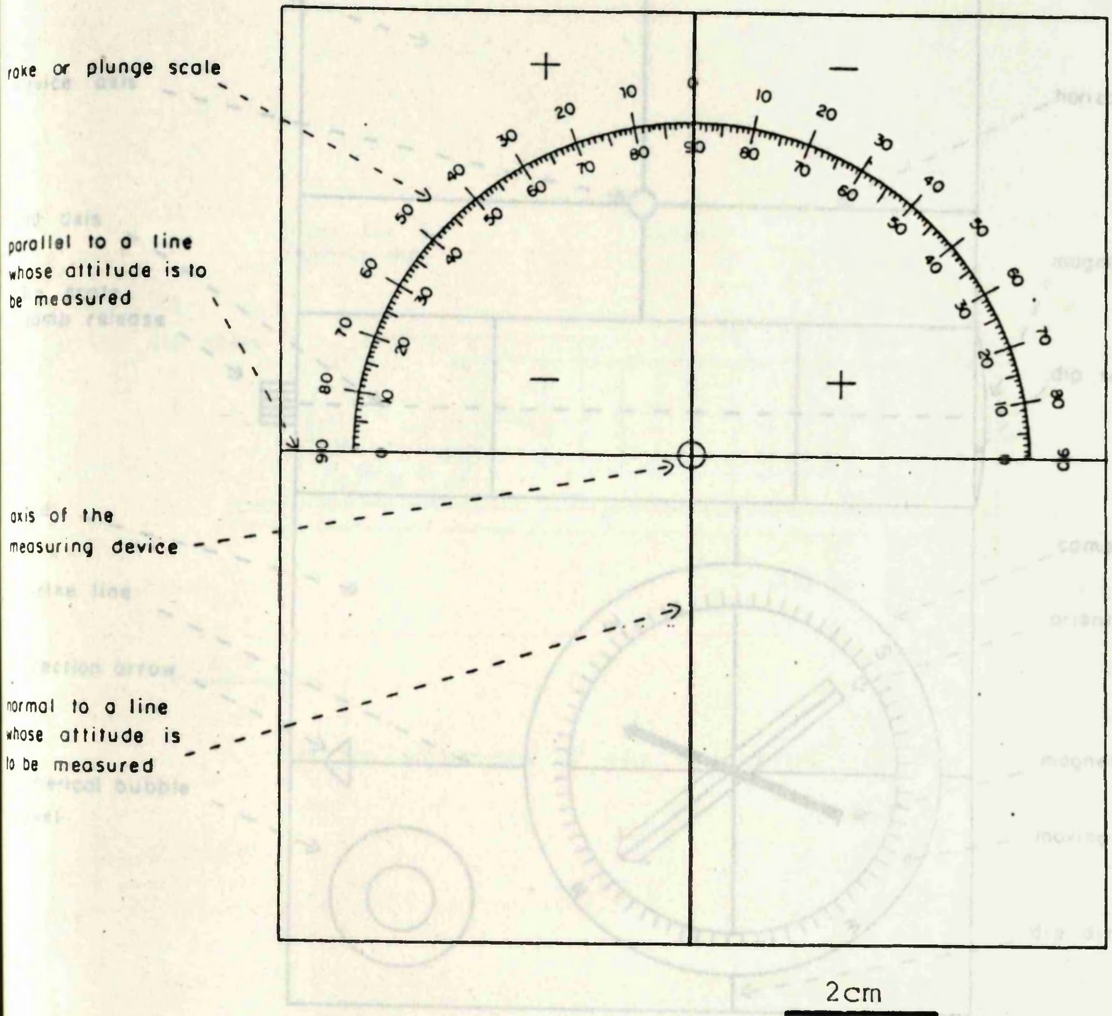

FIG. 1 - BASE PLATE

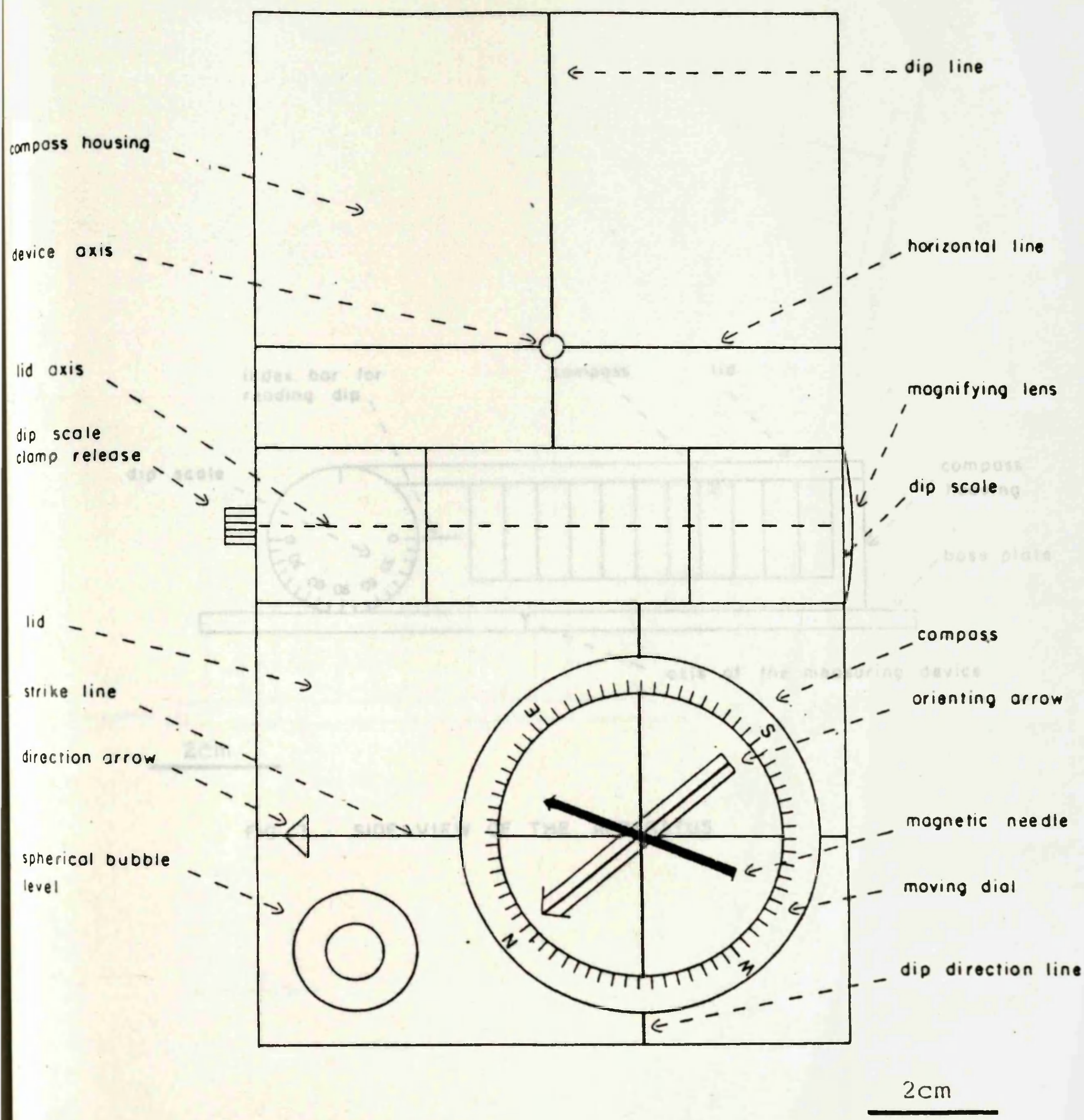

FIG. 2 - MEASURING DEVICE (fully open) -

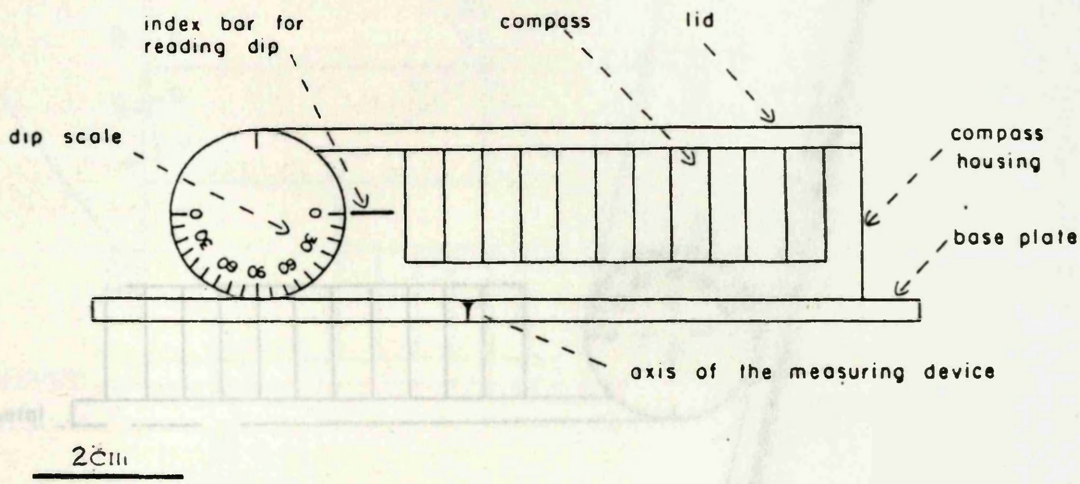

FIG 3 - SIDE VIEW OF THE APPARATUS

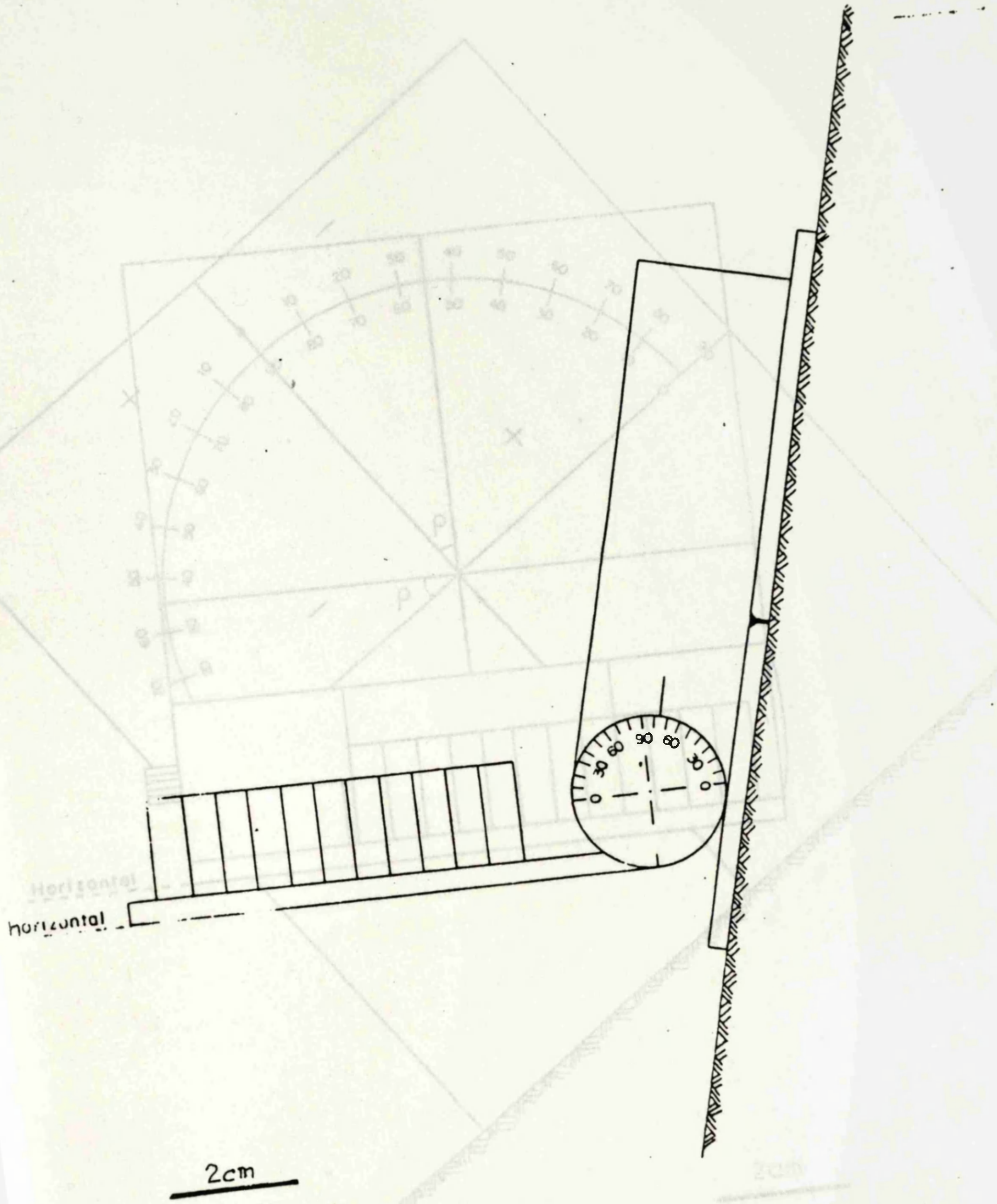

FIG. 4 - APPARATUS SET FOR MEASURING THE ATTITUDE OF A ROCK SURFACE

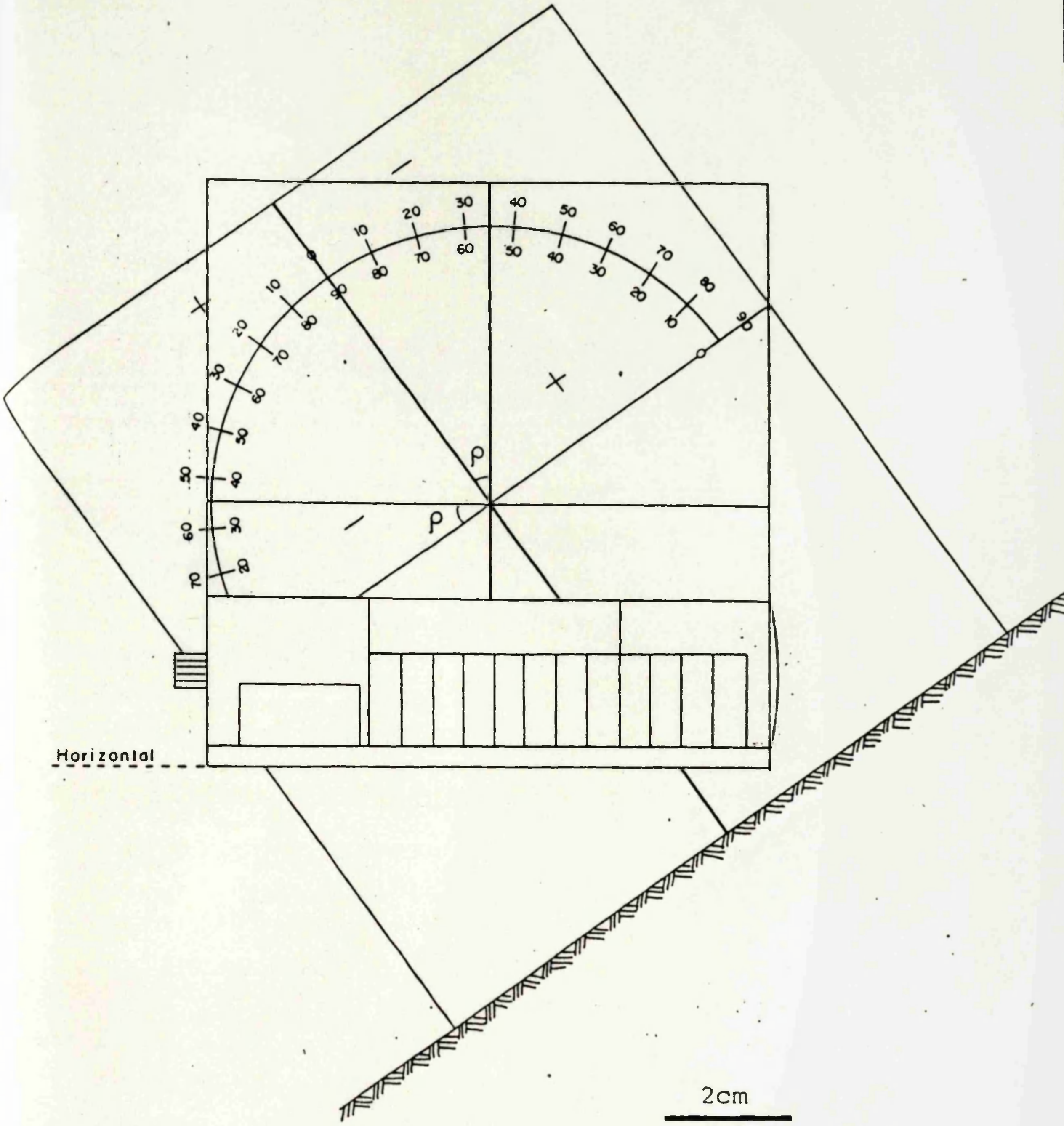

FIG. 5 - APPARATUS SET FOR MEASURING THE ATTITUDE OF A LINEATION ON A ROCK SURFACE. IF ONE CONSIDER THE BASE PLATE AS BEING VERTICAL THE ANGLE ρ REPRESENTS THE PLUNGE OF THE LINEATION. IF THE BASE PLATE IS INCLINED EITHER OUTWARDS OR TOWARDS THE READER THE ANGLE ρ IS THE RAKE OF THE LINEATION IN THE PLANE WHICH THE BASE PLATE REPRESENTS.

ORIGIN OF THE POLYPHASE DEFORMED AMPHIBOLITES OF THE DURNESS REGION, SCOTLAND

by

BRENO CORREA DA SILVA FILHO

1984

ABSTRACT

Evidence is presented showing that the polyphase deformed Lewisian amphibolites of the Durness region, Scotland, are related to basaltic parent magmas, irrespective if they are intercalated with quartzofeldspathic gneisses or calc-silicate rocks.

The original basaltic magma underwent diferentiation at shallow depths (< 15 km) acquiring composition varying from olivine-tholeiites to tholeiites. Although the original basaltic magma had similarities with modern ocean ridge basalts some geochemical differences suggest they were related to lava flow or shallow intrusions which moved through a crust somewhat thicker than a modern oceanic crust.

A geotectonic environment similar to that represented at present by Iceland is considered as more in accordance with the site of the basaltic outpourings during the early stage in the generation of the Lewisian amphibolites.

I. INTRODUCTION

In recent years the petrochemistry of amphibolites has found extensive application in the study of crustal evolution on Precambrian terranes (Condie et al., 1969; Naqvi & Hussain, 1973; Naqvi et al., 1974; Graham, 1976; Rivalenti, 1976). In the same light, this paper presents results of a geochemical investigation of amphibolites occurring in the Lewisian complex making up the Rhiconich group (Dash, 1967) in the Rispond peninsula area, Durness region, NW Scotland (Fig. 1). The main objectives are to assess the petrogenesis and tectonic significance of these amphibolites. Detailed descriptions of the geology of the area with which this study is concerned have been presented by Findlay (1970) and isotopic constraints are given by Lyon & Bowes (1977).

II. ROCK UNITS

In the Durness region the Rhiconich group is made up predominantly of banded quartzofeldspathic gneisses and amphibolites, together with subordinate metasedimentary units represented by calc-silicate rocks.(cf. Findlay, 1970).

The amphibolites occur amongst the quartzofeldspathic gneisses as bands or lenses concordant with the gneissose banding which is essentially tectonic in origin, and when associated with calc-silicate rocks they form a finely striped structure. They are dominantly composed of lineated idiomorphic green hornblende (45 - 60%), plagioclase (An_{25-35}; 25 - 40%) and irregular quartz (10 -15%) in aggregates with plagioclase parallel to the lineation. Hornblende shows pleochroism in greenish yellow or brownish yellow to dark green or olive green, with $C \wedge Z$ varying between 18° and 21°. Small, round quartz is commonly seen as inclusions in porphyroblasts of this mineral. The accessory minerals are represented by biotite, with pleochroism in light yellow to reddish brown, epidote, sphene, apatite and zircon. Epidote is associated with hornblende and biotite and can be found making up to 5% of the rock. Sphene (up to 2%) is associated with opaque minerals and sometimes can be seen forming rims around them. Apatite and zircon are seen as inclusions in hornblende crystals.

Findlay (1970) has demonstrated that the Lewisian rocks in the Durness region were affected by polyphase deformation and metamorphism. This author has related the rock sequence of this region to the structural sequence outlined by Dash (1967) for the area immediatly to the south, and reported the concordant amphibolites as exhibiting structural features relating the first deformational phase.

The mineralogical assemblage of the amphibolites is compatible with amphibolite facies metamorphism. Dash (1967) has claimed that the peak of metamorphism of the Rhiconich group took place during the second deformational phase, at temperatures about 600-700^{o} C and pressure about 5 Kb. According to Lyon & Bowes, (1977) this metamorphic event is related to late Archean (2.8-2.7.b.y.).

III. GEOCHEMISTRY

III.1. METHODOLOGY

For the present study chemical data were determined on 31 samples collected by the author in the Rispond peninsula area. The samples were crushed to 1 cm chips in a steel-jaw crusher and then pulverized to 100 mesh powder in an agate swing mill, and finally to 250 mesh in an agate ball-mill. The chemical analyses were carried out in the Department of Geology, University of Glasgow, using a Phillips fully automatic spectrometer for both major and trace elements, except for FeO, H_2O and CO_2, which were determined by conventional methods. Major elements were determined on fused beads whereas for trace elements pelletized rock powders were used.

The results of the chemical analyses are given in Table I, whereas the normative compositions and Niggli numbers are given in Table II.

III.2. ORIGIN OF THE AMPHIBOLITES

The igneous or sedimentary character of the parental material of amphibolites is a problem which has concerned a number of workers for many years. Basically, the approaches devised to establish the origin of such rocks may be divided into two groups, viz. (1) those based upon field information, such as structural characteristics and relations with associated rocks (Wilcox & Poldervaart, 1958; Walker et al., 1960; Heier, 1962), and (2) those based on the interpretation of chemical parameters (Evans & Leake, 1960; Leake, 1964; Karlsbeck & Leake, 1970, Van der Kamp, 1970).

The discrimination between ortho- and para-amphibolites on the basis of field criteria is often very difficult, particularly when such rocks consistently show concordant relations with lithological layered assemblages, as in the present area. On the other hand, as far as the chemical approach is concerned, some workers have shown that the most reliable method in discriminating between the two types of amphibolites is based upon the comparison of the trends of variation of certain critical elements, rather than on the comparison of differences in absolute values of the various chemical components. Following this approach the analyses of thirty-one amphibolites were recalcutated to Niggli numbers and plotted in different variation diagrams.

Evans & Leake (1960) and Leake (1964) placed much emphasis on Niggli mg, which shows a systematic decrease during differentiation of basic magmas. Leake (1964) also showed that amphibolites rich in Ni, Cr and Ti with low Niggli k values, are almost certainly of igneous origin. Thus, in order to determine the type of chemical variation of the rocks under investigation, plots of mg, alk, c, fm and al agaist si, and ti, c, alk and k against mg were compared with trends established by Evans & Leake (1960) for the Karroo dolerites, (Figs. 2 and 3, respectively). The general trends in figure 2, show increase of al and alk, and decrease of fm with increasing si, similarly to the trends shown by the Karroo dolerites taken for comparison. The systematic decrease of mg when compared with other Niggli parameters and the sharp rise of ti strongly suggests the existence of a differentiation process of basic magma and, on the other hand, shows that the trend displayed by alk can be in great part dependent upon such a process rather than on alkali metasomatism (Fig 3).

In the al-alk against c plot (Fig.4) the amphibolites also fall within the field of the Karroo dolerites. Similarly, in the 100 mg-c-(al-alk) triangular diagram (Fig.5) which illustrates the trend line of a typical differentiated basic igneous rocks (Karroo dolerites) as well as fields of typical pelites, limestones and dolomites, and the trend lines of sedimentary mixtures (Kalsbeck & Leake, 1970), the points representing the amphibolites follow a trend parallel to that of igneous rocks.

Karroo dolerites Plots of the same elements agains TiO_2 show a negative correlation (Fig. 7) what is again in accordance with results found by Leake (1964) for the Karroo dolerites.

In summary, on the basis of the evidence presented the polyphase deformed amphibolites from the Durness region irrespective if intercalated with quartzofeldspathic gneisses or calc-silicate rocks are interpreted as having an igneous origin.

The relation of the amphibolites with a parental magma of basaltic comp sition is also indicated by figures 8 and 9.

III.3 CHARACTER OF THE IGNEOUS ROCK SERIES

In the foregoing section it was determined that the amphibolites have an igneous origin. In the present section the character of the original igneous material will be discussed.

On the basis of the criteria set out by Yoder & Tilley (1962) for discriminating between tholeiitic and alkali basalts, it can be concluded that the polyphase **deformed** amphibolites from the Durness region are related to tholeiitic magmas, since the norms (Table II) usually contain hypersthene and quartz, little olivine, and only rarely nepheline According to Miyashiro (1975) one of the most striking features of a tholeiitic magma is its strong iron and titanium enrichment and slow SiO_2 variation during fractionation. This is apparent for the studied amphibolite in plots of <u>si</u> and <u>ti</u> against <u>mg</u> , and on an AFM diagram, as well (Figs. 2e, 3c and 10).

The tholeiitic character of the original magma is also confirmed by the relatively low amounts of TiO_2, P_2O_5 and Zr (Floyd & Winchester, 1975; Winchester & Floyd, 1976) and by a plot of Y against Nb (Fig.11) which according to Pearce & Cann (1973) discriminates between tholeiitic and alkali basalts even in altered samples. A further evidence of the tholeiitic character of the parents of the amphibolites is brought out by figures 12 and 13, which according to Irvine and Baragar (1971) discriminates between the more basic members of calc-alkaline and tholeiitic series on the basis of their alumina contents plotted against normative plagioclase composition. These authors have claimed that the most prominent chemical difference between basic calc-alkaline and tholeiitic is their alumina content, with tholeiitic basalts having characteristically less than 16% Al_2O_3.

Wood (1978) has considered the term tholeiite as confusing since it has more than one current usage in the literature. According to him, more commonly the term is used to refer to any basalt with normative hypersthene and often applied to Mg-rich basalts, as is normally the case when ocean-floor th leiite is referred to by some authors. In order to make the term tholeiite more precise, Wood (1978) established an index FM given by the FeO + MnO/FeO+MgO+MnO ratio to classify basaltic rocks. On these grounds, basaltic rocks with FM $\leq$ 71 are to be classified as olivive tholeiites, whereas those with 71 $\leq$ FM $\leq$ 78 are tholeiites.

On the basis of Wood's criterion the amphibolites are related to igneous rocks varying in composition from olivine tholeiites to tholeiites, along the differentiation trend of a parental basaltic magma (Fig. 14). This differentiation can be explained by crystal fractionation in a high crustal level magma chamber (Wood, 1978). This opinion is supported by a late-stage crystallization of magnetite and ilmenite, as indicated by the increasing contents of iron and titanium as the differentiation procceeded (Fig. 10 and 3c, respectively). This late-stage crystallization of magnetite is indicative of low TiO_2 (Osborn,1959) and might be related to a low water content of the magma.

IV. TECTONIC SETTING

The composition of the amphibolites is of paramount importance in attempting to establish the tectonic setting in which the igneous rocks formed.

In the last ten years a number of diagrams have been used to correlate chemical composition with the tectonic environment in which the rocks crystallized. As referred to by Pearce & Cann (1973) the most successful method in which the geochemical approach for identifying the original tectonic situation of igneous rocks has relied is that of comparison of trace elements concentration in the rock under investigation with their concentration in present day volcanic rocks, whose tectonic setting is known. The trace elements selected for determining the magmatic affinities of ancient metamorphosed rocks are those considered least influenced by metamorphism or metasomatism, i.e , the immobile elements. Elements such as Ti, Zr, Y, Nb and Sr have been considered as immobile and of value in discriminating between tectonic environments in various rock series (Pearce & Cann, 1971; Bloxan & Lewis, 1972; Bickle & Nisbet, 1972; Cann, 1971).

Following Pearce & Cann (1973)a Ti-Zr-Y diagram (Fig. 15) suggests that the amphibolites were not within plate basalts and most plot in the field of ocean-floor basalts. A Ti against Zr diagram (Fig. 16) also shows that most of the samples have affinities with ocean-floor basalts, althought some points plot outside the field relating to such rocks In addition, a Zr/Y against Zr diagram (cf. Pearce & Norry, 1979) also supports a similar conclusion with mid-ocean ridge basalts being indicated (Fig. 17) However, despite all these similarities with magmatic events relating mid-ocean ridges some amphibolites present characteristics in accordance with those of oceanic basalts, mainly with respect to the absolute values of the abundances of some trace elements. In addition, the fractionation process responsible for the variation of the magmas from high-magnesia basalts, through low-magnesia basalts to ferro-basalts (Fig. 14) is much in accordance with a situation as that represented at present by Iceland, where the fractionation of basaltic magmas has been interpreted by O'Hara (1973) as due to emplacement through a greater thickness of crust as compared to ocean-ridge basalts. This opinion makes much more sense if it is considered that on account of a higher geothermal gradient in the Archean, an extensional regime would lead to thinning rather than breaking of the crust (cf. Tarney ,1976), accompanied by mantle upwelling. Therefore, the initial site of magma deposition in the area under investigation is considered to have been related to a late mantle-activated rifting (Condie, 1982) of an older crust thinned during an early stage of extension on account of its ductile behaviour.

The scarcity of sedimentary material in the studied region, where just some small, restricted occurrences of calc-silicate rocks have been described (Findlay, 1970), as well as the absence of metagraywackes is favouring an environment far from either volcanic arcs (if any actually existed) or uplifted continental areas.

V. CONCLUSIONS

The Lewisian amphibolites, concordant with either the regional quartzofeldspathic gneisses or the calc-silicate rocks in the Durness region show characteristics typical of an assemblage of basic igneous rocks affected by amphibolite facies metamorphism and polyphase deformational processes. In the whole they correspond with tholeiitic basalts but a more detailed study of their chemical composition has unraveled a clear differentiation trend from high-magnesia basalts (olivine-tholeiites) through low-magnesia basalts to ferro-basalts (tholeiites). Petrogenetic evidence shows that the differentiation processes took place at shallow depth ($<$ 15 km).

The chemical characteristics of the parental magmas of the amphibolites resemble those of modern ocean-ridge basalts, as have been considered by some workers (Condie, 1982; Engel *et al.*, 1965) to be the case for Archean tholeiites in general. Nevertheless, some slight differences exist in relation to the chemistry of the modern ocean-ridge lavas, which are accounted for the fact that the crust which underwent rifting, to promote the outpouring of the basic lavas, was thicker than a modern oceanic crust. The rifting mechanism is thought to have been of the type mantle-activated (cf. Condie, 1982) with the crust behaving as ductile body (cf. Tarney *et al.*, 1976) rather than as a brittle one (Condie & Hunter, 1976) during an extensional regime.

REFERENCES

ARMBRUSTMACHER, T.J. 1977 Geochemistry of Precambrian mafic dykes, Central Bighorn Mountains, Wyoming, USA. Precamb.Res., 4:13-38.

BLOXAN, T.W. & LEWIS, A.D. 1972 Ti, Zr and Cr in some British pillow lavas and their petrogenetic affinities. Nature Phys.Sci, 237:134.

BICKLE, M.J. & NISBET, E. 1972 The oceanic affinities of some alpine mafic rocks based on their Ti-Zr-Y contents. J.Geol.Soc., 128:267.

CANN, J.R. 1971 Major element variation in ocean-floor basalts. Royal Soc.London Philos.Trans., Series A, 268:495-505.

CARMICHAEL, I.S.E. 1964 The petrology of Thingmuli: a Terciary volcano in eastern Iceland. J.Petro., 5:435-60.

CONDIE, K.C.; BARSKY, C.K. & MUELLER, P.A. 1969 Geochemistry of Precambrian diabase dykes from Wyoming. Geoch.Cosmoch.Acta., 33: 1371-88.

CONDIE, K.C. & HUNTER, D.R. 1976 Trace element geochemistry of Archean granitic rocks from the Barbeeton region, South Africa. Earth Planet.Sci.Letter, 29:389-400.

DASH, B. 1967 The geology of the Lewisian rocks between Strath Dionard and Rhiconich, Sutherland. Ph.D. Thesis, Univ. of Glasgow (unpublished)

ENGEL, A.E.J.; ENGEL, C.G.; HAVENS, R.G. 1965 Chemical characteristics of oceanic basalts and the upper mantle. Geol.Soc.Am.Bull., 76:719-34.

EVANS, B.W. & LEAKE, B.E. 1960 The composition and origin of the striped amphibolites of Connemara, Ireland. J.Petrol., 1(3):337-63.

FINDLAY, D. 1970 Studies of fold tectonics in the Lewisian of the Durness region, Sutherland. Ph.D. Thesis, Univ.of Glasgow (Unpubl.)

FLOYD, P.A. & WINCHESTER, J.A. 1975 Magma type and tectonic setting discrimination using immobile elements. Earth Planet.Sci.Letter, 27:211-18.

GRAHAM, C.M. 1976 Petrochemistry and tectonic significance of Dalradian metabasaltic ricks of the SW Scottish Highlands J Gol Soc London, 132:61-84.

HEIER, K.S. 1962 The possible origin of amphibolites in an area of high metamorphic grade. Norsk.Geol.Tidsskr., 42:157-65.

IRVINE, T.N. & BARAGAR, W.R.A. 1971 A guide to the chemical classification of the common volcanic rocks Can.J.Earth.Sci., 8:523-48.

KALSBEEK, F. & LEAKE, B.E. 1969 The chemistry and origin of some basement amphibolites between Ivigtut and Frederik Shab, Southwest Greenland. Grønlands Geologiske Undersøgels Bull. 90:1-21.

LEAKE, B.E. 1964 The chemical distinctions between ortho- and para-amphibolites. J.Petro., 5(2):238-54.

LYON, T.D.B. & BOWES, D.R. 1977 Rb-Sr, U-Pb and K-Ar isotopic study of the Lewisian complex between Durness and Loch Laxford, Scotland Krystalinikum, 13:53-72.

MEHNERT, K.R. 1969 The composition and abundance of common metamorphic rock types. In: K.H.Wedepohl, Ed. Handbook of Geochemistry, 1:272-96.

MIYASHIRO, A. 1975 Classification, characteristics and origin of ophiolites J.Geol., 83:249-81.

NAQVI, S.M. & HUSSAIN, S.M. 1973 Geochemistry of Dahwar metavolcanics and composition of the primeval crust of the peninsular India Geoch.Cosmoch.Acta, 37:159-64.

NAQVI, S.M.; DIVAKARARAO, V.; SATYANARAYANA, K. & HUSSAIN, S.M. 1974 Geochemistry of post-Dahmar basin dykes and the Precambrian crustal evolution of peninsular India. Geol.Mag., 11:229-36.

O'HARA, M.J. 1973 Non-primary magmas and dubious mantle plume beneath Iceland. Nature, 243:507-8.

OSBORN, E.F. 1959 Role of oxigen pressure in the crystallization and differentiation of basaltic magma. Am.J.Sci., 257:609-47.

PEARCE, J.A. & CANN, J.R. 1971 Ophiolite origin investigated by discriminant analysis using Ti, Zr and Y Earth Planet.Sci.Letters, 12:339-49.

PEARCE, J.A. & CANN, J.R. 1973 Tectonic setting of basic volcanic rocks determined using trace element analyses Earth Planet Sci Letters, 19:290-300

PEARCE, J.A. & NORRY, M.J. 1979 Petrogenetic implicati ns of Ti, Zr, Y and Nb variations in volcanic rocks, Contr.Miner.Petro., 69:33-47.

RIVALENTI, G. 1976 Geochemistry of metavolcanic amphibolites from southwest Greenland In: B.F.Windley, Ed. The early history of the Earth. John Wiley, New York p.213-23

TARNEY, J. 1976 Geochemistry of Archean high-grade gneisses with implication as to the origin and evolution of the Precambrian crust In: B.F.Windley, Ed. The early history of the Earth. John Wiley, New York. p.405-15.

Van De Kamp, P.C. 1970 The Green Beds of the Scottish Dalradian Series. Geochemistry, origin and metam rphism of mafic sediments. J.Geol , 78:281-303.

VILJOEN, M.T. & VILJOEN, R.P. 1969 The geol gy and geochemistry of the lower ultramafic unit of the Ouvermacht Group and a proposed new class of igneous rocks . Spec.Pub.GeolSoc.South Africa,2:55.

WALKER, K.R.; JOPLIN, G.A.; LOVERING, J.F. & GREEN, A. 1960 Metam rphic and metasomatic convergence of basic igneous rocks and lime-magnesia sediments of the Precambrian f n rthwestern Queensland. J.Geol.Soc.Australia, 6:149-177

WILCOX, R.E. & POLDERVAART, A. 1958 Metadolerite dyke swarm in Battersville-Roan Mountain area, N.Carolina. Geol.Soc Am.Bull., 69:1323-68.

WINCHESTER, J.A. & FLOYD, P.A. 1976 Geochemical magma type discrimination: application to altered and metamorphosed basic igneous rocks. Earth Planet.Sci.Letter, 28:459-69.

WOOD, D.A. 1978 Terciary lavas of eastern Iceland. J.Petro., 19: 393-436.

YODER, H.S. & TILLEY, C.E. 1962 Origin of basalt magmas: an experimental study of material and synthetic rock systems J.Petro , 3:342-532.

TABLE I. CHEMICAL COMPOSITION (MAJOR AND TRACE ELEMENTS) OF THE LEWISIAN AMPHIBOLITES FROM THE DURNESS REGION, SCOTLAND

Field n.	RA-19B	RA-20	RA-5	RA-6-1	RA-6-2	RA-16	RA-17	RA-18
SiO_2	50.33	49.91	49.15	47.62	48.74	50.57	49.12	50.44
TiO_2	0.79	9.87	1.12	1.14	1.15	0.76	0.93	0.64
Al_2O_3	13.14	14.57	13.22	13.22	13.27	14.84	12.33	13.77
Fe_2O_3	3.81	3.89	4.04	4.05	4.29	3.23	4.03	3.53
FeO	8.17	8.36	8.36	8.53	8.53	7.96	9.71	7.61
MnO	0.22	0.21	0.23	0.25	0.24	0.23	0.26	0.28
MgO	8.18	7.67	8.39	8.74	8.57	7.11	7.61	8.97
CaO	10.89	8.86	10.14	9.08	9.16	8.72	10.37	9.91
Na_2O	2.87	2.69	2.85	2.96	2.79	3.43	2.32	3.07
K_2O	0.97	1.41	1.54	1.69	1.73	1.39	0.90	1.33
P_2O_5	0.07	0.06	0.09	0.08	0.11	0.06	0.08	0.05
H_2O^+	1.16	1.64	1.46	1.70	1.70	1.28	1.42	1.45
CO_2	0.12	0.23	0.08	0.26	0.26	0.08	0.10	0.12
Total	100.72	100.37	100.67	99.32	100.54	99.66	99.18	101.17
Zr	52	54	61	60		52		42
Sr	124	133	159	140		183		150
Rb	19	29	26	32		26		25
Zn	76	80	92	97		119		100
Cu	39	32	11	11		59		10
Ba	53	100	129	124		97n		73
Ce	2	5	8	1		8		3
La	7	5	0	0		2		9
Nb	6	7	4	4		4		4
Ga	13	18	18	19		18		15
Pb	4	4	7	6		9		10
Co	53	52	65	60		58		58
Ni	101	81	145	151		64		100
Cr	194	44	230	222		67		256
Y	20	21	20	20		23		20
Th	0	1	1	1		1		1
U	1	2	1	1		2		1
S	167	77	50	122		74		96
CaO/Al_2O_3	0.83	0.61	0.77	0.69	0.69	0.59	0.84	0.72
Al_2O_3/SiO_2	0.26	0.29	0.27	0.28	0.27	0.29	0.25	0.27
Na_2O/K_2O	2.96	1.91	1.85	1.75	1.61	2.47	2.58	2.31
FM	0.59	0.61	0.59	0.58	0.59	0.60	0.64	0.55
Y/Nb	3.33	3.00	5.00	5.00	0.00	5.75	0.00	5.00
Ce/Y	0.10	0.24	0.40	0.05	0.00	0.35	0.00	0.15

$FM = \frac{FeO^+ + MnO}{FeO^+ + MnO + MgO}$; FeO^+ = Total iron as FeO

TABLE I. CONTINUED

Field n.	RA-19	RA-20	RA-22	DB-2-1	DB-2-2	DB-3	DB-6	DB-7
SiO_2	48 76	50 29	49.99	48 62	49.27	50 84	47 52	50 51
TiO_2	0.78	0 87	0.91	1 27	1.32	0.80	1 28	0 79
Al_2O_3	13 15	13 28	13.53	14.41	14 49	14.13	14.31	13.89
Fe_2O_3	3 57	3 17	3.04	3.69	3.69	2.73	3 96	3.54
FeO	8.16	9.02	9.07	8.81	8.81	7.76	8 83	7.36
MnO	0 27	0.26	0.26	0.22	0 23	0.23	0 22	0.24
MgO	8.28	7.32	7 08	7.90	7 78	8.67	7.57	8 43
CaO	10 79	10.22	10.25	9.16	9 22	11 02	9 18	11.16
Na_2O	3.13	2.93	3.03	2.89	2.65	2 11	3.01	2.23
K_2O	0 98	1 14	0 18	1.39	1.41	0 88	0 93	0.86
P_2O_5	0 07	0.07	0.07	0.08	0.08	0 06	0.08	0 05
H_2O^+	1.32	1 07	1.20	1.62	1.62	1.54	1.43	1.59
CO_2	0 06	0 04	0.04	0.10	0 10	0 14	0 25	0 10
Total	99.32	99.69	99.55	100.16	100 67	100 91	98.57	100 75
Zr	48	48	57	71		52	68	43
Sr	122	168	172	217		130	232	129
Rb	17	16	16	43		32	20	31
Zn	77	110	93	112		90	119	88
Cu	57	72	306	45		23	85	29
Ba	76	141	138	180		83	119	53
Ce	2	7	4	0		0	1	14
La	5	8	5	0		0	5	6
Nb	3	4	5	4		4	6	8
Ga	15	14	18	20		14	22	14
Pb	4	12	9	13		8	6	18
Co	50	56	56	61		56	61	54
Ni	96	111	102	143		115	149	109
Cr	223	196	171	203		241	215	243
Y	21	25	22	22		19	22	17
Th	0	0	2	1		1	1	0
U	2	0	3	0		2	1	1
S	137	363	87	83		46	77	63
CaO/Al_2O_3	0 82	0 77	0.76	0 63	0.64	0 78	0 64	0.80
Al_2O_3/SiO_2	0 27	0.26	0.27	0.30	0.29	0 28	0 30	0 27
Na_2O/K_2O	3 19	2 57	2.80	2 08	1 88	2 40	3 24	2 59
FM	0.58	0 62	0 63	0.61	0 61	0 54	0 62	0 56
Y/Nb	7.00	6.25	4 40	5 50	0 00	4 75	3 67	2 12
Ce/Y	0.09	0 28	0 18	0 00	0.00	0 00	0,04	0 82

$$FM = \frac{FeO^+ + MnO}{FeO^+ + MnO + MgO}$$; FeO^+ = total iron as FeO

TABLE I. CONTINUED

Field n.	DB-8	DB-9	RA-8	RA-13	RA-14	RA-15	RA-9	RA-10-1
SiO_2	49.31	50.24	51.54	52.27	52.22	51.89	51.75	51.85
TiO_2	0.89	0.80	1.13	1.11	1.13	1.11	1.18	1.14
Al_2O_3	14.80	13.86	13.33	13.64	13.63	13.74	13.61	13.30
Fe_2O_3	4.05	3.01	4.60	4.64	4.70	4.53	4.34	4.29
FeO	8.65	7.88	8.43	8.44	8.30	8.42	8.41	8.52
MnO	0.23	0.23	0.22	0.23	0.23	0.28	0.26	0.26
MgO	7.56	8.39	5.82	5.78	5.69	6.00	5.78	5.94
CaO	0.09	10.95	8.68	8.76	8.50	8.53	8.34	8.70
Na_2O	3.09	2.33	2.73	2.70	2.99	2.85	3.33	2.87
K_2O	1.51	0.81	1.40	1.41	1.29	1.31	1.37	1.31
P_2O_5	0.06	0.06	0.13	0.13	0.12	0.12	0.13	0.13
H_2O^+	1.35	1.34	1.36	1.14	1.42	1.32	1.25	1.20
CO_2	0.16	0.40	0.04	0.02	0.10	0.00	0.02	0.08
Total	100.75	100.30	99.41	100.27	100.31	100.10	99.76	99.59
Zr	57	51	112	110	113	114	116	108
Sr	154	132	210	205	185	187	218	198
Rb	33	29	22	22	19	21	25	24
Zn	101	89	110	105	110	112	113	97
Cu	12	29	75	102	24	23	58	115
Ba	110	86	158	220	96	113	156	206
Ce	5	6	30	20	26	27	26	29
La	2	4	12	9	14	15	12	10
Nb	4	4	7	9	10	10	10	8
Ga	17	14	20	17	20	18	17	16
Pb	12	8	10	7	14	3	11	5
Co	61	51	55	53	53	56	54	52
Ni	99	107	89	86	92	81	83	83
Cr	58	218	100	85	119	89	88	83
Y	21	19	28	26	29	29	29	27
Th	2	1	4	3	4	2	0	2
U	4	2	2	0	4	3	3	0
S	85	59	81	103	75	71	94	102
CaO/Al_2O_3	0.61	0.79	0.65	0.64	0.62	0.62	0.61	0.65
Al_2O_3/SiO_2	0.30	0.27	0.26	0.26	0.26	0.26	0.26	0.26
Na_2O/K_2O	2.05	2.88	1.95	1.91	2.32	2.17	2.43	2.19
FM	0.62	0.56	0.68	0.69	0.69	0.68	0.68	0.68
Y/Nb	5.25	4.75	4.00	2.89	2.90	2.90	2.90	3.37
Ce/Y	0.24	0.31	1.07	0.77	0.90	0.93	0.90	1.07

$FM = \dfrac{FeO^+ + MnO}{FeO^+ + MnO + MgO}$; FeO^+ = total iron as FeO

TABLE I. CONTINUED

Field n.	RA-11	RA-12	DB-5	DB-1	DB-4	DB-11	DB-12	A-4-3
SiO_2	50.06	50.03	50.27	49.85	50.09	48 96	50 42	50 27
TiO_2	1 10	1 09	1 16	2 25	1 46	1 39	1 47	0.82
Al_2O_3	13 55	14.12	14 14	14 75	15 80	17 13	15 94	13 55
Fe_2O_3	4.28	4 42	4 16	6 01	4 20	3 86	3 76	3 78
FeO	8.70	8 63	9 07	8.54	8 44	9 44	9 11	8 25
MnO	0 23	0.25	0 24	0 22	0 29	0 29	0 24	0 23
MgO	6 19	5 70	6 19	4 01	3.97	4.34	3 68	7 09
CaO	8.52	8 36	7 32	7.37	8 95	9.14	8 67	9 13
Na_2O	3.45	2 54	3.45	3.23	3 65	3 45	3.75	3 50
K_2O	1.35	1.39	1.46	1.18	1 04	1.24	1.00	1.28
P_2O_5	0.12	0 12	0 12	0 18	0.12	0 11	0.12	0 06
H_2O^+	1 40	1 18	1.56	1 35	1 02	1 19	1 14	1 12
CO_2	0 20	0.06	0 14	0 10	0.06	0 00	0.08	0 16
Total	99 15	99 89	99.28	99.04	99 19	100 54	99.38	99 24
Zr	113	107	106	156	108	98	115	54
Sr	199	168	333	243	211	246	218	240
Rb	21	23	27	32	20	22	19	13
Zn	111	106	113	136	119	109	112	103
Cu	39	60	17	313	30	24	29	44
Ba	143	135	63	258	174	162	174	144
Ce	24	20	27	38	16	9	14	15
La	7	12	8	15	9	3	7	21
Nb	8	10	7	12	9	10	6	5
Ga	16	17	20	26	18	22	20	15
Pb	6	13	22	15	12	13	6	11
Co	58	64	56	51	43	42	53	53
Ni	87	87	83	47	38	50	42	74
Cr	90	96	102	52	62	101	62	109
Y	26	27	26	35	27	28	29	22
Th	3	2	3	2	1	0	3	2
U	1	4	1	3	2	2	2	3
S	103	96	89	284	102	87	100	351
CaO/Al_2O_3	0.63	0.59	0.52	0.50	0.57	0.53	0 54	
Al_2O_3/SiO_2	0.27	0.27	0.27	0.29	0.31	0.35	0 32	
Na_2O/K_2O	2.55	1 83	2.36	2.74	3.51	2.78	3.75	
FM	0 67	0.69	0.66	0.78	0.76	0.75	0.77	
Y/Nb	3.25	2.70	3.71	2 92	3.00	2.80	4.83	
Ce/Y	0.92	0.74	1.04	1.08	0 59	0.32	0 48	

$$FM = \frac{FeO^+ + MnO}{FeO^+ + MnO + MgO}$$; FeO^+ = total iron as FeO

A-4-3 : Average of 4 amphibolites intercalated with calc-silicate rocks

TABLE II. CIPW NORMS AND NIGGLI NUMBERS OF THE LEWISIAN AMBPHIBOLITES FROM THE DURNESS REGION, SCOTLAND

Field n.	RA-19B	RA-2-	RA-5	RA-6-1	RA-6-2	RA-16	RA-17	RA-18
q	0.00	0.00	0.00	0.00	0.00	0.00	0.00	0.00
or	5.73	8.33	9.10	9.99	10.22	8.21	5.32	7.86
ab	24.28	22.76	24.11	23.37	23.60	29.02	16.63	25.97
an	20.11	23.52	18.73	17.79	18.56	20.99	20.57	19.86
di	26.50	15.10	24.66	20.29	19.82	17.40	24.29	22.77
hy	7.83	16.58	0.52	0.00	4.39	5.79	18.66	2.93
ol	7.40	4.26	13.47	16.19	12.73	10.27	1.00	13.29
mt	5.52	5.64	5.86	5.87	6.22	4.68	5.84	5.12
il	1.50	1.65	2.13	2.16	2.18	1.44	1.77	1.22
ap	0.16	0.14	0.21	0.19	0.26	0.14	0.19	0.12
cc	0.27	0.52	0.18	0.59	0.59	0.18	0.23	0.27
py	0.04	0.02	0.00	0.02	0.00	0.02	0.00	0.02
ne	0.00	0.00	0.00	0.90	0.00	0.00	0.00	0.00
si	112.58	116.24	109.37	106.59	109.34	120.45	112.41	112.22
al	17.32	20.00	17.34	17.44	17.54	20.83	16.63	18.05
fm	48.97	49.72	50.15	51.95	51.90	46.88	51.48	49.81
mg	0.56	0.54	0.55	0.56	0.55	0.54	0.50	0.60
c	26.10	22.11	24.18	21.78	22.02	22.25	25.43	23.62
alk	7.61	8.17	8.33	8.84	8.54	10.03	6.46	8.51
k	0.18	0.26	0.26	0.27	0.29	0.21	0.20	0.22
ti	1.33	1.52	1.87	1.92	1.94	1.36	1.60	1.07

TABLE II. CONTINUED

Field n.	RA-19	RA-21	RA-22	DB-2-1	DB-2-2	DB-3	DB-6	DB-7
q	0.00	0.00	0.00	0.00	0.00	0.16	0.00	0.24
or	5.79	6.74	6.38	8.21	8.33	5.20	5.20	5.08
ab	24.46	24.79	25.63	24.45	22.42	17.85	25.46	18.86
an	18.94	19.72	20.13	22.42	23.48	26.49	22.79	25.35
di	27.36	24.74	24.56	17.91	17.15	21.78	16.79	23.45
hy	0.00	8.41	6.17	4.91	11.66	21.72	6.64	18.94
ol	13.11	7.40	8.80	12.40	7.51	0.00	10.80	0.00
mt	5.18	4.60	4.41	5.35	5.35	3.96	5.74	5.13
il	1.48	1.65	1.73	2.41	2.51	1.52	2.43	1.50
ap	0.17	0.16	0.16	0.19	0.19	0.14	0.19	0.12
cc	0.14	0.09	0.09	0.23	0.23	0.32	0.57	0.23
py	0.02	0.07	0.02	0.02	0.00	0.00	0.02	0.02
ne	1.10	0.00	0.00	0.00	0.00	0.00	0.00	0.00
si	108.79	116.46	116.23	110.72	112.93	115.00	109.42	114.18
al	17.09	18.12	18.54	19.34	19.57	18.84	19.42	18.50
fm	48.75	48.26	47.49	49.91	49.83	48.56	49.84	48.34
mg	0.56	0.52	0.52	0.54	0.53	0.60	0.52	0.59
c	25.79	25.36	25.54	22.35	22.64	26.71	22.65	27.03
alk	8.16	8.26	8.43	8.40	7.95	5.90	8.09	6.13
k	0.17	0.20	0.19	0.24	0.26	0.22	0.17	0.20
ti	1.31	1.52	1.59	2.17	2.28	1.36	2.22	1.34

TABLE II. CONTINUED

Field n.	DB-8	DB-9	RA-8	RA-13	RA-14	RA-15	RA-9	RA-10-1
q	0 00	0.00	3.79	4 39	3 99	3 39	1.37	3 39
or	8 92	4 78	8.27	8.33	7 62	7 74	8 10	7 74
ab	26 14	19 71	23 09	22.84	25.29	24.11	28.17	24 28
an	22.05	24.97	19.98	20.93	19.93	20.83	18.14	19 54
di	17 60	21.41	17 95	17.61	17.00	.6 90	18.19	18 20
hy	3.18	20.22	15.51	15 59	15 33	16 55	15.38	16 09
ol	13 17	0.68	0 00	0.00	0.00	0.00	0 00	0.00
mt	5.87	4 36	6.67	6 73	6 81	6.57	6 29	6.22
il	1 69	1.52	2.15	2.11	2.15	2.11	2.24	2 16
ap	0 14	0.14	0 30	0.30	0 28	0 28	0 30	0.30
cc	0.36	0 91	0.09	0.04	0.23	0.00	0 04	0 18
py	0 02	0 02	0 02	0 02	0 02	0 02	0 02	0 02
ne	0 00	0 00	0 00	0 00	0 00	0 00	0 00	0 00
si	112 14	114.09	129 23	130 33	131.16	128 99	129.46	129.67
al	19 84	18.55	19.70	20 04	20.16	20 13	20.07	19.60
fm	49 01	48 50	48.11	47 78	47.62	48.21	47.32	48 03
mg	0.52	0.59	0.45	0.45	0.45	0 46	0 46	0 46
c	22 15	26.64	23.32	23.40	22.88	22.72	22.36	23.31
alk	9.00	6.30	8.88	8 77	9.35	8.95	10 26	9 05
k	0.24	0.19	0 25	0.26	0.22	0 23	0 21	0 23
ti	1.52	1 37	2 13	2.08	2 13	2 08	2.22	2.14

TABLE II. CONTINUED

Field n.	RA-11	RA-12	DB-5	DB-1	DB-4	DB-11	DB-12	A-4-3
q	0.00	5.04	0.55	5.09	0.18	0.00	0.07	0.00
or	7.98	8.21	8.63	6.97	6.15	7.33	5.91	7.56
ab	29.18	21.49	29.18	27.32	30.88	29.18	31.72	29.61
an	17.50	23.02	18.78	22.26	23.66	27.59	23.71	17.48
di	18.57	14.16	12.92	10.21	16.18	14.14	15.00	21.50
hy	10.65	17.63	18.56	11.93	11.40	2.98	12.85	4.44
ol	4.58	0.00	0.00	0.00	0.00	9.37	0.00	9.70
mt	6.21	6.41	6.03	8.71	6.23	5.60	5.45	5.48
il	2.09	2.07	2.20	4.27	2.77	2.64	2.79	1.56
ap	0.28	0.28	0.28	0.42	0.28	0.26	0.28	0.14
cc	0.45	0.14	0.32	0.23	0.14	0.00	0.18	0.36
py	0.02	0.02	0.02	0.06	0.02	0.02	0.02	0.07
ne	0.00	0.00	0.00	0.00	0.00	0.00	0.00	0.00
si	121.97	131.17	129.61	130.79	127.41	118.57	129.65	118.87
al	19.46	20.98	21.07	22.81	23.68	24.45	24.16	18.88
fm	48.05	48.00	48.30	46.28	41.23	41.82	40.97	48.03
mg	0.47	0.45	0.48	0.34	0.36	0.37	0.34	0.52
c	22.24	22.58	19.83	20.72	24.39	23.72	23.89	23.13
alk	10.25	8.44	10.81	10.19	10.69	10.02	10.99	9.95
k	0.20	0.26	0.22	0.19	0.16	0.19	0.15	0.19
ti	2.02	2.07	2.21	4.44	2.79	2.53	2.84	1.46

A-4-3 : Average of 4 amphibolites intercalated with calc-silicate rocks.

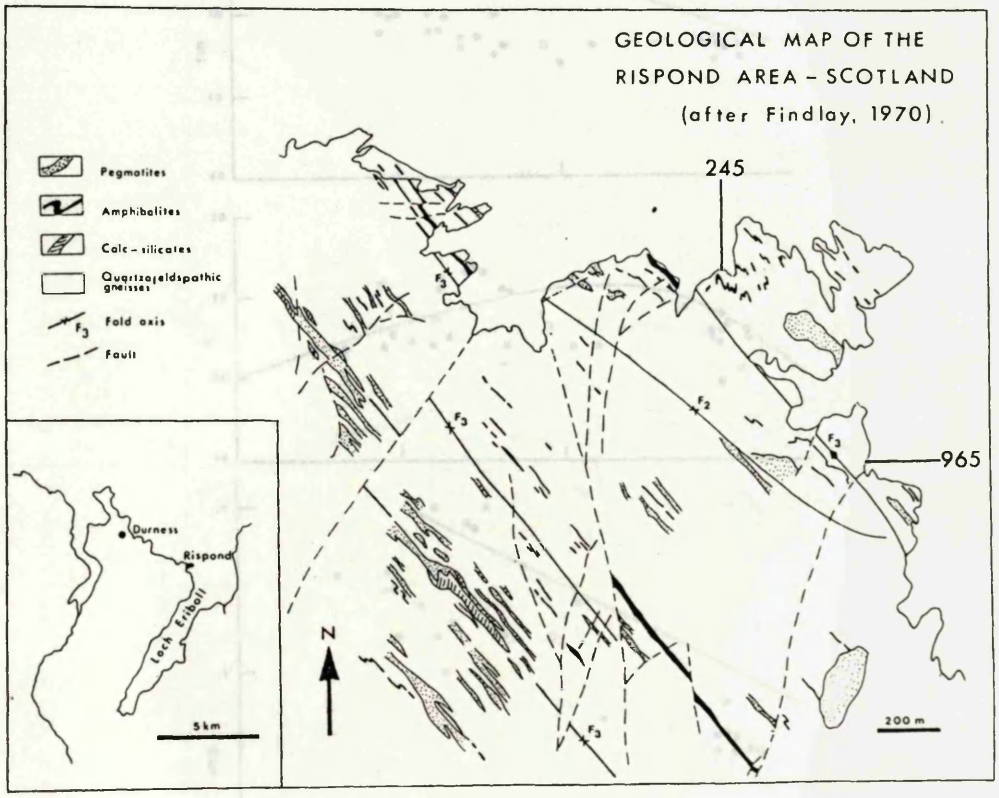
GEOLOGICAL MAP OF THE
RISPOND AREA - SCOTLAND
(after Findlay, 1970)
245
965
Pegmatites
Amphibolites
Calc-silicates
Quartzofeldspathic gneisses
Fold axis
Fault
Durness
Rispond
Loch Eriboll
5km
N
200 m

FIGURE 1

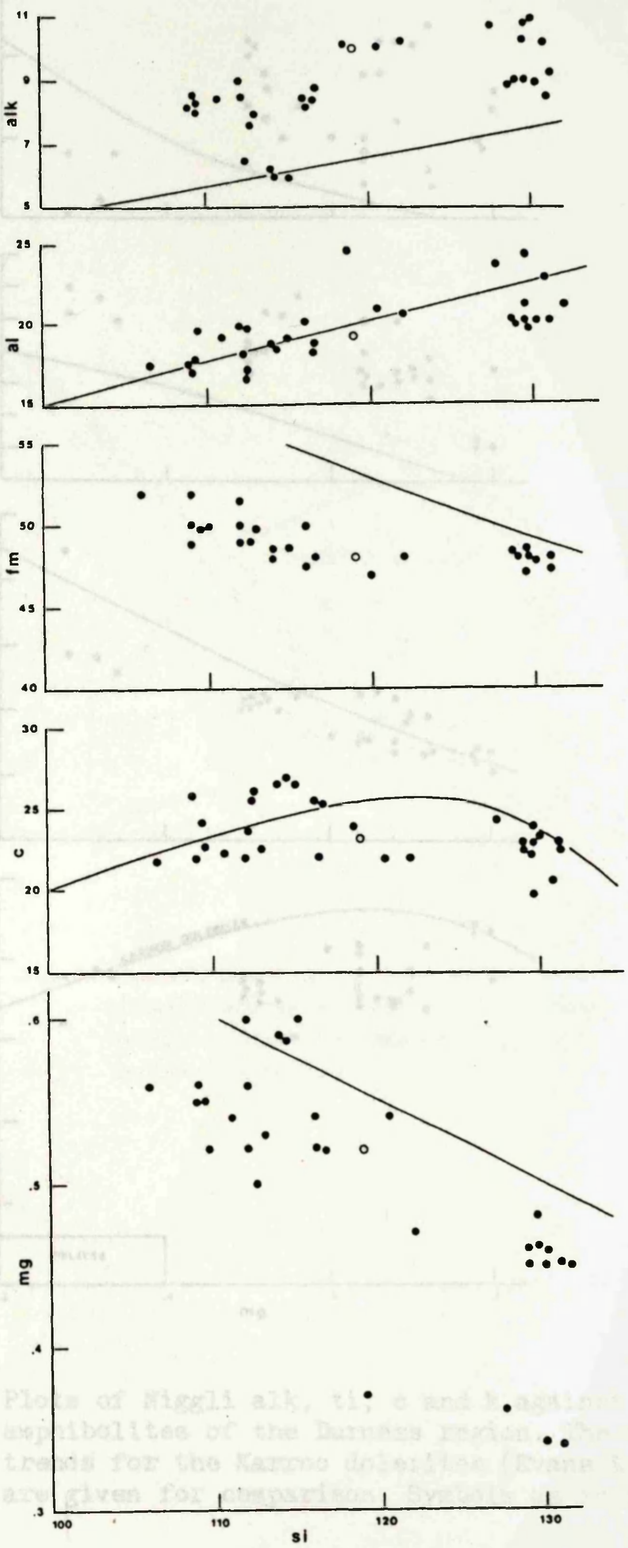

Figure 2. Plots of Niggli al, fm, c, alk and mg against si, for the amphibolites of the Durness region. The approximate trends for the Karroo dolerites (Evans & Leake, 1960) are given for comparison. Symbols: (●) amphibolites intercalated with quartzofeldspathic gneisses, (o) amphibolites intercalated with calc-silicate rocks.

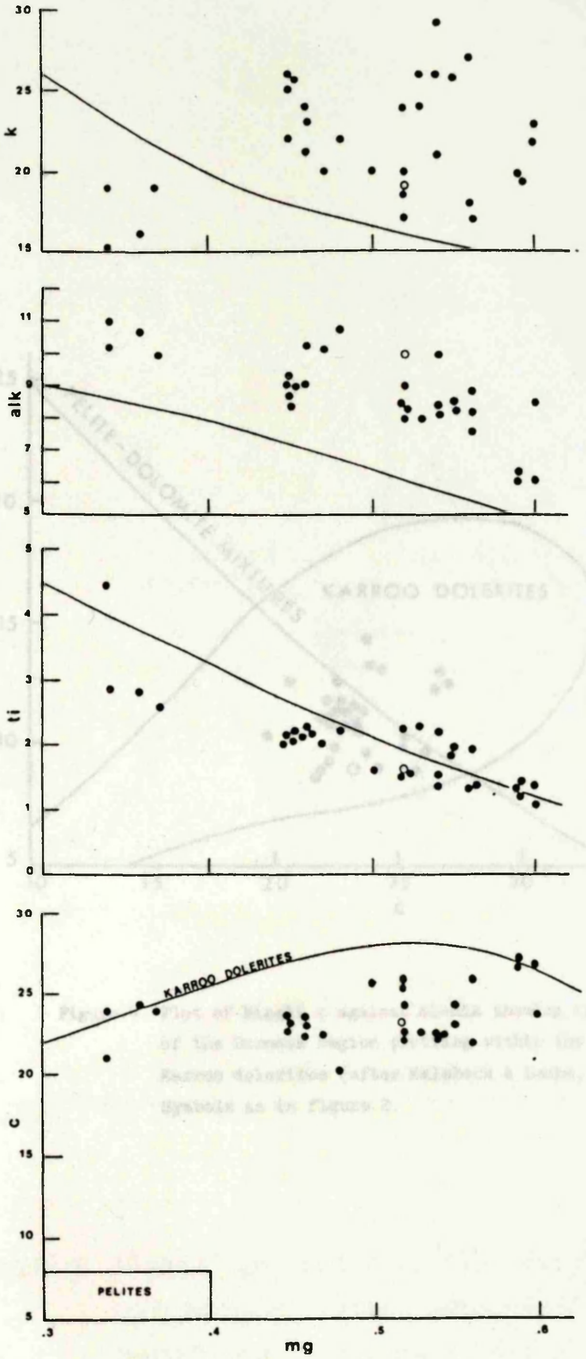

Figure 3. Plots of Niggli alk, ti, c and k against mg, for the amphibolites of the Durness region. The approximate trends for the Karroo dolerites (Evans & Leake, 1960) are given for comparison. Symbols as in figure 2.

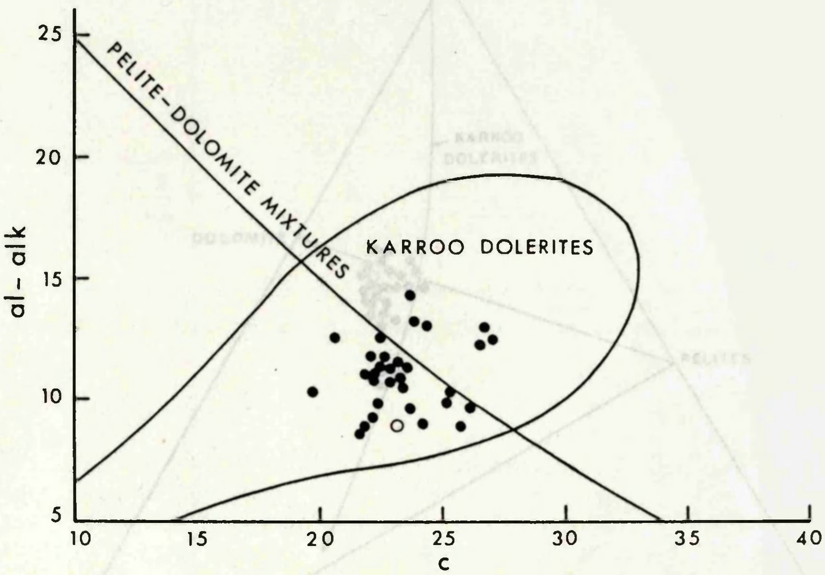

Figure 4. Plot of Niggli c against al-alk showing the amphibolites of the Durness region plotting within the field of the Karroo dolerites (after Kalsbeck & Leake, 1970) Symbols as in figure 2.

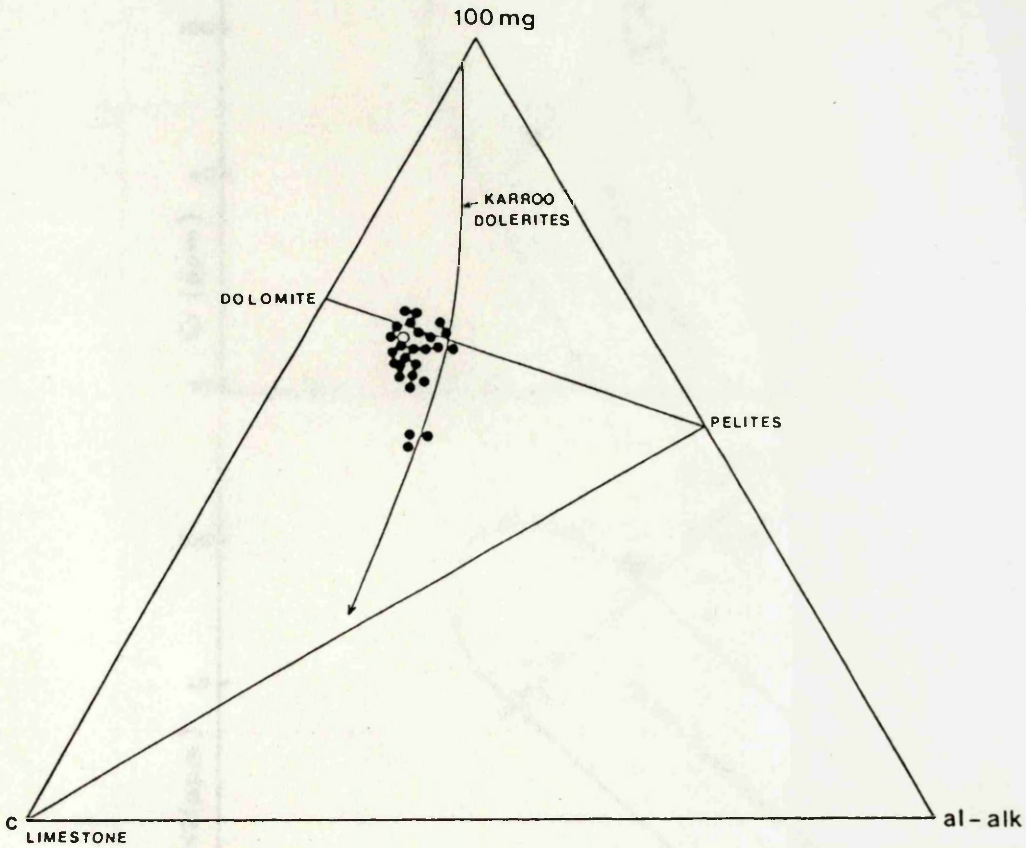

Figure 5. Niggli mg-c-(al-alk) plot for the amphibolites of the Durness region, after Leake (1964). Symbols as in figure 2.

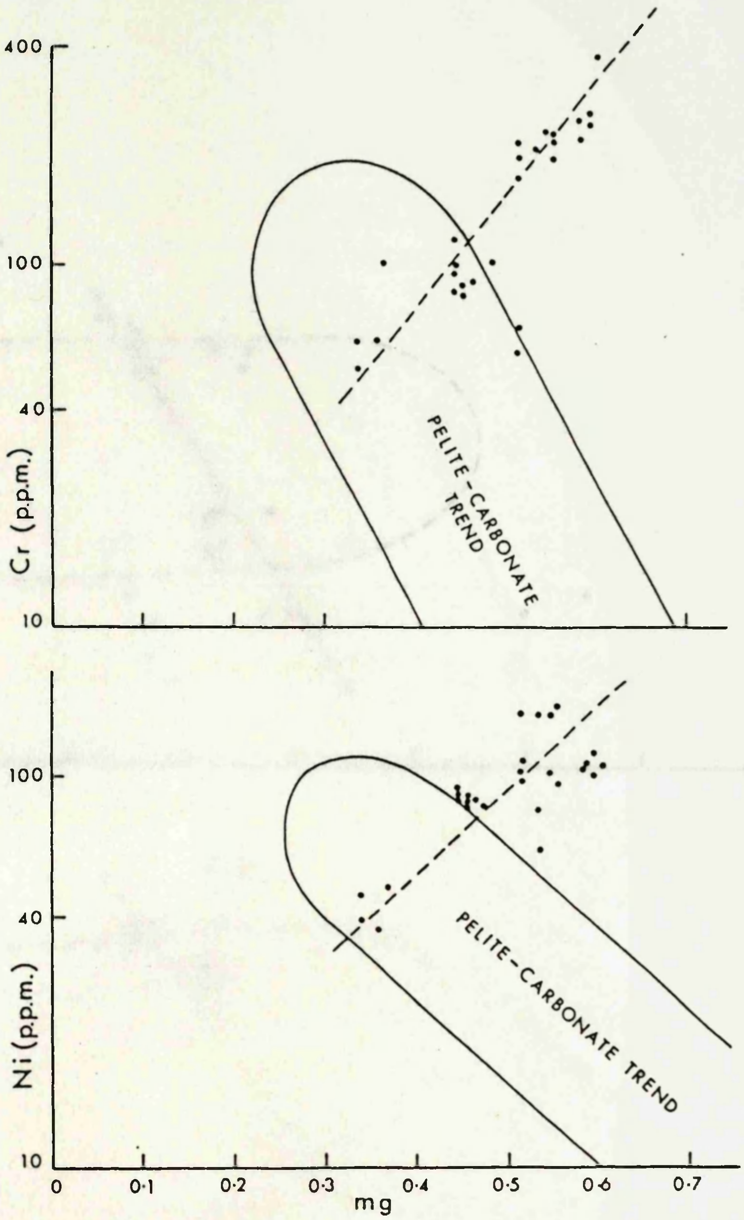

Figure 6. Niggli mg against Cr and Ni showing igneous trends for the amphibolites of the Durness region (after Evans & Leake, 1960). Field of pelite-carbonate mixtures from Van de Kamp (1970).
Symbols as in figure 2.

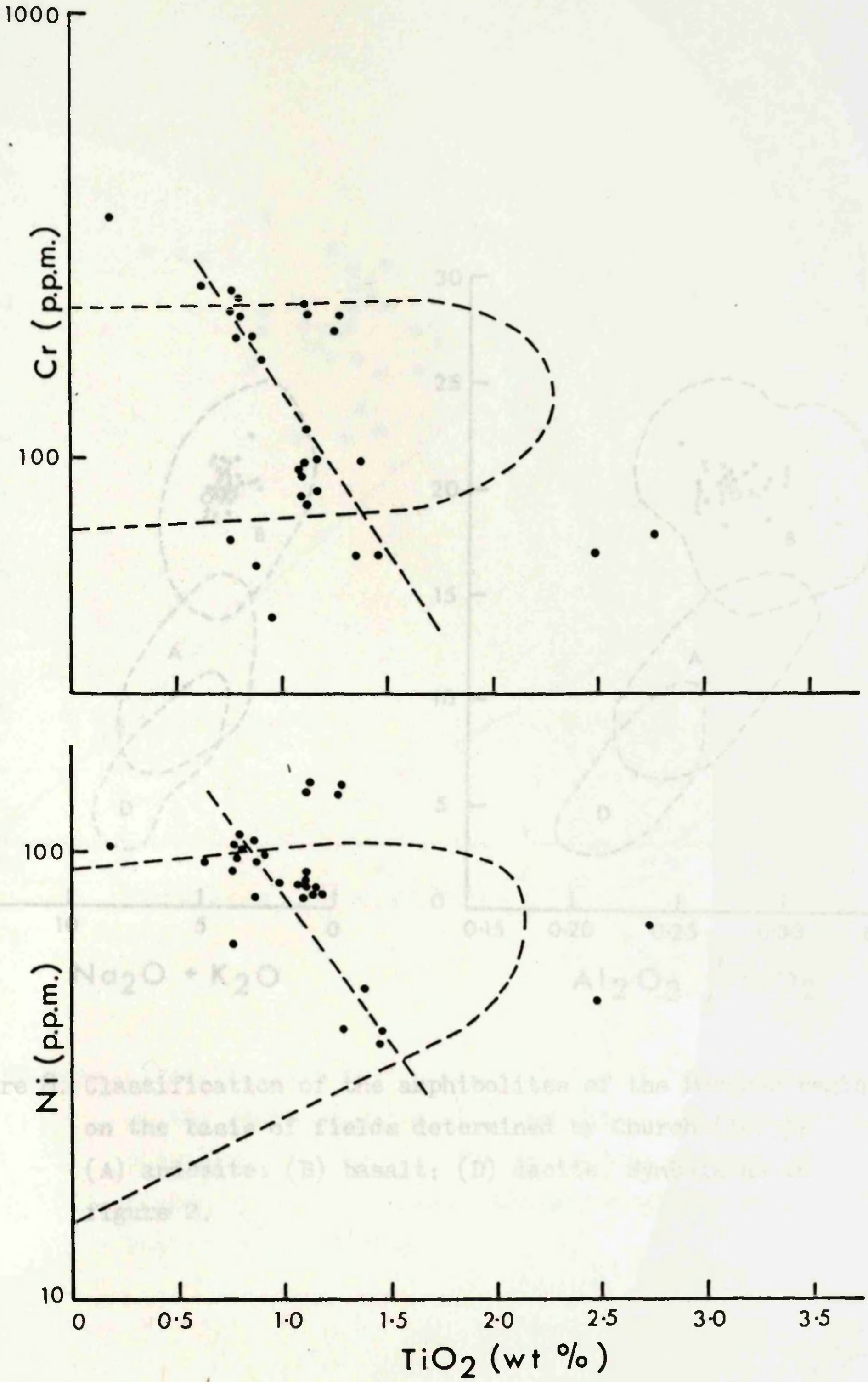

Figure 7. TiO_2 against Cr and Ni showing igneous trends for the amphibolites of the Durness region; the ringed area represents the field of pelites (cf. Leake, 1964). Symbols as in figure 2.

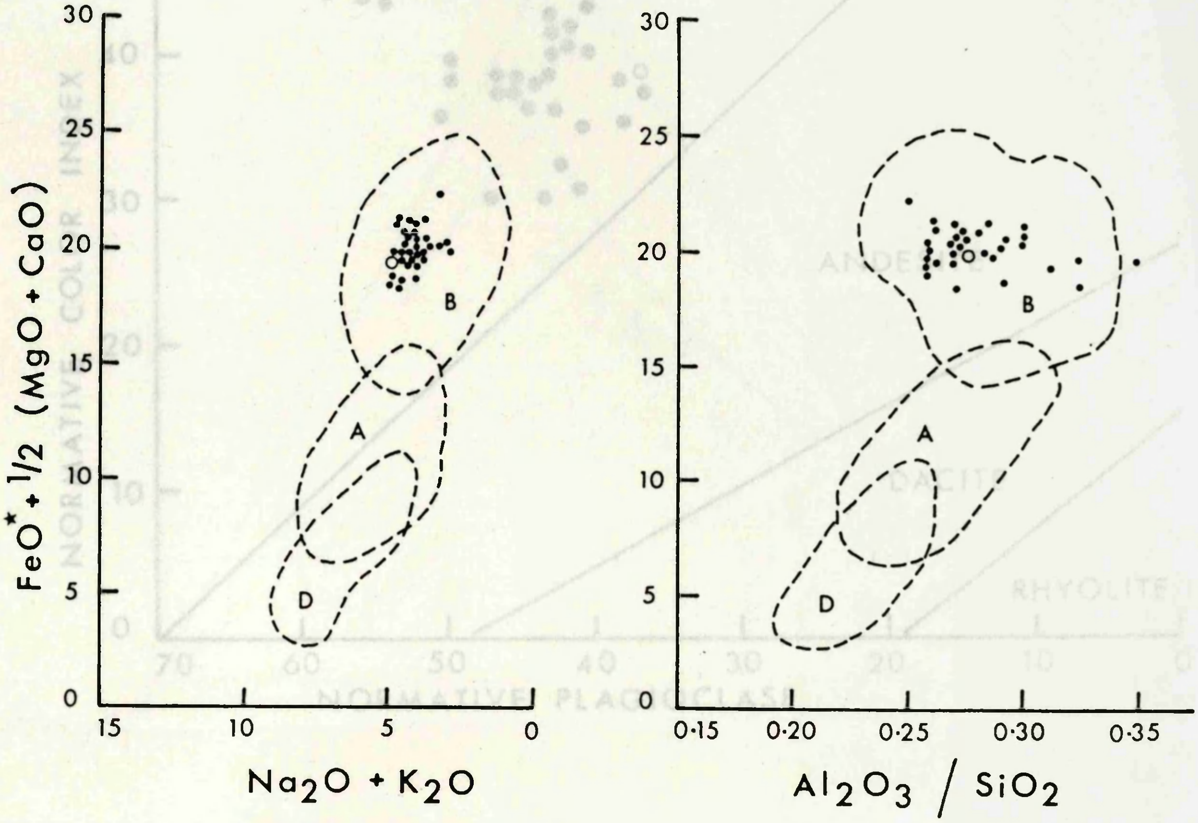

Figure 8. Classification of the amphibolites of the Durness region on the basis of fields determined by Church (1975): (A) andesite; (B) basalt; (D) dacite. Symbols as in figure 2.

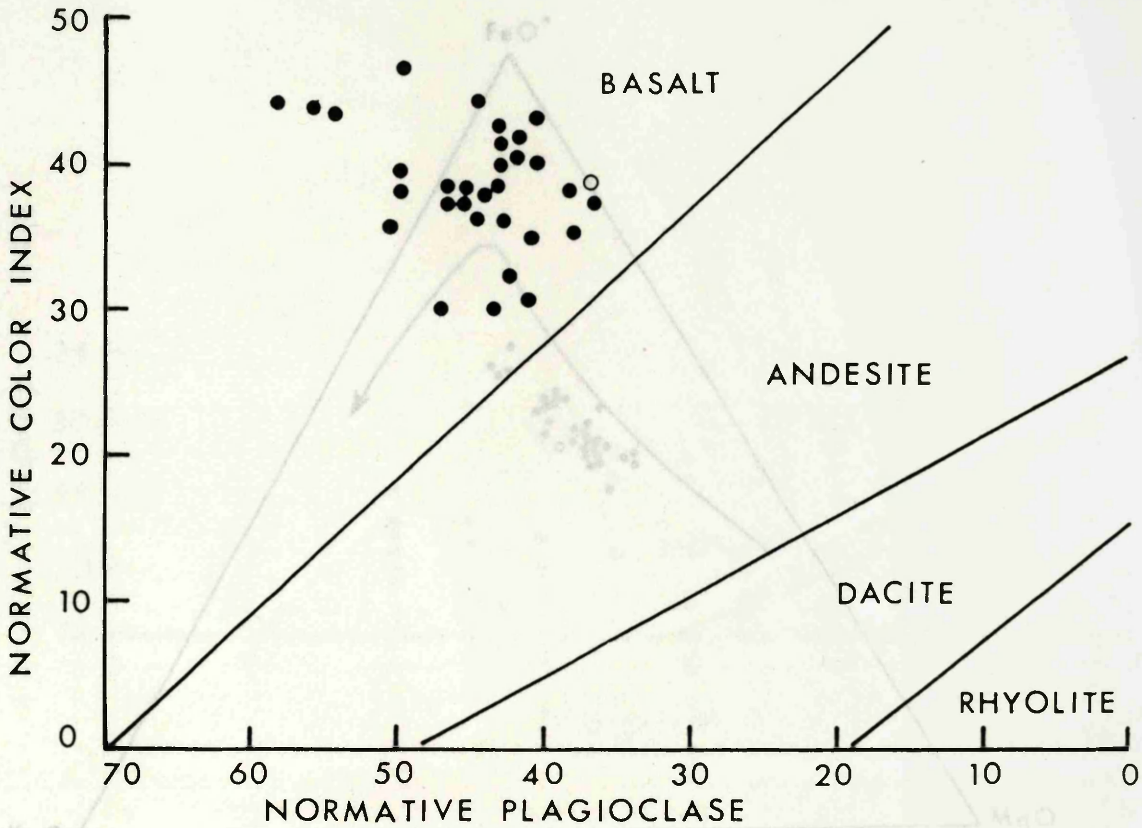

Figure 9. Classification of the amphibolites of the Durness region on the basis of plots of normative color index against normative plagioclase. The lines separating the different fields are from Irvine & Baragar (1971). Symbols as in figure 2.

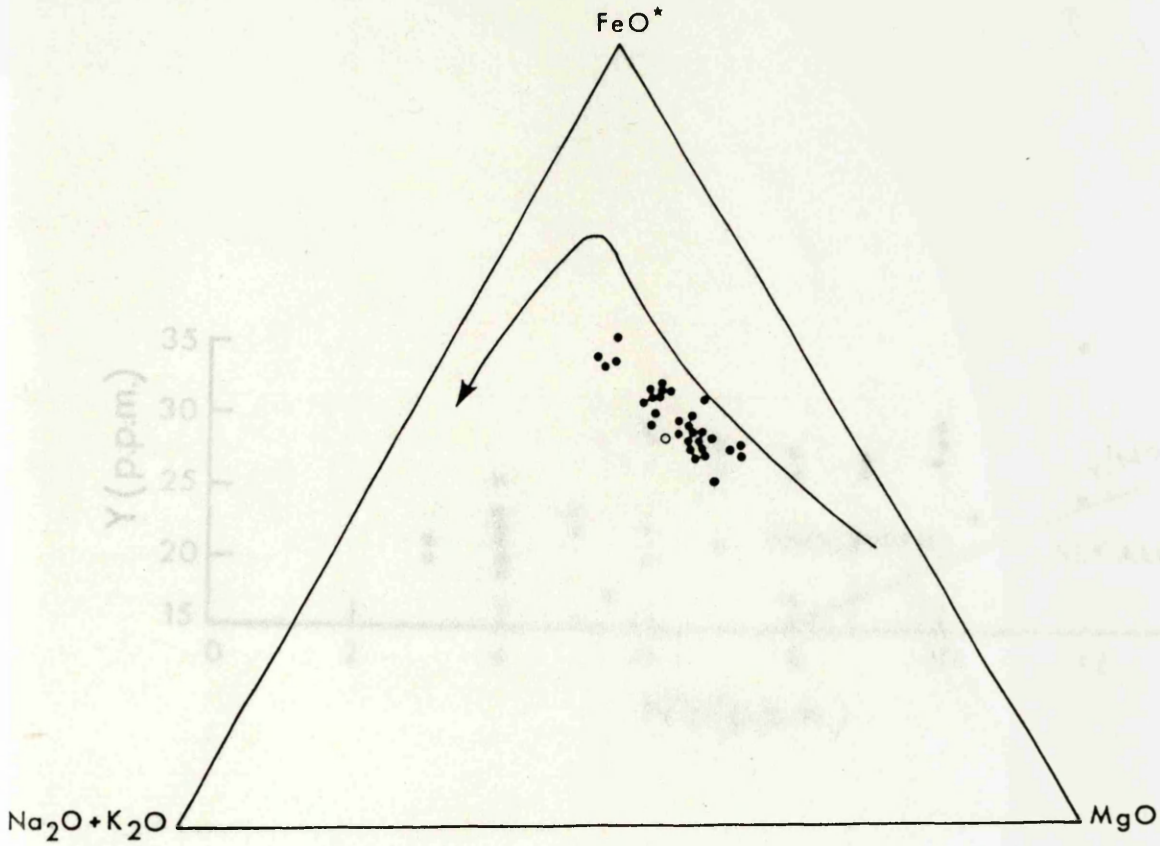

Figure 10. AFM diagram for the amphibolites from the Durness region. The Skaergaard trend (after Armbrustmacher, 1977) is given for comparison Symbols as in figure 2.

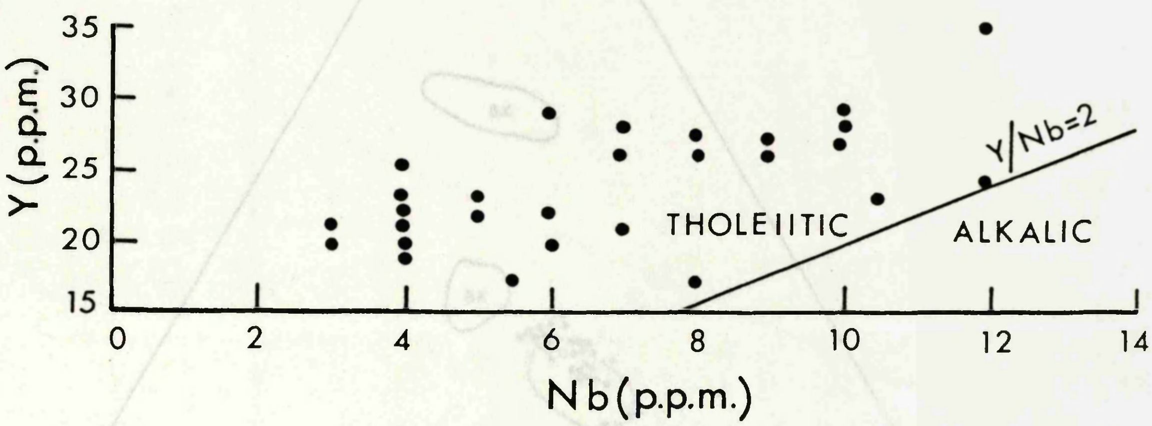

Figure 11. Plot of Y against Nb to discriminate between tholeiitic and alkalic parentage for the amphibolites of the Durness region (modified after Pearce & Cann, 1973). Symbols as in figure 2.

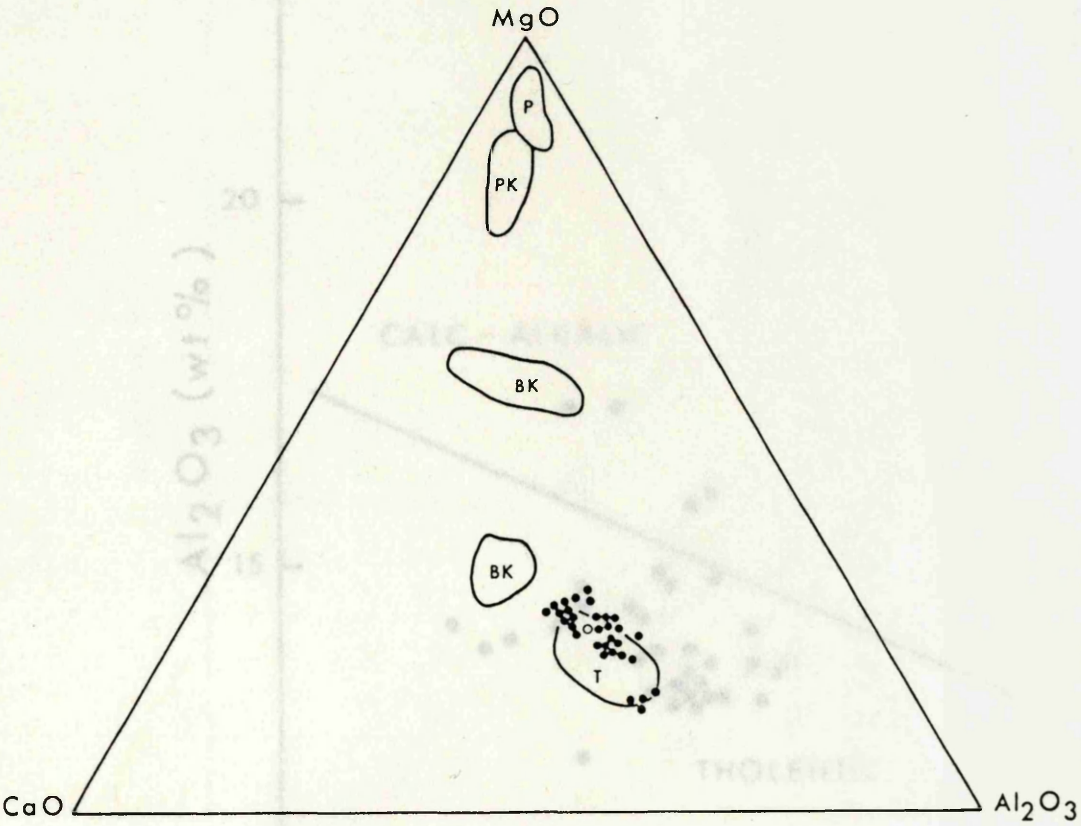

Figure 12. Ternary CaO-MgO-Al_2O_3 diagram for the amphibolites of the Durness region. The classification fields are from Viljoen & Viljoen (1969). (P) peridotite; (PK) peridotite-komatiite; (BK) basalt-komatiite; (T) tholeiite. Symbols as in figure 2.

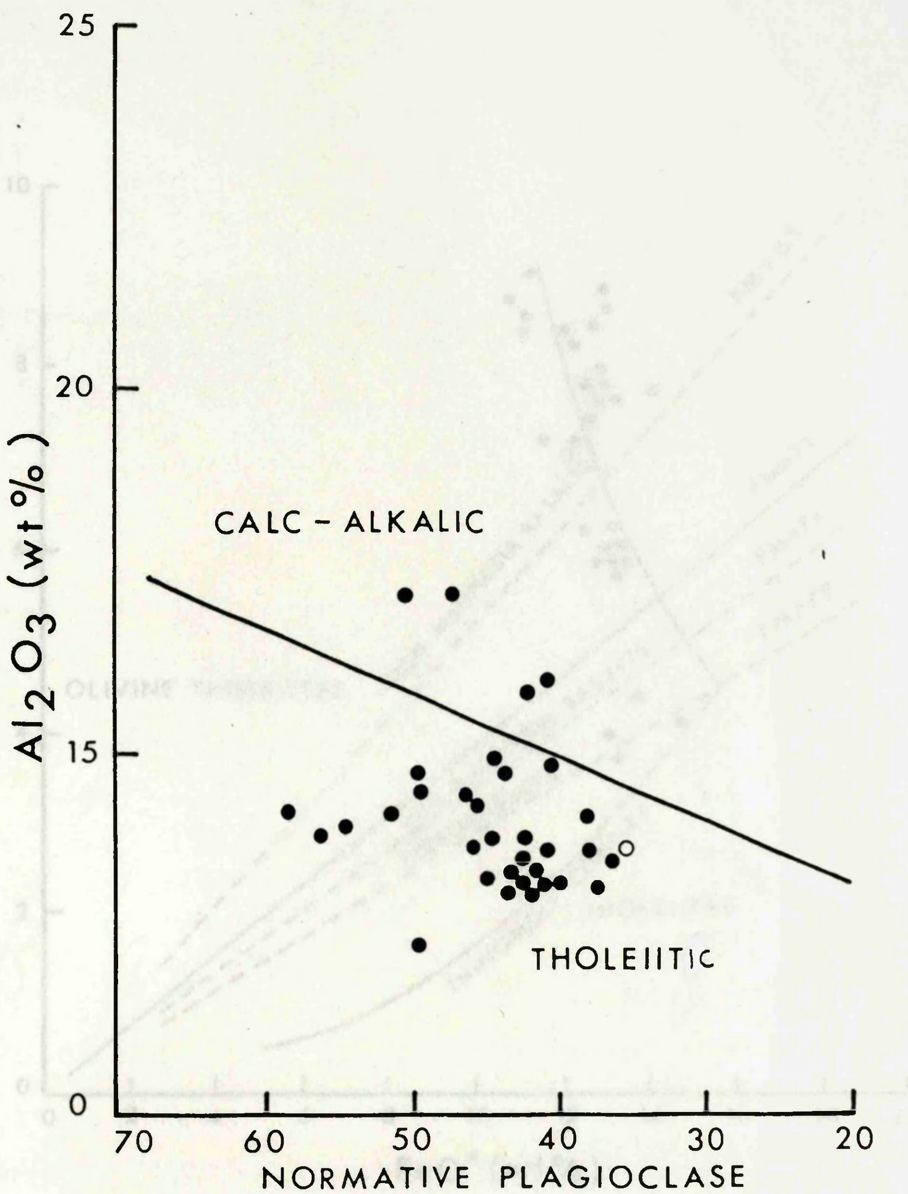

Figure 13. Plot of Al_2O_3 against normative plagioclase for discriminating between calc-alkaline and and tholeiitic sequences (after Irvine & Baragar, 1971). Symbols as in figure 2.

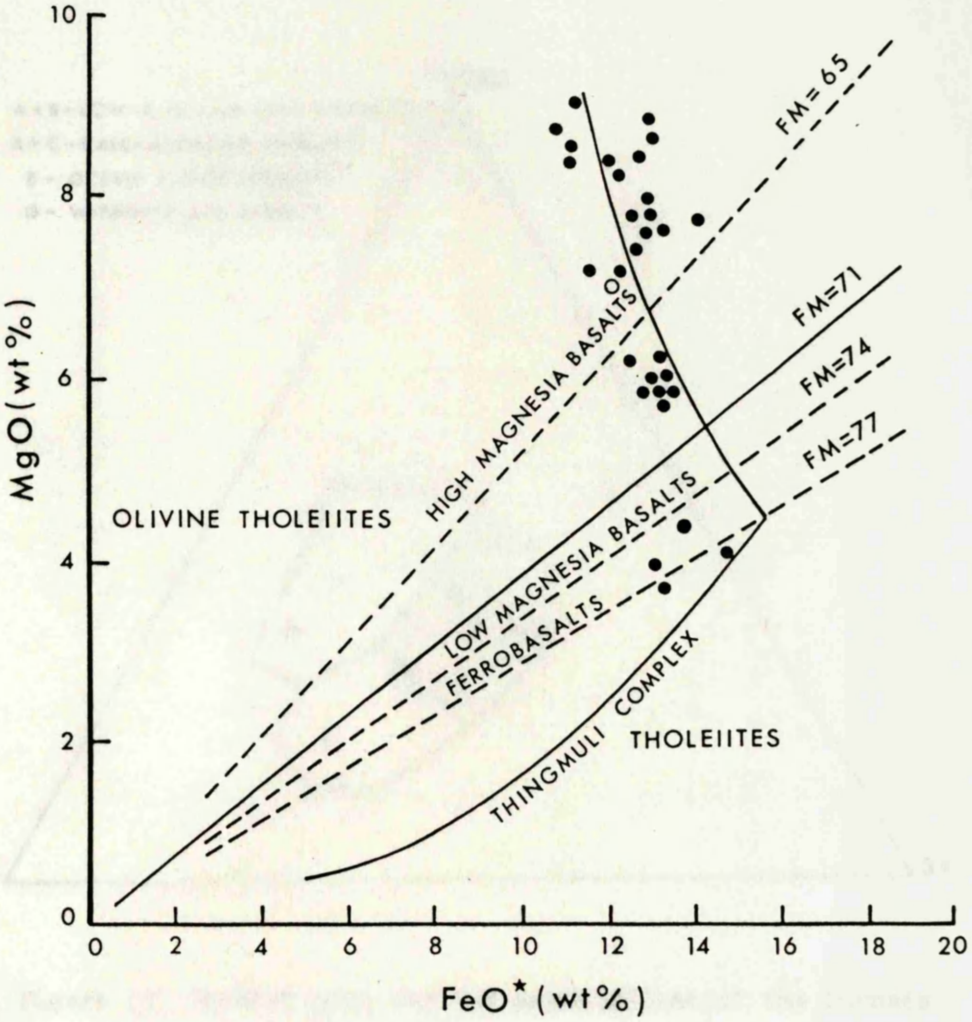

Figure 14. Plot of MgO against FeO^+(total iron as FeO) for discriminating between olivine tholeiites and tholeiites, for the amphibolites of the Durness region (after Wood, 1978). The trend line defined by the Thingmuli aphyric lavas, Iceland is given for comparison (after Carmichael, 1964). Symbols as in figure 2.

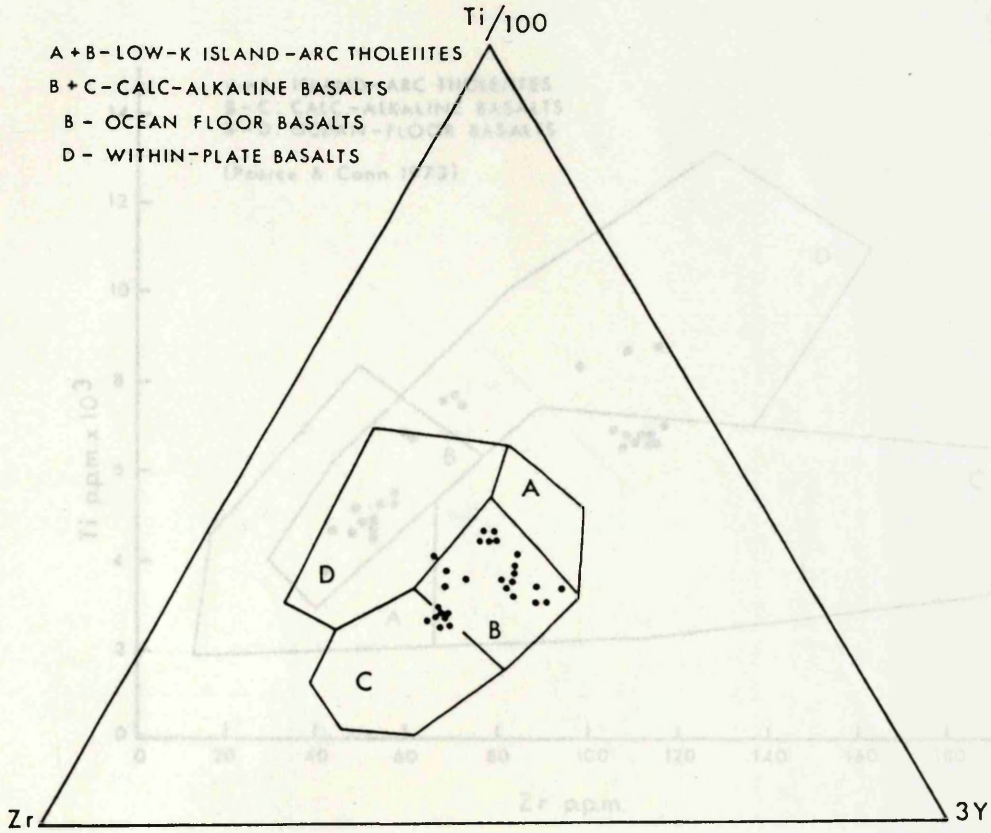

Figure 15. Ti-Zr-Y plot for the amphibolites of the Durness region. The different tectonic settings of recent volcanic rocks are from Pearce & Cann (1973). Within plate basalts (ocean island and continental) plot in field D; ocean floor basalts in field B; low-K island arc tholeiites in A and B; calc-alkaline basalts in B and C. Symbols as in figure 2.

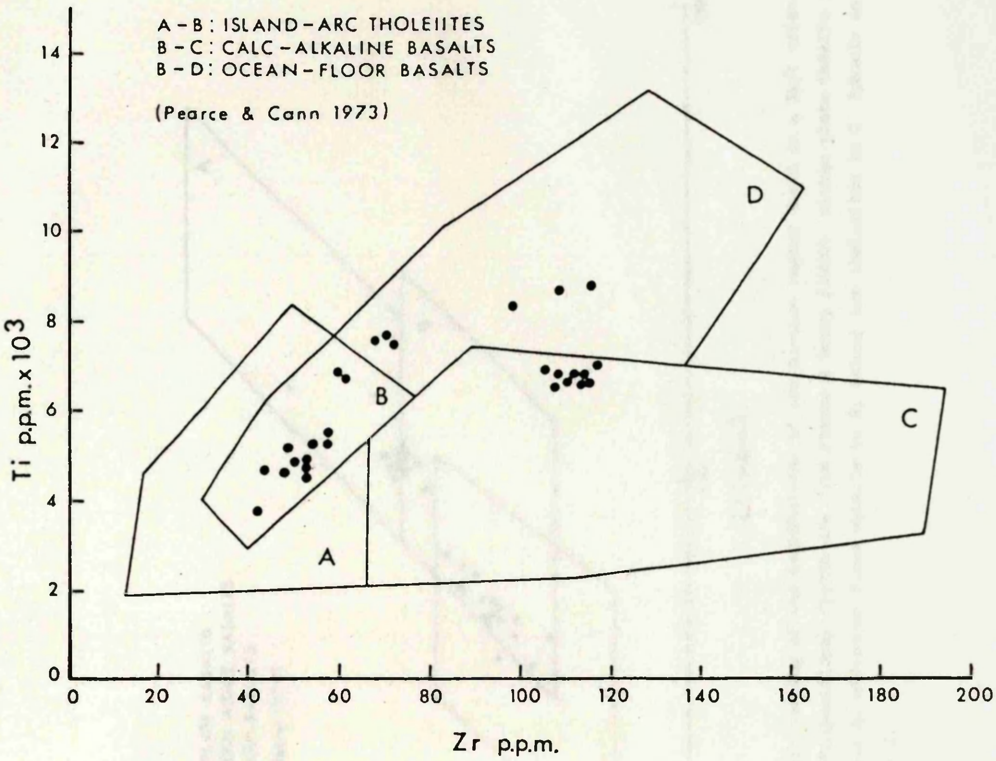

Figure 16. Tectonic setting of the amphibolites of the Durness region, based on a Ti versus Zr plot. Compositional fields from Pierce & Cann (1973). Ocean floor basalts plot in fields B and D; island arc tholeiites in A and B; calc-alkaline basalts in B and C. Symbols as in figure 2.

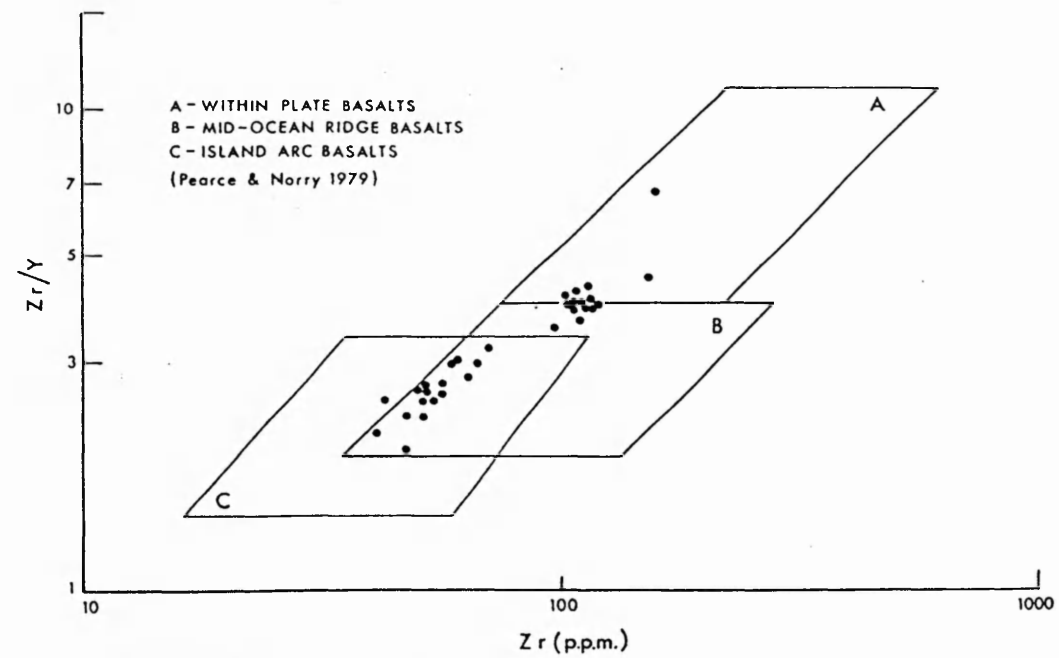

Figure 17. Tectonic setting of the amphibolites of the Durness region based on a Zr/Y versus Zr plot. Compositional fields are from Pierce & Norry (1979). Within plate basalts plot in field A; mid-ocean ridge basalts in B; island arc tholeiites in C Symbols as in figure 2.

XI.2 GEOLOGICAL MAPS

GEOLOGICAL MAP - SUBAREA II

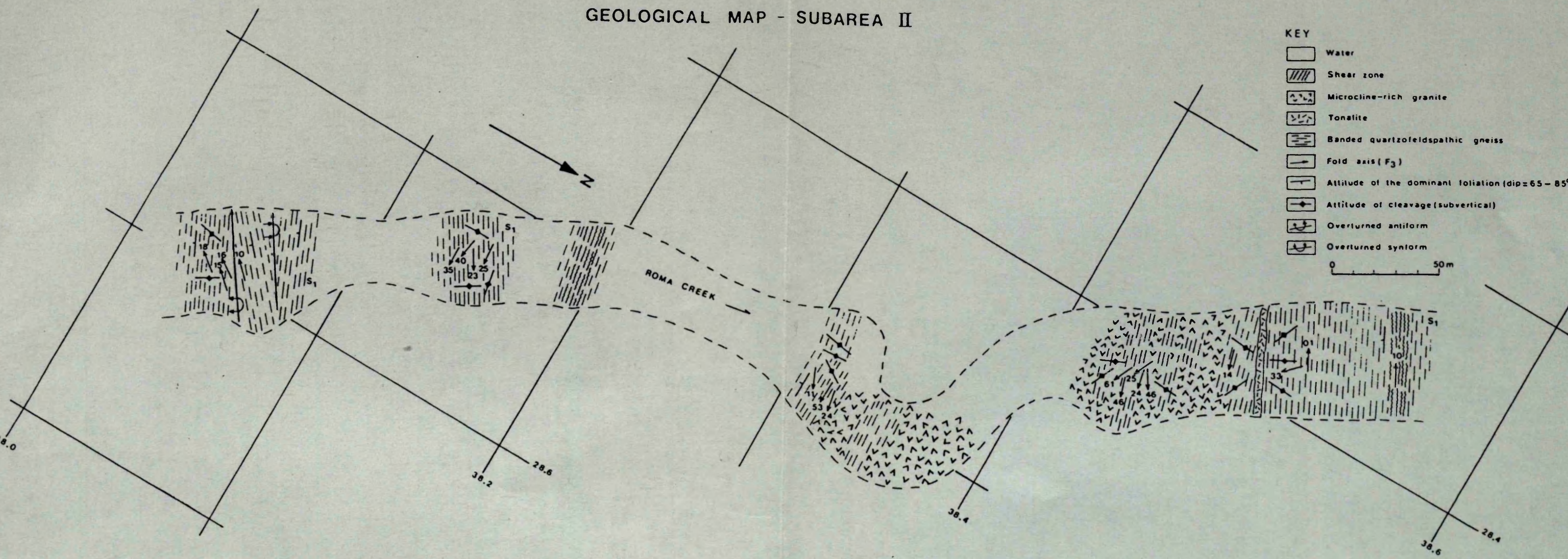

FIGURE.VII.3

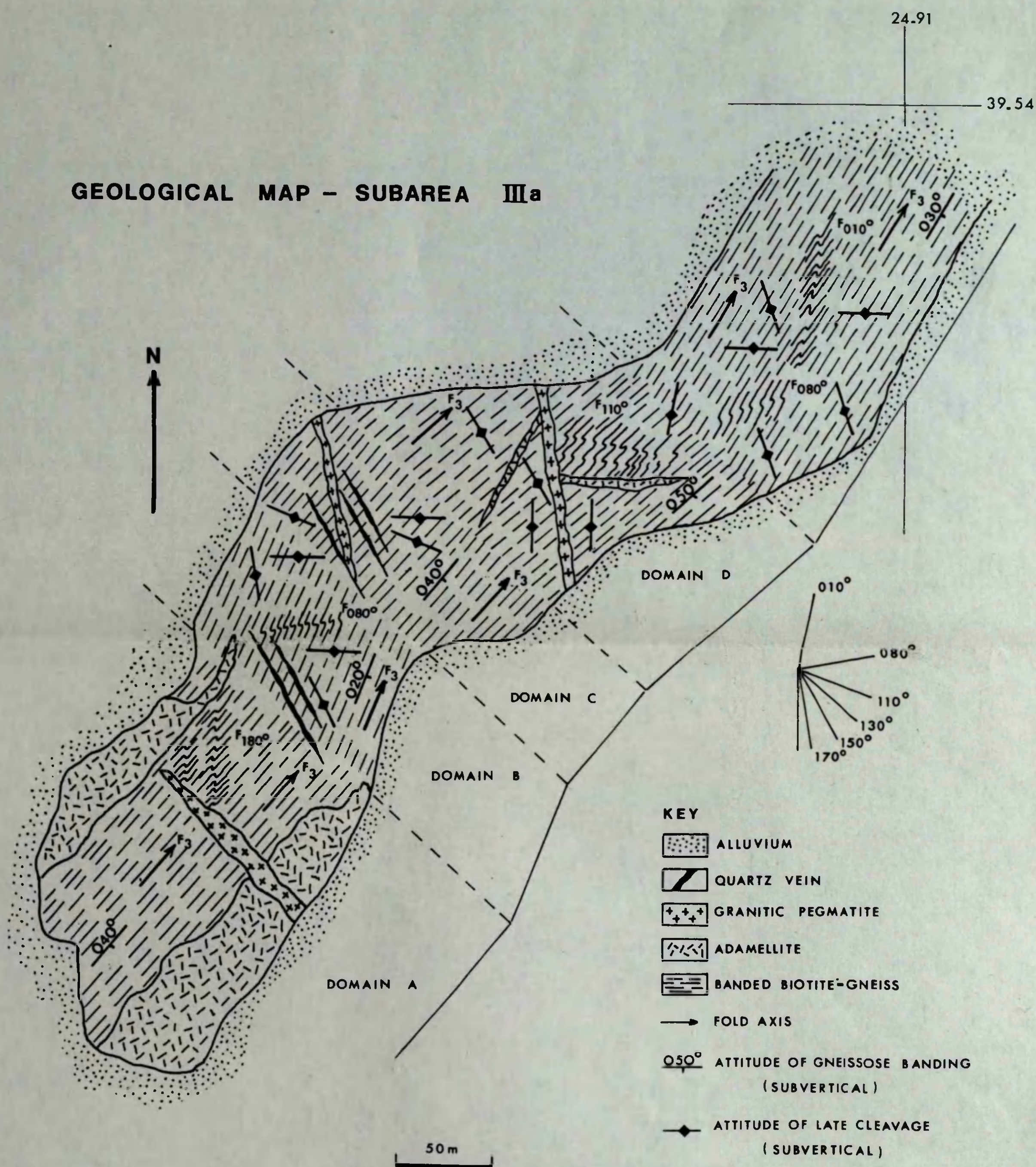
GEOLOGICAL MAP - SUBAREA IIIa
24.91
39.54
N
F010°
030°
F3
F080°
F110°
050°
040°
F080°
020°
F180°
040°
DOMAIN D
DOMAIN C
DOMAIN B
DOMAIN A
010°
080°
110°
130°
150°
170°
KEY
ALLUVIUM
QUARTZ VEIN
GRANITIC PEGMATITE
ADAMELLITE
BANDED BIOTITE-GNEISS
FOLD AXIS
050° ATTITUDE OF GNEISSOSE BANDING (SUBVERTICAL)
ATTITUDE OF LATE CLEAVAGE (SUBVERTICAL)
50m

FIGURE.VII.4

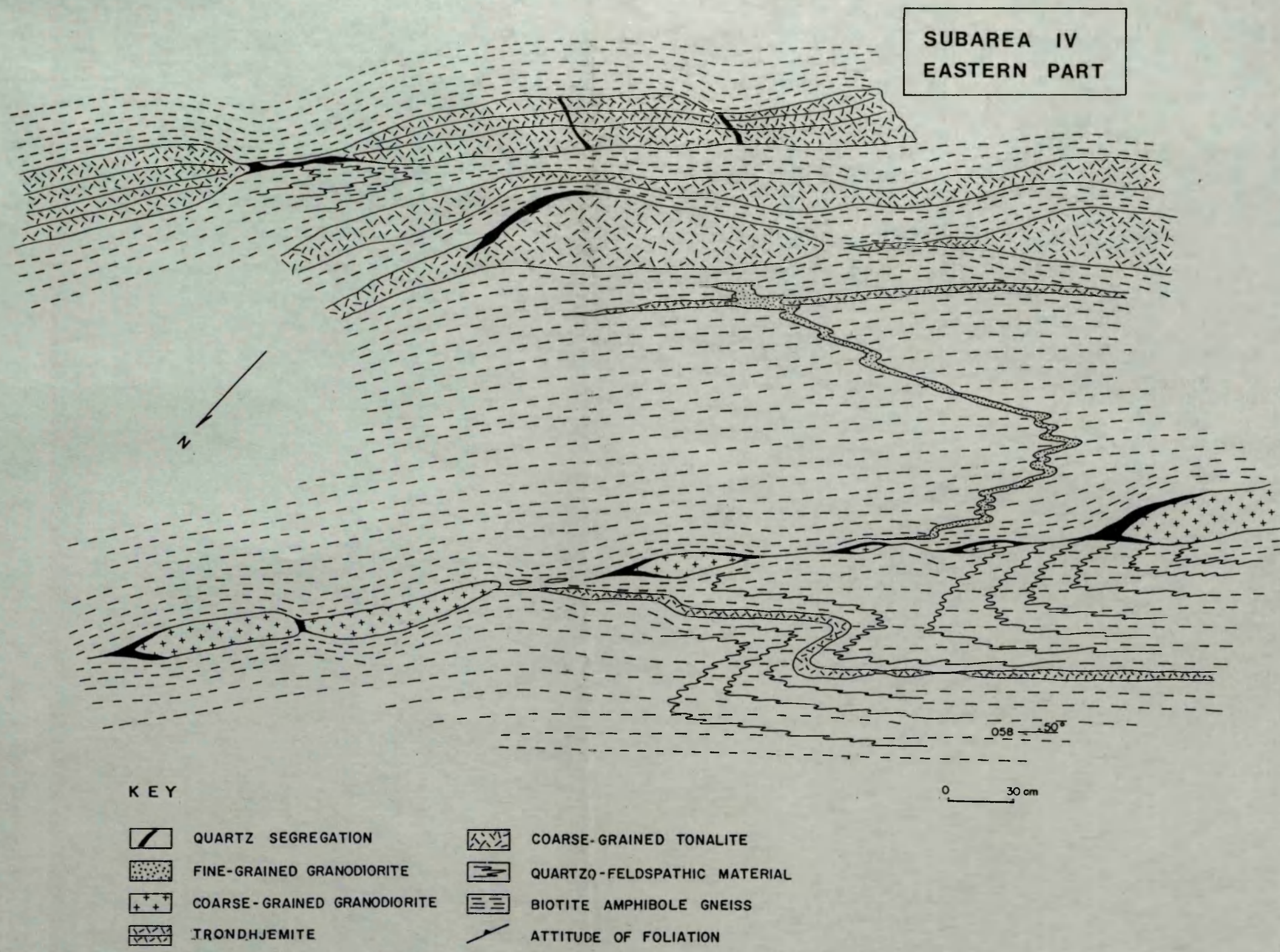
SUBAREA IV
EASTERN PART
N
058
50°
0
30 cm
KEY
QUARTZ SEGREGATION
FINE-GRAINED GRANODIORITE
COARSE-GRAINED GRANODIORITE
TRONDHJEMITE
COARSE-GRAINED TONALITE
QUARTZO-FELDSPATHIC MATERIAL
BIOTITE AMPHIBOLE GNEISS
ATTITUDE OF FOLIATION

FIGURE.VII.5

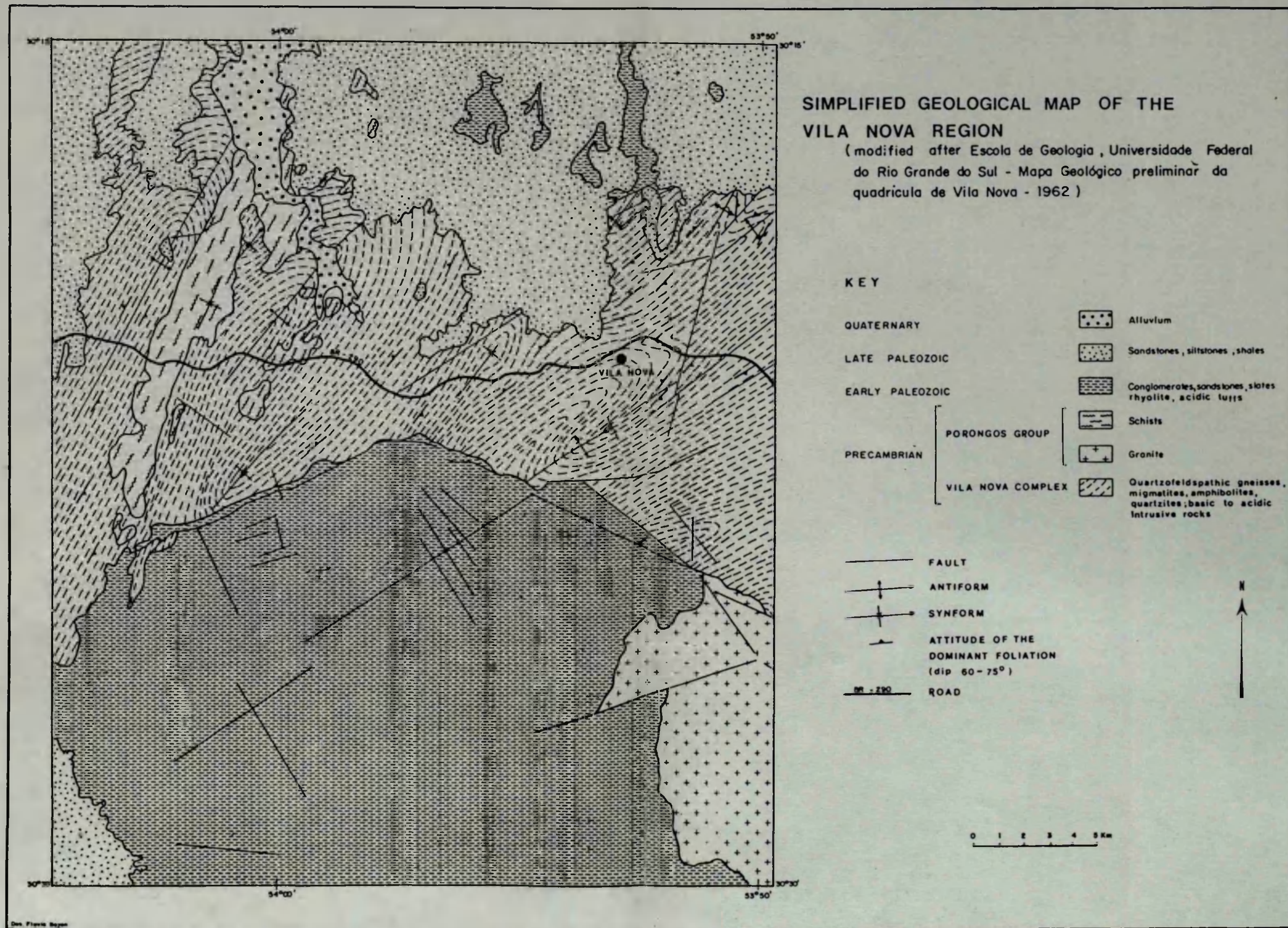
SIMPLIFIED GEOLOGICAL MAP OF THE VILA NOVA REGION
(modified after Escola de Geologia , Universidade Federal do Rio Grande do Sul - Mapa Geológico preliminar da quadrícula de Vila Nova - 1962)
KEY
QUATERNARY
Alluvium
LATE PALEOZOIC
Sandstones , siltstones , shales
EARLY PALEOZOIC
Conglomerates, sandstones , slates rhyolite, acidic tuffs
PRECAMBRIAN
PORONGOS GROUP
Schists
Granite
VILA NOVA COMPLEX
Quartzofeldspathic gneisses, migmatites, amphibolites, quartzites; basic to acidic intrusive rocks
FAULT
ANTIFORM
SYNFORM
ATTITUDE OF THE DOMINANT FOLIATION (dip 60 - 75°)
ROAD
N
0 1 2 3 4 5 Km
VILA NOVA
54°00'
53°50'
30°15'
30°30'

FIGURE.VII.1

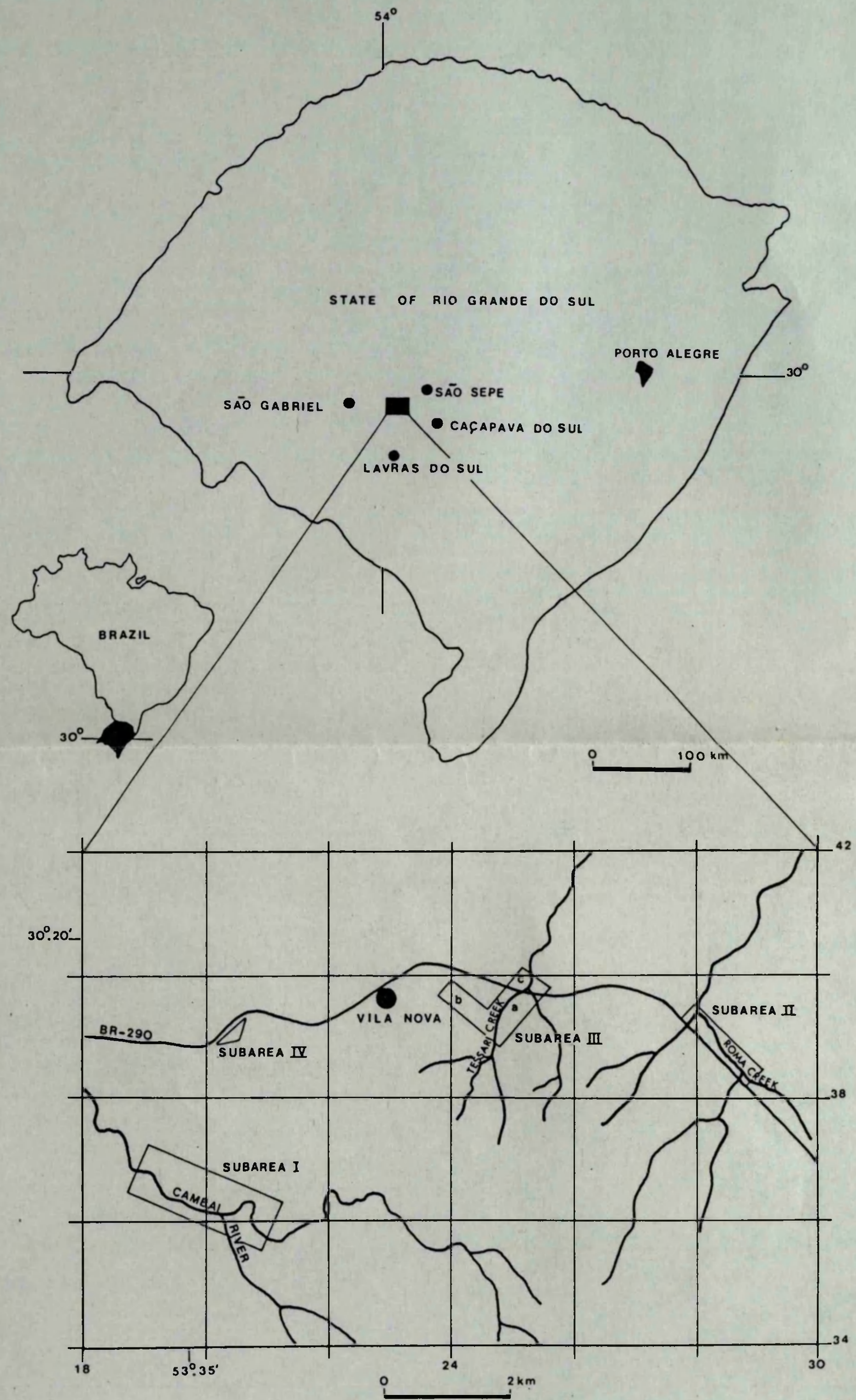

FIGURE. I. 1 _ LOCATION MAP

GEOLOGICAL MAP - SUBAREA I

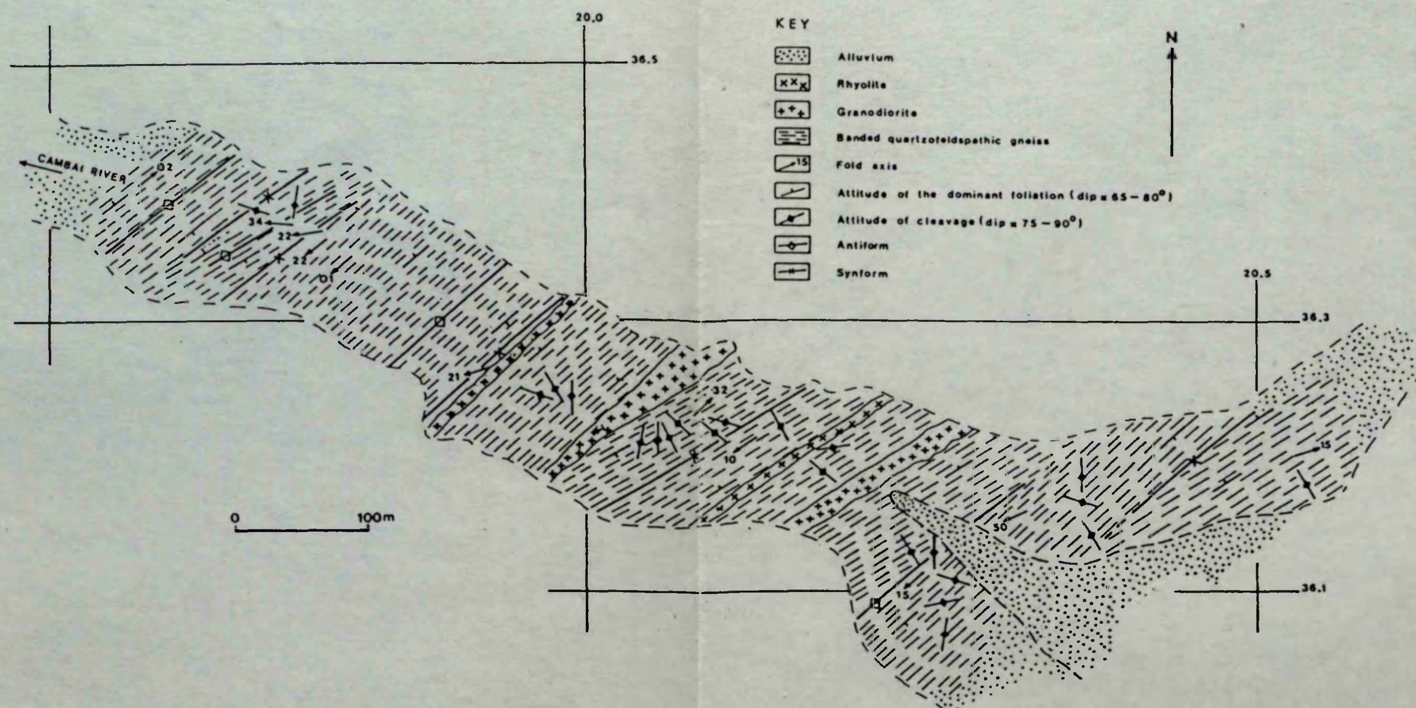

FIGURE. VII.2